Ochre and Biochar: technologies for phosphorus capture and re-use

Jessica Shepherd

Submitted for the degree of Doctor of Philosophy

School of GeoSciences

University of Edinburgh

2017

Dedicated to my parents, whose love, support and encouragement got me here.

In loving memory of Joy

Gone too soon from this world,

but always with me in my heart

Declaration

I confirm that this work has not been previously submitted for any other degree or professional qualification. This thesis has been composed by myself, except where work which has formed part of jointly authored publications has been included. I was the lead author of the published/submitted manuscripts and solely responsible for the laboratory work, (except stated otherwise), data analysis and manuscript writing. Co-authors provided feedback and contributed to the editing of the following one published and two submitted manuscripts and one manuscript intended for submission, which are listed in the following order according to how they appear as chapters in the thesis:

1. Shepherd, J.G., Sohi, S.P. and Heal, K.V. (2016) Optimising the recovery and re-use of phosphorus from wastewater effluent for sustainable fertiliser development. Water Research. 94. 155-165
2. Shepherd, J.G., Joseph, S., Sohi, S.P. and Heal, K.V. (2017) Biochar and enhanced phosphate capture: mapping mechanisms to functional properties. Chemosphere. 179. 57-74
3. Shepherd, J.G., Buss, W., Sohi, S.P. and Heal, K.V. (2017) Bioavailability of Phosphorus, nutrients and potentially toxic elements from marginal biomass-derived biochar assessed in barley (Hordeum vulgare) growth experiments. Science of the Total Environment. 584-585. 448-457
4. Shepherd, J.G., Sohi, S.P. and Heal, K.V. Plant availability of phosphorus from sewage sludge derived biochar used to capture aqueous phosphorus in barley rhizobox experiment

Details of the specific contributions of other people to the work are outlined at the beginning of each experimental chapter.

Jessica Grace Shepherd 16th April 2017

Lay summary

Phosphorus is an essential element for all life and is therefore an essential macronutirent for plant growth. To support global food security for a growing population, phosphorus fertilisers must be applied to soils to ensure crops grow to their maximum potential. Unlike carbon and nitrogen, however, the natural cycling of phosphorus occurs on a very slow timescale (hundreds of millions of years), and thus human intervention via the mining of phosphate rock for fertiliser production has a large impact on the phosphorus cycle. There have been recent predictions of 'peak phosphorus' occurring within 50 years and rapid spikes in phosphate rock prices which have triggered a response in the regulatory and research communities worldwide. With a limited supply of phosphate rock reserves, it is necessary to increase the efficiency of phosphorus use and the recycling of phosphorus wastes to ensure food security into the future.

In this project, materials to capture waste phosphorus from wastewater treatments plants have been designed and tested. These materials have also been tested as phosphorus fertilisers. They have been designed with the mechanisms of phosphorus uptake by plants in mind, so that they are optimised for agricultural use. The feedstocks they have been produced from are wastes, and the production processes have been purposefully simple to ensure the system is sustainable.

This research serves as a proof of concept, demonstrating the use of these sustainable materials to capture P from wastewater effluent and directly return it to soils as fertiliser.

Despite recent instability in the global supply of phosphate-rock derived fertiliser and the potential for this to continue into the future, the recovery of phosphorus (P) from wastewater treatment systems, where P is abundant and accessible, is well below maximum potential. Considerable resource is spent on removing P from wastewater in order to comply with environmental standards and to protect aquatic ecosystems from eutrophication, yet there is little emphasis on capturing the P in a way that is optimised for re-using it as agricultural fertiliser.

To address this lack of innovation in the face of climate change and food insecurity, a concept for a material capable of capturing P from wastewater was developed, with an emphasis on the utilisation of otherwise waste materials and the use of carbon neutral or negative production technologies. Based on the demonstrated P capture properties of coal minewater treatment waste (ochre) and biochar made from anaerobically digested feedstocks, a range of biochars were designed and produced using different mixtures of ochre ("OC"), sourced from the UK Coal Authority Minto minewater treatment scheme in Fife, Scotland and anaerobically digested sewage sludge ("AD"), sourced from the Newbridge wastewater treatment plant in Edinburgh.

A first generation of materials consisting of either AD or a 1:1 mixture (dry weight basis) of OC and AD were produced in a small-scale batch pyrolysis unit at two pyrolysis highest treatment temperatures (HTTs) (450 and 550°C) to give the biochars AD450, AD550, OCAD450 and OCAD550. These were tested for their P capture properties in repeated P-exposure experiments with pH buffering in comparison to unpyrolysed ochre, activated carbon and a natural zeolite. After 5 days of repeated exposure to a P solution at a wastewater-relevant concentration (20 mg P l^{-1}) replenished every 24 h, relatively high masses of P were recovered by ochre ($1.73 \pm 8.93\times10^{-3}$ mg P g^{-1}) and the biochars OCAD550 ($1.26 \pm 4.66\times10^{-3}$ mg P g^{-1}), OCAD450 ($1.24 \pm 2.10\times10^{-3}$ mg P g^{-1}), AD450 ($1.06 \pm 3.84\times10^{-3}$ mg P g^{-1}), and AD550 ($0.986 \pm 9.31\times10^{-3}$ mg P g^{-1}). The biochar materials had higher removal rates than both activated carbon ($0.884 \pm 1.69\times10^{-2}$ mg P g^{-1}) and zeolite ($0.130 \pm 1.05\times10^{-2}$ mg P g^{-1}). To assess the extractability of recovered P and thus potential plant bioavailability, P exposure was followed by repeated extraction of the materials for 4 days with pH 7-buffered deionised water. The AD biochars retained 55% of the P recovered, OCAD biochars 78% and ochre 100%. Assessment of potentially toxic element (PTE)

concentrations in the biochars against guideline values indicated low risk associated with their use in the environment.

A second generation of materials were produced to examine the scalability of the concept. Mixtures of AD and OC were pelletised with a lignin binder (89.1:9.9:1.0 ratio, dry weight basis) and AD was pelletised with binder (99:1 ratio, dry weight basis). The pelletised feedstocks were pyrolysed in a bench-scale continuous flow pyrolysis kiln at the same two HTTs to give the pelletised biochars PAD450, PAD550, POCAD450 and POCAD550. Analysis of digested biochar samples compared to the previous generation of biochars showed general similarities between the two groups, apart from the substantially lower Fe content.

Sub-samples of the pelletised biochars were exposed to a 20 mg l^{-1} P solution over 6 days, with the solution replaced every 24 h to give the P-exposed biochars EPAD450, EPAD550, EPOCAD450 and EPOCAD550. To probe the mechanisms of P capture by these materials and how feedstock preparation and pyrolysis conditions affected these, spectroscopic analysis using laser-ablation (LA) ICP-MS, X-ray diffraction, X-ray photo-electron spectroscopy (XPS) and scanning electron microscopy coupled with energy dispersive X-ray was performed. The results highlighted the general importance of Fe minerals in P capture and subsidiary roles for Al, Ca and Si.

A 3-week barley (*Hordeum vulgare*) seedling growth experiment was conducted using the pelletised and P-exposed biochars, in comparison with other biochars produced using feedstock which contained high amounts of PTEs. The biochars were also extracted using a range of different methods used to assess the bioavailability of PTEs and nutrients in soils, and the results compared to digests of barley leaves to identify whether any of these could reliably predict plant bioavailability in biochar. The above ground biomass and its total P concentration of barley grown in a 5% mixture of EPOCAD550 in sand was significantly higher than the control ($p < 0.05$ and $p < 0.01$, respectively). A significant positive correlation between mean leaf P mass and dry weight leaf yield ($R^2 = 0.865$, $p < 0.001$) was found, indicating that dry weight yield could be used as an indicator for the P fertilising capability of biochar for barley seedlings. Element concentrations in unbuffered and buffered and (pH 7) 0.01 M $CaCl_2$ biochar extractions were significantly positively correlated with plant leaf concentration for 6 of the 18 elements investigated, more than any of the other extractions.

A longer barley growth experiment was conducted, using rhizoboxes, to test the bioavailability of P in the biochars compared to conventional fertiliser. The pelletised and P-exposed biochars were applied to a sandy loam soil with P constraints. Biochar application rates were based on 2% formic acid extractable P, calculated for summer barley using Index 0 soil. Analysis of total leaf length at harvest (12 weeks), dry weight yield, leaf P concentration and leaf P mass showed no significant differences between the biochar treatments, NPK fertilised and NK fertilised controls. This shows that biochar, when applied at low total application rates based on extractable P, is as effective as conventional fertiliser.

Now that AD biochar materials have been shown to have useful phosphorus recycling properties in laboratory experiments, additional work is required to optimise their use in wastewater and agricultural systems. The next stage of research should determine their performance in flow-through filtration systems with simulated and real wastewater effluent, as well as their performance in field trials with different crops of interest to demonstrate their potential as viable alternative fertilisers.

Acknowledgements

Firstly, I would like to thank my supervisors, Professor Kate Heal and Dr Saran Sohi for their support and guidance over the years. I would especially like to thank Kate for responding to my enquiry those many years ago, and for going to great lengths to help me get the funding I needed to pursue this project in Edinburgh. She has provided both academic and emotional support when I needed it, and I am very grateful.

Outside of my academic supervision, I would also like to thank Colin Graham, Brian Cameron and Andy Cross for taking me under their wing at an early stage, involving me in the GeoScience Outreach course and teaching me about all things geoscience and outreach along the way. Brian, particularly, has provided counsel and support above and beyond, and I am very lucky to count him as a dear friend and a mentor. Thank you Andy for making me feel like family. Thanks also to Dawn Smith, who gave me the opportunity to learn from her as an intern and became a good friend in the process.

For their technical support, bad jokes and general tolerance of me, thanks to Andy Gray, John Mormon, Dr Clare Peters, Dr Lorna Eades, Dr Nic Odling, Jim Smith, Alan Pike for doing the things I couldn't do and thus making the research project possible. A number of people also assisted me at times when two hands weren't enough – my sincere thanks to Francesca Gregory, Flavien Poinçot, Dominic Greenslade, Lily Malich and Franziska Srocke for being there.

Thank you to Dr Chris Hepplewhite for arranging research funding from ICON, without which I could not have done any of this work. Thank you also for your encouragement.

Special thanks to Dr Roy Doyle for believing in me and joining me for the occasional breakfast beer in London. Thank you to those who have travelled long distances to visit - Kate, Annie, Emma, Andrew, Kelly, Daniel, Rob, Vera and the Green family.

Andrea Baxter must be acknowledged for her healing abilities in times of need. Thank you Miriam for stepping into my life at just the right time with a bubbly personality, can-do attitude and shared love of pad thai and wine. Thanks to everyone in the office, Lettice, Amy, Emma, Abbie, Qing and all the other Crewtons.

Finally, thank you to Mum, Dad, Kate and the rest of my family for your endless love and support. You are everything, and this is for you. Woli! Little did I know the impact you would make on my life. You have saved my experiments and saved me from breakdowns. You have helped me in so many ways and this wouldn't have been possible without you.

Table of Contents

List of Abbreviations

ANOVA	analysis of variance
BBF	British Biochar Foundation
DI	deionised
EBC	European Biochar Certificate
EBPR	enhanced biological phosphorus removal
HTT	highest treatment temperature
IBI	International Biochar Initiative
ICP-OES	inductively coupled plasma optical emission spectrometry
ICP-MS	inductively coupled plasma mass spectrometry
LA-ICP-MS	laser ablation inductively coupled plasma mass spectrometry
LOD	limit of detection
m/v	mass per volume
MWTP(s)	minewater treatment plant(s)
n/a	not available
n.c.	not calculated
PAH	polycyclic aromatic hydrocarbon
PTE(s)	potentially toxic elements(s)
ρ	Spearman's rank correlation coefficient (Spearman's rho)
r	Pearson's correlation coefficient
rpm	revolutions per minute
SEM	scanning electron microscopy
SEM-EDX	scanning electron microscopy with energy dispersive x-ray spectroscopy
UKBRC	UK Biochar Research Centre
WWTP(s)	wastewater treatment plant(s)
XPS	X-ray photoelectron spectroscopy
XRD	X-ray diffraction
w/w	weight per weight
wt%	weight percent

Feedstocks

AD	anaerobically digested sewage sludge
OC	ochre (from the Minto MWTP in Fife, UK)
OCAD	mixed ochre-AD feedstock
PAD	pelletised AD
POCAD	pelletised OCAD
ADX	*Arundo donax*
DW	demolition wood
FWD	food waste digestate
RH	rice husk
WHI	water hyacinth, India
WLB	willow logs, Belgium
WSI	wheat straw, India

Biochar

EPAD	PAD biochar after being exposed to a phosphate solution
EPOCAD	POCAD biochar after being exposed to a phosphate solution

List of Figures

List of Tables

Chapter 1

Introduction

"*Dear future generations: Please accept our apologies, we were rolling drunk on petroleum*"

- Kurt Vonnegut

The story of phosphorus (P) is closely interlinked with that of petroleum. For both resources, the discovery of large natural deposits spearheaded industrial developments which together enabled and demanded an exponential increase in their extraction and use. In the case of P, we are faced with significant challenges caused by the rapid extraction, unbalanced distribution and excessive use of P in a world with an expanding population and where food insecurity is already a reality for many. This chapter will outline the role of P in the current food system to explain how and why the natural phosphorus cycle has been broken by industrialisation. It will also outline relevant research into ochre and biochar technologies for the capture of P from organic waste streams and re-use as fertiliser, a strategy for restoring cycling within the global P system, which provides the theoretical basis for the research presented in this thesis. The research aims and questions, along with the thesis structure, will be presented at the end of the chapter.

1.1 Overview of the global phosphorus problem

On updating their assessment of Planetary Boundaries, the ‘safe operating space’ for humanity, Steffen et al. (2015) recognised the significant environmental risk posed by excessive application of P fertiliser to the world’s croplands. To mitigate this risk, it has been suggested that crop production could be supported by the redistribution of P from areas of excess to areas where soils are naturally P deficient (Carpenter and Bennett, 2011; MacDonald et al., 2011; Steffen and Stafford Smith, 2013). The capture of P from wastes and subsequent re-use in agriculture has occurred in various forms for thousands of years, such as the use of human excreta, or ‘night soil’, in rural Asia (Ashley et al., 2011). Urban development since the Industrial Revolution has led to a geographical separation of agricultural land and the waste-producing population. The development of water-based sanitation systems has further exacerbated this disconnection by facilitating the dumping of P rich waste into the ocean, where it would be returned to land by geological processes only after tens to hundreds of millions of years (Ashley et al., 2011; Smil, 2000). Before the Industrial Revolution, it is estimated that 1 Mt P y^{-1} was harvested in crops globally to support a population of 1 billion people, and approximately 15 Mt P y^{-1} was transferred to the ocean by human-induced erosion and runoff in excess of natural processes (Smil, 2000). By the year 2000, this had increased to 12 Mt P y^{-1} harvested for 6 billion people and around 70 Mt y^{-1} of anthropogenic increases in natural P fluxes (Smil, 2000). In order to return P biochemical flows to within the safe operating space of the Planetary Boundaries, P cycling must be re-established at relevant geospatial scales, which will require the redesign of many widely accepted waste management practices in order to be successful (Cordell et al., 2009; Shepherd et al., 2016; Steffen et al., 2015). An indication of the complexity of the system is demonstrated in Figure 1.1, a diagram of the modern global phosphorus cycle. The current acceleration of P flows caused by humans and dealt with in this research are highlighted in orange. The sections of the cycle targeted in this research to improve cycling in the anthropogenic P system are highlighted in green.

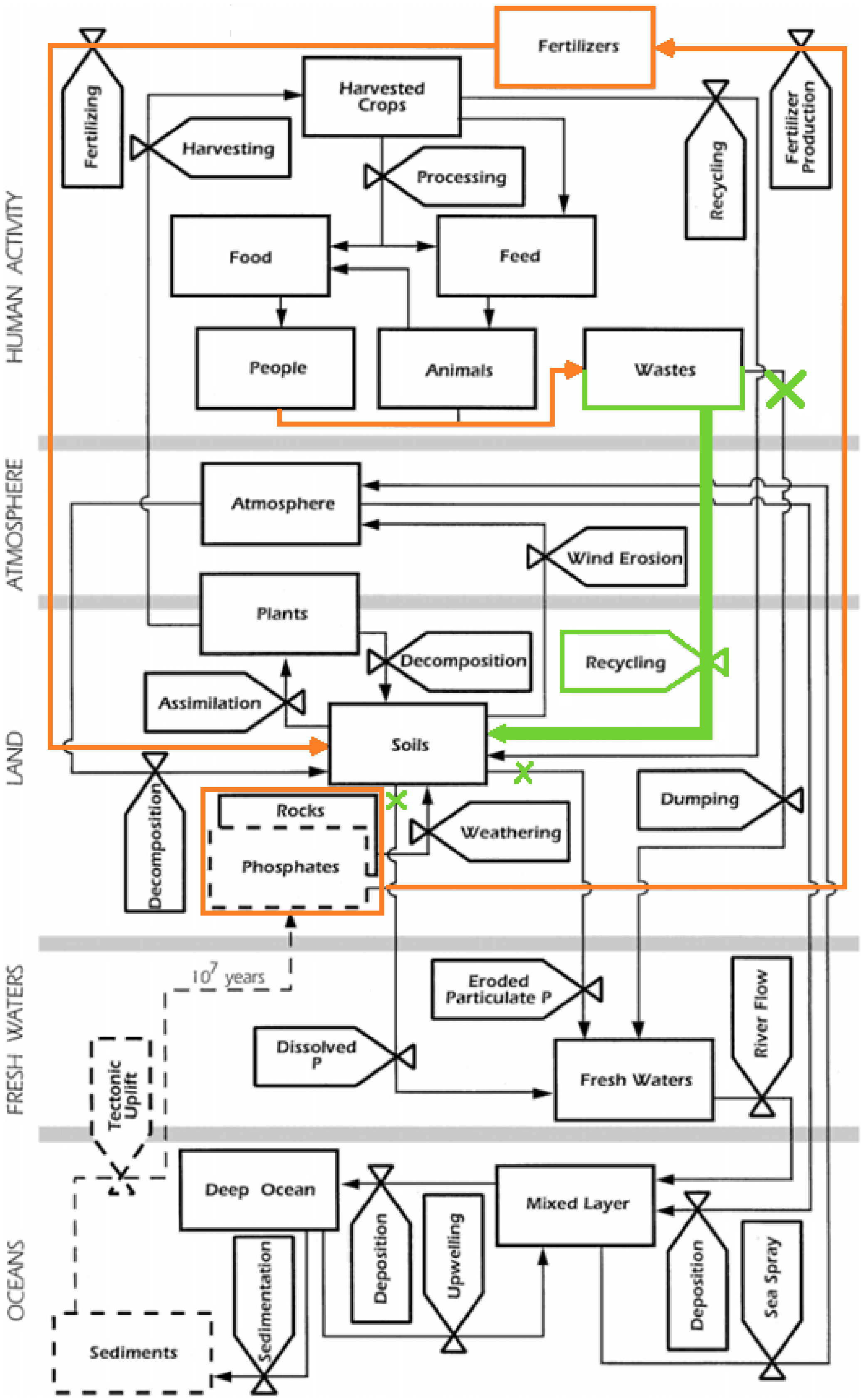

Figure 1.1 The global phosphorus cycle, separated into the different spheres, with flows relevant to the current research highlighted. From Smil (2000)

1.2 The role of phosphorus in natural systems

Phosphorus occurs primarily in the Earth's surface, with the main stores in rocks, soils, water and living organisms (Valsami-Jones, 2004). Unlike carbon (C) and nitrogen (N), under atmospheric conditions, P has no gaseous phase and so cycling of the element in the environment is via very different mechanisms (Tiessen et al., 2011; Valsami-Jones, 2004). The chemical properties of P are important for understanding P cycling processes.

Due to its high reactivity, P is never found on Earth as a free element (Desmidt et al., 2015). Instead, P exists most commonly as the phosphate anion (PO_4^{3-}), containing single and double bond linkages to oxygen (O). These linkages can be either inorganic, where none of the O atoms are bound to C, or organic, where one or more of the O atoms are bound to both P and C, to give phospho-esters (Bryant, 2004). The chemical flexibility of the phosphate anion can be explained in part due to the ability of one of the 3s or 3p electrons to be transferred into the 3d orbital, which allows different structures to be created (Valsami-Jones, 2004). Phosphate is an important part of biological reactions, forming part of the backbone of DNA and RNA, cell membranes, and the reactive functionality of adenosine triphosphate (ATP) (Figure 1.2) which is responsible for energy transfer in cells (Desmidt et al., 2015). Vital, therefore, for all life, P is one of the three essential plant macronutrients, along with N and potassium (K).

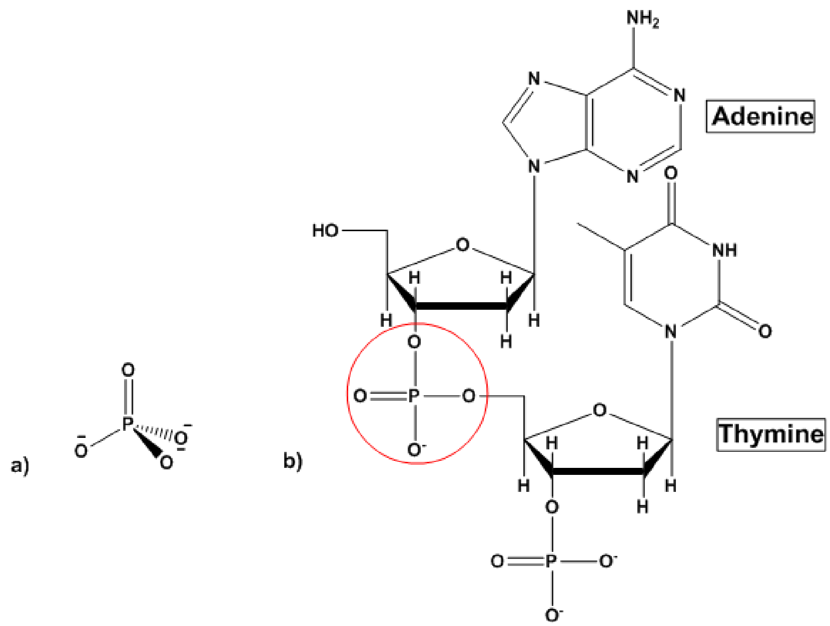

Figure 1.2 a) the trivalent phosphate anion, and b) the phosphodiester bond between adenine and thymine bases in DNA

1.3 Cycling of phosphorus in natural systems

The natural cycling of P is slow compared to the C and N cycles due to the absence of a gaseous phosphorus phase under atmospheric conditions (Smil, 2000). The processes involved in the natural P cycle occur over a timescale of 10^7 to 10^8 years (Smil, 2000). Initially, P is transferred from rocks to soils by weathering, and then transported to rivers and lakes, before being deposited into oceans. This is followed by deposition of P from shells and aquatic debris into marine sediments, followed by mineralisation and the tectonic processes of subduction, accretion and uplift (see Figure 1.3).

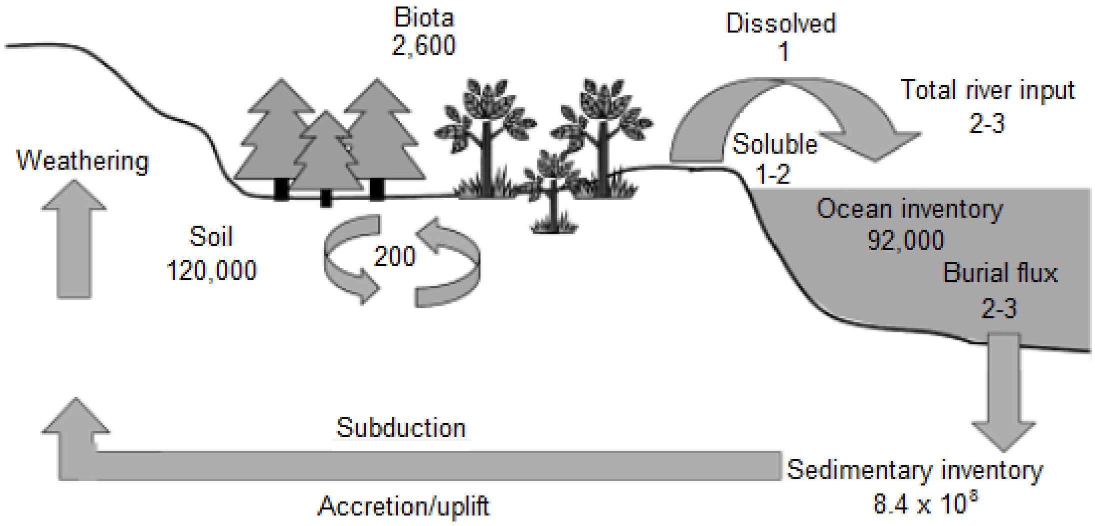

Figure 1.3 Natural cycling of phosphorus before anthropogenic influence. Reservoir capacities are in Mt P and fluxes in Mt P year^{-1}. From Valsami-Jones (2004) p. 22.

In water, orthophosphates ($H_2PO_4^-$ and HPO_4^{2-}) are the prevalent dissolved phosphate species. The relative concentrations of the different species are dependent on pH (Figure 1.4). The particulate fraction may account for as much as 95% of total water phosphate content, with up to 40% of particulate phosphate in organic forms (Follmi, 1996).

Phosphorus is present in soils at relatively low concentrations, around 100-3,000 mg kg^{-1} soil (dry weight) (Sharpley, 2000), in both inorganic and organic forms. Unbound inorganic P, present as orthophosphate in soil solution, is considered to be immediately bioavailable and is accessed by plants via uptake from roots. Orthophosphate can be found in soil bound to calcium (Ca), as in apatite ($Ca_5(PO_4)_3(F,Cl,OH,Br)$), and interacts with iron (Fe) and

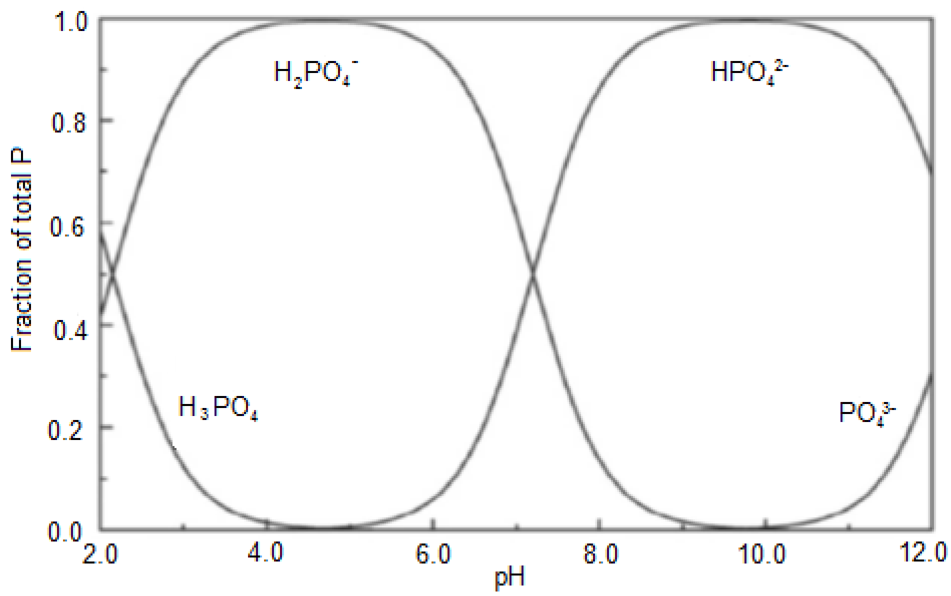

Figure 1.4 The speciation of phosphate in water with varying pH. After Oliveira et al. (2011)

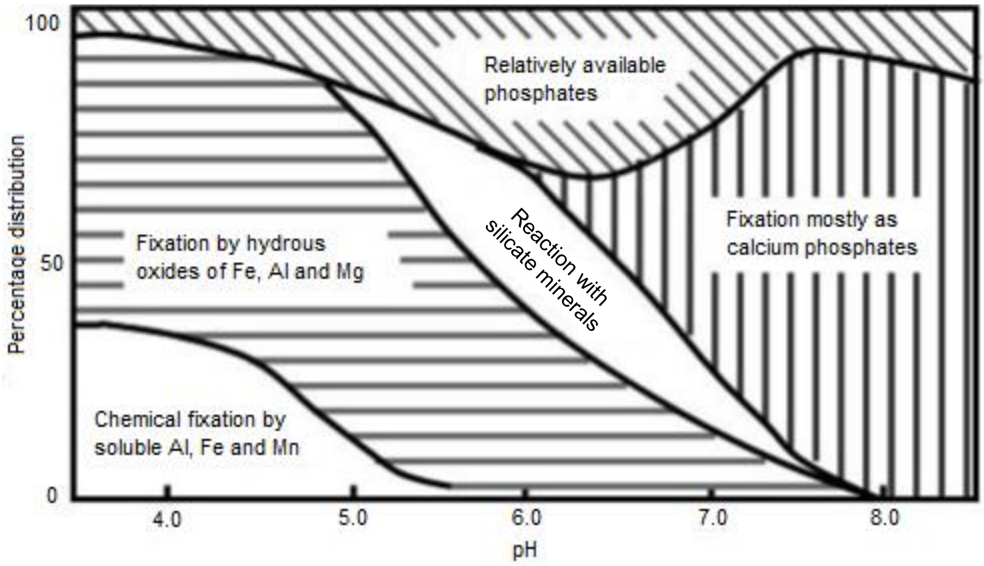

Figure 1.5 Phosphorus availability in soil with varying pH. From Valsami Jones (2004) p. 25

aluminium (Al) oxyhydroxides (Doolette and Smernik, 2011). There is a strong relationship between P bioavailability and soil pH, with the highest percentage of available P occurring at a pH of 6-7 (Figure 1.5). Cycling of P between soil and plants occurs on a relatively fast timescale compared to geological cycling (10^{-2} to 10^{0} years). It comprises plant uptake of P from soil through plant roots, followed by return of P to the soil through breakdown of dead plant matter in-situ (Figure 1.6). Bacteria and mycorrhizal fungi are essential in this process as they assist in the breakdown and solubilisation of phosphates from insoluble sources, giving plants access to nutrients (Frossard et al., 1995; Walker and Syers, 1976). Plant roots and microorganisms can excrete the enzyme phosphatase, which chemically converts organic phosphate to orthophosphate (Valsami-Jones, 2004). Roots also interact with mycorrhizae, which increase phosphorus availability by acting as an extension of the root system and excreting compounds which provide access to more plant available phosphate forms (Valsami-Jones, 2004).

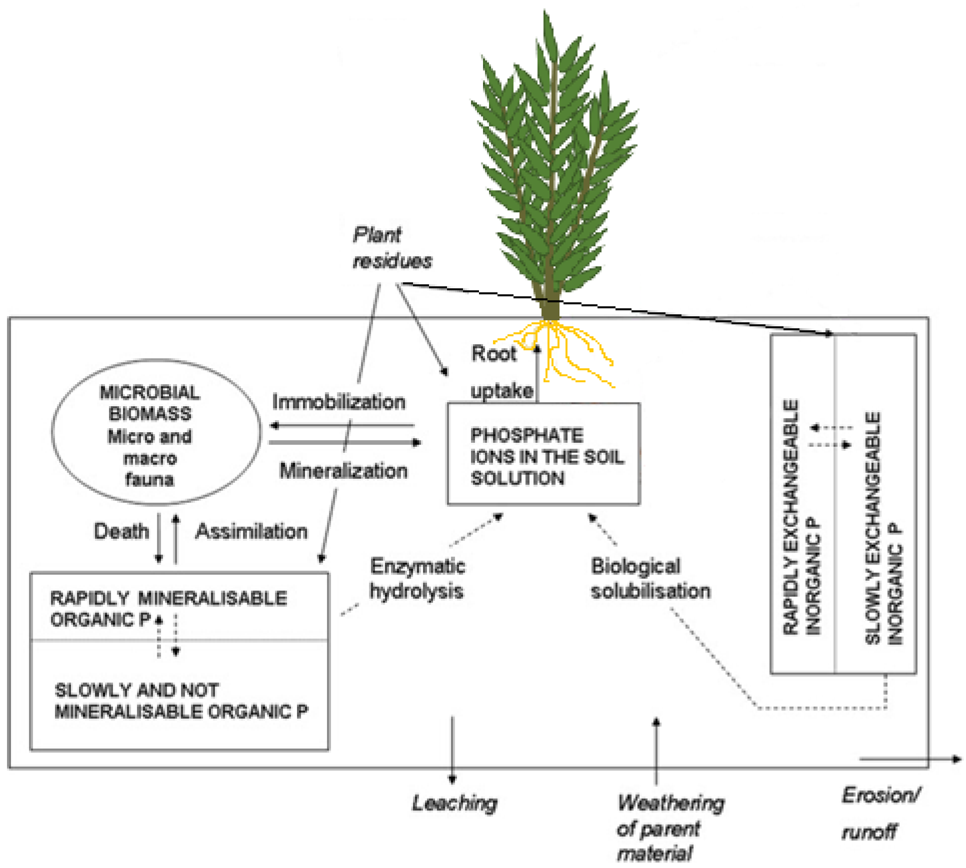

Figure 1.6 The soil-plant phosphorus cycle. Adapted from Frossard et al. (2011)

1.4 Human perturbation of the phosphorus cycle

Human intervention has significantly impacted the natural cycling of phosphorus, leading over time to a greatly increased rate of phosphorus flow from rock reserves into the ocean. Transportation – of rock phosphate from reserves around the world, through the agricultural, food and sanitation systems has been an important part of this development.

1.4.1 Inefficient use of phosphate rock-based fertiliser

In 2015, 223 million tonnes of phosphate rock was mined worldwide, predominantly for fertiliser production, compared to 180-190 Mt in 2011 (Jasinski, 2016, 2012). World phosphate rock resources are predominantly present as sedimentary marine phosphorites, with additional igneous occurrences found in Brazil, Canada, Finland, Russia and South Africa (Jasinski, 2016). Apatites such as fluorapatite ($Ca_3(PO_4)_3.CaF_2$) are the primary phosphorus bearing minerals in phosphate rock, with an average P content of 13% (Villalba et al., 2008). Mining of phosphate rock peaked in 1989, after which time P fertiliser use in developed countries started to decline (Desmidt et al., 2015). A second peak, driven by increasing fertiliser use in developing countries, occurred in 2009 (Desmidt et al., 2015).

Current global rock phosphate reserves may reach peak extraction in the next 50-100 years, with 85% of the remaining reserves controlled in just five countries: Morocco (majority of reserves in Western Sahara), China, the USA, Jordan and South Africa (Jasinski, 2010; Smil, 2000; Steen, 1998), with 77% of these reserves controlled by Morocco (Cooper et al., 2011). The control of rock phosphate is a serious global issue, where inequality in distribution and access has a strong negative impact on food security, especially in developing countries (Cordell and Neset, 2014; Shepherd et al., 2016). Soil phosphate requirements differ between regions. Oversupply of phosphate to soils is a problem in the Netherlands and Northern USA whereas undersupply affects soils in eastern Europe, Russia, Australia, South America and Sub-Saharan Africa (Cordell et al., 2009) (Figure 1.7).

The conversion of phosphate rock into fertiliser results in the transfer of P to soils and plants, and is largely responsible for the increases in crop yields since the 1950s (Tilman et al., 2002). In 2015 43.7 Mt of P_2O_5 (equivalent to 19.1 Mt of P) was applied to soil as fertiliser worldwide (Jasinski, 2012). This is in addition to approximately 2.5 Mt of P applied to crops in recycled manures (Liu et al., 2008). Based on FAO data from 2005, of this approximately 22 million tonnes y^{-1} of applied P, 12.7 is harvested in crops, 8.2 of which

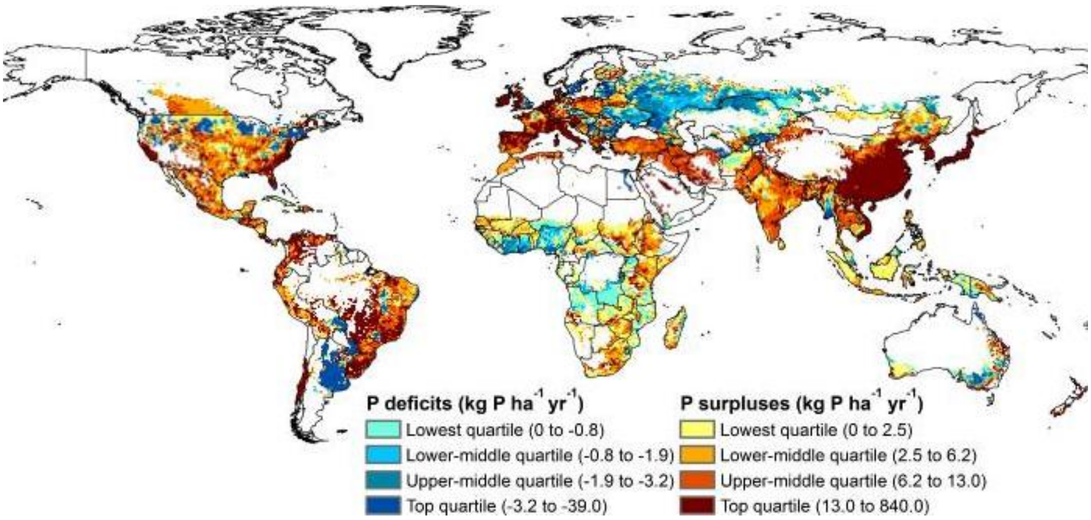

Figure 1.7 Map of global agronomic P imbalances for the year 2000, classified according to quartiles, determined for each 5° grid cell. From MacDonald et al. (2011)

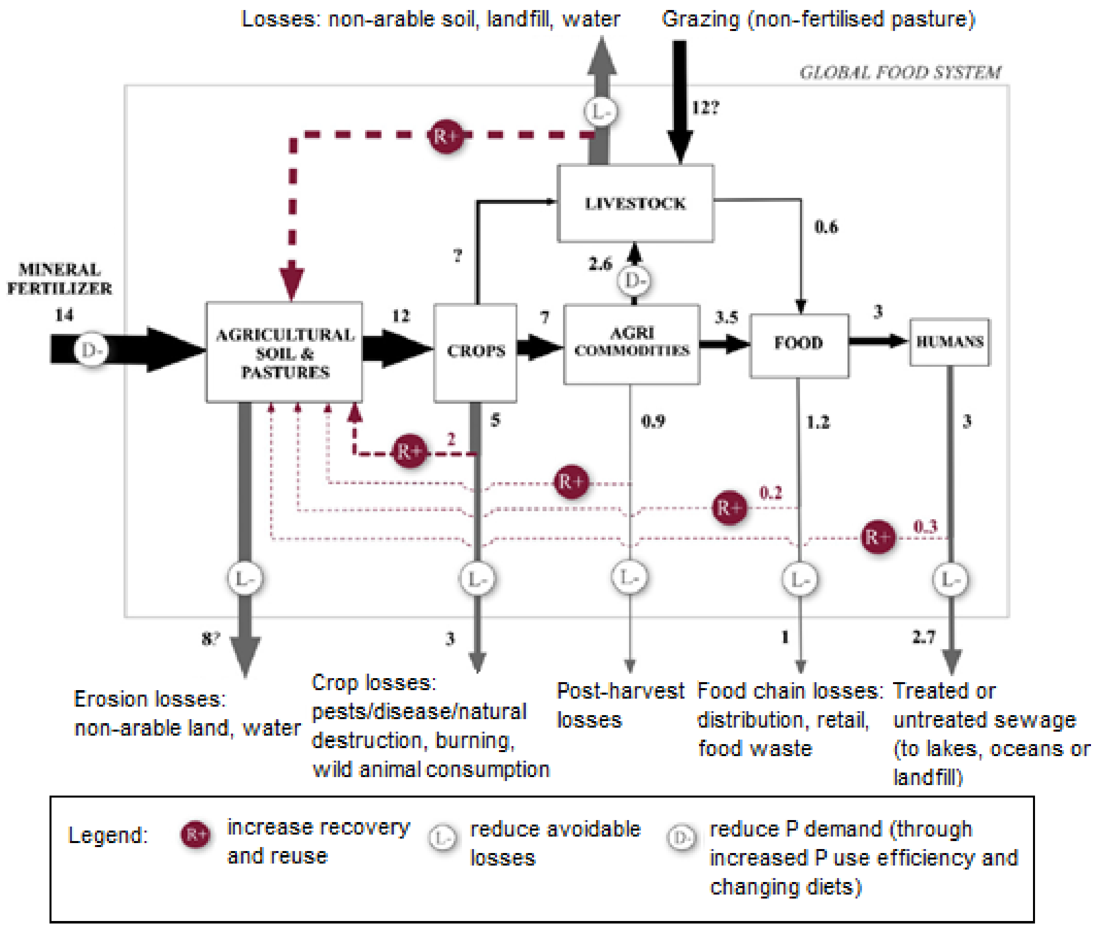

Figure 1.8 The flow of phosphorus through the global food system, highlighting losses and potential for recovery and re-use. From Cordell et al. (2011). Numbers represent current P flows in Mt P year^{-1}

is in grain (Liu et al., 2008). By the time the food is produced, 90% of P input from phosphate rock is lost from the soil (Clift and Shaw, 2012), as shown in Figure 1.8 of the flows of P through the global food system. Phosphorus use must become more sustainable through a combination of increased use efficiency and the implementation of recovery and re-use technologies in order to maintain a secure supply of food into the future. Understanding of soil P requirements with tailoring of fertiliser use will contribute to more sustainable use of P globally.

1.4.2 Phosphorus pollution of aquatic ecosystems

Transfer of P from soils to water and from animal excreta to soils, then water are considered diffuse sources of aquatic P pollution. Point sources of P pollution include industrial sites, such as wastewater treatment plants (WWTPs). Phosphate pollution from both point and diffuse sources presents a threat to water quality, with an estimated 8.5-9.5 Mt $year^{-1}$ of P transported from land to oceans (Bennett et al., 2001; Mackenzie et al., 2002), around eight times the natural rate of P transportation (Rockstrom, 2009).

The main impact of phosphate pollution is eutrophication, the process of nutrient enrichment of aquatic ecosystems, resulting in accelerated growth of algae and other aquatic plants (Haygarth and Condron, 2004; Pierzynski et al., 2000). Interactions between the aquatic ecosystem and nutrient levels are complex, so it is difficult to define criteria for phosphate concentrations that will predictably cause eutrophication, however phosphate concentrations in excess of 10 µg P l^{-1} remove constraints to the growth of many algae species (Valsami-Jones, 2004). Human activities contribute 22 Mt of P $year^{-1}$ into oceans, resulting in more than 400 dead zones across the world (Bennett et al., 2001; Diaz and Rosenberg, 2008). As the biggest cause of damage to global freshwater ecosystems, eutrophication costs more than £114 M per year in the treatment and restoration of affected water bodies in England and Wales alone (Pretty et al., 2003; Smith and Schindler, 2009).

In developed countries, improvements in the management of phosphate release from WWTPs, driven by the setting and enforcement of pollution control legislation, has led to a shift in focus towards addressing diffuse sources of phosphate pollution (Haygarth and Condron, 2004). A number of different phosphorus removal techniques are employed by WWTPs to minimise the risk of eutrophication in receiving waters.

1.4.3 Wastewater treatment

Treatment of wastewater to remove phosphate is a major engineering undertaking. Each year approximately 4.6 Mt P is passed through wastewater treatment plants (WWTPs) (Scholz et al., 2014). Wastewater composition varies, depending on the diet and sanitary habits of each country (Parsons and Stevenson, 2004). Typical raw wastewater in the UK has concentrations of around 10-50 mg l^{-1} ammonia-N, 0-5 mg l^{-1} nitrate-N and 5-10 mg l^{-1} phosphate-P (Parsons and Stevenson, 2004). The maximum permissible P concentrations to be discharged from WWTPs vary between countries, but European Council Directive 91/271/EEC allows 2 mg l^{-1} Total P for WWTPs treating 10,000-100,000 population equivalents (p.e.) of sewage per day and 1 mg l^{-1} Total P for >100,000 p.e. treatment plants (Desmidt et al., 2015).

Wastewater treatment typically occurs in three stages, the last of which is for final control of nutrient release. Primary treatment involves gravity-driven sedimentation to remove gross solids, removing approximately 11% of inflow P load (Cornel and Schaum, 2009). In secondary treatment microorganisms are utilised to consume organic C and nutrients, separating them from the water, and removing a further 20-30% of P in surplus sludge (Parsons and Smith, 2008). Tertiary treatment involves chemical or biological removal of phosphate and other nutrients (Parsons and Stevenson, 2004). Organic phosphates are contained in the sludge produced in primary treatment, whereas secondary treatment converts remaining organic phosphates in the system into inorganic forms (Smil, 2000).

1.4.3.1 Tertiary treatment

Tertiary treatment may involve removal of P from wastewater through chemical precipitation of phosphate or enhanced biological P removal (EBPR). Chemical precipitation commonly involves the addition of Fe(II),(III) and Al(III) chlorides or sulphates, to react with phosphates to form sparingly soluble compounds which are separated by filtration of the resulting sludge from the treated water (Parsons and Berry, 2009; Parsons and Stevenson, 2004). Under optimum conditions, up to 90% phosphate removal is possible (Parsons and Berry, 2009) but large quantities of chemicals are required and high volumes of sludge are produced (Desmidt et al., 2015).

EBPR uses specialised phosphate-accumulating microorganisms (Parsons and Smith, 2008) cycling between anaerobic and aerobic phases to remove 80-90% of influent P (McGrath and Quinn, 2004). Sludge produced in this process can be chemically converted into struvite, a magnesium ammonium phosphate which has a demonstrated use as a fertiliser (Parsons and Smith, 2008).

The P-rich sludges arising from wastewater treatment are spread on land, landfilled, incinerated and landfilled or disposed of into waterbodies (although this is banned in the EU) (Cordell et al., 2011). In the EU, 31% of sludge is landfilled as sludge and ashes (Scholz et al., 2014).

1.5 Phosphorus recovery and reuse from wastewater

The drive to develop P capture systems in the past has focussed on the prevention of eutrophication, but not on the re-use of captured phosphorus. Treatment of wastewater significantly reduces the concentration of phosphate released into the aquatic environment, but efficiency varies significantly between treatment plants. Septic tanks and nutrient-laden agricultural soils also contribute to phosphorus leaching into watercourses. Technologies for capture of phosphate are therefore necessarily diverse to reflect the different situations in which they are required. There is great opportunity in the UK, for example, to reduce reliance on P imports, as in 2009 the equivalent of 40% of total P imports were processed in UK WWTPs (Cooper and Carliell-Marquet, 2013). There are a number of different approaches to recover P from wastewater treatment including struvite precipitation, extraction of P from incinerated sewage sludge ash and capture of P using reactive substrates such as ochre. Advances in pyrolysis technologies means that P rich char (biochar) may begin to replace ash from incineration as the main solids output from WWTPs.

1.5.1 Struvite production

Phosphorus can be recovered at three different stages in WWTPs: the liquid phase, the sludge phase, or from monoincinerated ash (A, B and C, respectively, in Figure 1.9 (Desmidt et al., 2015).

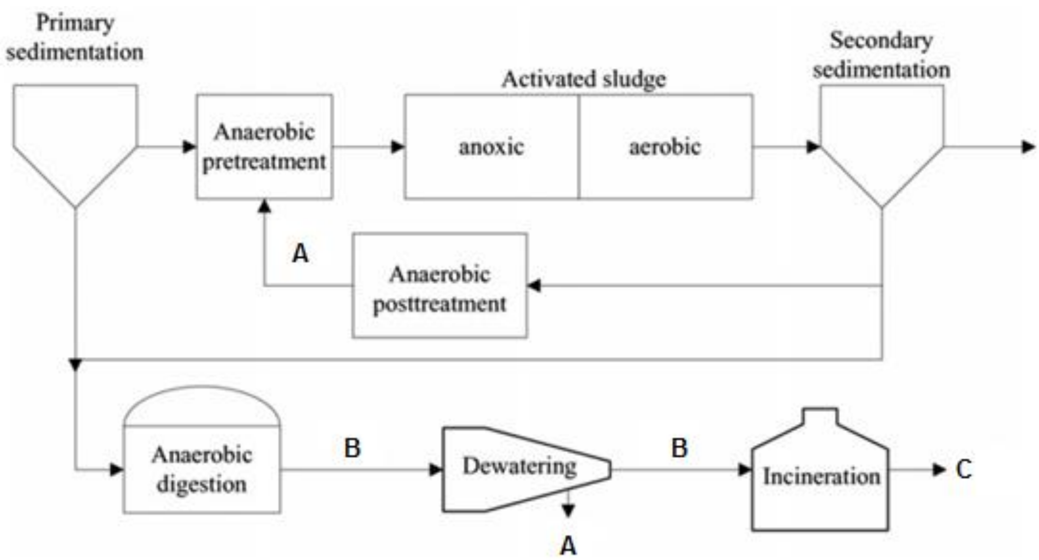

Figure 1.9 Locations which can be targeted for P recovery from wastewater treatment systems. Adapted from Desmidt et al. (2015).

The most developed technology to date for P recovery is the production of struvite, a white crystalline substance containing Mg, NH_4, and PO_4 in equi-molar concentrations that can be collected from both liquid and sludge phases. Formation of struvite in pipes of WWTPs reduces internal diameters and increases the energy required to pump sludge through the network, while removing deposits significantly increases maintenance effort and hence cost (Doyle and Parsons, 2002). A number of full scale systems for P recovery as struvite are already operational (Table 1.1). Struvite produced from human wastewater is sold as a fertiliser in Japan, and from Canadian-based company Ostara, which collects struvite produced using its PEARL™ system from WWTPs across northern America and Europe (Köhler, 2004; Ostara, 2016). In a recent analysis of the implementation of the Ostara system at Slough WWTP in England, £113,000 in savings were identified in the first year of operation due to reduced operational costs (Kleemann, 2015). Struvite fertiliser was as effective as single superphosphate for growing perennial ryegrass (*Lolium perenne L.*) in P-deficient loamy sand soil, and more effective for growing lettuce (*Lactuca satica L.*) in the same type of soil (González Ponce et al., 2009; Plaza et al., 2007). In a comparison of pot experiments using struvite and diammonium phosphate (DAP) to grow spring wheat (*Triticum aestivum*) over 30-90 days, struvite acted as a slow release fertiliser with equivalent rates of P uptake by spring wheat as from DAP, but needed to be blended with DAP to meet crop requirements in early growth stages (Talboys et al., 2016).

1.5.2 Recovery of P from ash

Incineration of sewage sludge has been viewed as an attractive option for sludge disposal due to the large volume reduction, destruction of toxic organic compounds, odour minimisation and the potential to recover energy from the sludge, which has a similar energy value to brown coal (Fytili and Zabaniotou, 2008). The ash produced can be incorporated into bricks, cement and concrete and made into light weight aggregates (Donatello and Cheeseman, 2013). Phosphorus recovery from sewage sludge ash has been achieved, with the commercial systems Ash Dec, BioCon, LEACHPHOS and Thermphos currently operational in Europe (Desmidt et al., 2015; Kleemann, 2015). The BioCon and LEACHPHOS systems use wet chemical leaching to extract P, whilst the Ash Dec process uses a complex and energy intensive thermo-chemical process. A greenhouse pot-scale experiment comparing ash-derived P fertiliser which met Swiss fertiliser regulations with conventional fertiliser treatments found them to be equally effective for plant growth (Franz, 2008).

Table 1.1 Full scale systems for struvite production from wastewater currently in operation. Adapted from Desmidt et al. (2015)

Process name	Technology or reactor type for P recovery	Input flow (m^3 day^{-1})	Influent P concentration (mg l^{-1})	Struvite production (tonnes day^{-1})	Removal efficiency (wt%)
ANPHOS	Liquid phase in batch reactor	100 or 4800	580 or 58	0.45 or 2	80-90
PHOSPHAQ	Liquid phase in a continuous stirred tank reactor	2400-3600	60-65	0.8-1.2	80
NuResSys	Liquid/sludge phase in a continuous stirred tank reactor	1920-2880	60-150	1.43-1.58	85
Phosnix	Liquid phase in fluidised bed	650	100-110	0.50-0.55	90
Ostara Pearl	Liquid phase in fluidised bed	500	100-900	0.50-4	85
AirPrex	Sludge phase in a continuous stirred tank reactor	1680-2000	150-250	1-2.5	80-90
Seabourne	Wet chemical recovery from sludge in a continuous stirred tank reactor	110	600	0.58	~ 90

1.5.3 Sorption technologies

Distinct from chemical extraction technologies, P can be captured from wastewater using substrates that are reactive towards P. These include soils, sediments, minerals and rocks, industrial by-products and tailor-made materials (Johansson Westholm, 2006). Comparison of studies investigating the P sorption capacity and hydraulic properties of a large range of materials highlighted wollastonite (a calcium metasilicate) and slag materials as promising for P removal from wastewater (Johansson Westholm, 2006). Another comparison of the literature identified zeolite, blast furnace slag, fly ash, Polonite, shell sand and red mud as materials with moderate to very high P sorption capacity (Cucarella and Renman, 2009). Various ochres, the by-product of the treatment of metal-rich mine water, also have high to very high P sorption capacities if assessed by the same standards (Heal et al., 2005).

Table 1.2 Comparison of the P adsorption capacity of ochres to other substrates identified for use as a P removing substrate, based on Johansson Westholm, (2006), Cucarella et al. (2007), Cucarella and Renman (2009) and Carr (2012).

Material	Adsorption capacity (mg P g^{-1})
Bauxite	0.61
Blast furnace slag	0.42
Burnt oil shale	0.65
Limestone	0.01-0.68
Polonite	70-120
Red mud	113.87
Shell sand	9.6-17
Wollastonite	0.064-0.065
Zeolite	0.46
Ochres	
Avoca ochre	21.0
Friendship Hill ochre	23.9
Polkemmet ochre	21.5
Minto ochre	18.2
Toby Creek ochre	22.6
WV ochre	32.0

1.5.3.1 Ochre for phosphorus recovery

Ochre is a compound comprised of Fe (oxy)hydroxides ($Fe(OH)_3$ and FeO.OH) and is produced in large quantities in the treatment of water discharged from flooded coal and metal mines. The precipitates formed from the treatment of coal mine drainage will differ chemically to those produced from other coal and metal mine drainage due to the differences in mine rock geochemistry between sites. Although there is no widespread end-use for ochre, it has been shown to have a high capacity for phosphorus adsorption and new industrial uses are emerging (Heal et al., 2003; Sapsford et al., 2015; Sibrell et al., 2009; Sibrell and Tucker, 2012). It has also been demonstrated as an effective as a slow-release P fertiliser without causing a significant increase in levels of toxic trace metals in soils and crops (Dobbie et al., 2005). A number of studies in the last 10 years have shown that ochre can successfully recover phosphate (Adler and Sibrell, 2003; Dobbie et al., 2009; Fenton et al., 2009; Heal et al., 2003, 2005; Littler et al., 2013; Na and Park, 2004; Sibrell et al., 2009; Sibrell and Tucker, 2012) and this phosphorus-enriched ochre has a secondary use as a soil fertiliser (Dobbie et al., 2005; Heal et al., 2003).

Ochre is therefore particularly interesting as a phosphorus recycling material as it makes use of an otherwise waste material and can be used directly as fertiliser. In the UK approximately 2,900 t y^{-1} are produced from around 70 coal mine water treatment plants (MWTPs), containing between 37-43 wt% iron (Moorhouse and Watson, 2015). Contamination of these ochres with potentially toxic elements (PTEs) is not generally a problem (Hancock, 2005). The mechanism of phosphorus binding to ochre has been previously investigated (Parfitt, 1989; Sibrell et al., 2009). High silicate concentration in ochre has been correlated with a low P sorption capacity, whilst high sorption capacities were found in ochres containing a mixture of Fe and Al (Sibrell et al., 2009). Conflicting results have been reported for the influence of pH on the P sorption capacity of different ochres, where either an inverse correlation or no significant correlation have been reported (Sibrell and Tucker, 2012; Wei et al., 2008). Phosphorus adsorption was shown to be relatively independent of the presence of other ionic species in the wastewater (Wei et al., 2008).

The physical properties of ochres differ based on their chemical compositions and the nature of the mine water treatment system. The chemical properties of the wastewaters and soils to which P-enriched ochre is to be applied will also have an effect on how each ochre performs as a phosphate recovery material. Differences in the physical properties of ochres sourced from the Polkemmet and Minto minewater treatment plants (MWTPs) in the UK, for instance, make them suitable for different phosphate sorption applications (Heal et al., 2003). The high saturated hydraulic conductivity of Polkemmet ochre (26-32 m day^{-1}) makes it more suitable for use as a substrate in constructed wetlands after the tertiary stage of wastewater treatment, whereas the low hydraulic conductivity and fine-grained texture of the Minto ochre (0.7-1.7 m day^{-1}) makes it more suitable for dosing of wastewater in a holding

Figure 1.10 The Minto minewater treatment plant wetland in Fife, Scotland (Photographs courtesy of Professor Kate Heal)

tank for P removal by adsorption and settlement, such as in a septic sewage treatment system (Heal et al., 2003).

Pelletisation has been investigated as a means of improving handling and sorption capacities of ochre-based phosphate sorption materials. A three-year experiment at the Leitholm WWTP, Scotland, diverting secondary-treated wastewater through a trough containing either Polkemmet ochre or ochre pellets (made from Polkemmet and Acomb MWTP ochre and Portland cement) showed that the former had a significantly higher hydraulic conductivity compared the latter (22×10^3 m day^{-1}) (Dobbie et al., 2009). Under optimal conditions, phosphorus removal rates were up to 65 ± 48 mg total P kg^{-1} ochre day^{-1}. In a nine month study of ochre pellets in horizontal and vertical flow configurations within a tank at Windlestone WWTP, England, phosphorus removal rates were up to 195 mg total P kg^{-1} ochre day^{-1} (Dobbie et al., 2009).

The re-use of phosphate recovered by ochre as a fertiliser has been successfully demonstrated (Dobbie et al., 2005; Heal et al., 2003). Pot and field experiments with grass, barley, birch and spruce seedlings using Polkemmet ochre saturated with phosphorus from KH_2PO_4 solution showed that addition of ochre increased both plant-available and total phosphorus concentrations in the soils. During the experiments, initially unavailable phosphorus in the ochre and soil was converted to available forms, probably via biological mechanisms (Dobbie et al., 2005). Crop yields from the ochre treatments were greater, but not always significantly, compared to no phosphate and conventional phosphate treatments. No contamination of soils or plant materials by potentially toxic elements was identified in the experiments.

Biochar is a charcoal analogue produced by the pyrolysis of biomass at temperatures above 250°C under oxygen-limited conditions. The difference between biochar and charcoal is in the intended use of the material, where biochar is produced for an environmental application and charcoal for energy (Lehmann and Joseph, 2009). Biochar can be made from a wide variety of biomass and bioresources, including wastes. Due to the large range of feedstocks from which biochar can be produced, and the variation possible in pyrolysis conditions such as highest treatment temperature (HTT), kiln residence time and gas flow, the resulting materials and have very different properties (Downie et al., 2009). Because of this variation, a classification system for biochar based on its potential benefits has been developed (Camps-Arbestain et al., 2015).

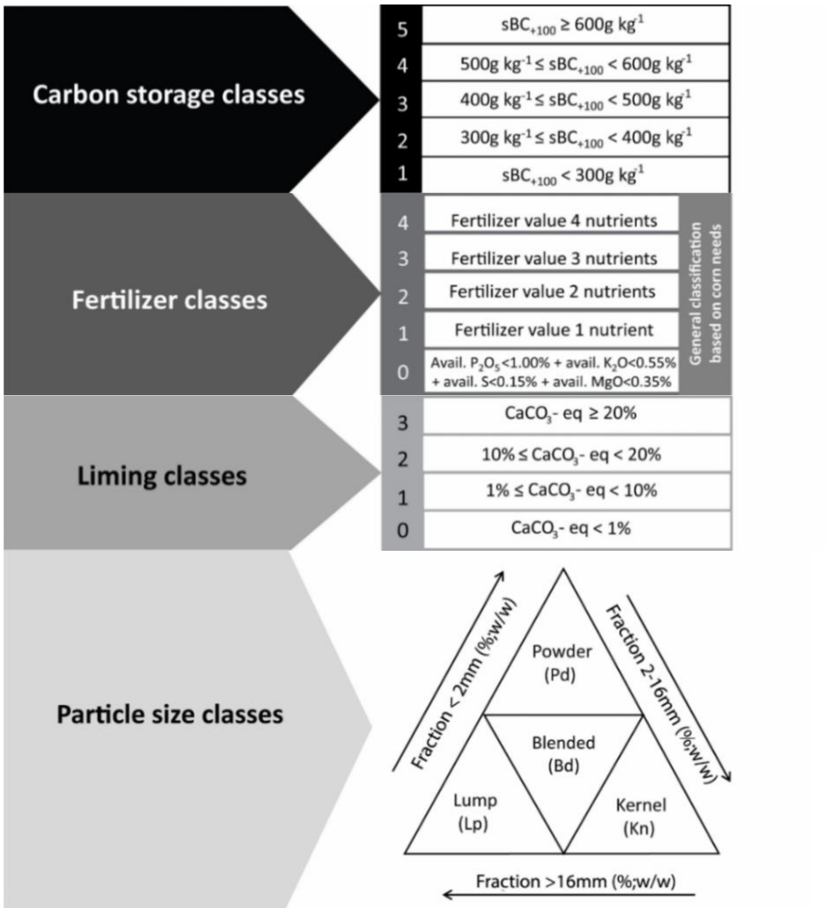

Figure 1.11 Biochar classification classes proposed by Camps-Arbestain et al. (2015), reflecting the diverse characteristics of biochars. sBC_{+100} is the C storage value, calculated by multiplying the organic C content of the biochar by the estimated organic C fraction that remains stable in soil for more than 100 years.

1.6.1 Biochar for phosphate capture

The phosphate sorption capacity of unmodified biochar is greatly varied, but generally low (Table 1.3). In addition, the residual levels of phosphate in some biochars may be sufficient to provide phosphate for plant growth without the addition of phosphate via sorption/capture (Kloss et al., 2012).

The surface chemistry of biochar is expected to be of primary importance to its phosphate binding capacity. Electron donor groups are unlikely to interact with phosphate, whilst Fe, Al and Mg mineral phases in biochar ash are more likely to interact with phosphate (Chernyakhovskii, 1985; Streubel et al., 2012; Volceanov et al., 2003). Furthermore, the charge of functional groups on the surface of biochar is affected by pH (Amonette and Joseph, 2009), where higher pH results in more negative, electron donating functional groups.

Table 1.3 Examples of Biochar P sorption from P solution by non-modified biochars in the literature

Biochar feedstock	Pyrolysis HTT	P Sorption	Reference
Anaerobically digested sugar beet tailings	600°C	133 mg P g^{-1}	Yao et al., 2011
Ingá (*Inga edulis* Mart.) biomass	400°C	~ 0.25 mg P g^{-1} (from 40 mg P l^{-1} solution)	Morales et al., 2013
Embaúba (*Cecropia hololeuca* Miq.) biomass	400°C	~ 0.5 mg P g^{-1} (from 40 mg P l^{-1} solution)	Morales et al., 2013
Lacre (*Vismia guianenses* Aubl. Pers) biomass	400°C	~ 0.4 mg P g^{-1} (from 100 mg P l^{-1} solution)	Morales et al., 2013
Corn stover	650°C	~ 3.1 mg P g^{-1} (from 100 mg P l^{-1} solution)	Chintala et al., 2014
Switchgrass	650°C	~ 3.1 mg P g^{-1} (from 100 mg P l^{-1} solution)	Chintala et al. 2014
Ponderosa Pinewood residue	650°C	~ 0.93 mg P g^{-1} (from 100 mg P l^{-1} solution)	Chintala et al. 2014

1.6.2 Unmodified biochars for phosphate capture

Biochars produced from anaerobically digested feedstocks have been shown to have a high capacity for removing phosphate from solution (Streubel et al., 2012; Yao et al., 2011). Biochar produced from anaerobically digested sugar beet tailings (DSTC) at 600°C via slow pyrolysis was more effective than activated carbon in phosphate removal from aqueous solution (Yao et al., 2011). Compared to biochar produced from undigested sugar beet tailings (STC), DSTC had a higher surface area, a less negatively charged surface but similar pH (9.45 and 9.95, respectively) and surface functional groups (Yao et al., 2011). DSTC contained a higher percentage of P and Ca compared to STC, and colloidal and nano-sized MgO, which has been shown to have a strong affinity for phosphate (Chernyakhovskii, 1985; Volceanov et al., 2003), was identified by X-ray diffraction and Scanning Electron Microscope-Energy Dispersive Spectroscopy (SEM-EDS) on the surface of DSTC but not STC. The highest concentrations of Mg in biochars investigated by Kloss et al. (2012) were in those produced at temperatures between 400 and 460°C.

Biochar produced from pelletised dairy fibre (separated from anaerobically digested cow manure in the digestion system) at 500°C captured a mean of 63% of P (mass basis) in a pilot-scale filtration system treating effluent from dairy lagoons, increasing to 70% after 15 days. However loss of weakly associated phosphate into drainage waters during removal of biochar from the filtration system resulted in an overall removal rate of around 30% (Streubel et al., 2012). The total P concentration of the biochar increased from 9.2 g kg^{-1} to 11.1 g kg^{-1} after 15 days of effluent filtration. Before disturbance of the biochar P capture rate was 9.6 g P kg^{-1} biochar (640 mg P kg^{-1} day^{-1}). When the filters were removed and the biochar analysed, however, on average only 29 g of phosphorus had been captured by biochar (129 mg P kg^{-1} day^{-1}) with an additional 17 g (76 g P kg^{-1} day^{-1}) of phosphorus recovered from the fibre that had collected around the biochar in the filters.

1.6.3 Modified biochars for phosphate capture

The majority of biochars assessed for P capture properties have demonstrated low affinity for P in solution, especially for low-ash biochar (Hale et al., 2013; Morales et al., 2013; Yao et al., 2012). Consequently, most biochars that have demonstrated P capture properties have been chemically modified (either feedstock modification pre-pyrolysis, or biochar post-pyrolysis) to increase porosity and enrich the biochar surfaces with Mg, Al, or Fe oxides (Chen et al., 2011; Li et al., 2016; Park et al., 2015; Ren et al., 2015; Yao et al., 2011; Zhang et al., 2013, 2012). Whilst chemical modifications are relatively simple and easy to optimise, the alternative of producing biochar with these desired characteristics by identifying and incorporating suitable mineral wastes (rather than chemical reagents) into the feedstock is more complicated but also less resource intensive.

1.6.4 Biochar application to soil

In order to develop a suitable fertiliser from P recovered in biochar, it is necessary to also consider the N fertilisation capacity and potential for PTE contamination of soil. There is a vast body of literature detailing the results of the application to soil/crop systems of biochar in varying quantities, produced from different feedstocks using different pyrolysis systems. It has become increasingly clear that specific biochar types are suited to specific soil/crop systems, as discussed below, so a 'one size fits all' approach is not appropriate (Jeffery et al., 2015; Joseph et al., 2013; Verheijen et al., 2014). In order for biochar to be adopted as a soil fertility technology by farmers and approved for use by legislators, it is necessary to show that biochar can produce reliably positive effects on soil characteristics and crop growth, and that is does not cause harm to the environment. The lack of standardisation of experimental methods and logical tailoring of biochars for specific scenarios has contributed to the emergence of literature showing negative effects of biochar on plant growth in various plant growth experiments (e.g. Mukherjee et al., 2014; Oleszczuk et al., 2013; Quilliam et al., 2012; Rajkovich et al., 2012; Spokas et al., 2012; van Zwieten et al., 2010).

There are also many examples of the positive benefits of biochar application to soils, including remediation of metal contamination via reduction in availability and toxicity of potentially toxic elements (PTEs) and increased P availability in column and plant growth experiments (Beesley et al., 2014, 2011; Buss et al., 2012; Jeffery et al., 2015; Méndez et al., 2012; Uchimiya et al., 2011).

The EU are currently developing fertiliser regulations which will cover recycled nutrients such as those found in biochar (European Commission, 2016). It is therefore essential to be able to demonstrate the positive characteristics of biochar and how any potential risks of their application to soil can be mitigated.

1.6.4.1 Biochar and nutrients

Soil nutrient availability is essential for optimal crop yields, but nutrients which are very soluble can be easily leached from the system, requiring additional fertiliser application and potential pollution in downstream environments. Some biochars provide plant nutrients originating from the feedstock (Hossain et al., 2011; Ippolito et al., 2015), whilst others reduce the leaching of P and N already in the system via interactions between surfaces and nutrients (de la Rosa et al., 2014; Uzoma et al., 2011). Application of biochar to soils assists in enhancing P availability to plants, but this is dependent on specific soil and biochar characteristics, such as pH, mineral and nutrient content (Shen et al., 2016). The availability of P, N, Ca, Mg and Mo can be increased by biochar addition to soil which results in an increase in soil pH (Jeffery et al., 2015).

The availability of N originating from feedstocks is influenced by pyrolysis conditions. Organic nitrogen in feedstock is gradually transformed into pyridine-like compounds, with plant available N concentrations significantly decreased above pyrolysis temperatures of 600°C (Bagreev et al., 2001). Therefore, biochars produced at temperatures exceeding 600°C would be less suitable for use as fertilisers. Biochar interactions with N in soil have been identified, which, depending on whether the system is nutrient deficient or enriched, can result in positive or negative effects on the system (Deenik et al., 2010; Nelissen et al., 2014; Prommer et al., 2014; Rondon et al., 2007; Shenbagavalli, S and Mahimairaja, 2012).

1.6.4.2 Biochar and potentially toxic elements

Application of biochar produced from feedstocks which contain high concentrations of PTEs may pose a risk of contaminating the soil and connected environment, causing phytotoxicity, or elevated uptake of PTEs into plant tissues, which may in turn cause harm to animal and human health. As mentioned previously, biochar has been used to successfully remediate PTE contaminated soils (Beesley et al., 2014) thus, as with nutrients, understanding of the specific characteristics of each biochar is necessary to estimate the level of risk involved in application to a particular soil. By increasing the soil pH, biochar can immobilise PTEs (Beesley et al., 2014). Functional groups on biochar surfaces can also interact with PTEs via complexation, ion exchange, electrostatic attraction, precipitation and non-covalent π interactions (Beesley et al., 2014; Ding et al., 2016).

Guidelines have been developed by the International Biochar Initiative, the European Biochar Foundation and the British Biochar Foundation to provide some means of governance for biochar production and provide criteria by which the quality of biochars on the market can be assessed (BBF, 2014; EBC, 2012; IBI, 2012). Each of these stipulate limits on the total concentrations of PTEs permissible in biochar, but this does not take into account the low bioavailability of elements in biochar that have been identified experimentally.

It remains difficult to predict the bioavailability of PTEs (and nutrients) in biochar as the methods traditionally utilised to assess bioavailability have been developed for soils, which have very different properties to biochar. Nonetheless, extraction-based assessments of bioavailability are useful to help compare biochars with each other in terms of varying extractability.

1.6.5 Sewage sludge biochar

Sewage sludge contains high concentrations of the nutrients N, P and K but can also contain high amounts of PTEs. The disposal of sewage sludge to land now occurs less due to concerns around the build-up of PTEs in soils, as well as the potential for PTEs and nutrients to leach from the soil and cause pollution downstream (Stutter, 2015; Waqas et al., 2014). Pyrolysis of sewage sludge is an attractive alternative to incineration, as it is a more efficient and cleaner technology for energy production (Kleemann, 2015). Application of biochar made from sewage sludge, rather than the unpyrolysed feedstock, may be more acceptable to environmental regulators as PTEs in sewage sludge biochar can be less bioavailable after pyrolysis (Agrafioti et al., 2013; Méndez et al., 2012; Waqas et al., 2014).

Several studies have demonstrated the effect of sewage sludge biochar application to soil on crop quality. A plant growth experiment using sewage sludge biochar as a fertiliser produced cherry tomatoes (*Lycopersicon esculentum*) which met Australian food standards for PTE concentration in the fruit (Hossain et al., 2010). Yields of cherry tomatoes were 64% higher in biochar treatments (applied to a low P chromosol at a rate of 10 t ha^{-1}) compared to soil-only controls, showing the fertiliser potential of sewage sludge biochars. Non-pyrolysed sewage sludge and sewage sludge biochars were applied to Cd and Zn contaminated soil at rates between 2-10% (mass basis), in which cucumber (*Cucumis satvia L.*) was grown (Waqas et al., 2014). The bioavailability of PTEs was lower in the biochar-amended soils than in the sewage sludge amended soils. Bioaccumulation of As, Cd and Cu in cucumber fruit was significantly lower in the biochar treatments than the contaminated soil control and sewage sludge treatments for all application rates, whilst bioaccumulation of Zn was only lower than the soil control for the highest application rate (10%). Although significantly lower than the contaminated soil and sewage sludge treatment values, the concentration of As in the cucumber fruit in the biochar treatments still exceeded Chinese regulatory guidelines for bioaccumulation. Bioaccumulation of Cd was significantly increased in the biochar treatments compared to the unamended soil.

These studies demonstrate that PTEs are not normally a concern in the application of biochars produced from sewage sludge to agrosystems, especially when soils are not heavily PTE contaminated in the first instance.

1.7 Research aims and objectives

Based on the background presented in this introduction, an opportunity exists to investigate the potential for biochars produced from waste feedstocks to be used to capture P from wastewater effluent and return it to soil as fertiliser to create a more sustainable P cycle. Evidence points towards anaerobically digested feedstocks as the most suitable for producing P-reactive biochars. In the case of anaerobically digested sewage sludge, the physical characteristics of the material (soft, workable) also make it an ideal candidate as a binding material for ochres which have high P sorption capacity but insufficient hydraulic conductivity (i.e. are powders) for use in filtration systems to remove P from wastewater.

The overall aim of this research was to design and test tailored biochars to be used as P recycling materials as a way of using wastewater effluent P to meet agricultural crop P requirements. The research has a mechanistic approach, focusing on the interactions between biochar, phosphate, soil and plants to improve P use efficiency in these systems.

In order to assess the suitability of these theoretical biochar materials for use in both wastewater treatment and agricultural fertilisation, their function in each system must be demonstrable. If such functionality is demonstrated, it must also be shown that the materials pose no risk to the environments in which they will be used, i.e. they do not contain or release unsafe levels of PTEs.

The objectives of the research presented in this thesis were therefore:

1) <u>Material design</u>
   a) To determine whether a mixed anaerobically digested sewage sludge and ochre biochar material could be produced using simple mixing techniques and standard pyrolysis systems;
   b) To identify whether the biochars met different current quality guidelines regarding PTE contents.

2) <u>P capture from wastewater</u>
   a) To assess the reactivity of mixed anaerobically digested sewage sludge and ochre biochars towards P, and determine whether they were more or less reactive than biochars produced from the sewage sludge alone;
   b) To identify whether pyrolysis highest treatment temperature affected the P capture properties of the biochars;

c) To identify the chemical mechanisms behind any observed differences in P capture between the biochars;

d) To determine whether P-reactive biochars could be used over an extended period of time.

3) Recycling of captured P to plants

a) To assess methods for the estimation of plant availability of nutrients and PTEs from the biochars and P-exposed biochars;

b) To determine whether native biochar-P and P captured by the biochars can be accessed by plants;

c) To compare the performance of the biochars and P-exposed biochars against soluble P fertiliser in a plant growth experiment.

1.7.1 Thesis structure

The objectives of the research are addressed in four experimental chapters in this thesis, which have been prepared in journal paper format, and one general discussion chapter. Chapter 2 investigates the production and P capture and release properties of the biochars, addressing objectives 1) a,b and 2) a-d. Chapter 3 presents the upscaled production of the biochars, as well as a mechanistic study of P capture using spectroscopic and microscopic techniques, addressing objectives 1) a,b and 2) a-d also. In Chapter 4 the biochars are assessed for P and PTE bioavailability using soil extraction methods and a rapid plant growth experiment, addressing objectives 3) a and b. Chapter 5 presents a longer plant growth experiment in which the performance of the P-exposed biochars as P fertiliser are compared against a highly soluble P source, addressing objectives 3) b and c. Chapter 6 presents a general discussion of the research in Chapters 2-5, bringing the research chapters together. Conclusions, possibilities for further research and finally the relevance of the research in the context of P sustainability are presented in Chapter 7.

Chapter 2

Optimising the recovery and re-use of phosphorus from wastewater effluent for sustainable fertiliser development

J.G. Shepherd, S.P. Sohi and K.V. Heal

Published in *Water Research* Volume 94 (2016) pages 155-165

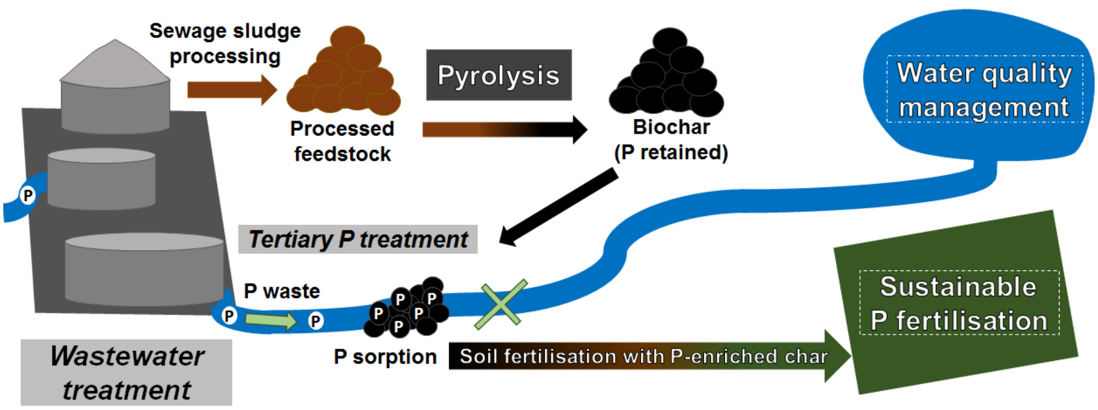

The candidate, as lead author, performed the experiments and laboratory analysis. Data analysis and writing of the paper was carried out by the candidate. Co-authors provided support and guidance on the scope and design of the project, the analyses performed and editing of the manuscript. Pyrolysis was performed by Dr Clare Peters. AutoAnalyser analyses were performed by Andy Gray and John Mormon.

2.1 Introduction

As a limiting factor for plant growth, the current food production system relies on constant inputs of phosphorus (P) into soils to satisfy the growing demand of the human population. Phosphate rock, the dominant source of P for phosphate fertilisers, is a limited resource, with current world reserves estimated to last between 30 to 300 years (Cordell and Neset, 2014; Reijnders, 2014). In contrast, eutrophication caused by the discharge of excess P from wastewater and agricultural runoff into aquatic systems is a global environmental problem (Dodds et al., 2009; Steffen et al., 2015). Worldwide 17.5 Mt $year^{-1}$ P is harvested from rock reserves and 9.5 Mt $year^{-1}$ released into inland and coastal waters (Cordell et al., 2009). Human society currently perpetuates a P paradox where both a problematic scarcity and a detrimental profusion of P exists in different parts of the same system. P wastage occurs in almost all stages of the current food system and there is therefore great potential to address this paradox (Cordell and White, 2013; J. G. Shepherd et al., 2016a).

Recovery and redistribution of P from wastewater to agricultural land is one mechanism for reconciling P wastage and scarcity. During wastewater treatment the majority of P is precipitated into the solid sludge fraction using iron salts. Transfer of treated sludge to agricultural land is already an important method of sludge disposal within the UK as well as Cyprus, Denmark, France, Ireland, Luxemburg, Portugal and Spain (SEPA, 2015). Managed under the EU Sewage Sludge Directive (86/278/EEC), the UK Sludge Use in Agriculture Regulations 1989 and Safe Sludge Matrix, 75% of treated sludge in England and Wales is transferred in this way (Defra, 2011). In 2008 approximately two thirds of the 1.6 Mt of sewage sludge produced in the UK was also treated by anaerobic digestion before use (Defra, 2011). Anaerobic digestion reduces the pathogen load of sewage sludge and produces methane, but does not address acceptability issues relating to odour. Distribution of wet digestate is also expensive but drying followed by granulation or pelletising is energy intensive. Another alternative for sludge treatment is incineration, which reduces bulk, removes odours and yields P-rich ash from which P can be recovered. Various processes for the extraction of P from incineration ash have been developed (Donatello and Cheeseman, 2013) and the utility of the fertiliser products demonstrated (Franz, 2008). However incineration converts nitrogen (N) and carbon (C) to the gaseous phase, losing their potential value in agricultural re-use. Whilst there are many sludge treatment methods in use which allow for the recycling of P, few of the products of sludge treatment are truly optimised for agriculture.

Pyrolysis is an alternative thermal treatment technology in which a proportion of C is conserved in solid phase as well as P and some N, depending on the highest treatment temperature (HTT) (Xie et al., 2015). The term biochar has been adopted to describe the solid product of pyrolysis, especially if it is designed for use in soil. Pyrolysis of anaerobically digested sewage sludge has a better energy balance than its non-digested counterpart (Cao and Pawłowski, 2012), possibly because methanogenesis does not involve fractions that are volatile at pyrolysis temperatures. Sludge pyrolysis is environmentally and economically viable for energy production and solid waste treatment in the wastewater treatment industry (Mills et al., 2014). Productive uses of biochar improve the economic case for this mode of sludge management, however environmental regulators require evidence that addition of biochar from sludge pyrolysis will not cause contamination of soils by potentially toxic elements (PTEs) that they may contain.

In the near future the permissible concentrations of P in discharge from wastewater treatment will decrease in the EU under the Water Framework Directive, from 1–2 mg P l^{-1} to 0.1 mg P l^{-1}. This may necessitate the use of tertiary treatment specifically to meet these requirements. To date, various materials have been suggested for removing P from wastewater effluent: ochre, zeolite, Polonite, opoka, blast furnace slags and Filtra P, amongst others (Cucarella et al., 2008; Dobbie et al., 2005, 2009; Heal et al., 2005). Ochre is produced during the treatment of metal-rich water from flooded coal and metal mines. Each year around 50,000 t of ochre are produced from UK coal minewater treatment plants (MWTPs) with no specific recycling option (Johnston et al., 2008). Ochre from a variety of MWTPs and other sources has been used previously to remove phosphate from wastewater in batch, column and field-scale experiments (Adler and Sibrell, 2003; Fenton et al., 2009, 2012; Heal et al., 2005; Na and Park, 2004; Sibrell and Tucker, 2012; Sibrell et al., 2009). However the properties of each ochre are specific to the mine geochemistry, treatment processes and design at the respective MWTP and thus not all are ideally suited for use in a flow-through filtration system. Screening of ochre prior to use is required as leaching of toxic metals from ochre from particular mine sources has been reported (Fenton et al., 2009, 2012). Low hydraulic conductivity is an important current barrier to widespread use of ochre for P filtration in wastewater treatment plants (WWTPs) (Heal et al., 2003, 2005). To improve the hydraulic properties of ochre in P filtration systems, pelletised ochre-composites bound using cement have been developed (Dobbie et al., 2009; Sibrell, 2007), but the use of cement is not consistent with the development of an energy and resource-efficient system. The system would be improved if a successful alternative binder and binding system were to be identified.

Purposeful precipitation of struvite (magnesium ammonium phosphate) is performed at some treatment facilities to simultaneously manage both P and N, but some P remains in the solid waste stream, requiring additional treatment. Despite encouraging results in both P extraction and plant growth studies for products of P recovery systems, traditional P management systems remain the most commonly utilised in the wastewater and agricultural industries. Regulatory and industrial attitudes towards P have nonetheless shifted and so technological innovations are focussing on treating P as an increasingly scarce resource rather than an environmental pollutant (EC, 2013).

Biochars produced from anaerobically digested materials have been shown to recover P from aqueous media in laboratory (Yao et al., 2011) and field (Streubel et al., 2012) experiments. More recently, enhancement of biochar P recovery properties has been achieved by chemical pre-treatment of feedstocks (Liu et al., 2015; Zhang et al., 2013, 2012) and post-treatment of biochar (Park et al., 2015; Ren et al., 2015). However, a challenge in the assessment of biochars for P recycling is to make useful comparisons with existing materials. Methods for characterising biochar have often been based on existing soil science methods, perhaps since biochar is intended for addition to soil. Due to several features of biochar, such as its hydrophobicity and the recalcitrance of the carbon structure to chemical and biological breakdown, these methods may not provide the intended information. The relative infancy of the topic means that new assessment methods are under development and there is much scope for their testing and improvement to better predict the potential of biochar for P recycling.

The overall aim of our research is to design and test novel materials for capture of P from wastewater that are environmentally sustainable and economically viable. It is desirable that the P captured can be subsequently recycled P to the soil as a fertiliser, rather than becoming a waste product of the process. Our objective in the present study was to develop a robust methodological framework to compare biochar P filters made using materials already generated in wastewater treatment to other established materials for P filtration, namely ochre, activated carbon and zeolite. Anaerobically digested (AD) sewage sludge was selected to act as an alternative to cement as a binder for ochre to produce a combined feedstock (OCAD) for pyrolysis. In addition to providing additional nutrients to the ochre, it was hypothesised that the AD component in OCAD feedstock would also exhibit P recovery characteristics. Both AD and OCAD biochar feedstocks were therefore assessed to determine whether P recovery in the composite OCAD biochar materials would be due to each component or ochre alone. To test and rank the diverse materials considered in our work, the design of novel batch recovery experiments that considered the distinctive chemistry of biochar was required. Specifically, methods for buffering solution pH were investigated due to the high variability of P capture with changing pH. We allowed for P release as well as recovery, so that our results would be relevant to both P recovery from wastewater and its subsequent release into soil. We also tested for inherent nutrients and PTEs in the materials and compared these against current biochar contaminant guidelines to assess whether the use of these biochars posed any risk to the environment.

2.2 Materials and Methods

2.2.1 Material selection and processing

The ochre used in this study was selected for characteristics representative of coal mine water treatment ochre, with typically low concentrations of PTEs but low hydraulic conductivity. Ochre was collected from the Coal Authority Minto mine water treatment scheme in Fife, Scotland. Anaerobically digested sewage sludge (AD) was collected from the Newbridge WWTP, Edinburgh, Scotland. The AD feedstock (20% dry solids) was prepared by first making a slurry from the untreated digestate cake and deionised (DI) water, followed by shaking on an orbital platform shaker at 150 rpm overnight, and then drying and sterilising by heating in an oven at 80°C for 12 h, 180°C for 2.5 h and finally 80°C for a further 48 h. A mixed AD and ochre feedstock (OCAD) was produced by making a slurry from the untreated digestate cake with the addition of air-dried ochre (1:1 ratio, dry weight basis) in DI water, shaking to homogenise the sewage solids and ochre, followed by drying and sterilising as above. In order to compare the results of these experiments with experiments in the future, a commonly available activated carbon produced from peat was sourced from Sigma Aldrich (St Louis, Missouri, USA) to run as a standard. It was selected based on its easy acquisition and the fact that it is structurally and chemically similar to biochar. A natural zeolite from RS Minerals (Guisborough, UK) was also selected for comparison in these experiments as zeolites, although cation exchangers like biochar, have also shown P filtration properties (Agrawal et al., 2011; Sakadevan et al., 1998).

Pyrolysis was undertaken at the UK Biochar Research Centre (University of Edinburgh, UK) using the small-scale batch pyrolysis unit described in Crombie et al. (2013). The surface chemistry of biochar is expected to be of primary importance to its phosphate binding capacity. Electron donor groups are unlikely to interact directly with phosphate, so adsorption and retention will likely take place via a metal-mediated mechanism. The highest treatment temperature (HTT) is one of the most important pyrolysis parameters for controlling chemical and physical properties of the resulting biochar. Structural complexity, in both chemical and macro-physical terms, decreases with increasing HTT (Brown et al., 2006; Downie et al., 2009; Lua et al., 2004), therefore two relatively low HTTs were selected to increase the number of potential reactive sites in the biochar.

Samples of both feedstock types were heated at a rate of 25°C min^{-1} to a HTT of 450°C or 550°C, held for 30 min. The resulting biochars (AD450, AD550, OCAD450 and OCAD550) were each left in the reactor with N_2 flow overnight to cool before being transferred into a N_2-purged container. OCAD biochars were cooled to 4°C before air was allowed to slowly diffuse into the container to prevent spontaneous combustion due to rapid re-oxidation of reduced elements within the material.

2.2.2 Characterisation of materials

2.2.2.1 Nutrients and potentially toxic elements (PTEs)

The materials were digested and analysed by ICP-OES to determine the concentrations of nutrients (Ca, K, Mg, Mn, P, S) and PTEs (Al, As, B, Cd, Co, Cr, Cu, Fe, Mo, Na, Ni, Pb, Zn). All materials (biochars and biochar feedstocks) and blanks were prepared in triplicate for analysis using the method described by Buss et al. (2016a), which is based on the modified dry ashing procedure proposed by Enders and Lehmann (2012) and prescribed by IBI (2012). The purpose of the modifications was to improve element detection by decreasing the dilution of samples during the digestion process. Due to the high concentration of Fe in the biochars and ochre prepared for this study HCl was used instead of H_2O_2.

Elemental quantification was performed on digests by ICP-OES, using a Perkin Elmer Optima 5300DV instrument (Waltham, USA). The majority of elements were analysed in axial mode, with the exception of Al, Ca, Fe, K, Mg and Na, which were present in sufficient concentrations to necessitate the use of radial mode. Standards were prepared and run during each analysis session for calibration and to check the accuracy of measurements. The limit of detection of the instrument was determined as described in Buss et al. (2016a).

2.2.2.2 pH and electrical conductivity (EC)

The pH and EC of the materials were determined in DI water in duplicate using the method recommended by the IBI (Rajkovich et al., 2012).

2.2.3 Testing of buffers

To determine whether buffer addition affected P sorption, a batch experiment was carried out using AD550 and a 0.02 g P l^{-1} solution (from K_2HPO_4) with either 5 mM or 10 mM 3-(*N*-

morpholino)propanesulfonic acid (MOPS), following the procedure described in section 2.3. All supernatants were refrigerated at 4°C before analysis for soluble reactive P (SRP) by automated colorimetry (Molybdenum blue method, Auto Analyser III, Bran & Luebbe, Norderstedt, Germany). Each adsorption experiment was performed with four replicates and results reported as means ± 1 S.D. All experiments were conducted at room temperature (21°C) concentrations were measured as described above. One-way ANOVA and Tukey HSD tests were completed using RStudio and used to identify statistical differences ($p<0.05$) between the total P adsorbed by the materials and no statistically significant difference was found between the treatments.

2.2.4 Batch adsorption experiments

As is standard for the investigation of material adsorption properties, a laboratory batch adsorption experiment was conducted and both the Langmuir and Freundlich isotherms fitted to the results.

The Langmuir equation describes single-layer adsorption and can be expressed as:

$$S = \frac{S_{max}KC}{1 + KC}$$

Where S is the concentration of solute adsorbed by the material (mg g^{-1}), S_{max} is the calculated maximum adsorption capacity of the material (mg g^{-1}), K is the Langmuir coefficient, which refers to binding strength (higher K indicates stronger binding) and C is the concentration of the solute remaining in solution at equilibrium (mg l^{-1}).

The Freundlich equation allows for multi-layer adsorption and can be expressed as:

$$S = K_f C^n$$

Where S and C are the same as for the Langmuir equation, K_f is the Freundlich coefficient which indicates relative adsorption capacity (but not specifically a maximum adsorption capacity), and n is the Freundlich exponent which is a constant describing heterogeneity of the material (Cucarella and Renman, 2006). The reciprocal of the Freundlich exponent is also used in the literature to describe the adsorption affinity, with higher values indicating higher affinity (Castaldi et al., 2014; Holford, 1982). Therefore a lower n value also indicates a higher affinity for the solute.

While the pH in P batch adsorption experiments is usually adjusted manually to 7 using acid or base at the beginning of the experiment, it is typical for phosphate adsorption isotherms to be determined for biochar without the use of buffering or even without any pH adjustment at the start of the experiment (Chen et al., 2011; Liu et al., 2015; Park et al., 2015; Ren et al., 2015; Yao et al., 2012, 2011; Zhang and Zhang, 2013; Zhang et al., 2013), even though P adsorption is generally highly dependent on pH (Antelo et al., 2005; Kanematsu et al., 2011; Kumar et al., 2010). The pH of biochar measured using a DI water–biochar mixture is typically between 6 and 11. When added to soil, biochar tends to have a liming effect, raising soil pH over a period of time (Beesley et al., 2011; Biederman and Harpole, 2013). This is, however, dependent on the initial soil pH and associated buffering capacity as well as the biochar type. Hence, if relevant comparisons are to be made between biochars and with other materials, the pH of batch experiments should be controlled for the duration of the experiment. The effect of materials in different soils can then be inferred separately, using information on specific soil properties. Although most buffers may interfere with reaction conditions, some (known as 'Better Buffers') have been developed for use in biological systems where buffer interactions with cations are undesirable (Kandegedara and Rorabacher, 1999; Yu et al., 1997). They are a set of tertiary amines with nitrogen substituents which are at least 2 carbon atoms in length, meaning they lack donor atoms on the α, β and γ carbons with which a metal cation could react to form a closed ring structure with the nitrogen atom (Yu et al., 1997). Within this group of compounds, MES (2-(N-morpholino)ethanesulfonic acid) and MOPS (3-(*N*-morpholino)propanesulfonic acid) have been found to have no effect on P adsorption (Mao et al., 2012). MOPS was tested in our experimental system at increasing concentrations (see 3.2.4) and as in the literature, no interference was observed. Therefore phosphate solutions of concentrations ranging from 0–800 mg P l^{-1} were prepared for the batch experiments using DI water buffered to pH 7 with 10 mM MOPS/$NaNO_3$ and K_2HPO_4.

The median particle size of the Minto ochre is 0.02-0.06 mm (Heal et al., 2003), which is smaller than that of the other materials tested, however it does form natural aggregates. Therefore it was prepared by breaking up the aggregates in a pestle and mortar and removing manually any visible organic matter. Rather than matching the primary particle size of ochre for all materials, the biochar (AD450, AD550, OCAD450, OCAD550), activated carbon and zeolite samples were passed through a sieve to obtain a 0.5–1.0 mm size fraction, since crushing of the OCAD materials may have separated the ochre and AD components spatially and prevented direct interaction between fractions relevant to P adsorption. Due to the highly hygroscopic nature of the biochars, their moisture content at room temperature was determined by weighing, drying at 105°C overnight and re-weighing a subsample of each material immediately after cooling in a desiccator. The calculated water content was accounted for in subsequent calculations. Aliquots of MOPS buffered P solution (36 ml, prepared as outlined above) were added to 0.100 g of each material in 50 ml centrifuge tubes. The tubes were laid on their side and shaken on an orbital platform shaker at 150 rpm for 24 h. The samples were centrifuged at 3500 rpm for 30 min and the supernatant filtered using 0.45 µm syringe filters (Millipore, Watford, UK). All filtrates were refrigerated at 4°C before analysis for soluble reactive P (SRP) by automated colorimetry (Auto Analyser III, Bran & Luebbe, Norderstedt, Germany). Each adsorption experiment was performed with four replicates and a set of blank samples, with results reported as means of the blanks subtracted from the means of the treatment results ± 1 S.D. All experiments were conducted at room temperature (21°C).

2.2.5 Repeat exposure experiments

To rank the materials, an experiment was designed to provide repeated exposure to P at three different concentrations. The lowest P concentration used in the experiment described in section 2.3 (0.02 g P l^{-1}) was selected to simulate the typical maximum P concentration of tertiary wastewater effluent. Higher concentrations (0.8 and 3 g P l^{-1}) were selected to probe the maximum P recovery rate. The experiments were designed with repeated removal and replenishment of the P solution, rather than a flow-through column system (which would more accurately simulate a wastewater treatment system), as the objective was to design a simple screening method that could be adopted using readily available equipment.

After the addition of the appropriate MOPS-buffered P solution in a 1:20 solid to liquid ratio (m/v) in 50 ml centrifuge tubes, the samples were laid on their side and shaken on an orbital platform shaker at 150 rpm for 20 h, stood for 4 h and then centrifuged at 3500 rpm for 30 min, filtered and analysed for P as described in 2.2.3. A fresh P solution was added in the same solid to liquid ratio and the process repeated until the samples had been exposed for 5 days. P recovery was determined by calculating the difference in SRP concentration in the blank control samples and each treatment collected after 24 h for each of the 5 days. Data were analysed using the Shapiro-Wilk test for normality, followed by one-way ANOVA and Tukey HSD tests using RStudio (R Core Team, 2015) to identify any significant differences ($p<0.05$) between the cumulative P captured by the materials over the 5-day experiment. Where the data were not normally distributed, the Wilcoxon rank sum test was used instead to identify any significant differences.

2.2.6 Phosphorus release from P-enriched materials

To probe the potential for recovered P to be released from the materials, an extraction experiment analogous to the repeat exposure experiment was designed, where the P solutions were substituted by DI water buffered at pH 7. There are more than ten standard soil-P bioavailability test methods in use but no clear ‘best method’, reflecting the large number of variables which influence the plant availability of P in different soils (Jordan-Meille et al., 2012). Biochar has strongly contrasting properties to soil and no specific methods have so far emerged. Some guidelines (IBI, 2012) recommend 2% formic acid extraction as described in Wang et al., (2012) but this method has limited validation to date. In our study buffered DI water was chosen to simulate soil pore water, which is buffered to varying extents in the soil system, based on the finding that most native P in biochar is water extractable (Angst and Sohi, 2013). Therefore, the P extracted represents the plant available P that might become immediately available in soil at pH 7. The P-enriched materials from each treatment were oven-dried at 35°C for 3 days. Using pH 7 MOPS-buffered DI water, the samples were extracted over 4 days, following the method described in 2.4, with SRP concentrations measured every 24 h.

2.3 Results and Discussion

2.3.1 Biochar production and analysis

2.3.1.1 Feedstock processing

The OCAD feedstock was prepared by combining AD sewage sludge with Minto ochre in a 1:1 ratio (dry weight basis) therefore it was expected that the elemental concentrations measured in the resulting OCAD biochar would approximate to the mean of the sum of the concentrations of the two materials, expressed in g kg^{-1}. ICP-OES analyses of digests of the OCAD feedstock revealed that, with the exception of S, which was enriched by 51%, and Cu, which was 28% lower, all elements measured were present at expected concentrations. Although it is difficult to explain the exceptions with certainty and it should be noted that the mass amounts are small, it is probable that Cu was lost during the altered modified dry-ashing protocol and S enrichment owed to sample contamination during the same process or during pyrolysis.

2.3.1.2 Assessment of potential toxic effects of the novel biochar materials

Evaluation of the chemical composition of the novel biochar materials against the International Biochar Initiative (IBI) Certification (IBI, 2012) and the European Biochar Certificate (EBC) guidelines (EBC, 2012) provides an indication of the potential for re-use of the filter materials as P (and other nutrient) fertiliser in soils within existing environmental regulations. Although these certification systems are not officially recognised by environmental regulators, they have been developed (primarily by academics) to assist in the development of suitable frameworks. PTE concentrations measured in all the biochars are reported in Table 2.1.

Of the elements listed by the IBI guidelines (IBI, 2012), no thresholds values were breached by any of the biochars for As, Hg, Co, Cr, Cu, Ni, Pb, and Se. Of the EBC guidelines (EBC, 2012), none of the premium biochar thresholds were exceeded for Cu, Cr, Hg, Ni or Pb. With respect to PTE concentrations, both OCAD450 and OCAD550 were below thresholds in the IBI guidelines and EBC premium grade specification, but close to exceeding Zn thresholds. Notably, the AD feedstock itself contains 461 ± 16.5 mg Zn kg^{-1}, so blending with ochre before pyrolysis reduced the final concentration in OCAD450 and OCAD550 below threshold values.

Table 2.1 Mean PTE concentrations (n=3) of the materials as determined by ICP-OES of sample digests expressed in mg kg^{-1} ± standard deviation (dry weight basis). Values expressed as "< x" were below the limit of detection of the method (x).

	AD	Ochre	OCAD	AD450	OCAD450	AD550	OCAD550	ZEO	AC
Al	$29.8\times10^3 \pm 913$	$2.09\times10^3 \pm 227$	$15.8\times10^3 \pm 131$	$38.1\times10^3 \pm 2.20\times10^3$	$20.1\times10^3 \pm 3.59\times10^3$	$62.7\times10^3 \pm 1.29\times10^3$	$24.9\times10^3 \pm 689$	$19.6\times10^3 \pm 357$	649 ± 16
As	< 0.72	< 0.72	< 0.72	1.42 ± 2.01	< 0.72	< 0.72	< 0.72	44.0 ± 5.1	< 0.72
B	16.7 ± 1.7	43.8 ± 6.1	28.3 ± 0.7	13.4 ± 1.5	45.1 ± 1.5	22.7 ± 0.569	46.8 ± 2.9	4.58 ± 1.63	< 0.36
Cd	0.249 ± 0.033	< 0.04	< 0.04	3.34± 0.40	< 0.04	0.542 ± 0.042	< 0.04	0.591 ± 0.111	0.310 ± 0.202
Co	4.90 ± 0.16	9.65 ± 0.06	7.56 ± 0.17	6.57 ± 0.53	11.7 ± 0.5	8.22 ± 0.20	11.2 ± 0.7	0.47 ± 0.04	0.25 ± 0.01
Cr	10.5 ± 0.5	< 0.49	< 0.49	15.3 ± 1.3	< 0.49	21.8 ± 0.80	< 0.49	< 0.49	5.76 ± 0.17
Cu	41.7± 4.1	< 0.06	15.1 ± 0.6	93.1 ± 3.8	23.5 ± 1.1	72.8 ± 1.6	33.8 ± 3.2	0.694 ± 0.097	7.36 ± 0.50
Fe	$72.8\times10^3 \pm 1.37\times10^3$	$520\times10^3 \pm 7.44\times10^3$	$352\times10^3 \pm 14.1\times10^3$	$44.6\times10^3 \pm 3.85\times10^3$	$406\times10^3 \pm 86.0\times10^3$	$101\times10^3 \pm 2.29\times10^3$	$451\times10^3 \pm 20.7\times10^3$	$8.01\times10^3 \pm 172$	$1.31\times10^3 \pm 64.1$
Mo	2.12 ± 0.23	< 0.21	< 0.21	7.62 ± 1.44	< 0.21	5.56 ± 0.15	< 0.21	< 0.21	< 0.21
Na	$1.37\times10^3 \pm 37$	186 ± 30	863 ± 34	$1.65\times10^3 \pm 48$	$1.01\times10^3 \pm 36.0$	$1.96\times10^3 \pm 118$	999 ± 56	$1.26\times10^3 \pm 102$	406 ± 16
Ni	11.1 ± 0.4	5.90 ± 0.08	9.53 ± 0.43	22.3 ± 2.4	15.9 ± 0.7	23.4 ± 0.7	15.7 ± 0.7	< 0.09	0.465 ± 0.064
Pb	15.2 ± 0.8	10.1 ± 0.8	14.8 ± 3.8	34.9 ± 2.7	22.8 ± 4.1	36.4 ± 0.8	20.4 ± 2.2	17.0 ± 2.7	59.5 ± 10.5
Zn	461 ± 17	60.6 ± 1.0	270 ± 4	518 ± 41	397 ± 25	900 ± 13	400 ± 12	9.88± 1.02	< 0.47

Concentrations of PTEs in AD450 biochar exceeded the following threshold values (threshold values given in parentheses): Cd (IBI 1.4-39 mg kg^{-1} and EBC basic grade 1.5 mg kg^{-1}), Mo (IBI 5–75 mg kg^{-1}) and Zn (IBI 416–7400 mg kg^{-1} and EBC basic grade 400 mg kg^{-1}). AD550 moderately exceeds the IBI threshold for Mo at 5.56 ± 0.14 mg kg^{-1} and exceeds both the IBI and EBC basic grade threshold for Zn at 900 ± 12.9 mg kg^{-1}.

2.3.2 Fertiliser value

Fertiliser value and relevant characteristics of the novel materials (Table 2.2) were determined to assess their potential for use in agriculture. All the biochars had a pH close to neutral (7.3–7.9), which is lower than typical for biochar, but expected due to their high ash content as indicated by high yields and metal concentrations in Tables 2.1 and 2.2. Application of these biochars to acidic soil may still result in a liming effect but, more importantly, application is not likely to have negative effects on pH of soil at ideal pH values for optimum fertility (~7).

The concentration of P in each of the biochar materials before retention of additional P is high in the context of the dose required to match fertiliser applications. Assuming all biochar P is plant accessible in the first season after application, 0.4–1.1 t ha^{-1} of non-P-enriched material would satisfy UK recommendations for barley grown on P-depleted soil (110 kg P_2O_5 ha^{-1}, equivalent to 48 kg P ha^{-1}) (DEFRA, 2010). Production of biochar from sewage sludge should also be economically feasible due to the low cost of sewage sludge as a feedstock (Shackley et al., 2011).

Nutrient retention during pyrolysis is desirable as it preserves the fertiliser value of the final biochar materials. Compared to their feedstocks, AD550, OCAD450 and OCAD550 each were enriched in Ca, K, Mg, Mn, P and S, maintaining the fertiliser value of the materials. This enrichment is expected as none of these elements are extremely volatile at the pyrolysis temperatures used (although small amounts of Ca and Mg can be lost), thus as C and other volatile elements are lost the relative concentration of other nutrients increases.

Table 2.2 Characteristics of the biochar feedstock, biochar and comparison materials. Nutrient values were determined by ICP-OES of samples and the mean values (n=3) ± standard deviation are given (dry weight basis).

	AD	Ochre	OCAD	AD450	OCAD450	AD550	OCAD550	ZEO	AC
Yield %	-	-	-	52.6	67.3	50.5	65.1	-	-
pH (n = 2)	-	7.9 ± 0.0	-	7.3 ± 0.0	7.6 ± 0	7.9 ± 0.0	7.7 ± 0.1	8.1 ± 0.2	10.3 ± 0.0
EC (µS cm^{-1}) (n = 2)	-	518 ± 20	-	596 ± 62	692 ± 28	375 ± 0	738 ± 200	223 ± 9	424 ± 52
Nutrients (g kg^{-1})									
Ca	38.4 ± 1.1	18.8 ± 0.44	28.9 ± 0.63	28.7 ± 2.8	32.4 ± 8.3	70.0 ± 1.6	39.7 ± 1.6	16.6 ± 0.2	34.3 ± 0.3
K	2.12 ± 0.08	0.349 ± 0.048	1.35 ± 0.02	2.75 ± 0.07	3.05 ± 1.94	3.42 ± 0.09	1.84 ± 0.05	12.8 ± 0.2	2.29 ± 0.02
Mg	7.39 ± 0.19	3.03 ± 0.059	5.02 ± 0.12	6.03 ± 0.50	5.97 ± 1.15	12.8 ± 0.3	7.06 ± 0.24	2.72 ± 0.13	2.72 ± 0.01
Mn	0.286 ± 0.013	0.891 ± 0.005	0.615 ± 0.015	0.493 ± 0.046	1.03 ± 0.05	0.565 ± 0.008	0.961 ± 0.052	0.120 ± 0.017	0.528 ± 0.005
P	71.2 ± 2.6	1.92 ± 0.13	36.6 ± 0.6	46.9 ± 3.1	44.9 ± 1.7	126 ± 4	49.8 ± 1.6	0.301 ± 0.090	24.5 ± 0.3
S	8.83 ± 0.24	3.32 ± 0.12	9.18 ± 0.22	8.25 ± 0.53	12.2 ± 0.2	15.6 ± 0.3	12.3 ± 0.2	0.207 ± 0.020	2.78 ± 0.00

2.3.3 Phosphorus recovery

2.3.3.1 Batch adsorption experiments

The calculated parameters for the best fits of the Langmuir and Freundlich isotherms are shown in Table 2.3. The lowest fits of the Langmuir isotherm were found for ochre (R^2 = 0.400), zeolite (R^2 = 0.269), activated carbon (R^2 = 0.458) and OCAD550 (R^2 = 0.848). In general, good fits were not obtained for any of the materials, indicating that single-layer absorption does not describe the dominant adsorption kinetics in these systems For the AD and OCAD biochars adsorption capacity (S_{max}) increased with pyrolysis temperature, but binding strength decreased, suggesting that the additional P may be more easily re-dissolved.

The Langmuir isotherm plot (Figure 2.1.1) has been extended to compare the theoretical P adsorption at the highest concentration tested in the repeat uptake experiments. Visual inspection of the plot indicates that the 550°C biochars should retain more P than the 450°C biochars at higher concentrations of P. It also shows the rapid reaction of ochre with P compared to the other materials. The calculated isotherms and raw data are plotted for each of the materials in Figure 2.1.2.

In general, the Freundlich isotherm did not provide good fits for the materials, with the exception of AD550, OCAD450 and OCAD550 (R^2>0.93) (Table 2.3 and Figure 2.1.3). The K_f for AD450 was more than 5 times that for AD550, and the K_f for OCAD450 was more than 2 times greater than that of OCAD550, suggesting that the lower temperature biochars should have higher adsorption capacities, in contrast to those estimated from the Langmuir isotherm. The K_f of ochre was 10 times higher than for the next highest material (OCAD450) which, again, was not replicated in the Langmuir results. The smaller particle size of the ochre compared to the other materials results in a higher surface area available to react with P. Activated carbon and zeolite both had a K_f in the range of the biochar materials. Sorption affinity ($1/n$) was in the order: ochre > OCAD450 > AD450 > activated carbon > OCAD550 > AD550 > zeolite.

Examining these results in the context of the proposed use of the materials, whilst ochre may be an excellent P filter, it may not readily release the P into soils. However this may not mean that the P is inaccessible to plants, as P-enriched ochre has been shown to be as effective as conventional phosphate treatment in a plant pot trial (Dobbie et al., 2005). This

Table 2.3 Best-fit Langmuir and Freundlich parameters determined for the materials.

	Langmuir parameters			**Freundlich parameters**		
	Smax (mg g^{-1})	*K*	R^2	K_f	*n*	R^2
AD450	6.68	0.01	0.92	0.44	0.41	0.85
AD550	8.25	0.00	0.94	0.08	0.64	0.97
OCAD450	6.70	0.01	0.94	0.50	0.40	0.97
OCAD550	7.33	0.00	0.85	0.20	0.52	0.93
Ochre	7.59	7.30	0.40	5.71	0.07	0.31
Zeolite	0.30	0.03	0.27	0.03	0.89	0.22
Activated carbon	3.11	5.40×10^{-3}	0.46	0.14	0.45	0.67

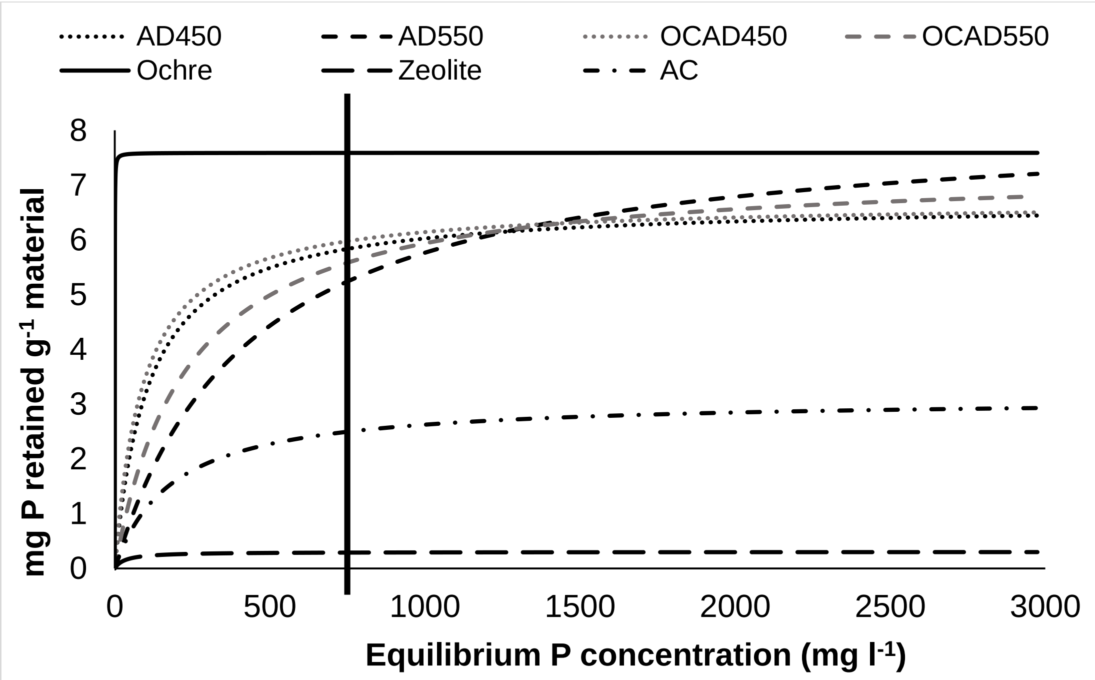

Figure 2.1.1 Langmuir isotherms plotted for all materials. The vertical line on the x axis shows the highest treatment concentration in the batch adsorption experiments (0.8 g P l^{-1}). The isotherms have been extended to the highest treatment concentration in the repeat uptake experiments (3 g P l^{-1}) to show the predicted adsorption capacity at these concentrations.

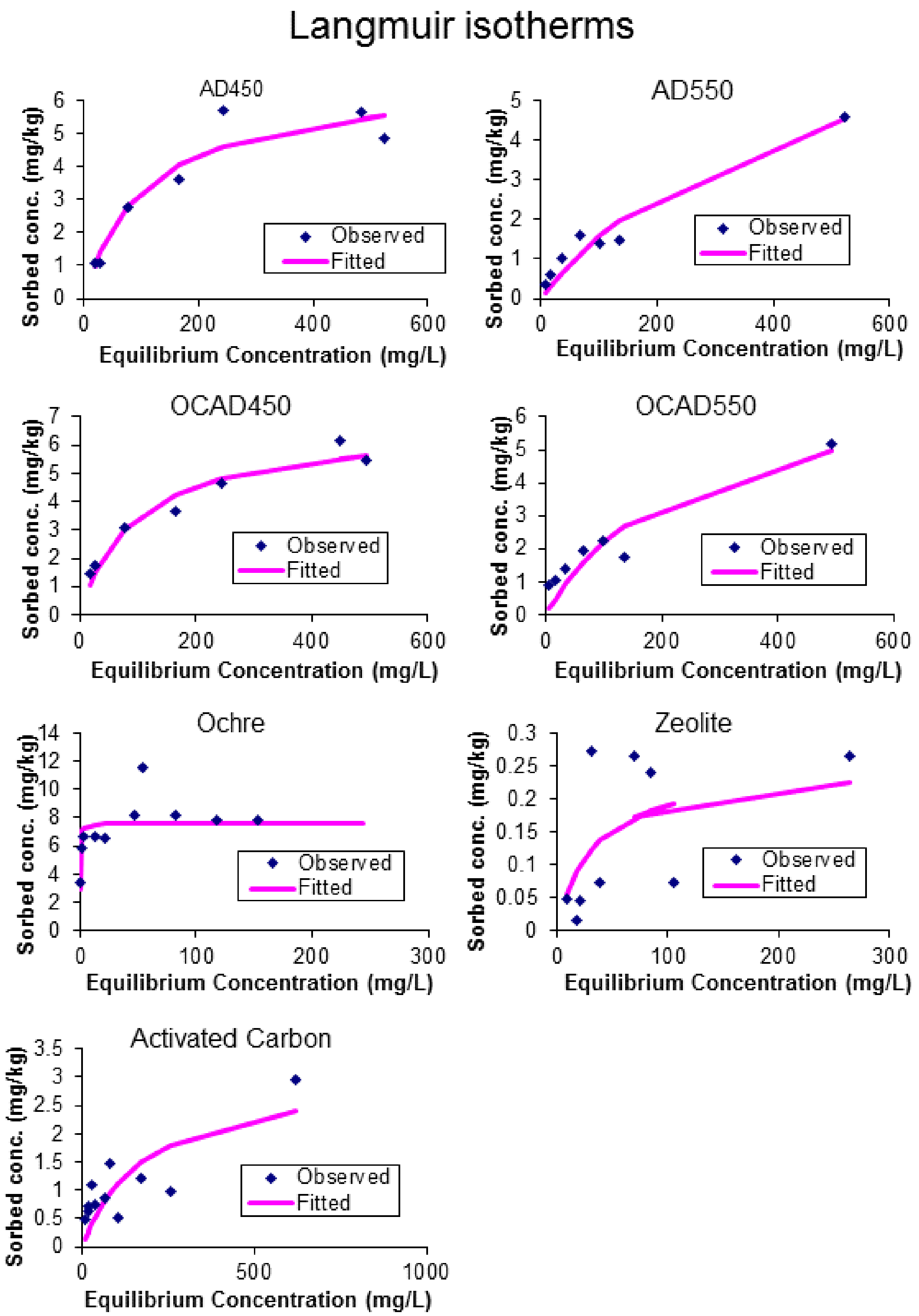

Figure 2. 1.2 Langmuir isotherms and raw data plots for each of the 7 materials.

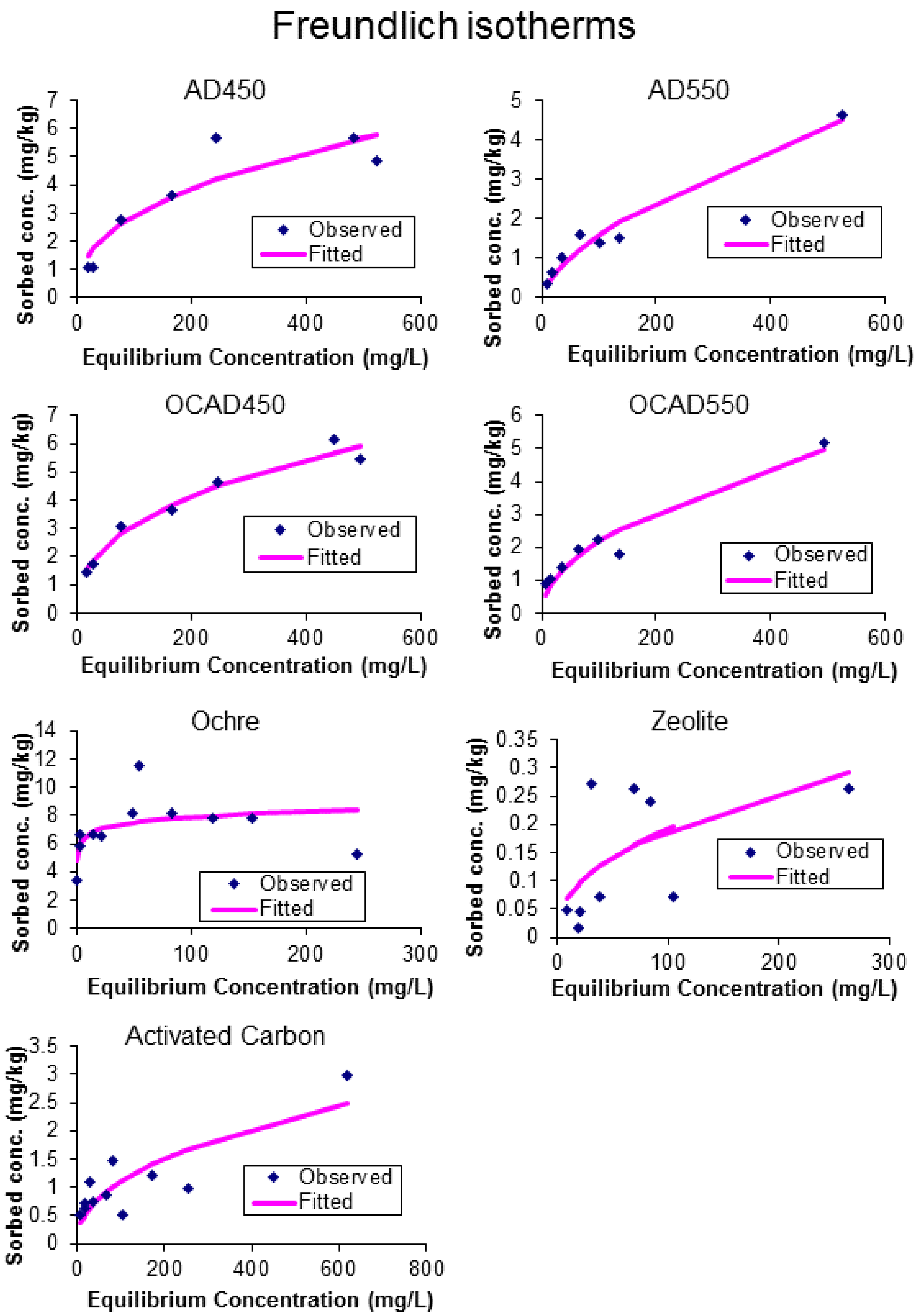

Figure 2.1.3 Freundlich isotherms and raw data plots for each of the 7 materials.

finding is important as the experiments reported here were all buffered at pH 7.0, at which phosphate is at its most soluble. Overall, the biochar materials and activated carbon also demonstrate promising retention properties for recycling P. The more similar results observed for the biochars and activated carbon are likely due to their similar carbon structure. The higher concentration of metals in the biochars with which P can interact compared to the activated carbon explains their superior retention properties. Using these testing methods, the zeolite analysed is not suitable for P capture from wastewater and subsequent release to soil.

2.3.3.2 Assessment of P recovery characteristics of the novel biochar materials

After 5 days repeated exposure to 0.02 g P l^{-1} solutions, ochre removed the highest amount of P, closely followed by OCAD550 and OCAD450 (Figure 2.1.4). As expected, P removal rates of the OCAD biochars were in between those of ochre and the AD biochars, and the values were closer to AD biochars than ochre. Significant differences ($p < 0.01$) between all materials were found in the 0.02 g P l^{-1} experiment except OCAD550 and OCAD450 (For the 0.02 g P l^{-1} treatment, ochre was found to retain the most recovered P, both in concentration and percentage of recovered P (Figure 2.1.4, Table 2.5). It also released the smallest amount of P after 4 days of buffered DI water extraction. As expected, both the OCAD450 and OCAD550 biochars had similar behaviours to ochre, retaining more P and therefore having a higher concentration of remaining P than the non-ochre containing materials. No difference was observed between pyrolysis temperatures for the OCAD biochars in the release of adsorbed P.). It appears that the co-pyrolysis of ochre with AD sewage sludge may reduce the removal capacity of the ochre component (on a w/w basis) of the biochar produced, although the differences in particle size between the treatments may also contribute to the observed differences. All of the biochars removed more P than activated carbon and zeolite. There was no significant effect of pyrolysis temperature for the OCAD biochars, but AD450 removed significantly more P than AD550 ($p < 0.001$). As AD550 contains a higher concentration of metals which are expected to interact with P than AD450 (Ca: 2.4 times higher, Mg: 2.1, Al: 1.6 and Fe: 2.3) it was expected to remove more P, however this is not the case. It is possible that the difference in pH (AD450: 7.3 vs AD550: 7.9) may have been the cause of the small but significant difference in P retention due to increased electrostatic repulsion of negatively charged phosphate (PO_4^{3-}) by more negatively-charged surfaces of AD550 compared to AD450.

Higher P solution concentrations were included to probe the actual recovery capacities of the materials without a prolonged experiment. Rather than providing definitive capacity results, however, these experiments highlighted the importance of solution concentration on recovery kinetics. Whilst higher P recovery was measured for each material in the 0.8 and 3 g P l^{-1} experiments as expected, the relative ranking of the materials was different. Most notable was the higher P recovery by zeolite, which ranked lowest in the 0.02 g P l^{-1} experiment but second highest in the 0.8 g P l^{-1} experiment. With the exception of AD450, the other biochar materials were ranked in decreasing order of P-interacting metal concentration (OCAD >AD, 550 >450), as would be expected. Statistically however, the materials did not perform differently. For the 3 g P l^{-1} experiment, AD450 recovered more P than activated carbon and ochre ($p < 0.05$), but no other significant differences were found between materials, noting that 550°C biochars were not included in this experiment.

The P recovery observed in both the 0.8 g P l^{-1} and 3 g P l^{-1} experiments exceeded the S_{max} values calculated by the Langmuir isotherm. The fits of the Langmuir isotherms were generally poor, and so the calculated adsorption capacity values do not reflect actual recovery capacities of these materials. Hence, as discussed by Cucarella and Renman (2009) and Barrow (2015) with reference to other materials, despite being widely used, batch adsorption experiments may not be an appropriate method for estimating P recovery capacity for biochar materials. The repeated exposure experiments show the capacity for biochar materials to continuously take up P from solution as the biochar becomes less hydrophobic and, as a result, more of the reactive sites come into contact with the P solution. The adsorption of P into soil (Barrow, 2015) and ochre (Sibrell et al., 2009) particles has been shown to occur in two stages: initial adsorption onto surfaces, followed by passive diffusion of P into the particle along a concentration gradient until the particle is saturated. The energy required for the forwards reaction (sorption, or capture) is similar to that of the backwards reaction (release) (Barrow, 1979) so a higher concentration of P in solution increases the concentration gradient, allowing for P to be taken up into the particle at a faster rate. This lends support to use of a method involving repeated exposure to a constant concentration of P which is relevant for the intended use of the material, in order to observe the relevant kinetics of the system. In a flow-through filtration system, rate of recovery under the relevant conditions is just as important as total capacity for P uptake.

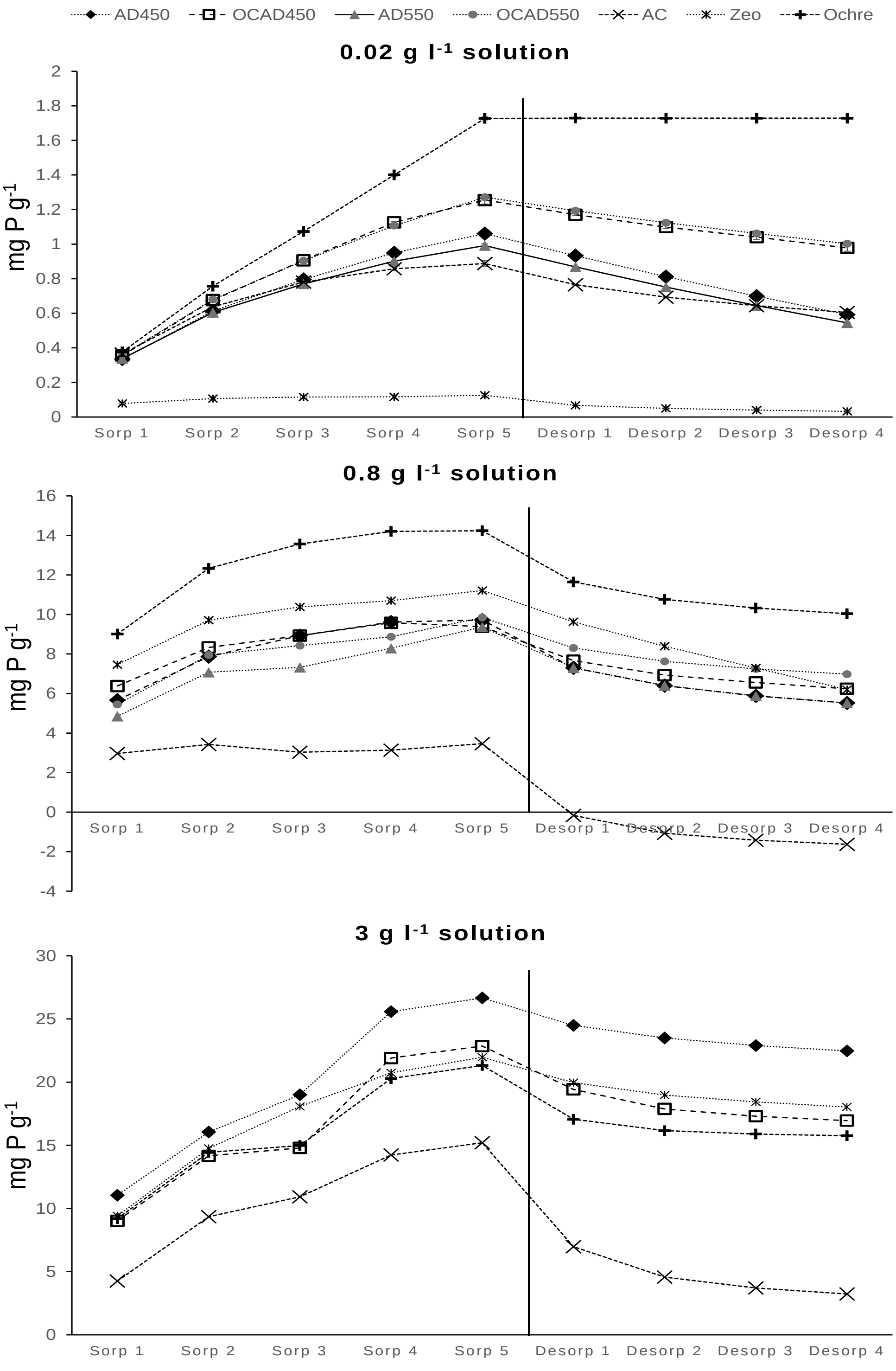

Figure 2.1.4 Sorption and desorption of P from the materials in experiments with solutions of (a) 0.02 g P l^{-1}, (b) 0.8 g P l^{-1} and (c) 3 g P l^{-1}. Values are cumulative and are the mean of 4 replicates. Error bars are shown for the 0.02 g P l^{-1} experiment (± 1 standard deviation from the mean) but most are not visible due to small deviations between the replicates. Error bars are not shown for the 0.8 or 3 g P l^{-1} experiments to allow trends to be clear. Negative values for desorption of P for activated carbon (AC) in the 0.8 g P l^{-1} experiment show release of native P rather than enriched P, as the values have been calculated relative to total sorption.

2.3.4 P release from enriched materials

Whilst strong interactions with P are important characteristics of materials for P extraction from wastewater, they may not be optimal for fertiliser re-use. Previous studies of native P release from different biochars have shown continuous release over repeated extractions and throughout a greenhouse experiment (Angst and Sohi, 2013; Wang et al., 2014), suggesting that P interactions within biochar lattices were not so strong as to prevent P release entirely. This also indicates high-P biochars should be suitable P fertiliser alternatives. To estimate the accessibility of P recovered by biochar to plants from soil pore water, repeated water extractions at each of the three experimental P enrichment concentrations were conducted.

Table 2.4 Total P capture of the materials after 5 days exposure to solutions of different P concentrations. Materials are grouped according to statistical differences (ANOVA and Tukey HSD tests, as indicated by the letters a–l) and ranked in descending order of P sorption. Values for sorption reported are the mean of 4 replicates with propagated standard error.

P solution	**Ranking**		**P sorption (mg P g^{-1})**
0.02 g l^{-1}	a	Ochre	1.73 (± 0.01)
	b	OCAD550	1.26 (± 0.01)
	b	OCAD450	1.24 (± 0.02)
	c	AD450	1.06 (± 0.00)
	d	AD550	0.99 (± 0.01)
	e	Activated carbon	0.88 (± 0.02)
	f	Zeolite	0.13 (± 0.01)
0.8 g l^{-1}	g	Ochre	14.20 (± 1.77)
	h	Zeolite	11.20 (± 1.46)
	h,i	OCAD550	9.82 (± 2.01)
	h,i	AD450	9.72 (± 0.66)
	i	OCAD450	9.37 (± 0.87)
	i	AD550	9.35 (± 2.21)
	j	Activated carbon	3.47 (± 1.52)
3 g l^{-1}	k	AD450	25.9 (± 5.1)
	k,l	Zeolite	21.5 (± 5.0)
	k.l	OCAD450	20.4 (± 6.4)
	l	Ochre	20.0 (± 5.7)
	l	Activated carbon	15.1 (± 4.4)

For the 0.02 g P l^{-1} treatment, ochre was found to retain the most recovered P, both in concentration and percentage of recovered P (Figure 2.1.4, Table 2.5). It also released the smallest amount of P after 4 days of buffered DI water extraction. As expected, both the OCAD450 and OCAD550 biochars had similar behaviours to ochre, retaining more P and therefore having a higher concentration of remaining P than the non-ochre containing materials. No difference was observed between pyrolysis temperatures for the OCAD biochars in the release of adsorbed P.

Table 2.5 Percentage of P extracted from the P-enriched samples in pH 7 buffered deionised water after 24 h, repeated for four days. The concentration of material P enrichment (in mg P g^{-1}) is shown for reference. The percentage of enriched P remaining after the four extractions is also given. AD550 and OCAD550 were not included in the 3 g l^{-1} P experiment as they became available after the initial experiment was run. All values are the mean of four replicates with propagated standard error shown.

			% enriched P extracted after 24 h treatment				
Treatment		**P enrichment (mg P g^{-1})**	**Day 1**	**Day 2**	**Day 3**	**Day 4**	**% enriched P remaining**
AD450	0.02 g l^{-1}	**1.06** ± 0.00	**12.1** ± 0.3	**11.4** ± 0.5	**10.7** ± 0.6	**10.1** ± 0.7	**55.8**
	0.8 g l^{-1}	**9.72** ± 0.66	**25.8** ± 2.8	**12.5** ± 2.9	**6.7** ± 2.9	**4.8** ± 2.9	**50.3**
	3 g l^{-1}	**25.9** ± 5.1	**9.9** ± 3.1	**4.1** ± 3.2	**2.7** ± 3.6	**1.9** ± 4.0	**81.5**
OCAD450	0.02 g l^{-1}	**1.24** ± 0.02	**6.8** ± 0.4	**5.7** ± 0.6	**4.6** ± 0.8	**5.0** ± 1.0	**77.9**
	0.8 g l^{-1}	**9.37** ± 0.87	**18.3** ± 1.2	**7.9** ± 2.1	**3.95** ± 2.2	**3.4** ± 2.2	**66.5**
	3 g l^{-1}	**20.4** ± 6.4	**18.7** ± 3.3	**8.3** ± 5.7	**3.10** ±7.6	**1.9** ± 9.3	**68.0**
AD550	0.02 g l^{-1}	**0.986** ± 0.009	**12.4** ± 0.1	**11.7** ± 0.1	**10.8** ± 0.2	**10.1** ± 0.2	**54.9**
	0.8 g l^{-1}	**9.35** ± 2.21	**22.6** ± 5.0	**9.7** ± 5.3	**5.7** ± 5.4	**3.9** ± 5.4	**58.2**
	3 g l^{-1}	n/a	n/a n/a	n/a n/a	n/a n/a	n/a n/a	**n/a**
OCAD550	0.02 g l^{-1}	**1.26** ± 0.00	**6.2** ± 0.2	**5.4** ± 0.3	**4.9** ± 0.3	**4.7** ± 0.4	**78.8**
	0.8 g l^{-1}	**9.82** ± 2.01	**15.8** ± 2.0	**6.9** ± 2.2	**4.0** ± 2.2	**2.7** ± 2.3	**70.6**
	3 g l^{-1}	**n/a**	n/a n/a	n/a n/a	n/a n/a	n/a n/a	**n/a**
AC	0.02 g l^{-1}	**0.884** ± 0.017	**13.8** ± 0.4	**8.1** ± 0.5	**5.6** ± 0.6	**4.4** ± 0.7	**68.1**
	0.8 g l^{-1}	**3.47** ± 1.52	**89.3** ± 11.6	**22.2** ± 12.1	**8.9** ± 12.2	**5.2** ± 12.2	**-25.6**
	3 g l^{-1}	**15.1** ± 4.4	**64.1** ± 8.9	**18.6** ± 13.6	**6.6** ± 17.5	**3.6** ± 20.8	**7.03**
OCHRE	0.02 g l^{-1}	**1.73** ± 0.00	**0** n/a	**0** n/a	**0** n/a	**0** n/a	**100**
	0.8 g l^{-1}	**14.2** ± 1.77	**18.3** ± 1.9	**6.1** ± 2.0	**3.1** ± 2.0	**2.0** ± 2.0	**70.4**
	3 g l^{-1}	**20.0** ± 5.71	**23.2** ± 2.2	**4.9** ± 3.3	**1.5** ± 4.2	**0.7** ± 4.9	**69.8**
ZEOLITE	0.02 g l^{-1}	**0.130** ± 0.011	**46.3** ± 1.3	**13.9** ± 4.2	**8.2** ± 5.1	**5.6** ± 6.1	**26.0**
	0.8 g l^{-1}	**11.2** ± 1.5	**14.2** ± 1.8	**10.9** ± 2.1	**9.9** ± 2.3	**9.6** ± 2.4	**55.3**
	3 g l^{-1}	**21.5** ± 5.0	**12.5** ± 4.1	**6.1** ± 7.2	**3.3** ± 9.9	**2.5** ± 12.4	**75.6**

In contrast, both the AD450 and AD550 biochars release a higher concentration of P than any of the other materials (AD450 more so than AD550) and, apart from zeolite, both released the greatest percentage of recovered P. Activated carbon ranked in between the AD and OCAD biochars. As potential P fertilisers, these materials should provide more readily-available P to plants than ochre-based products, but are less effective at recovering P from solution, particularly zeolite.

Where release was less than the amount of P recovered, the released P was probably derived from the pool of recovered P, rather than the P native to the materials. To confirm this interpretation, extraction of non-enriched materials was undertaken which demonstrated that water soluble P was much lower than that of the enriched samples (Table 2.6). Comparison of the results from the 0.02 g P l^{-1} treatments to the other treatments shows differences in the rate of P loss over time. For example, the rate of P loss for the AD biochars at the lowest concentration treatment was approximately constant, whereas in the higher concentration treatments there was greater release on the first extraction than in subsequent extractions. This suggests a different mechanism of P sorption and retention at higher concentrations which results in less strongly bound P. Thus when materials saturated with P are added to soil, P release could be faster initially, a pattern that may be better synchronised with plant growth.

Table 2.6 Total concentration of P released from the materials after 5 consecutive extractions in deionised water

	mg P g^{-1}
AD450	0.209
OCAD450	0.101
Zeolite	0.001
AC	0.001
Ochre	0.000

2.3.5 Alternative P fertilisers from wastewater P

Systems in which biochar production recycles P from sewage sludge and wastewater to agriculture have great potential. Our results show that selected biochars can be used to actively extract P from wastewater, and that they might subsequently function as fertilisers with more favourable characteristics to established fertiliser products from biosolids or phosphate rock.

Using these results, the biochar requirement to reduce the outflow P concentration in a WWTP to 0.01 mg P l^{-1} from a concentration of 20 mg P l^{-1} (0.02 g l^{-1}), assuming achievement of only 50% of the highest laboratory-measured efficiency in the 0.02 g P l^{-1} experiments after the first 24 h (see Sorp 1, Figure 2.1.4) is 114 g biochar l^{-1}. For a WWTP producing 80×10^3 l treated water d^{-1}, 9 t of biochar would be required to bring all water to 0.01 mg P l^{-1} before discharge. For a plant producing 5×10^6 l d^{-1}, 570 t of biochar would be required. These are large quantities of biochar, but if a 50% total recovery capacity is also assumed (using the highest P sorption values from the 3 g l^{-1} P experiment), the char would not be saturated with P until after 70 days. However, applying these calculations and assumptions to achieve a WWTP outflow P concentration of 0.1 mg P l^{-1} from the current limit of 2 mg l^{-1}, the biochar required would be 0.9 t and 54 t respectively, which may be more feasible in terms of the physical space required for filtration.

Using the approximate density of biochar of 0.3 g ml^{-1}, the smaller of the two WWTPs would require a filter of dimensions 1 m × 2 m × 15.2 m to treat an outflow P concentration of 20 mg l^{-1} or 1 m × 2 m × 1.45 m for an outflow of 2 mg P l^{-1}. The larger WWTP would require 1 m × 2 m × 947 m and 1 m × 2 m × 90.4 m, respectively. Whilst the largest of these volumes does appear unfeasible, the rest look to be achievable. Biochar from WWTPs of these sizes would produce enough P enriched material each year to fertilise between 1.8 and 3261 ha of Index 0 soil at the rates calculated in section 3.3.1. These calculations support the assertion that these materials could be used to supplement or replace conventional P fertiliser, especially for land in the vicinity of individual WWTPs.

Understanding the chemical and physical properties of biochars used for P capture and release from wastewater will be important for managing (for example) the diminishing sorption expected when biochar surfaces become negatively charged through phosphate sorption. It will also help to identify non-ochre mineral waste materials that might improve sorption efficiency. Technical responses might also be considered, such as filtration designs that permit periodic resting for diffusive penetration of phosphate into biochar and which have been shown to increase phosphate sorption of other materials (Barrow, 2015; Sibrell et al., 2009).

2.4 Conclusions

Biochars with promising P recovery and recycling properties can be made from anaerobically digested sewage sludge. We show that addition of ochre to the feedstock not only improves P recovery properties, but also produces biochars that comply with guidelines relevant to possible future regulation of biochar application to soil. The results also indicate that the ideal pyrolysis temperature for these materials depends on feedstock characteristics, and that the P capture and retention properties of the biochars were equal to or better than other potential P recycling materials tested for comparison. Robust methods using pH buffering that are applicable to diverse, novel materials and are meaningful in the context of their intended use as fertilisers have been demonstrated. Future experiments should aim to improve the design of the biochars by probing the sorption mechanisms more deeply, using plant growth experiments to directly evaluate their potential use as fertilisers.

Chapter 3

Biochar and enhanced phosphate capture: mapping mechanisms to functional properties

J.G. Shepherd, S. Joseph, S.P. Sohi and K.V. Heal

Published in *Chemosphere* Volume 179 (2017) pages 57-74

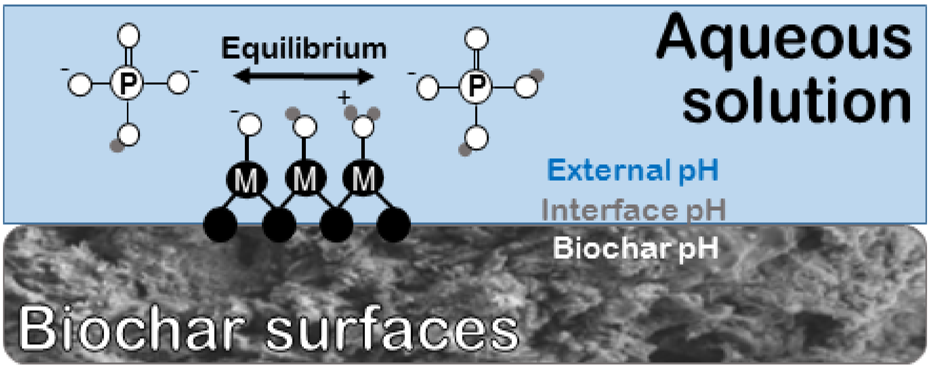

The candidate, as lead author, performed the experiments and laboratory analysis with the following exceptions: Professor Stephen Joseph jointly performed the SEM-EDX analyses with the candidate, XRD was performed by Ben Pace, XPS and LA-ICP-MS analyses were performed by technical staff at the University of New South Wales Mark Wainwright Analytical Centre, pyrolysis was performed by Dr Wolfram Buss and AutoAnalyser analyses were performed by Andy Gray and John Mormon. Data analysis and writing of the paper was carried out by the candidate. Co-authors provided support and guidance on the scope and design of the project, the analyses performed and editing of the manuscript.

3.1 Introduction

Freshwater and coastal ecosystems are at a high risk of damage caused by excess flows of phosphate from land application and wastewater (Steffen et al., 2015). Concurrently there is growing interest in the research, innovation and regulatory sectors to improve the recovery and recycling of phosphate as agricultural fertiliser in response to predicted future mineral phosphorus (P) scarcity (Reijnders, 2014). Traditional flocculation techniques may not be effective for limiting P concentrations in wastewater discharges to watercourses to reduce the risk of environmental damage to acceptable levels, for example the 0.1 mg l^{-1} level proposed by Greenop and Wentworth (2014). Therefore, alternative tertiary treatment methods are required, such as constructed wetlands increasingly utilised in smaller wastewater treatment plants (WWTPs), using combinations of plant, soil, and reactive materials to remove phosphate and nitrate to prevent environmental damage downstream.

In order to recycle P from wastewater it is important that the materials used to recover P are economic and the underlying mechanisms of P capture well understood. Low-cost, bulk filter materials investigated to date include ochre, zeolite and blast furnace slags (Cucarella et al., 2008; Dobbie et al., 2009; Drizo et al., 2006). The main mechanisms of P capture in these systems are either chemisorption and precipitation by Fe or Al (oxy)hydroxides, or precipitation with Ca (Arai and Sparks, 2001; Sakadevan et al., 1998). Activated carbons have also been developed for this purpose (Z. Wang et al., 2012), but the manufacture of these materials is more expensive than the direct recycling of secondary organic resources. A number of biochar materials, because of their similarities to activated carbon, have also been investigated. Biochars produced from anaerobically digested sugar beet tailings, digested sewage sludge and mallee tree (*Eucalyptus polybractea*) have all been shown to have phosphate capture functionality (Chapter 2; Yao et al., 2011; Zhang et al., 2016), but most studies have involved either feedstock pre-treatment (Chapter 2, Chen et al., 2011; Yao et al., 2011; Zhang et al., 2013a, 2012) or post-treatment of the biochar (Li et al., 2016; Park et al., 2015; Ren et al., 2015; Zhang et al., 2016) to increase porosity and enrich the biochar with Mg, Al or Fe oxides.

Although many P sorption studies are reported in the literature, there is still no definitive model for biochar–phosphate interactions. Adding to the complexity of the system, many biochars have been shown to release, rather than capture phosphate into water and/or phosphate solutions (Angst and Sohi, 2013; Morales et al., 2013; Schneider and Haderlein, 2016).

It has been suggested that phosphate may react with hydroxyl and carboxyl groups on the biochar surface (Laird and Rogovska, 2015) but such a reaction can only occur in the natural environment under extreme conditions or, in the case of biota, with the assistance of specialised enzymes (Gull et al., 2014). It is possible that the various phosphate anion species ($H_2PO_4^-$, HPO_4^{2-}, PO_4^{3-}) interact with C surfaces through hydrogen bonding and cation-mediated outer-sphere electrostatic interactions. These are weak compared to inner-sphere chemisorption and precipitation reactions which would occur with minerals, and thus are unlikely to be long-lived, unless in a relatively static system such as undisturbed soil. It has been suggested that adsorption of P by biochar will be dependent on the concentration and accessibility of cations in the biochar ash fraction (Streubel et al., 2012). This is supported by reports of low affinity for P of low-ash biochar in aqueous solution (Hale et al., 2013; Morales et al., 2013; Yao et al., 2012). Even in biochar that has not been chemically modified, the identified mechanisms of P capture have been related to a native mineral ("ash") phase (Yao et al., 2011; Zhang et al., 2016), rather than functional carbon groups.

The focus of subsequent optimisation of P capture properties has thus been on increasing the concentration and effectiveness of mineral phases on biochar surfaces. This can be likened to the research and development of activated carbon, where the activation step for improving P capture properties usually involves the addition of a metal reagent such as Fe or Zn (Bhatnagar and Sillanpää, 2011; Namasivayam and Sangeetha, 2004; Z. Wang et al., 2012). Drawing on the general principles of coordination chemistry suggested by Streubel et al. (2012), we support a dominant role for minerals, but emphasise the mineral-carbon interface. The specific role of Fe, Al, Ca and Mg will vary with pH, as has been widely documented (Barrow, 1983; Goldberg and Sposito, 1985; Parfitt and Russell, 1977; Parfitt, 1989; Parfitt et al., 1975; Reddy et al., 1999; Sibrell et al., 2009; Torrent et al., 1992). This needs to be understood in the context of interface interactions.

In a previous study, we tested biochars made from a novel mix of anaerobically digested sewage sludge and ochre (Chapter 2). The mix captured a greater amount of P from solution on a mass basis than activated carbon, ochre, or biochar from digested sludge only. To investigate the mechanisms underlying the P-capture function of that biochar we initiated the present study, with the overall goal of furthering the practical design of P capture materials in general. Consistent with this more practical context, we prepared new biochars using the original ingredients but pelletised before pyrolysis. We also used lower ochre content in mixed feedstock, namely 1:9 rather than 1:1 mass ratio. The surface properties were studied before and after exposure to aqueous P using a range of spectroscopic and visualisation techniques. Our overarching hypothesis was that P capture would be driven predominantly by mineral associations on surfaces and less by functional carbon groups.

3.2 Materials and methods

A summary of the materials, procedures and analyses used in this study and their respective aims is given in Table 3.1. The biochars collectively encompass the range of ochre (and therefore Fe), ash constituents and carbon components that allows the relative contribution to P capture to be assessed. Characterisation was undertaken on sub-samples with and without prior exposure to aqueous P solution, and of exterior and/or interior surfaces of individual particles or pellets. Different characterisation techniques covered different physical surface areas or surface thickness (i.e. sample volume); they also provide information at different levels of detail, e.g. elemental composition, functional groups, or oxidation state.

3.2.1 Biochars

3.2.1.1 Non-pelletised biochars

Biochars from non-pelletised feedstock were from the previous study (Chapter 2). They were produced in a small batch pyrolysis system at highest treatment temperatures (HTTs) of 450 and 550°C. The feedstocks were anaerobically digested sewage sludge (giving biochars AD450 and AD550) and the same sludge mixed with ochre at a dry-mass ratio of 1:1 (giving biochars OCAD450 and OCAD550). These relatively low HTTs were originally chosen so as to produce biochar with reactive sites potentially related to carbon functional groups (Downie et al., 2009).

3.2.1.2 Pelletised biochars

Biochars were made from pelletised feedstocks using a bench-scale continuous pyrolysis unit. It is more practical to pelletise feedstock than biochar; screw-feeders used in scalable, continuous flow pyrolysis systems also perform best with feedstock in pelletised form. The digested sewage sludge and ochre were sourced from the same locations as in the previous study. Anaerobically digested sewage sludge (50 kg wet mass) was sampled from the Newbridge WWTP (Edinburgh, Scotland) and oven dried. Ochre was obtained from the Minto minewater treatment plant (Fife, Scotland) and sieved to < 1 mm. Pellets were prepared from the sludge and/or ochre and a lignocellulose binder agent in the ratios 89.1:9.9:1.0 and 99.0:0:1.0. The mixtures were passed through a die to form pellets approximately 0.5 cm diam. × 2 cm in length. The pellets were pyrolysed at the UK Biochar

Table 3.1 Summary of the materials, analyses and their aims described in this study. First generation biochar materials AD450, AD550, OCAD450, OCAD550 as well as ochre and activated carbon were characterised in Chapter 2 and are indicated in italics. Elemental concentrations of these materials determined previously by modified dry ashing/ICP-OES are outlined in Chapter 2 Table 2.1 Table 2.2. The pelletised materials were produced for this study and were characterised by the techniques listed

	Analyses							
Material	**P capture and Release**	**Correlation of P capture/element concentrations**	**Modified dry ashing/ICP-OES**	**pH and EC**	**XRD**	**XPS**	**LA-ICP-MS**	**SEM-EDX**
AD450	✓*(previous work)*	✓	✓*(previous work)*	✓*(previous work)*	-	-	-	-
AD550	✓*(previous work)*	✓	✓*(previous work)*	✓*(previous work)*	-	-	-	-
OCAD450	✓*(previous work)*	✓	✓*(previous work)*	✓*(previous work)*	-	-	-	-
OCAD550	✓*(previous work)*	✓	✓*(previous work)*	✓*(previous work)*	-	-	-	-
Ochre	✓*(previous work)*	✓	✓*(previous work)*	✓*(previous work)*	-	-	-	-
Activated carbon	✓*(previous work)*	✓	✓*(previous work)*	✓*(previous work)*	-	-	-	-
PAD450	✓ (capture only)	-	✓	✓	✓	-	-	✓
PAD550	✓ (capture only)	-	✓	✓	✓	-	-	✓
POCAD450	✓ (capture only)	-	✓	✓	✓	✓	✓	✓
POCAD550	✓ (capture only)	-	✓	✓	✓	✓	✓	✓
EPAD450	N/A	N/A	-	-	✓	-	-	✓
EPAD550	N/A	N/A	-	-	✓	-	-	✓
EPOCAD450	N/A	N/A	-	-	✓	✓	✓	✓
EPOCAD550	N/A	N/A	-	-	✓	-	✓	✓
Mechanistic and chemical information obtained	Determination of P capture/release characteristics	Effect of elemental composition on P capture and release	Effect of feedstock, processing and/or pyrolysis conditions and pyrolysis HTT on elemental composition	Effect of feedstock, processing and/or pyrolysis conditions and pyrolysis HTT on pH and EC	Effect of feedstock, pyrolysis HTT and P exposure on mineral phases	Effect of P exposure on surface and whole properties	Effect of pyrolysis HTT and P exposure on surface properties	Effect of feedstock, pyrolysis HTT and P exposure on surface properties
Biochar nomenclature	AD – Anaerobically digested sewage sludge OCAD – 50% Minto ochre and AD mixture (pre-pyrolysis) PAD – Pelletised Anaerobically digested sewage sludge POCAD – Pelletised 10% Minto ochre and AD mixture (pre-pyrolysis)				EPAD – P exposed PAD biochar EPOCAD – P exposed POCAD biochar 450 – 450°C highest treatment temperature (HTT) for pyrolysis 550 – 550°C highest treatment temperature (HTT) for pyrolysis			

Research Centre (UKBRC) using the bench-scale continuous flow unit described previously (Buss et al., 2016a). The HTTs used in the previous study (Chapter 2) were used to produce the four new biochar materials: PAD450, PAD550, POCAD450 and POCAD550.

3.2.1.3 P–exposed pelletised biochars

To investigate the mechanisms of P capture on biochar surfaces, pelletised biochars defined above were exposed to aqueous P using a MOPS-buffered (3-(*N*-morpholino) propanesulfonic acid, Sigma Aldrich, St Louis, MI) K_2HPO_4 solution containing 20 mg P l^{-1}, following the procedure described previously (Chapter 2) modified as described here. Each biochar (30 g, PAD450, PAD550, POCAD450 and POCAD550) was used to provide representative particles of the physically heterogeneous samples, selecting only particles of diameter 0.25–15 mm. The P solution was added in a 1:20 solid to liquid ratio (m/v) and shaken with the biochar for 24 h. After this time the solution was poured off from the biochar and replaced with fresh P solution. This was repeated for 6 days to ensure sufficient uptake of P on the external surfaces of the biochar to analyse using the chosen techniques. At the end of each 24 h treatment two samples of the solution were analysed colorimetrically (Auto Analyser III, Bran & Luebbe, Norderstedt, Germany) to determine the amount of P captured by the biochars. The P-exposed samples were designated EPAD450, EPAD550, EPOCAD450 and EPOCAD550.

3.2.2 Characterisation

3.2.2.1 pH – pelletised biochars

To provide insights on surface protonation of pelletised biochars, the pH of crushed samples was determined in duplicates for PAD450, PAD550, POCAD450 and POCAD550, in DI water using the method recommended by the International Biochar Initiative (IBI) (IBI, 2012).

3.2.2.2 P capture and release – non-pelletised biochars

P-capture and release dynamics of the non-pelletised biochars (AD450, AD550, OCAD450 and OCAD550) were described and reported in the previous study (Chapter 2). It is the statistical analysis of the results in the light of new characterisation data that is the main focus of the present study. Briefly, replicate (n = 4) 1.0 g samples of each biochar, the ochre and an activated carbon (Sigma Aldrich, St Louis, MI) were repeatedly exposed for 24 h repeated over 5 days to 20 ml solutions of either 20 or 800 mg l^{-1} P (from K_2HPO_4, Sigma

Aldrich, St Louis, Missouri, USA) buffered at pH 7 using MOPS and $NaNO_3$ as a background electrolyte. To test the release of the captured P, the P-enriched materials were then exposed to pH 7 MOPS-buffered deionised (DI) water for 24 h repeatedly over 4 days.

3.2.2.3 Bulk elemental composition – pelletised and non-pelletised biochars, ochre and activated carbon

Samples were digested prior to ICP-OES analysis using the modified dry ashing method (Enders and Lehmann, 2012), as per published modifications (Chapter 2, Buss et al., 2016a). Briefly, 0.5 g samples were taken from sub-sampled and crushed materials, ashed in a muffle furnace then digested in HNO_3 and HCl. The materials and blanks were digested in triplicate and ICP-OES elemental quantification was performed using a Perkin Elmer Optima 5300DV instrument (Waltham, USA). Most elements were analysed in axial mode, except for Al, Ca, Fe, K, Mg and Na, which were present in sufficient concentrations to necessitate the use of radial mode. Standards were run with each analysis session for calibration and to check the accuracy of measurements over the time of the sample run. The limit of detection for each element was determined using an existing method (Buss et al., 2016a).

3.2.2.4 X-ray diffraction (XRD) – pelletised biochars

Cobalt Kα XRD was performed in duplicate on PAD450, PAD550, POCAD450, POCAD550, EPAD450, EPAD550, EPOCAD450 and EPOCAD550 using an Empyrean thin-film XRD (PANalytical, Almelo, the Netherlands). Analyses were initially attempted using standard Cu Kα XRD, but confounded by the large background signal from amorphous carbon phases.

3.2.2.5 X-ray photoelectron spectroscopy (XPS) – pelletised biochars

Surface layer functional groups and elemental composition was examined for one randomly sampled pellet fragment of POCAD450, EPOCAD450 and POCAD550. Mono-chromated Al Kα XPS was applied using an ESCALAB250Xi instrument (Thermo Scientific, Waltham, MA). The analysis parameters were as follows: 1486.68 eV photon energy, 150 W power and spot size of 500 μm. The core level binding energies (BEs) were aligned with C1s peak BE of 285.0 eV. Data were analysed with Avantage software (Thermo Scientific, Waltham, MA). The surfaces of POCAD450 and EPOCAD450 pellets were analysed to identify differences in properties before and after P exposure, respectively. Surfaces of POCAD550 were also analysed to identify whether pyrolysis HTT had an effect on surface composition in these biochars. To gain an insight as to the effect on pellet size on the utilised capacity for

P interaction measurements were also conducted on interior surfaces of the analysed POCAD and EPOCAD, exposed by crushing the pellet.

3.2.2.6 Laser ablation-ICP-MS – pelletised biochars

To study the relationship between P and other elements on the surface of P-exposed and non-treated biochar to a depth of 5 µm, elemental analysis by laser ablation (LA) ICP-MS was used. The analysis was applied to a randomly selected pellet of each of POCAD450, POCAD550, EPOCAD450 and EPOCAD550 using a NWR213 Laser Ablation unit (ESI New Wave, Portland, OR) coupled to a NexION 300D ICP-MS (Perkin Elmer, Waltham, MA). Laser ablation parameters were as follows: wavelength 213 nm, repetition frequency 10 Hz, laser energy density 0.48 J cm^{-2} (at 30%), spot size 110 µm and scan speed 20 µm s^{-1}. ICP-MS was performed at Rf power of 1150 W, helium gas flow rate of 0.8 l min^{-1}, argon gas flow rate of 0.6 l min^{-1}, in peak hopping scan mode and with a dwell time of 0.05 s. NIST610 and NIST612 glass standards were used to estimate the elemental concentrations of the biochar obtained in three separate 2 mm line scans for each pellet (resulting in between 219 and 223 sample locations for each pellet).

3.2.2.7 Scanning electron microscopy with energy-dispersive X-ray spectroscopy (SEM-EDX)

SEM-EDX analyses were performed on all P-exposed and non-exposed biochars (PAD450, PAD550, POCAD450, POCAD550, EPAD450, EPAD550, EPOCAD450 and EPOCAD550) to a depth of approximately 6 µm. Data was gathered using Nova Nano SEM 230 and 450 field-emission scanning electron microscopes (FEI, Hillsboro, OR), each configured with a Bruker silicon drift detector energy dispersion X-ray spectrometer (Bruker, Billerica, MA), as well a Sigma SEM (Zeiss, Jena, Germany). Samples were sputter coated with chromium prior to analysis. The resolution of EDX scans was 6 µm. To encompass as many P phases as possible, the whole region was quantified; many P phases have a dimension in the µm range. Elemental mapping provided by EDX was used to visualise the association of P and other elements in support of the other analyses.

3.2.3 Statistical analysis

3.2.3.1 Correlation of biochar element concentration and P capture and release – non-pelletised biochars

To identify whether specific elements were associated with P capture or release, mean P capture and release results (n = 6) were correlated against the concentration of 19 elements in AD450, AD550, OCAD450, OCAD550, ochre and activated carbon determined as described in 3.2.2.3. The cumulative results for 1 and 5 days x 20 mg l^{-1} P repeated exposure and 1 and 4 days x treatments for P release as described in section 2.2.2 were used. Pearson's product-moment correlation coefficients were calculated since all data were found to be normally distributed by the Shapiro-Wilk test. Where element concentrations were below the limit of detection for two or more of the materials (i.e. resulting in $n < 4$), the element was excluded from the analysis. RStudio (RStudio Team, 2015) was used for all statistical analyses, with significance indicated by $p < 0.05$.

3.2.3.2 Analysis of Laser ablation ICP-MS results

Correlation analysis between P and other elements measured by LA-ICP-MS was performed using the approach described in 3.2.3.1, with Spearman's rho calculated where one or both sets of data were not normally distributed. To further interpret elemental composition on biochar surfaces, we applied Principal Component Analysis (PCA) to the results for each sample location using the prcomp function in RStudio (RStudio Team, 2015) with data centring, scaling and specifying a tolerance of 0.3 to filter out noise and thereby limit the number of identified principal components. PCA provides insights into elemental clustering as well as the localisation of P on sample surfaces before and after exposure to P solution.

3.3 Results

3.3.1 Bulk properties

3.3.1.1 Elemental composition

The lower content of ochre in the POCAD feedstock compared to OCAD (10 vs 50%) explained some differences in nutrient and other element concentrations between PAD and POCAD (Table 3.2Table 3.3) compared to their non-pelletised analogues (AD and OCAD). In general, the non-pelletised biochars appeared to show greater elemental loss on a mass basis, compared to their feedstocks, than for the pelletised biochars (See Chapter 2 Table 2.1 and Table 2.2 for more detail). Calcium and P present in the feedstocks was retained to a higher extent in the pelletised biochars, suggesting that either pelletisation and/or the continuous flow bench scale pyrolysis process provides conditions less conducive for volatilisation of Ca and P than small scale batch pyrolysis.

The main difference between the PAD and POCAD biochars was in the concentration of Fe, reflecting feedstock composition (see Table 3.3). The incorporation of 10% ochre (dry weight) to the feedstock resulted in a Fe concentration in POCAD twice that of PAD. Despite similar concentrations in PAD and POCAD feedstocks, POCAD contained relatively less Cr than PAD at both HTTs (24.9 ± 0.880 and 21.1 ± 1.16 mg g^{-1} for POCAD vs 33.8 ± 1.25 and 30.1 ± 0.538 mg g^{-1} for PAD) (mean ± 1 standard deviation, n = 3). Compared to the non-pelletised biochars, the PAD and POCAD biochars contained more Al, Cr, Cu, Mo, Na, Ni and Zn, but less B and Co. The lower Co concentration reflects a lower concentration in the feedstock, but this is not the case for B, which may have also been lost during digestion in the modified dry ashing process. The concentrations of Mo and Na in the pelletised feedstocks are higher than in non-pelletised, explaining part of the difference in concentration in the biochars. In addition, there is considerably more Cr, Cu and Zn in POCAD than OCAD, probably from contamination of feedstock during the pelletisation process. Overall, the data indicate that pelletisation and/or continuous flow pyrolysis favours greater retention of some elements in biochar. The pH of the pelletised biochars ranged from 7.39 to 8.25, which is slightly higher than for the non-pelletised analogues. This is likely to be related to the relative retention of salts discussed above.

Table 3.2 Mean nutrient concentrations (n=3) of the materials (dry weight basis) as determined by ICP-OES of sample digests expressed in g kg^{-1} ± 1 standard deviation. See Table 3.1 for sample nomenclature.

	PAD	Ochre	POCAD	PAD450	POCAD450	PAD550	POCAD550
Yield %	-	-	-	**29.4**	**38.7**	**37.9**	**38.0**
pH (n=2)	-	**7.9** ± 0.014	-	**7.49 ± 0.02**	**7.39 ± 0.05**	**8.25 ± 0.08**	**7.85 ± 0.03**
Nutrients (g kg^{-1}) n=3							
Ca	28.7 ± 0.6	18.8 ± 0.4	28.8 ± 0.4	59.9 ± 2.0	58.1 ± 0.5	62.0 ± 1.1	53.9 ± 1.1
K	2.53 ± 0.04	0.349 ± 0.048	2.10 ± 0.03	5.09 ± 0.14	4.59 ± 0.07	5.51 ± 0.07	4.20 ± 0.13
Mg	5.12 ± 0.08	3.03 ± 0.06	5.09 ± 0.06	10.4 ± 0.28	10.5 ± 0.1	10.8 ± 0.1	9.52 ± 0.21
Mn	0.142 ± 0.001	0.891 ± 0.005	0.183 ± 0.003	0.327 ± 0.001	0.373 ± 0.005	0.336 ± 0.010	0.357 ± 0.009
P	52.1 ± 0.1	1.92 ± 0.13	51.5 ± 0.6	109 ± 3	103 ± 2	114 ± 1	98.7 ± 1.7
S	9.82 ± 0.43	3.32 ± 0.12	8.81 ± 0.16	16.8 ± 0.4	18.1 ± 0.3	16.3 ± 0.2	16.6 ± 0.2

Table 3.3 Mean potentially toxic element concentrations (n=3) of the materials (dry weight basis) as determined by ICP-OES of sample digests expressed in mg kg^{-1} ± 1 standard deviation. See Table 3.1 for sample nomenclature.

	PAD	Ochre	POCAD	PAD450	POCAD450	PAD550	POCAD550
Al	23.6×10^3 ± 121	2.09×10^3 ± 227	22.7×10^3 ± 151	46.5×10^3 ± 953	46.6×10^3 ± 354	49.5×10^3 ± 666	43.4×10^3 ± 1130
As	< 0.72	< 0.72	< 0.72	< 0.72	< 0.72	< 0.72	< 0.72
B	9.26 ± 0.09	43.8 ± 6.1	15.3 ± 3.5	18.6 ± 0.4	19.8 ± 1.5	18.0 ± 0.2	16.1 ± 0.4
Cd	0.281 ± 0.018	< 0.04	< 0.04	1.77 ± 0.04	0.169 ± 0.011	1.15 ± 0.09	0.322 ± 0.085
Co	2.94 ± 0.26	9.65 ± 0.06	3.10 ± 0.06	6.05 ± 0.14	6.71 ± 0.12	6.30 ± 0.17	6.10 ± 0.19
Cr	11.8 ± 0.2	< 0.49	10.6 ± 0.7	33.8 ± 1.3	24.9 ± 0.9	30.1 ± 0.5	21.1 ± 1.2
Cu	44.0 ± 1.2	< 0.06	39.1 ± 0.6	110 ± 2	103 ± 2	112 ± 8	98.9 ± 3.7
Fe	38.9×10^3 ± 719	520×10^3 ± 7.44×10^3	77.0×10^3 ± 2.51×10^3	80.8×10^3 ± 2.93×10^3	130×10^3 ± 2.00×10^3	84.5×10^3 ± 1.53×10^3	130×10^3 ± 1.92×10^3
Mo	10.9 ± 0.6	< 0.21	12.5 ± 0.9	21.9 ± 0.5	26.7 ± 0.6	23.8 ± 0.8	24.3 ± 0.3
Na	5.11×10^3 ± 274	1.86×10^2 ± 30	1.33×10^3 ± 44	9.90×10^3 ± 219	5.23×10^3 ± 49	10.5×10^3 ± 208	3.75×10^3 ± 171
Ni	7.14 ± 0.54	5.90 ± 0.08	7.23 ± 0.18	29.4 ± 1.0	23.0 ± 0.1	26.3 ± 0.9	18.8 ± 0.4
Pb	11.8 ± 0.4	10.1 ± 0.8	13.2 ± 1.8	31.9 ± 4.2	25.1 ± 0.4	29.8 ± 0.8	28.3 ± 3.7
Zn	360 ± 5	60.6 ± 1.1	350 ± 3	787 ± 10	746 ± 7	825 ± 16	706 ± 12

3.3.1.2 Phosphorus exposure of the pelletised biochars

Repeated exposure of biochars to 20 mg P l^{-1} MOPS-buffered solution resulted in P capture of 0.57 ± 0.26 mg P g^{-1} for PAD450 (mean ± 1 standard deviation, n = 2), 0.70 ± 0.40 mg P g^{-1} for PAD550, 0.95 ± 0.18 mg P g^{-1} for POCAD450 and 0.95 ± 0.23 mg P g^{-1} for POCAD550. The P capture by non-pelletised biochars AD and OCAD (Chapter 2) were higher: 0.99 ± 9.3×10^{-3} mg P g^{-1} to 1.3 ± 4.7×10^{-3} mg P g^{-1}. This may be attributed to the larger size of analysed pellet fragments (0.25–15 mm) compared to crushed particles (0.5–1.0 mm).

This P-exposure methodology was different than that used in Chapter 2 for the non-pelletised biochars as the purpose of P-exposure was to enrich the surfaces of the biochar pellets and pellet fragments with P relative to the interior of the biochar. The approach was selected so that a comparison of surface and bulk properties could be undertaken, for example in the case of XPS, and so that large fragments could be easily manipulated and imaged using the microscopy techniques. A consequence of this, however, was that the P capture data from the non-pelletised and pelletised biochars could not be incorporated with spectroscopic and microscopic data into a predictive model for P capture. The large differences between particle size distribution in the two experiments would have confounded any results from such modelling.

3.3.1.3 Elemental associations in P capture and release for non-pelletised biochars

The significant correlations between P capture and release and bulk element concentrations are shown for AD450, AD550, OCAD450, OCAD550, ochre and activated carbon in Table 3.4. After 1 day (1 x 24 h) exposure to a 20 mg P l^{-1} solution, P capture from solution was correlated negatively and strongly significantly with biochar Al, Cu, K, Na and Zn concentration. After 5 days (5 x 24 h) of exposure only Pb was significantly correlated (negatively), although Pb concentration of the materials was also very low ($< 3.2 \times 10^{-3}$ g kg^{-1}). After 5 days, P capture was positively and strongly significantly correlated with Fe, which was present in biochar at 44.6–451 g kg^{-1}.

In terms of P release following P exposure, after 1 day shaking in MOPS-buffered pH 7 DI water, P release was significantly negatively correlated with Fe, suggesting that higher Fe content is associated with lower solubility of captured P at pH 7. After 4 days the negative correlation with Fe was no longer significant, but P release was significantly positively correlated with both initial biochar Cu and Na concentration, indicating that these elements may be present in P compounds of greater solubility after P capture.

1.1.1.1 Mineral phases identified by X-ray diffraction

Due to the presence of amorphous C in the pelletised biochars, few mineral elements were identified, even using the Co method (Table 3.5). The analysed biochars all contained SiO_2 (quartz). Other detectable minerals were mostly complex silicates containing different combinations of Al, Ca, K, Mg, Mn and Na. The only phosphate-containing mineral detected was Al phosphate in EPOCAD450. Interestingly, no iron minerals were identified, indicating that Fe is either amorphous or present in a diversity of crystalline forms at very low individual concentrations.

Table 3.4 Pearson's product-moment correlation coefficients for elements where a statistically significant correlation between elemental concentration and P capture or P release was determined (n = 6) at the start or end of the experiments for the first generation materials using a 20 mg P l^{-1} solution reported in Chapter 2. * = $p < 0.05$, ** = $p < 0.01$, *** = $p < 0.001$

	P capture		**P release**	
	Day 1	**Day 5**	**Day 1**	**Day 4**
Al	-0.886*	-0.412	-0.194	0.0916
Cu	-0.961**	-0.478	0.642	0.860*
Fe	0.605	0.878*	-0.858*	-0.740
K	-0.850*	0.465	0.528	0.748
Mn	0.194	0.711	-0.609	-0.382
Na	-0.967**	-0.521	0.664	0.879*
Pb	-0.292	-0.887*	0.786	0.536
Zn	-0.854*	-0.358	0.487	0.730

Table 3.5 Minerals detected in the pelletised biochars using Co Kα X-ray diffraction. See Table 3.1 for sample nomenclature.

Sample	Minerals detected
PAD450	SiO_2 $Na_2S_2O_3$ $K_{1.2}Al_4Si_8O_{20}(OH)_4.4H_2O$ $Na_3Mg_3Ca_5Al_{19}Si_{117}O_{272}$
PAD550	SiO_2 $Na_2S_2O_3$ $Na_{0.3}(AlMg)_2Si_4O_{10}(OH)_2.6H_2O$
EPAD450	SiO_2
EPAD550	SiO_2 $NaNO_3$
POCAD450	SiO_2 $Na_2S_2O_3$ MgS
POCAD550	SiO_2 $K_{1.2}Al_4Si_8O_{20}(OH)_4.4H_2O$
EPOCAD450	SiO_2 $Na_2S_2O_3$ $NaAl(SO_4)_2.11H_2O$ $Na_4Mn_5Si_{10}O_{24}(OH)_4.6H_2O$ $AlPO_4$
EPOCAD550	SiO_2

3.3.2 Surface characterisation of the pelletised biochars

3.3.2.1 X-ray photoelectron spectroscopy

XPS analysis was conducted on the exterior surfaces of POCAD450, POCAD550 and EPOCAD450 pellets and the interior surfaces of a crushed pellet for POCAD450 and EPOCAD450. A comparison of the C1s A, B, C and D; O1S A and B; and N1sA and B bond states is depicted in Figure 3.1. Compared to the whole pellet, the POCAD450 surface was comparatively enriched with C-C/C-H, C-O/C-OC and C=O -type C bonds, as well as NH_4/NH_2 and N-C-COOH/pyridone -type N bonds, but contained a lower percentage of O=C-O -type C bonds and metal oxide O-bonds and a similar percentage of organic C=O -type O bonds (Table 3.6). The decrease in the metal oxide O-bonds between the surface and whole analyses could be due to reactions that have taken place between ochre and C within the pellet during pyrolysis.

Comparison of the POCAD450 and EPOCAD450 whole pellet XPS results reveals a general increase in the proportion of C-C/C-H and C=O -type C bonds and a decrease in C-O/C-OC

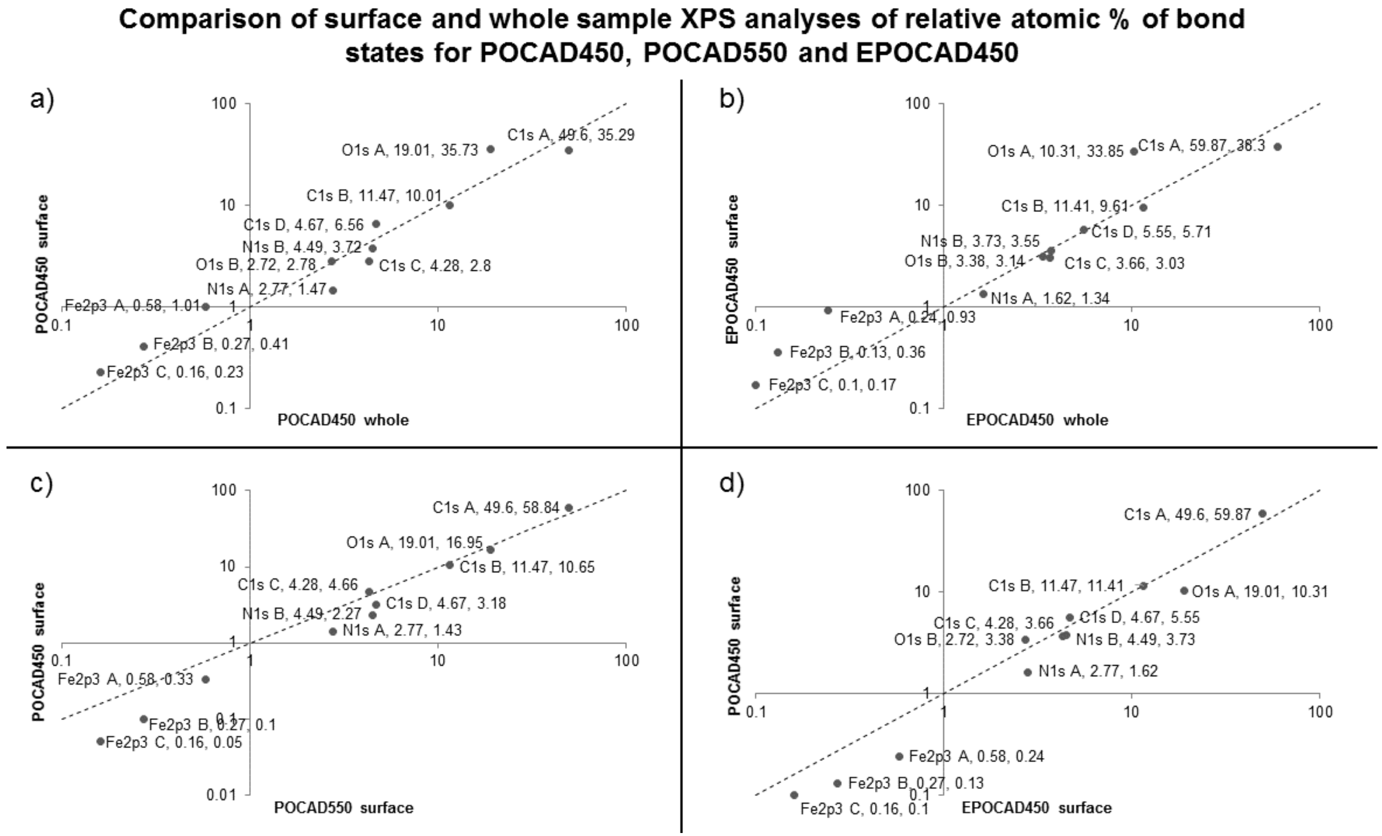

Figure 3.1 Comparative $\log_{10}$-$\log_{10}$ plots of relative atomic percentage of bond states identified by XPS. a) Comparison of POCAD450 surface and whole sample analyses. b) Comparison of EPOCAD450 surface and whole sample analyses. c) Comparison of POCAD450 and POCAD550 surface analyses. Bond state O1s B was detected for POCAD450 (relative atomic precentage 2.72 %) but not POCAD550, so this does not appear on the plot d) Comparison of POCAD450 and EPOCAD450 surface analyses.

and O=C-O –type C bonds after P treatment. An increase in organic C=O bonds was observed after P treatment, with a decrease in metal oxide O-bonding. There was an overall decrease in the proportion of NH_4/NH_2 and N-C-COOH/pyridine –type N bonding in EPOCAD450 compared to POCAD450. In contrast to the whole pellets, the surface of EPOCAD450 was found to have a higher proportion of O=C-O and a lower proportion of C=O –type C bonds compared to the surface of POCAD450.

The POCAD550 surface was enriched in C-C/C-H –type bonds compared to the POCAD450 surface, with a similar distribution of other organic C –type bonding. There was a lower occurrence of N bonding in POCAD550 compared to POCAD450, and notably only one O1s peak was identified for POCAD550 at 532.21 eV, in between the peaks identified for POCAD450 (at 531.55 and 533.59 eV). Peaks in this region could be due to SiO_2, metal carbonates or organic C-O –type O bonding.

The Fe2p3 results for POCAD450 and EPOCAD450 did not support the presence of Fe(0) or predominantly Fe(II) state iron compounds, as these were not detectable. The binding energy spectra indicate the possible presence of the Fe(III) compound Fe_2O_3 or FeOOH on the surface of POCAD450 with a peak at 710.85 eV, whilst the Fe2p3 A peak observed at 711.51 eV in the interior surface indicates the presence of either the Fe(II)/(III) compound Fe_3O_4 and/or surface Fe-O-PO_3^{2-}. This suggests that the overall concentration of Fe_2O_3 or FeOOH is relatively small compared with the concentration of Fe_3O_4 and/or surface Fe-O-PO_3^{2-}. The surface of the EPOCAD450 also produced a Fe2p3 peak at 711.56 eV rather than 710.85 eV. The shifting of the Fe2p3 A peak from 710.85 eV and associated Fe^{3+} satellite peak at 718.65 eV on the surface of POCAD450 to 711.56 eV and 720.33 eV respectively in EPOCAD450 may indicate Fe-O-PO_3^{2-} bonding during P exposure, as phosphate-iron interactions have been observed to cause similar energy shifts in previous studies (Arshadi et al., 2015; Fang et al., 2015; Mallet et al., 2013). Both spectra indicate the presence of iron sulfate compounds, which may be important.

The Fe2p3 peaks observed for the surface of POCAD550 differ slightly from those of the 450°C pair. The Fe2p3 A peak, similar to the surface of EPOCAD450, is observed at 711.52 eV, indicating either the presence of the Fe(II)/(III) compound Fe_3O_4 and/or surface Fe-O-PO_3^{2}. The Fe2p3 B peak indicates the presence of $FeSO_4$, and/or is a satellite of a Fe^{2+} peak. Importantly, the POCAD550 Fe2p3 C peak was uniquely located at a lower energy of 708.82 eV, which indicates the presence of reduced Fe compounds such as FeS_2, FeO and/or FeS.

Table 3.6 Comparison of surface and whole sample C1s, O1s, N1s and Fe2p3 bonding states and their relative atomic percentage of POCAD450, POCAD550 and EPOCAD450 biochar as determined by XPS (regional scan).

Bond state	**POCAD450 Surface**			**POCAD450 Whole**			**EPOCAD450 Surface**			**EPOCAD450 Whole**			**POCAD550 Surface**		
	Functional groups	Peak BE (eV)	At. %	Functional groups	Peak BE (eV)	At. %	Functional groups	Peak BE (eV)	At. %	Functional groups	Peak BE (eV)	At. %	Functional groups	Peak BE (eV)	At. %
C1s A	C-C/C-H	284.79	49.6	C-C/C-H	284.68	35.29	C-C/C-H	284.80	59.87	C-C/C-H	284.64	38.30	C-C/C-H	284.83	58.84
C1s B	C-O/C-OC	286.33	11.47	C-O/C-OC	285.79	10.01	C-O/C-OC	286.10	11.41	C-O/C-OC	285.67	9.61	C-O/C-OC	286.32	10.65
C1s C	C=O	288.05	4.28	C=O	286.98	2.80	C=O	287.58	3.66	C=O	286.79	3.03	C=O	287.92	4.66
C1s D	O=C-O	290.37	4.67	O=C-O	288.5	6.56	O=C-O	289.42	5.55	O=C-O	288.41	5.71	O=C-O	289.61	3.18
O1s A	Metal oxide	531.55	19.01	Metal oxide	531.79	35.73	Metal oxide	531.96	10.31	Metal oxide	531.73	33.85	SiO_2, organic C-O/C=O, metal carbonate	532.21	16.95
O1s B	Organic C=O	533.59	2.72	Organic C=O	533.61	2.78	Organic C=O	533.48	3.38	Organic C=O	533.37	3.14	nd	nd	nd
N1s A	NH_4/NH_2	398.60	2.77	NH_4/NH_2	398.60	1.47	NH_4/NH_2	398.75	1.62	NH_4/NH_2	398.52	1.34	NH_4/NH_2	398.72	1.43
N1s B	N-C-COOH /Pyridone	400.35	4.49	N-C-COOH /Pyridone	400.34	3.72	N-C-COOH /Pyridone	400.53	3.73	N-C-COOH /Pyridone	400.31	3.55	N-C-COOH /Pyridone	400.63	2.27
Fe2p3 A	$FeOOH/Fe_2O_3$	710.85	0.58	Fe_3O_4 / Fe-OPO_3^{2-}	711.51	1.01	Fe_3O_4 /Fe-OPO_3^{2-}	711.56	0.24	Fe_3O_4 /Fe-OPO_3^{2-}	711.41	0.93	Fe_3O_4 /Fe-OPO_3^{2}	711.52	0.33
Fe2p3 B	$Fe_2(SO_4)_3$	714.04	0.27	Fe^{2+} satellite/ $FeSO_4$	714.90	0.41	Surface Fe^{3+}/satellite	715.55	0.13	$Fe_2(SO_4)_3$	714.76	0.36	Fe^{2+} satellite/ $FeSO_4$	714.95	0.10
Fe2p3 C	Fe^{3+} satellite	718.65	0.16	Fe^{3+} satellite	719.10	0.23	Surface Fe^{3+}/satellite	720.33	0.10	Fe^{3+} satellite	718.88	0.17	FeS_2/FeO/FeS	708.82	0.05

Table 3.7 Comparison of bonding states and their relative atomic percentage of C, N, O and mineral elements in surface and whole samples of POCAD450 and EPOCAD450 and surface of POCAD550. nd = not detected.

	POCAD450 Surface		**POCAD450 Whole**		**EPOCAD450 Surface**		**EPOCAD450 Whole**		**POCAD550 Surface**	
	Peak BE (eV)	At. %	Peak BE (eV)	At. %	Peak BE (eV)	At. %	Peak BE (eV)	At. %	Peak BE (eV)	At. %
Al2p	74.40	1.47	74.54	3.52	74.88	0.85	74.45	3.35	75.05	1.58
P2p	133.3	1.16	133.52	2.35	133.66	0.59	133.35	2.34	134.04	0.77
Si2s	102.43	2.37	102.75	5.02	102.89	1.25	153.50	5.82	103.32	2.21
S2s	169.00	0.88	232.57	0.42	164.14	0.54	232.20	0.35	169.40	0.31
C1s	284.76	63.88	284.81	46.80	284.80	76.47	284.65	48.18	285.14	72.69
Ca2p3	347.38	0.67	347.3	1.29	347.63	0.35	347.08	1.29	347.95	0.54
N1s	399.34	7.11	399.73	4.56	399.78	5.46	399.57	4.67	400.30	4.62
O1s	531.47	20.4	531.68	33.14	532.16	13.78	531.57	31.49	532.48	16.27
F1s	685.47	0.39	684.87	0.30	nd	nd	684.91	0.11	nd	nd
Fe2p	711.13	1.08	711.80	1.62	711.30	0.46	711.80	1.58	712.61	0.65
Co2p3	780.70	0.04	Nd	Nd	nd	nd	nd	nd	nd	nd
Na1s	1071.08	0.16	1071.76	0.19	nd	nd	1071.90	0.18	nd	nd
Mg1s	1303.82	0.40	1305.04	0.79	1304.57	0.26	1305.13	0.63	1304.69	0.36

Interpretation of the C, N, O and mineral peaks showed no differences in the proportion of P, S, Ca, Fe and Na between POCAD450 and EPOCAD450 (Table 3.7). In terms of P, there is no difference in surface P concentration after P exposure as it is very low relative to the native P concentration. The abundance of Si, C and N was higher in relative terms for the EPOCAD450 pellet, while Al, O, F and Mg were relatively less abundant. The only element present at a higher proportion on the surface of EPOCAD450 compared to POCAD450 was C. In contrast to the whole sample results, in the surface EPOCAD450 sample there was also lower detection of P, Si, Ca, N, Fe, and Na compared to the surface of POCAD450.

Comparison of results for the surfaces of POCAD550 and POCAD450 pellets indicates a higher proportion of C overall and lower proportions of P, S, N, O and Fe in POCAD550. Heating of pure goethite (FeOOH) at temperatures > 600°C results in sintering (Cornell and Schwertmann, 1996), so it is possible that the detection of a lower proportion of Fe reflects sintering of Fe minerals at the 550°C HTT and a decrease in overall Fe area, rather than loss of Fe from the biochar surface. The fact that there was no difference in the distribution of the proportions of Al, Si, Ca and Mg probably reflects the stability of minerals that contain these elements at higher temperatures (Steenari and Lindqvist, 1998). At higher HTTs a higher proportion of C relative to O may be expected, as O and H are more completely eliminated. It is possible that proportionally more feedstock N, P and S was also eliminated in the preparation of POCAD550 than POCAD450, on account of their own volatility (Magdziarz and Wilk, 2013).

3.3.2.2 Laser ablation ICP-MS

Mass spectral data from LA-ICP-MS analysis of POCAD450, POCAD550, EPOCAD450 and EPOCAD550 were analysed to identify correlation of P with the abundance of selected other elements: Al, Ca, Cu, Fe, K, Mg, Mn, Na, P, Pb, S and Si. The selection of these elements was based on their predicted association with P and/or their high concentrations within the biochars. The results are shown in Table 3.8. Phosphorus was significantly positively correlated with Mg, Al, K, Mn, Fe, Cu and Pb for POCAD450, whilst after P exposure (EPOCAD450) the only strong significant correlation ($\rho < 0.650$) was positive and was with Al. For POCAD550 there was strong positive and significant correlation between P and Mg, Al, Si, K, Ca, Mn, Cu and Pb. After P exposure (EPOCAD550), the correlations with Al, Si, K, Ca and Cu remained highly significant. There was a marked difference between POCAD450 and POCAD550 in the correlation coefficient of P with Fe (0.807 vs 0.462). For this reason, correlations of Fe with other elements were also calculated (Table 3.8). Fe was strongly and significantly positively correlated with P, Mg, S, Mn, Cu and Pb in

POCAD450, but only S and Mn in POCAD550. In EPOCAD550 the only significant correlation with Fe that remained strong ($\rho < 0.650$) was with S, which was also positive.

Principal Component Analysis (PCA) was also conducted on the LA-ICP-MS data to identify the main clustering patterns of the elements on the surface of the biochars. The PCA results are shown in Figure 3.2 and detailed information on the Principal Components (PCs) of each sample is in Tables 3.9 – 3.12. Three PCs were identified for POCAD450. The first PC axis separated sample locations from the line scans (~220 for each biochar) enriched in Fe, Mn, S and Cu from sample locations enriched in all other elements except for P, which was invariant along the second PC axis. The concentration of all analysed elements increased along the second PC axis apart from P. The clustering of elemental concentrations in the sample locations was different after P exposure. Six PCs were identified for EPOCAD450. Along the first PC axis, the concentrations of Al, Si, Ca, K, Na, Pb and S varied in the same direction, whilst Mg, Cu, P, Mn and Fe concentrations varied together and separately from the other group of elements. Again, the second PC axis separated sample locations that contained either higher or lower concentrations of all of the analysed elements. Analysis of the POCAD550 data revealed five PCs and similar sample locations distribution to POCAD450 along the first PC, with a strong association between the concentrations of Fe and S, the variance of which was also related to that of Mn. All other elemental concentrations varied together, apart from Cu and Pb, which were invariant along the second PC axis. Similar to EPOCAD450, quite different elemental sample location distributions were identified after P exposure in EPOCAD550. Six PCs were identified, with sample locations enriched in Na, Mg and Al separated from sample locations enriched in Ca, Cu. Pb, Mn, Fe and S along the first PC axis. Iron and S were still strongly covariant, whilst K, P and Si were invariant along the second PC axis. Along the second PC axis, samples containing higher amounts of Fe and S separated from samples enriched in all other elements analysed. Unlike the transition observed in properties from POCAD450 to EPOCAD450, there was no evidence of dissociation of Fe and S in the higher temperature POCAD550 biochar after P exposure.

3.3.2.3 Scanning electron microscopy with energy dispersive X-ray spectroscopy

Visual comparison of SEM-EDX images from PAD450 and EPAD450 (Figure 3.3a-b) highlights the typical effect of P exposure on pores and mineral phases at the biochar exterior surface. Although the EDX spectra show similar element proportions overall, there is more P and Fe as well as considerably more exposed C (and somewhat less S) in EPAD (Figure 3.3c-d). SEM highlighted surface heterogeneity at various scales in the pelletised biochars

Table 3.8 Correlation coefficients of P and Fe to other elements analysed by LA-ICP-MS (n = ~ 220). Spearman's ρ is reported, except for correlations marked with ^{P}, where all data were normally distributed so Pearson's product-moment correlation has been reported. N.S. = no significant correlation. * = p<0.05, ** = p< 0.01, *** = p< 0.001, **** = p< 0.0001.

	POCAD450		EPOCAD450		POCAD550		EPOCAD550	
	P	Fe	P	Fe	P	Fe	P	Fe
Na	0.330^{****}	0.160^{*}	0.385^{****}	N.S.	0.432^{****}	0.324^{****}	0.433^{****}	N.S.
Mg	0.767^{****}	0.679^{****}	0.572^{****}	0.348^{****}	0.651^{****}	0.419^{****}	0.629^{****}	N.S.
Al	0.789^{****}	0.618^{****}	0.665^{****}	0.333^{****}	0.772^{****}	0.396^{****}	0.818^{****}	N.S.
Si	0.521^{****}	0.397^{****}	0.515^{****}	0.202^{**}	$0.669^{P,\ ****}$	0.453^{****}	0.748^{****}	N.S.
S	0.568^{****}	0.866^{****}	0.156^{*}	0.342^{****}	$0.348^{P,\ ****}$	0.857^{****}	N.S.	0.838^{****}
K	0.737^{****}	0.601^{****}	0.586^{****}	0.209^{**}	0.671^{****}	0.373^{****}	0.866^{****}	N.S.
Ca	0.520^{****}	0.446^{****}	0.517^{****}	0.286^{****}	0.772^{****}	0.480^{****}	0.850^{****}	N.S.
Mn	0.747^{****}	0.861^{****}	0.585^{****}	0.788^{****}	0.696^{****}	0.888^{****}	0.515^{****}	0.628^{****}
Fe	0.807^{****}	-	0.484^{****}	-	0.462^{****}	-	N.S.	-
Cu	0.713^{****}	0.688^{****}	0.402^{****}	0.467^{****}	0.742^{****}	0.497^{****}	0.737^{****}	N.S.
Pb	0.765^{****}	0.697^{****}	N.S.	0.270^{****}	$0.714^{P,\ ****}$	0.530^{****}	0.624^{****}	N.S.

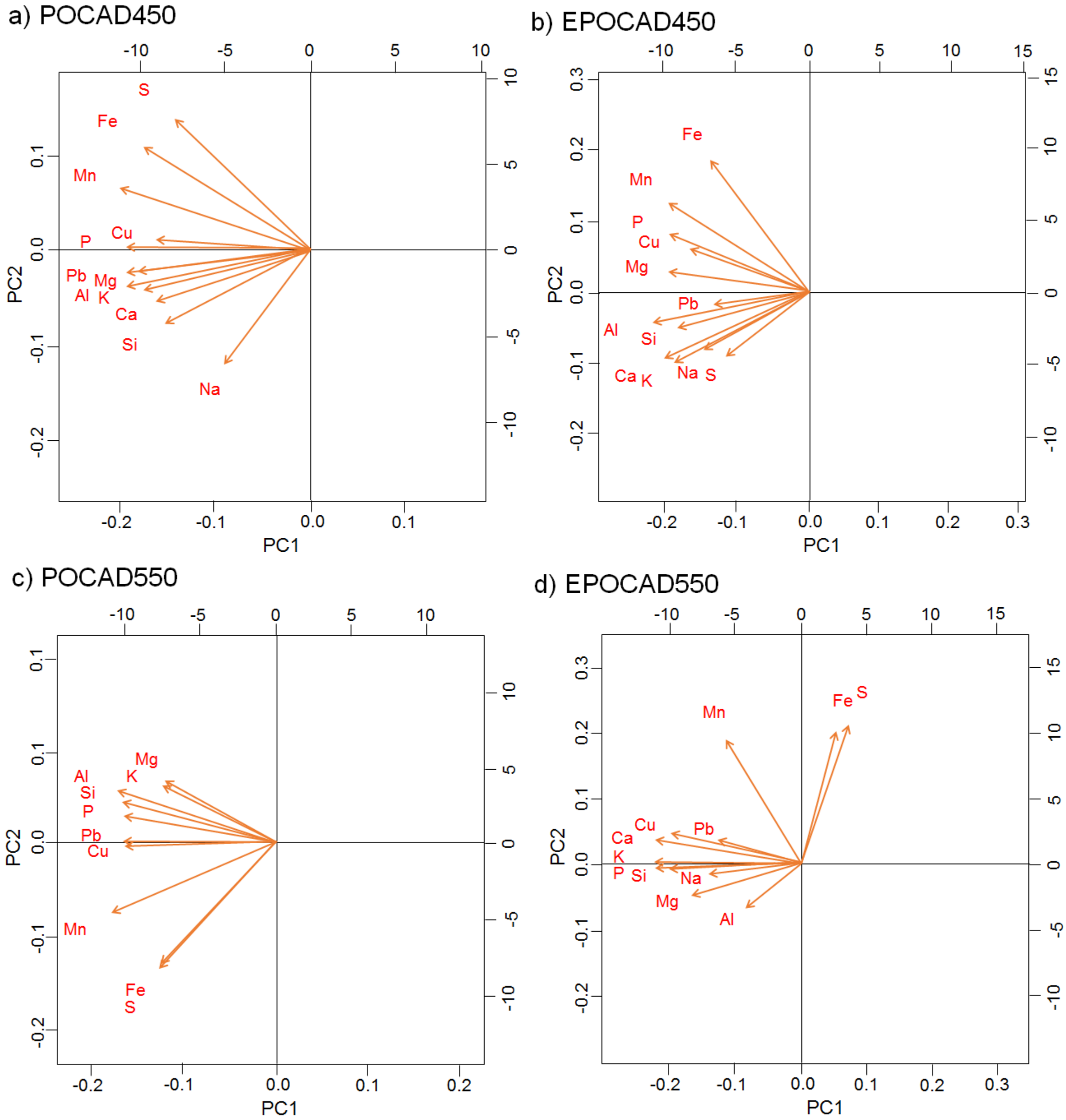

Figure 3.2 Principal component analysis of LA-ICP-MS spectral data obtained from a) POCAD450 b) EPOCAD450 c) POCAD550 and d) EPOCAD550. For each analysis n = ~220. The bar plots show proportion of variance of each principal component identified in the analysis, with further details provided in Tables 3.9-3.12. The adjacent plots how the distribution of samples along the first and second principal component axes, with arrows indicating the direction of the relevant vectors.

EDX mapping was used to visualise the co-location of elements in SEM images of EPOCAD450 in a spot identified as carbon framework with mineral deposits (and representative of other sites with similar morphology) (Figure 3.5). The map shows clear separation of the carbon-rich area from other elements aside from O. The mineral deposits were shown to contain predominantly P, Si, Al and O. EDX mapping of a spot on POCAD550 (Figure 3.6) highlights the general elemental heterogeneity of the external surfaces of the biochars observed during the SEM analyses. The maps show the location of native P relative to other elements. Compared to EPOCAD550, a lower proportion of C was measured at the surface of POCAD550. The same was observed for EPOCAD450 compared to POCAD450. Aluminium, P, Fe and O were present across the whole spot of POCAD550 mapped in Figure 3.7, but were also concentrated in small 1–10 μm domains. Calcium was found to be located diffusely across the right side of the image, but only in concentrated domains to the left. Sulfur, Si and Mg were predominantly found in concentrated phases. The relative distribution of P, C, Ca, Si, Al and Fe can be seen in the overlay maps at the bottom of Figure 3.8 which supports the findings of Ca, Si and Al co-variation and Fe and P covariation in the LA-ICP-MS analysis of POCAD550 in Figure 3.2. Additional structural and chemical detail can be found in additional SEM images, EDX spectra and maps in Figures 3.9 – 3.12.

Table 3.9 Output of the principal component analysis of LA-ICP-MS data for POCAD450. PCA was calculated from 219 individual measurements.

POCAD 450			
	PC1	PC2	PC3
Standard deviation	2.727	1.1468	0.91127
Proportion of Variance	0.7761	0.1373	0.08666
Cumulative Proportion	0.7761	0.9133	1
Loadings	PC1	PC2	PC3
Na	-0.814		0.346
Mg	-0.21		-0.241
Al			-0.463
Si	-0.129	-0.198	-0.439
P	-0.176	0.19	-0.202
S		0.654	0.147
K	-0.343		-0.122
Ca	-0.32		-0.156
Mn		0.381	-0.165
Fe		0.565	
Cu		0.103	-0.39
Pb	-0.106		-0.366

Table 3.10 Output of the principal component analysis of LA-ICP-MS data for EPOCAD450. PCA was calculated from 222 individual measurements.

EPOCAD450						
	PC1	PC2	PC3	PC4	PC5	PC6
Standard deviation	2.45	1.28	1.04	0.910	0.873	0.737
Proportion of Variance	0.553	0.151	0.0988	0.0763	0.0703	0.0501
Cumulative Proportion	0.553	0.705	0.803	0.880	0.950	1
Loadings						
Na						
Mg						
Al						
Si						0.996
P						
S			-0.958			
K	-1					
Ca						
Mn		0.706	0.195			
Fe		0.708	-0.192			
Cu				-0.999		
Pb					-1	

Table 3.11 Output of the principal component analysis of LA-ICP-MS data for POCAD550. PCA was calculated from 222 individual measurements

POCAD550					
	PC1	PC2	PC3	PC4	PC5
Standard deviation	2.49	1.23	1.06	0.916	0.748
Proportion of Variance	0.606	0.149	0.109	0.0819	0.0547
Cumulative Proportion	0.606	0.755	0.864	0.945	1
Loadings					
Na				0.908	0.12
Mg	0.175				0.826
Al	-0.385				0.244
Si	-0.184			0.101	0.373
P	-0.56				
S		-0.629			
K			0.615	-0.323	0.243
Ca			0.769	0.228	-0.164
Mn	-0.18	-0.435			
Fe		-0.628			
Cu	-0.516				
Pb	-0.402				

Table 3.12 Output of the principal component analysis of LA-ICP-MS data for EPOCAD550. PCA was calculated from 222 individual measurements.

	EPOCAD550					
	PC1	PC2	PC3	PC4	PC5	PC6
Standard deviation	2.32	1.52	0.983	0.889	0.842	0.712
Proportion of Variance	0.505	0.217	0.0902	0.0738	0.0663	0.0474
Cumulative Proportion	0.505	0.722	0.812	0.886	0.953	1
Loadings						
Na				-0.947		
Mg						-0.95
Al			-0.998			
Si	-0.334			0.169		-0.268
P	-0.456					
S		0.605				
K	-0.441					
Ca	-0.4					-0.107
Mn	-0.302	0.501				
Fe	0.118	0.602		-0.189		
Cu	-0.453					
Pb					-0.997	

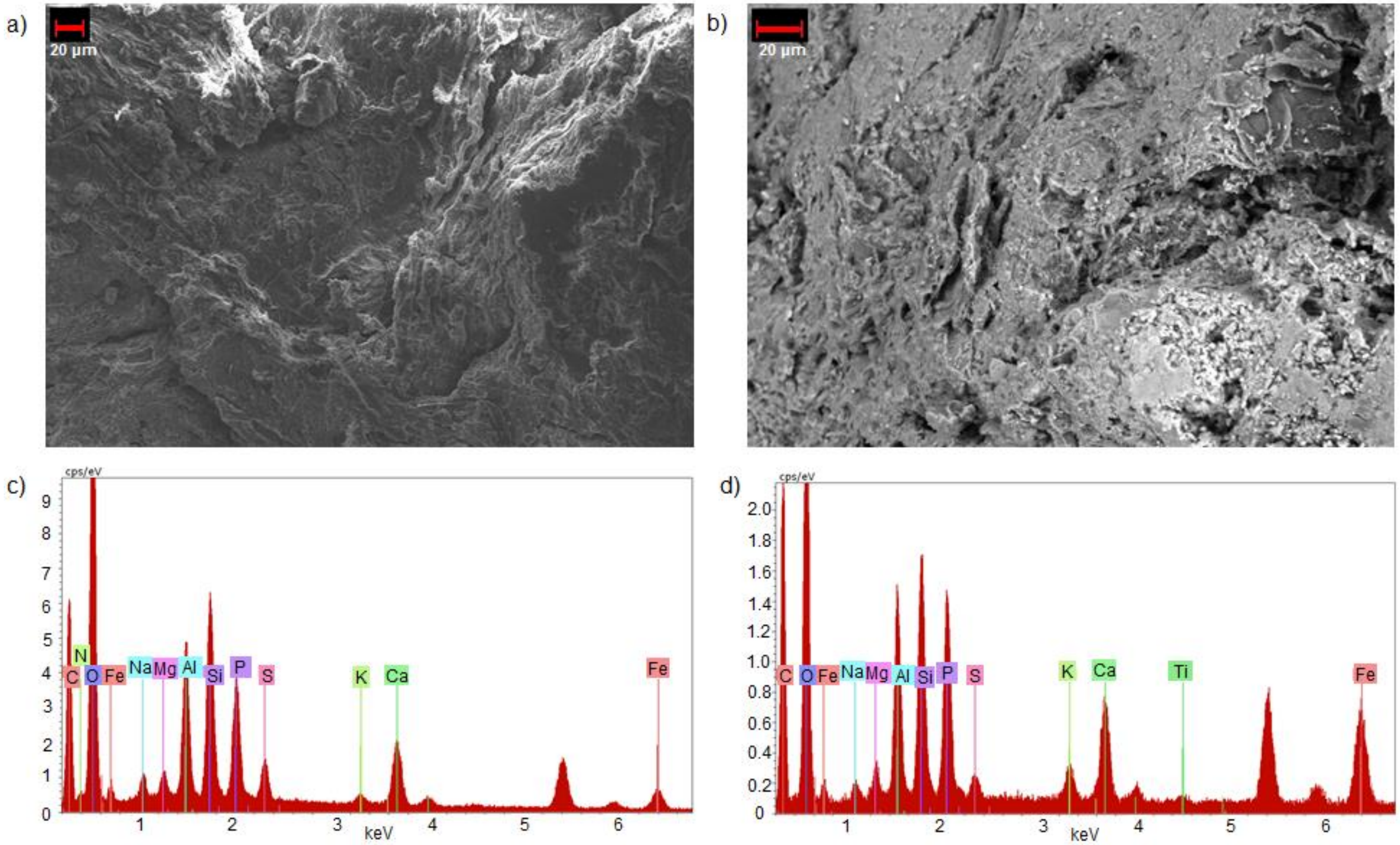

Figure 3.3 SEM and EDX spectrum of PAD450 (a,c) and EPAD450 (b,d) showing differences in surface morphology pre (PAD450) and post (EPAD450) P exposure.

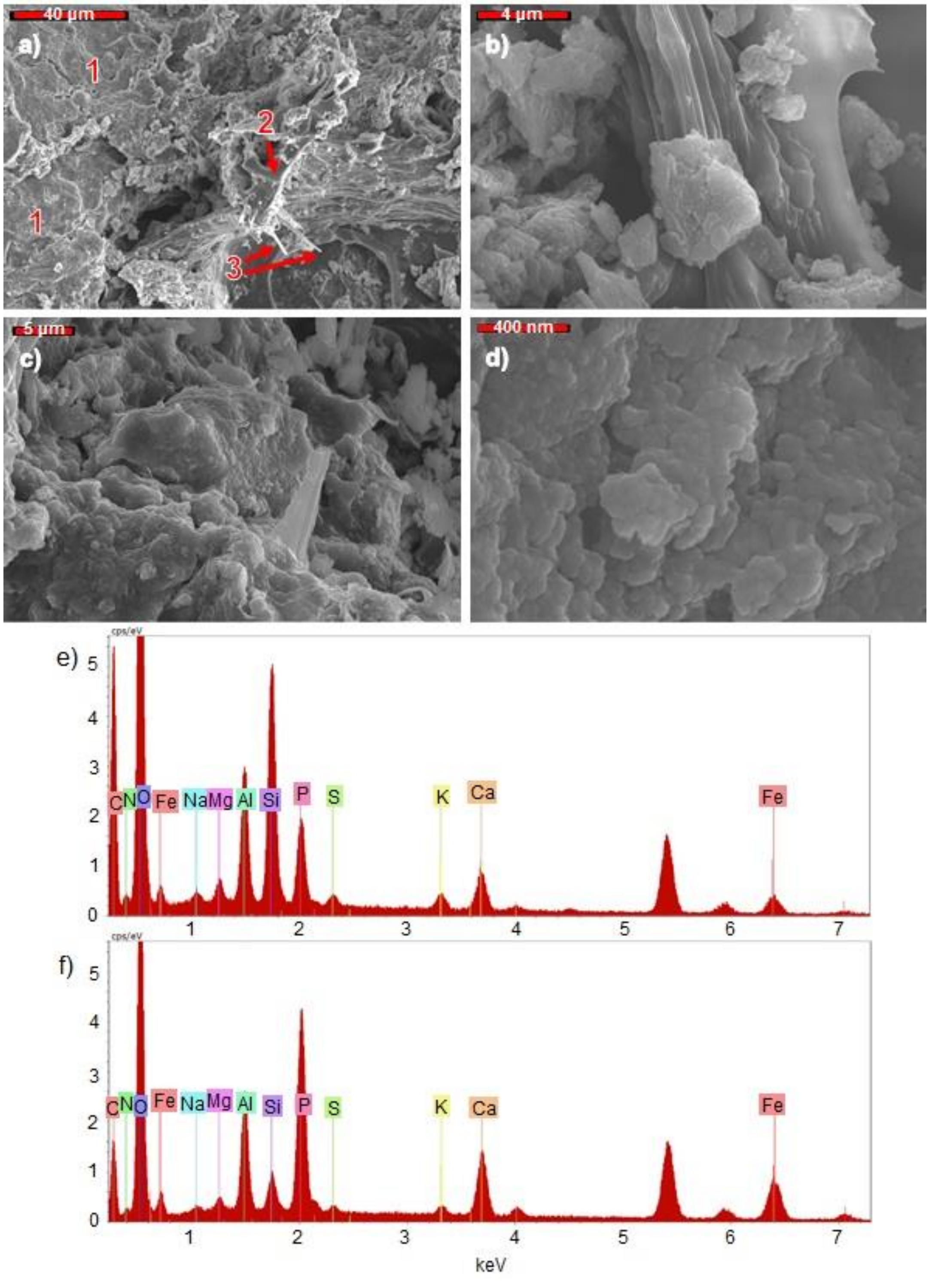

Figure 3.4 SEM-EDX data obtained from EPOCAD450. SEM image a) shows clay mineral phases (1), exposed carbon lattice (2) and newly formed or exposed mineral phases (3). SEM image b) shows mineral particles around the carbon lattice. Image c) shows the heterogeneous nature of the surface, and EDX spectrum d) shows the elements present in c), e) shows high magnification SEM image and EDX spectra of P deposits on the surface of EPOCAD and f) shows the elements present in e).

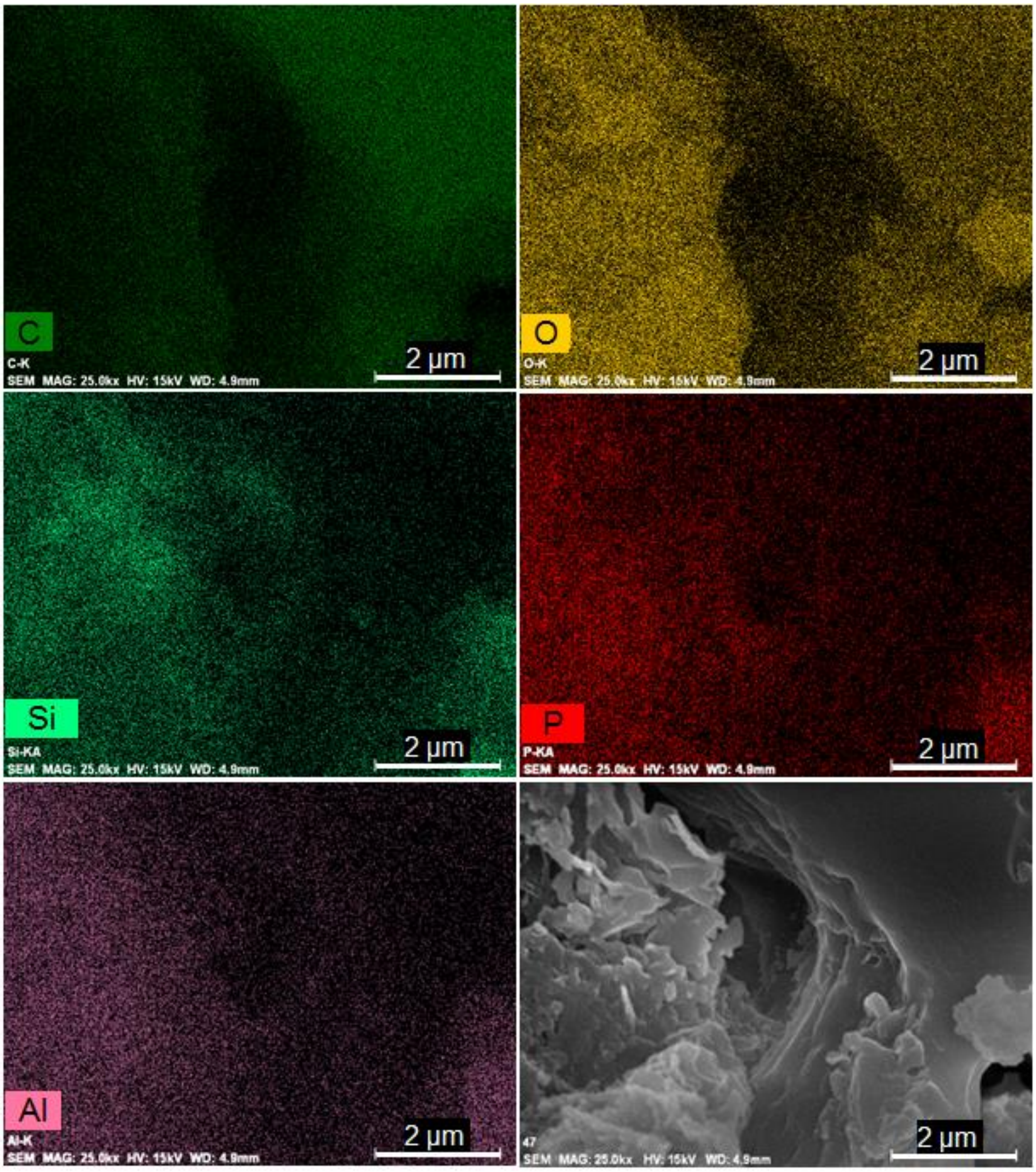

Figure 3.5 SEM-EDX map of EPOCAD450, showing spatial separation of C with O, Si, P and Al.

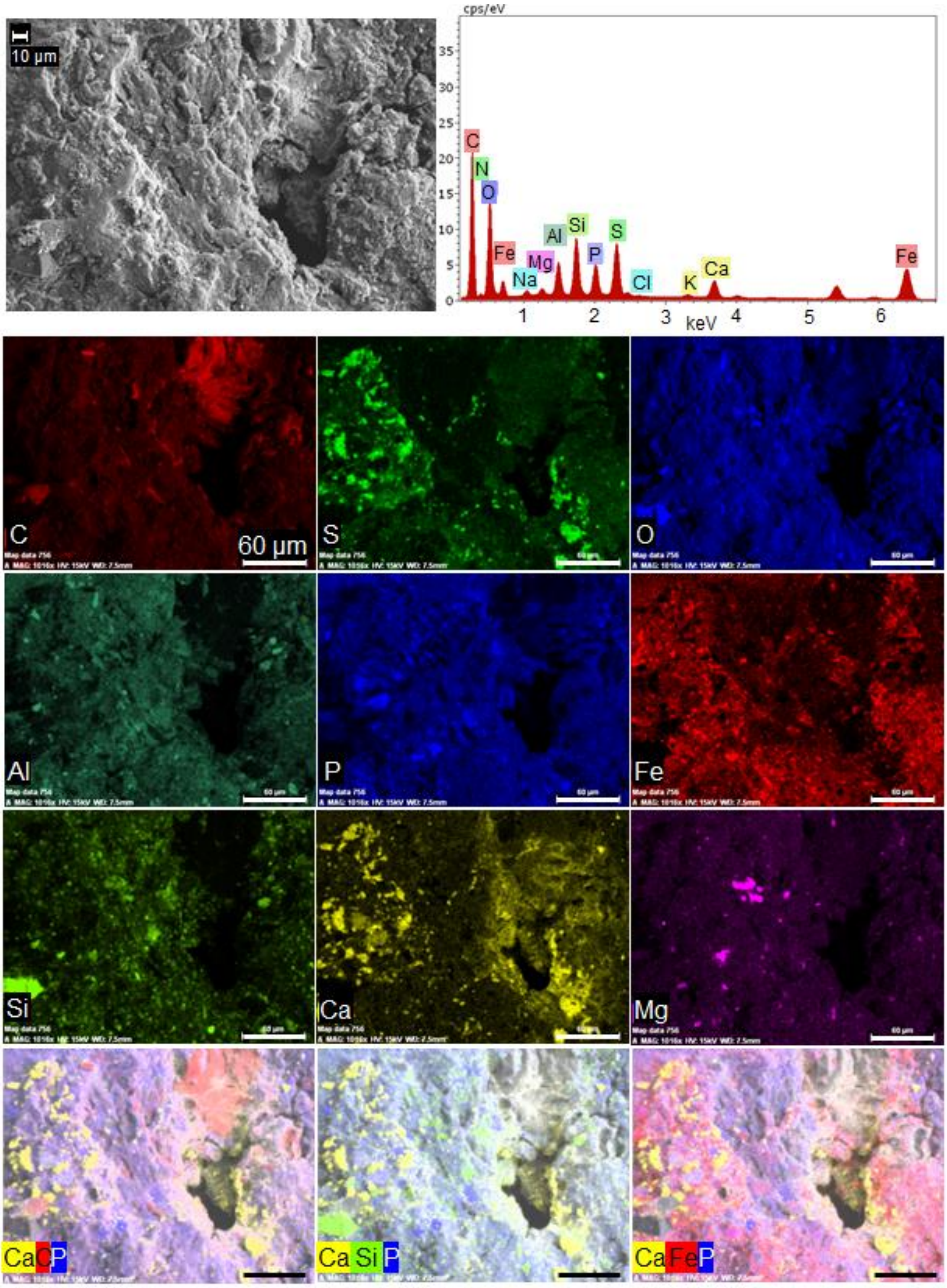

Figure 3.6 SEM-EDX map of POCAD550, showing the localisation of native P (centre), as well as C, S, O, Al, Fe, Si, Ca, and Mg. Overlay maps of C (red), Ca (yellow) and P (blue); Ca (yellow), Si (green) and P (blue); and Ca (yellow), P (blue) and Fe (red) are also shown.

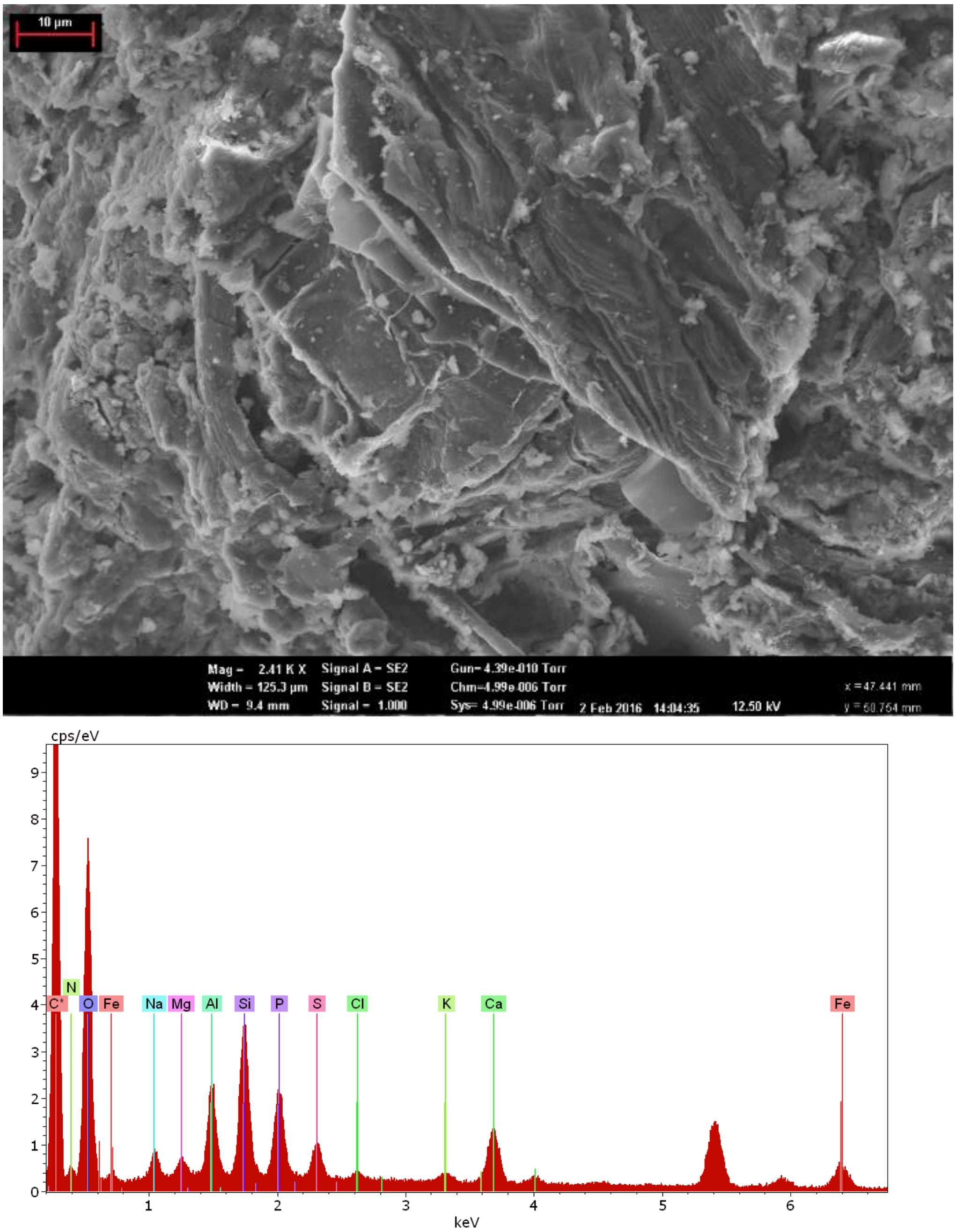

Figure 3.7 SEM image and EDX spectra of the surface of PAD450

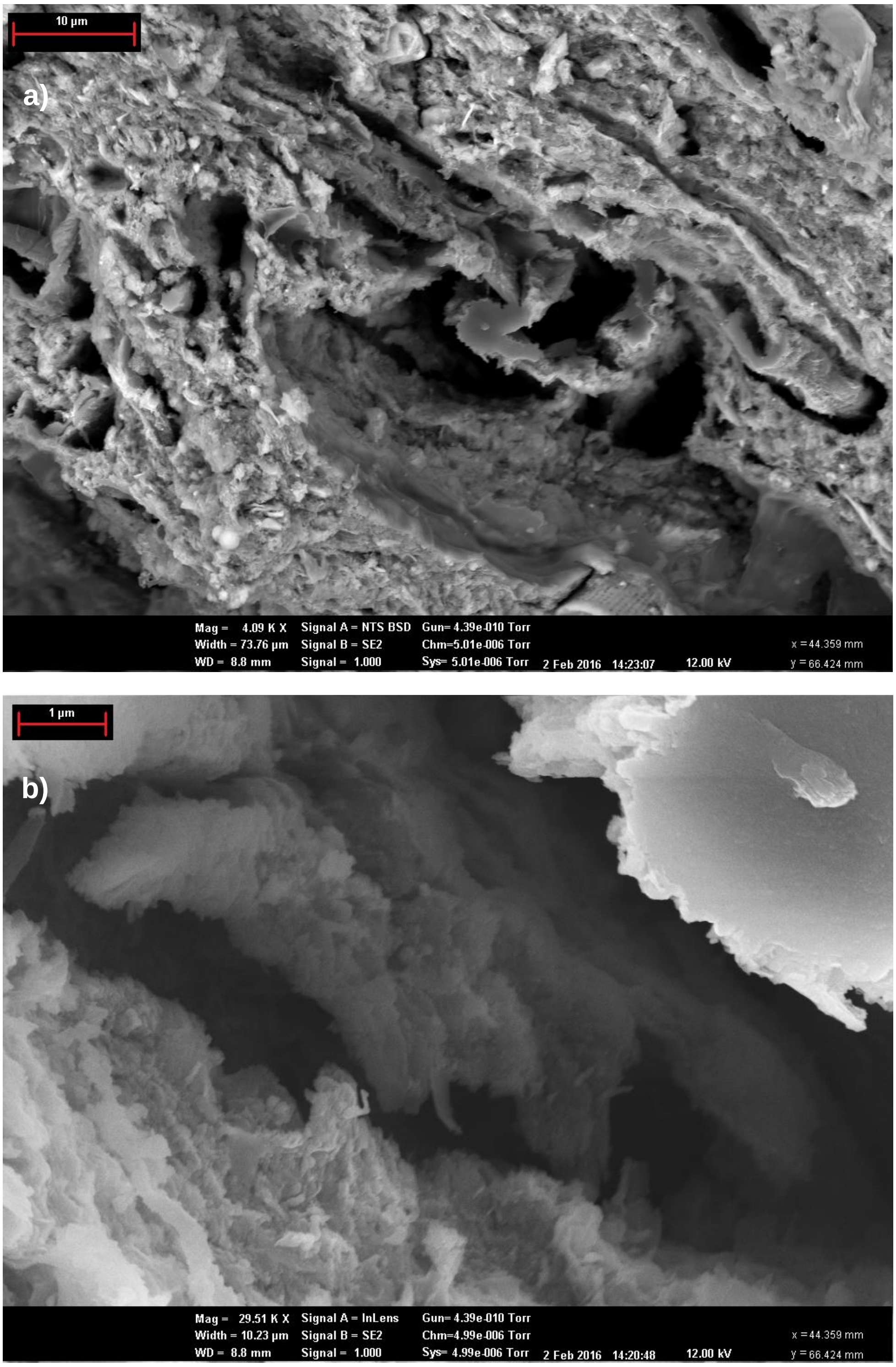

Figure 3.8 SEM image of a) the surface of EPAD450 and b) inside a pore of EPAD450

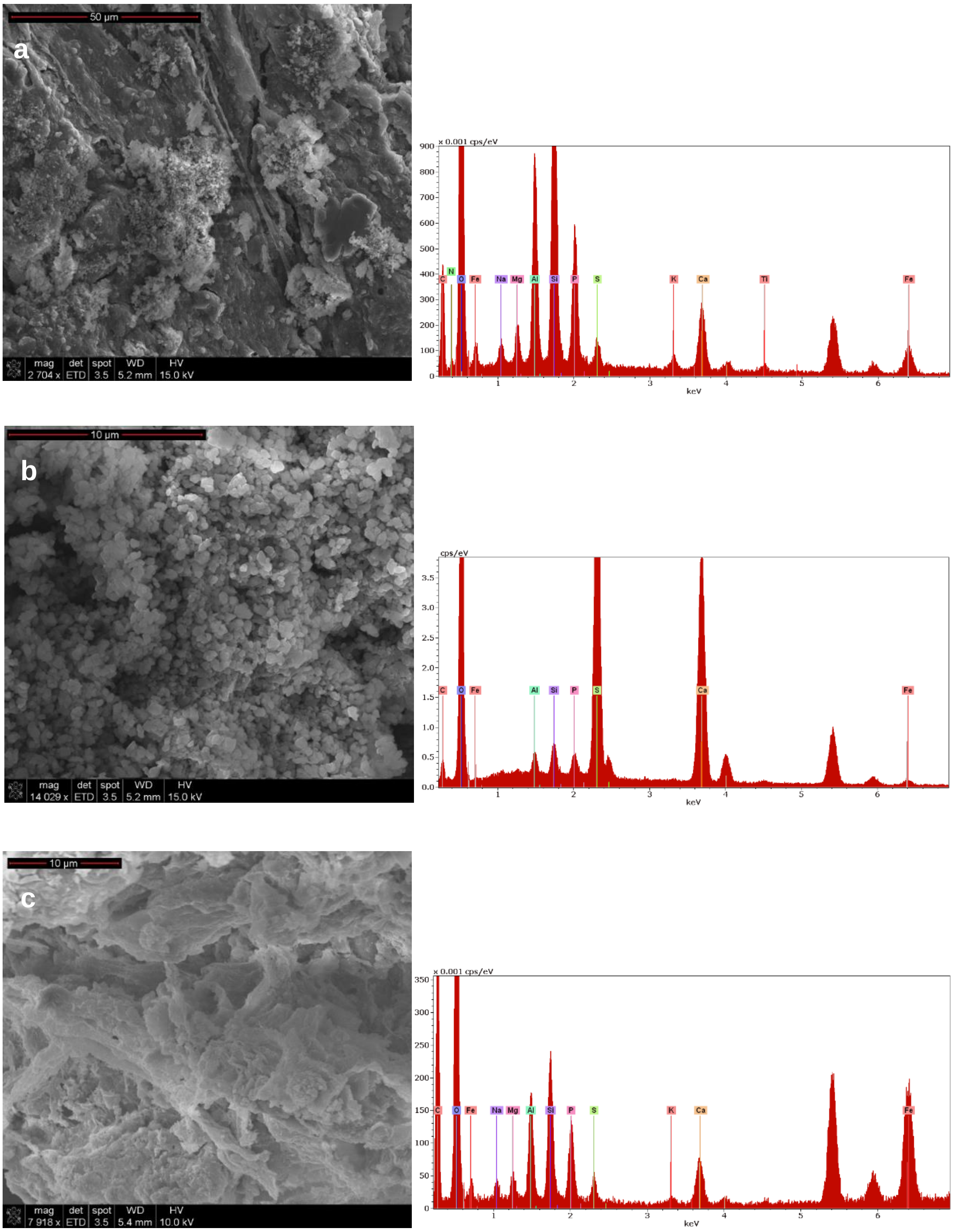

Figure 3.9 SEM image and EDX spectra of a) the surface of POCAD450 b) a mineral phase on the surface of POCAD450 and c) a surface on another particle of POCAD450

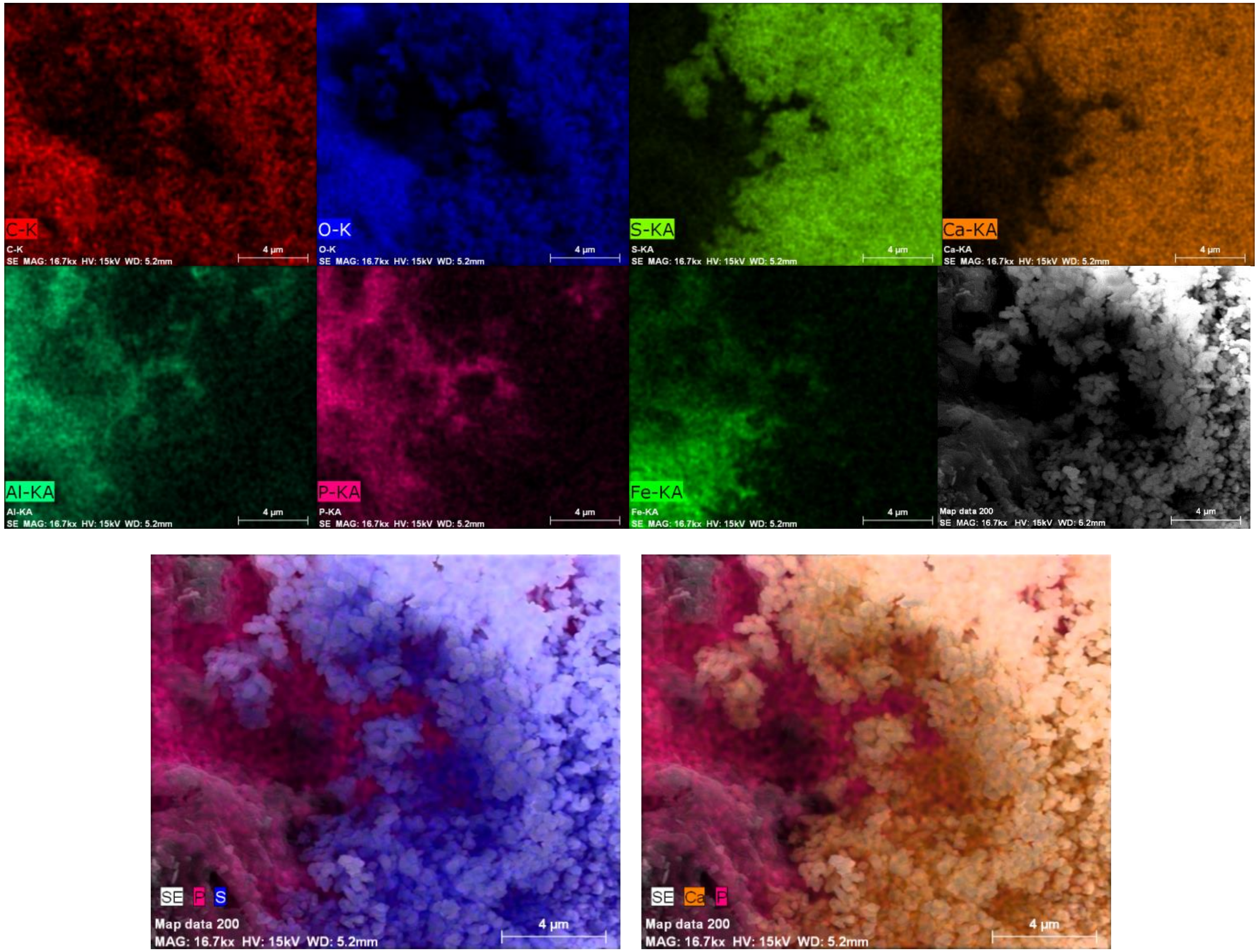

Figure 3.10 SEM-EDX map of the interface between the biochar surface of POCAD450 and the crystal phase identified in Figure 3.9 b), including two overlay maps showing the spatial separation of P with S and Ca.

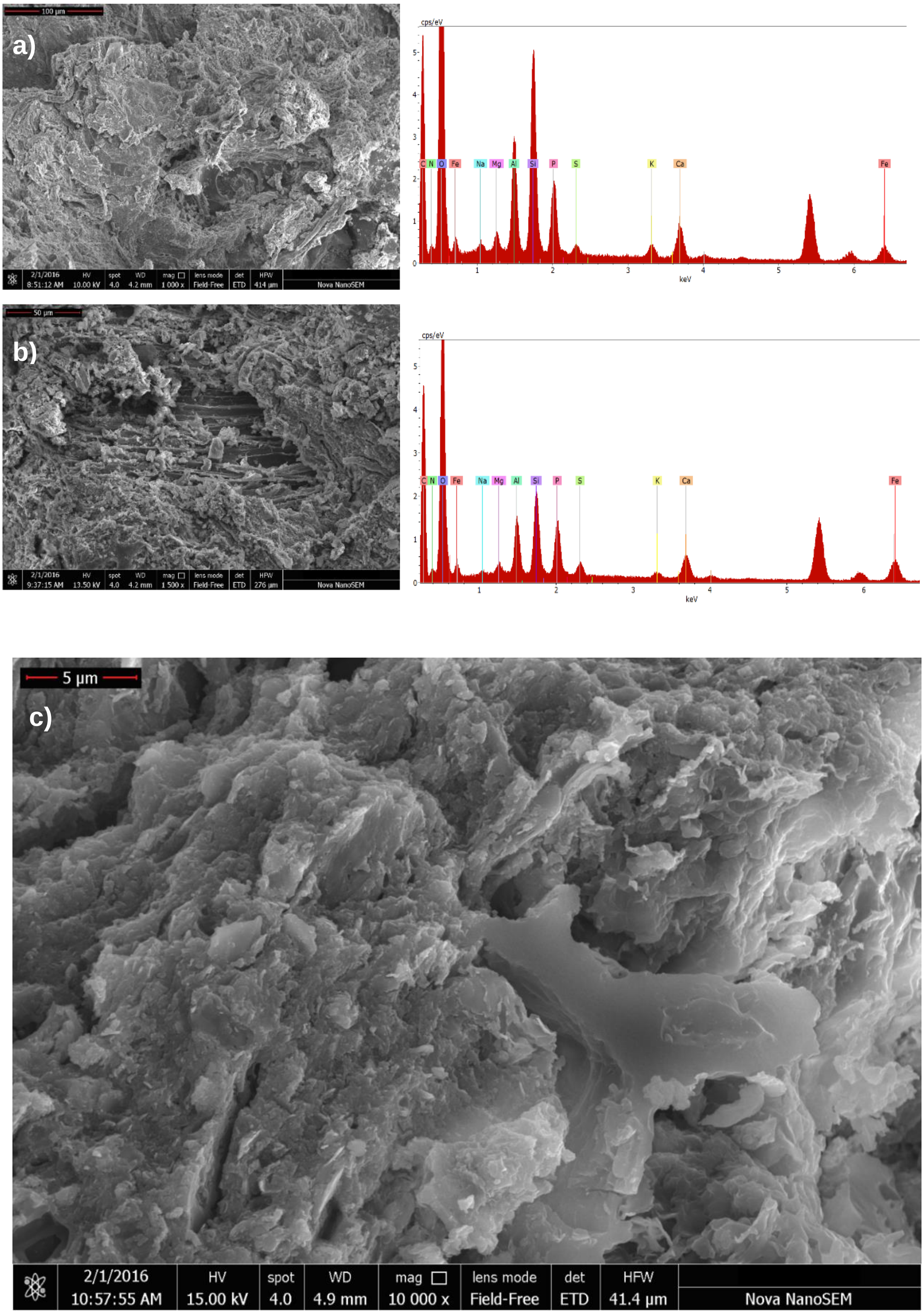

Figure 3.11 a) and b) SEM images and EDX spectra of the general surface structure of EPOCAD450, and c) SEM image of EPOCAD450 showing the exposure of the carbon lattice after P exposure.

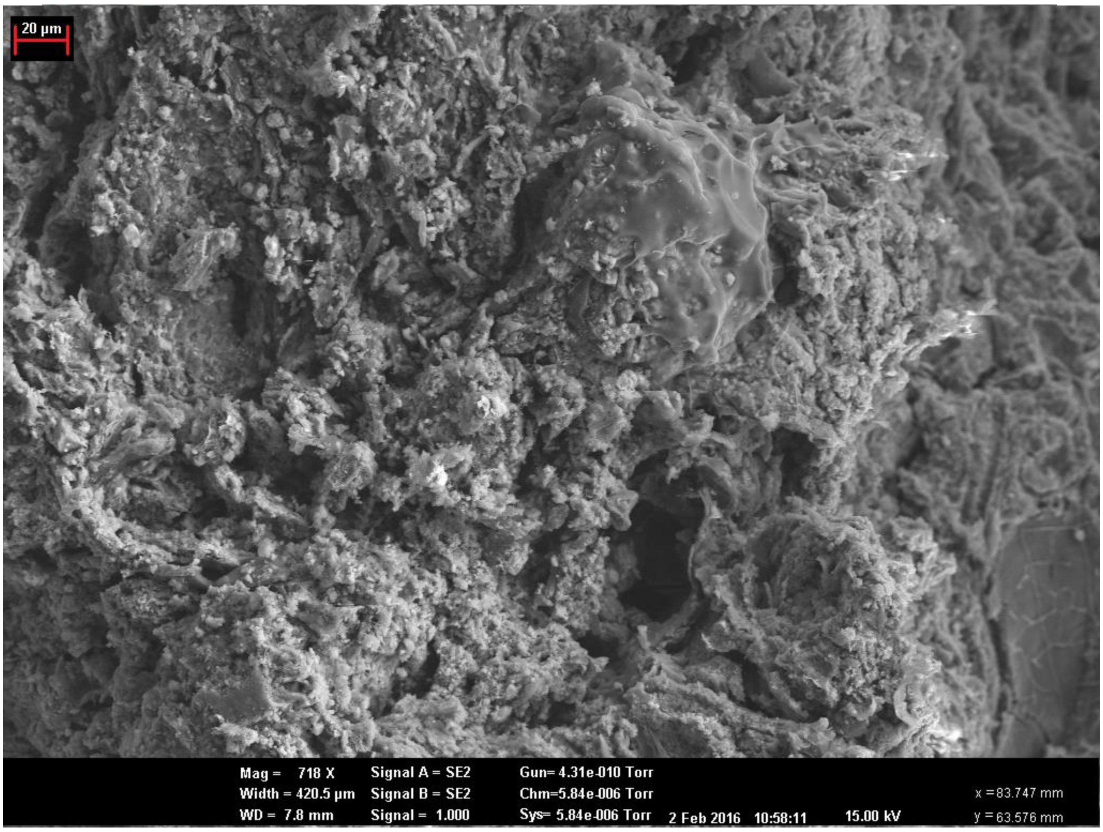

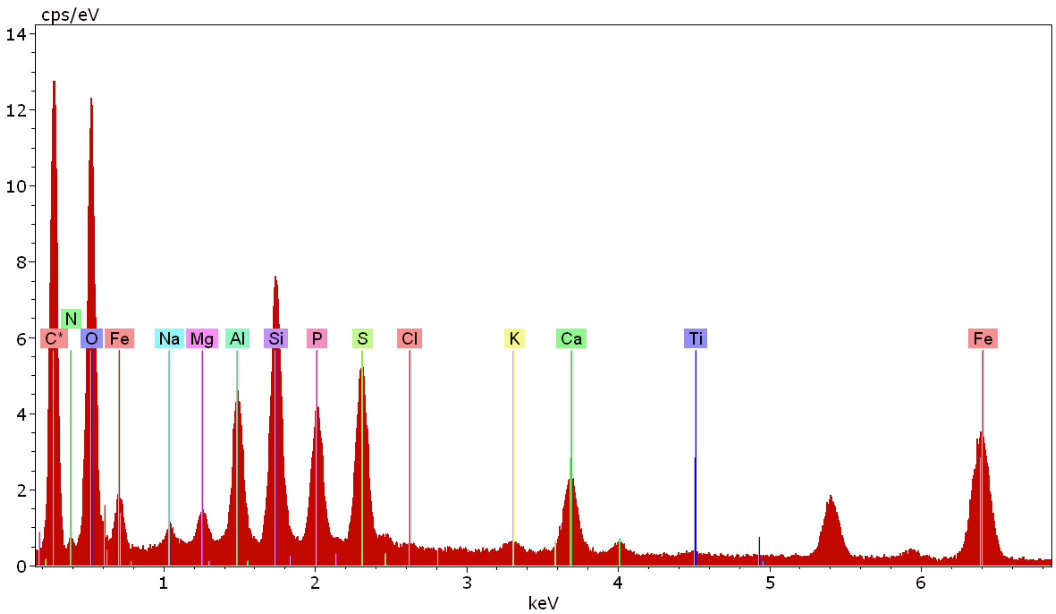

Figure 3.12 SEM image and EDX spectrum of the general surface of POCAD550

3.4 Discussion

3.4.1 Effect of feedstock composition, processing and pyrolysis conditions on P capture

The results of this study demonstrate that the interaction of P (as phosphate) with sewage sludge-derived biochar is not a simple process which can be described by one specific mechanism or element within the biochar matrix. At the macroscale (i.e. the particle scale – mg and mm), each specific sewage sludge/ochre biochar material is quite homogeneous, as demonstrated by the low standard deviations of replicated determinations of total element composition by ICP-OES analyses of sample digests (Tables 3.2 and 3.3) and of P uptake in the experiments with more uniform material size (Chapter 2). This reflects sufficient feedstock blending and indicates that the pyrolysis process has occurred uniformly throughout the materials. In contrast, the results of the XRD, SEM and LA-ICP-MS analyses highlight the microscale heterogeneity of the materials. Although microscale heterogeneity is not necessarily important for overall P capture capacity, more detailed studies of biochar microscale structure in future work would provide better insights into mineralogy, which may further assist in the selection of optimal HTT and feedstock blends for P capture and release, especially when mineral wastes of variable composition are used as the source of P-reactive elements.

3.4.1.1 Iron plays a key role in P capture for biochars produced at 450°C

Relatively small additions of ochre (10 % w/w) in the feedstock increased the Fe concentration in pelletised POCAD biochars by 54–61% compared to the sewage sludge-only equivalents (PAD). This is important, as Fe was the only element found to be strongly and significantly correlated positively to P uptake after 5 days exposure to P.

Considering the findings of Sibrell et al. (2009) examining P capture in ochres with differing chemical compositions, it is possible that the superior P capture characteristics demonstrated by AD450 could be related to the relatively equal content of Al and Fe in AD450 compared to AD550 (1:1.12 vs 1:1.6). Although the ochre-containing biochars captured more P from 5 days repeated exposure to a 20 mg l^{-1} solution, the mean P capture by AD450 was slightly higher (though not significantly) than that of OCAD450 from both the 800 mg l^{-1} P (9.72 ± 0.657 mg P g^{-1} compared to 9.37 ± 0.872 mg P l^{-1}) and the 3 g l^{-1} P solutions (25.9 ± 5.10 mg P g^{-1} compared to 20.4 ± 6.35 mg P g^{-1}). This indicates that, although a greater concentration of Fe may increase the rate of P capture at low concentrations of external P solution, a balance of Al and Fe may favour the reaction kinetics for P removal at higher external P concentration (Ainsworth et al., 1985). This is an important consideration for feedstock design, as mineral waste rich in Al may be more suitable for combination with Fe-rich sewage sludge than iron ochre for applications targeted at capturing P from high concentration P sources, but only if they are to be used in non-acidic soils, or in conjunction with liming treatments to mitigate Al toxicity to plants. Al was strongly and significantly correlated with P before and after P exposure in the LA-ICP-MS analyses, further indicating the importance of Al for P capture by biochar.

3.4.1.2 Feedstock pelletisation affects elemental composition of biochar

Comparison of the newly prepared pelletised biochars and non-pelletised biochars previously described in Chapter 2 showed that pelletisation and/or continuous (rather than batch) pyrolysis processing results in greater overall retention of elements within the biochar matrix, relative to carbon. This is most likely due to a reduction in the loss of material to the gas phase, or a different trajectory of pyrolytic reactions in the continuous-flow furnace compared to the gradual heating process in a batch kiln. Rapid expulsion of gases from the pellets as the cold feedstock reaches the hot continuous-flow kiln may result in different pyrolytic reactions than if the feedstock was slowly heated to the same temperature, similar to the reported explanation for the differences between gas, oil and solid yield between fast and slow pyrolysis (Onay and Kockar, 2003).

3.4.1.3 Increasing highest treatment temperature changes iron oxidation state, sulfur interactions and mineral structure

Comparison of elemental variation in the first PC in the analysis of LA-ICP-MS results shows great similarity between POCAD450 and POCAD550, accounting for 77 and 61% of sample variance respectively. Covariance of Fe, S and Mn was identified in both, however the correlation of Fe and S was much stronger in POCAD550 than POCAD450 (Figure 3.2), indicating possible differences in mineral structure due to pyrolysis HTT.

The stronger relationship between Fe and S in POCAD550 compared to POCAD450 was supported by visual evidence from SEM-EDX. EDX analyses of POCAD450 revealed sites where Fe and S were covariant (as in

Figure 3.9a), and non-covariant (as in Figure 3.9b-c and Figure 3.10), whilst the same analysis of POCAD550 revealed more sites where Fe and S were found in higher concentrations together (Figures 3.11 and 3.12). These results may suggest reduced iron species (Fe(I) or Fe(II)) are present in POCAD550, but not POCAD450 or EPOCAD450, where Fe appears to be present in Fe(III) and mixed Fe(II/III) compounds.

Considering these points together, is possible that at the 550°C HTT insoluble, reduced Fe/S compounds have formed to a greater extent than at 450°C, in addition to complex mixed mineral phases that contain both Fe and S. Further high-resolution analysis using Thermogravimetric analysis–mass spectroscopy (TG-MS), soft X-rays and Transmission electron microscopy (TEM) would be required to clarify this.

The ochre used in this study consisted of 100% goethite (Carr, 2012). When heated to temperatures between 140–500°C in the presence of air, goethite transforms to haematite by thermal dihydroxylation (Cornell and Schwertmann, 1996). Under reducing pyrolysis conditions and the presence of carbon, it is also possible that magnetite (Fe_3O_4, Fe (II)(III) oxide) and maghemite (γFe_2O_3, Fe(III) oxide) forms (Campbell et al., 1997). Thermal treatment of goethite results in the development of microporosity due to expulsion of water from the mineral lattice, creating more surfaces with which P can react. Pore sizes increase further as temperatures increase, however, as previously discussed, above 600°C the mineral sinters, which results in a large decrease in porosity (Cornell and Schwertmann, 1996). Hence pyrolysis HTTs of less than 600°C may be necessary for biochars containing large amounts of iron oxyhydroxides if high surface area and P reactivity are desired.

3.4.2 P capture processes

3.4.2.1 The role of organic functional groups on biochar surfaces in P capture

Despite the modest pyrolysis temperatures used in this study, SEM-EDX mapping and XPS analysis did not provide strong evidence for C-O-P bonding, or carbon functionality generally. It has been suggested that phosphate could undergo ligand exchange with hydroxyl or carboxyl groups on the surface of the biochar carbon lattice (Laird and Rogovska, 2015), however ligand exchange reactions only occur in metal complexes. Synthesis of the proposed phosphoester species proceeds via a condensation reaction, is favoured by decreasing pH (inconsistent with biochar surfaces), and requires high temperatures, condensing agents or condensed phosphate reagents, which also require significant temperatures for synthesis (Gull et al., 2014). In biological systems (at pH values closer to 7) the phosphorylation reaction requires enzyme catalysis, so the proposed mechanisms are unlikely to occur on biochar surfaces in environmental systems unless mediated by an organism which has some biological need to perform this reaction.

There is no evidence, in this study or in the literature, to suggest that the carbon fraction of biochar plays a major role in P capture, other than providing an essential support on which the mineral elements which do interact with P can be anchored, and improving the value of the end-product for use in agriculture. A significant increase in P sorption was observed in washed compared to unwashed oak biochar (Hollister et al., 2013), however the concentration of P sorbed by even the washed biochar was quite small (0.077 mg P g^{-1}, 13.5% of the lowest amount of P captured in this study), so the effect of washing to expose carbon surfaces appears to be over-estimated. The increasingly common practice of adding chemical elements to biochar for P capture enhancement is additional evidence for this assertion (Chen et al., 2011; Fang et al., 2015; Li et al., 2016; Park et al., 2015; Ren et al., 2015; Yao et al., 2011; Zhang et al., 2013, 2012). It is evident that metal cation-mediated interactions with organic functional groups on biochar surfaces (or precipitation reactions) explain the high P capture capacities demonstrated by particular biochars.

The point of zero charge (PZC) of biochars reported in the literature are generally low (Mukherjee et al., 2011; Qiu et al., 2009; Silber et al., 2010), so it is likely that at pH > 3 biochar surfaces will be negatively charged. Theoretically, at high pH a hydroxyl or carboxyl group on the surface of biochar will be deprotonated in solution, forming an oxyanion which will be resonance stabilised by the delocalisation of electrons in the aromatic biochar structure. This makes these groups more acidic than the equivalent group in an aryl alcohol. The oxyanion will be nucleophilic, and could attack the phosphate P (capturing the phosphate from solution), which, under basic conditions, will be relatively electron poor due to the presence of two electronegative oxyanions and a C=O group. The likelihood of these two negatively charged species coming together for reaction is low, however, due to electrostatic repulsion. Cations in solution may reduce this effect but, even so, the nucleophilic attack of the phosphate P by the biochar oxyanion is also sterically hindered. The equivalent argument can be made for the potential interactions between phosphate and N-heterocycles on biochar surfaces. Whilst not chemically impossible, the likelihood is low of these reactions contributing in any significant way to P capture mechanisms in biochar materials in wastewater treatment systems.

3.4.3 Conceptual model of P capture by biochar from aqueous solution

3.4.3.1 Initial solubilisation and mobilisation of native biochar components

In the P capture experiments biochar is held in aqueous P solution buffered at pH 7. A simplified reaction mechanism for the interaction of aqueous phosphate with metal oxides on the biochar surface is given in Figure 3.13. Soluble organic and mineral compounds are presumably released into solution at a rate that depends on their proximity to the surface of the biochar (limited by pore size and connectivity) as well as their solubility in the P solution and binding mechanisms. As demonstrated for soil, the energy required for P exchange from soil water to soil particles is very similar to that of the reverse reaction (Barrow, 2015), so the direction of this reaction in biochar (i.e. P capture or release) will be similarly dictated partly by the amount of P already within the biochar structure relative to its capacity for P uptake (probably related to the concentration and composition of certain mineral components).

The initial process of solubilisation of different phases within the biochar structure is likely to open up the pore structure, as evident in Figures 3.3-3.12. It is possible that, due to the comparatively low ratio of C compared to minerals in the sewage sludge feedstock, the carbon structure will contain a range of pore sizes. Physical determinations of porosity were not undertaken in this study, but visual SEM observation supports this hypothesis. During pyrolysis non-volatile mineral elements are likely to restrict the formation of aromatic sheets and promote pore formation (Rawal et al., 2016).

XPS analysis of surface and whole samples of POCAD450 and EPOCAD450 revealed a “loss” of P, Si, Ca, N, Fe, and Na from the exterior (but not interior) surfaces after P exposure. It is possible that this reflects solubilisation and loss of these elements from the surface into solution during P exposure, but another explanation is that the elements were re-arranged on the surface after initial solubilisation, forming localised mineral complexes (Figures 3.14-15). The formation of these complexes would result in exposure of the carbon lattice, as seen in the SEM images, coupled with mineral expansion out from (rather than laterally across) exterior surfaces. In XPS analysis after P exposure mineral elements located closer to the biochar surface might not be detected owing to masking by mineral layers and thus falsely appear to been “lost”. The LA-ICP-MS results also indicate that solubilisation

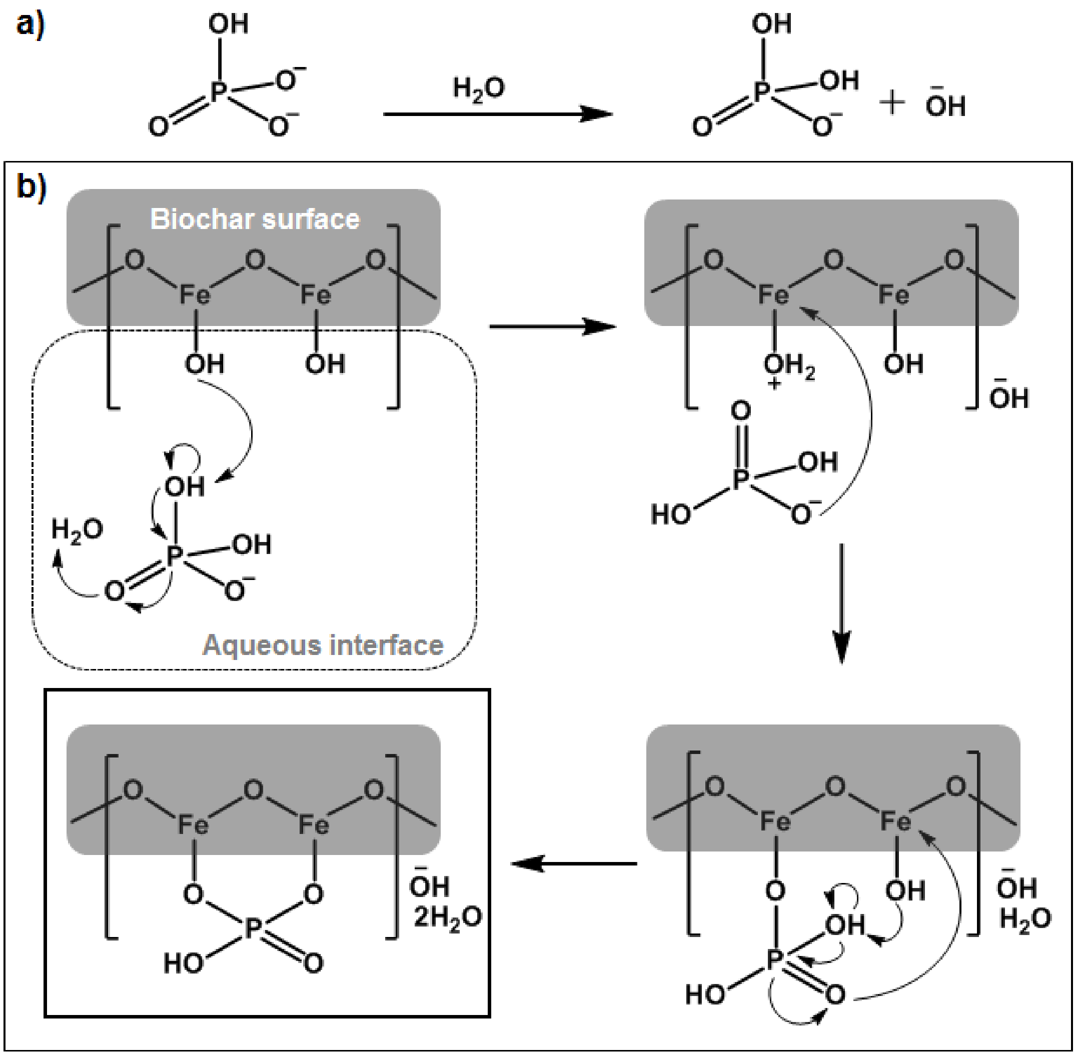

c)

$$H_2O + 2(O_x)FeOH + H_2PO_4^- \longrightarrow (O_x)Fe_2HPO_4 + 2H_2O + OH^-$$

$$2H_2O + 2(O_x)FeOH + HPO_4^{2-} \longrightarrow (O_x)Fe_2HPO_4 + 2H_2O + 2OH^-$$

Figure 3.13 Likely predominant AD sewage sludge biochar P sorption mechanism where the metal = $M^{2+/3+}$. Iron oxyhydroxides are presented based on the experimental evidence pointing to their significance in these biochars. (a) In a pH 7 buffered aqueous environment the basic phosphate species HPO_4^{2-} reacts with water to form the acidic $H_2PO_4^-$ species. (b) Deprotonation of a phosphate hydroxide moiety by the iron oxyhydroxide, followed by phosphate rearrangement and subsequent deprotonation of a water molecule, producing hydroxide, regenerates $H_2PO_4^-$ and renders the iron prone to nucleophilic attack by phosphate. The process can repeat on an adjacent ironoxyhydroxide moiety, forming a stabilised ring structure. (c) Balanced equations for the overall reaction where either $H_2PO_4^-$ or HPO_4^{2-} is the starting species.

and re-association occurred, with the number of significant correlations between P and other elements lower in EPOCAD than corresponding POCAD biochars.

The SEM-EDX, LA-ICP-MS and XRD analyses collectively suggest that non-soluble mineral phases remain on and in the biochar structure after P exposure. If this is correct, non-soluble phases anchored on biochar surfaces via soluble organic or mineral phases would become detached from the surface over time, as other phases dissolve. Minerals on the external surface of the biochar would then be lost from biochar into solution, those remaining in pores either being washed out over time or remaining trapped. Surface area to volume ratio and pore structure may affect the release of less soluble mineral phases.

3.4.3.2 Interaction of P with biochar surfaces and mobilised elements

In a solution phosphate interacts with solubilised mineral elements to form phosphate complexes which, depending on the phosphate coordination mechanism, can also interact with soluble organic compounds or organic surface-bound functional groups. Once chemically bound or precipitated onto a surface phosphate-mineral and -organomineral compounds can interact with other elements in solution. Phosphate ligands can be labile and coordinate to metals in different ways, e.g. monodentate vs bidentate coordination via O atoms (Arai and Sparks, 2001). Thus the way in which phosphate binds to the surface of biochar is dependent on the other species present and will change over time as different compounds dissolve and the local environment changes (see Figures 3.14-3.15).

3.4.3.3 Monovalent cations interrupt P capture and enhances P release

For the 20 mg l^{-1} P treatments (Chapter 2), Al, Cu, K, Na, and Zn concentrations in the biochars were all significantly negatively correlated with P capture on day 1. In addition, Pb was negatively correlated with P capture on day 5 (Table 3.4). The presence of high concentrations of mono- and divalent salts in the biochar samples that could dissolve in the P exposure experiments (Tables 3.2-3.3) may result in stabilisation of the $H_2PO_4^-$ anion in solution, reducing the rate of capture. Furthermore, K from the K_2HPO_4 used to make the phosphate solution would exacerbate this effect. Indeed the lack of similar correlations in the day 5 and 800 mg P l^{-1} treatments supports this interpretation, as by day 5 much of the K and Na will have leached from the biochar and, in the higher concentration experiments the concentration of phosphate will be much higher relative to the concentrations of K and Na leaching from the biochar. Positive correlation of Na with P release also supports this interpretation.

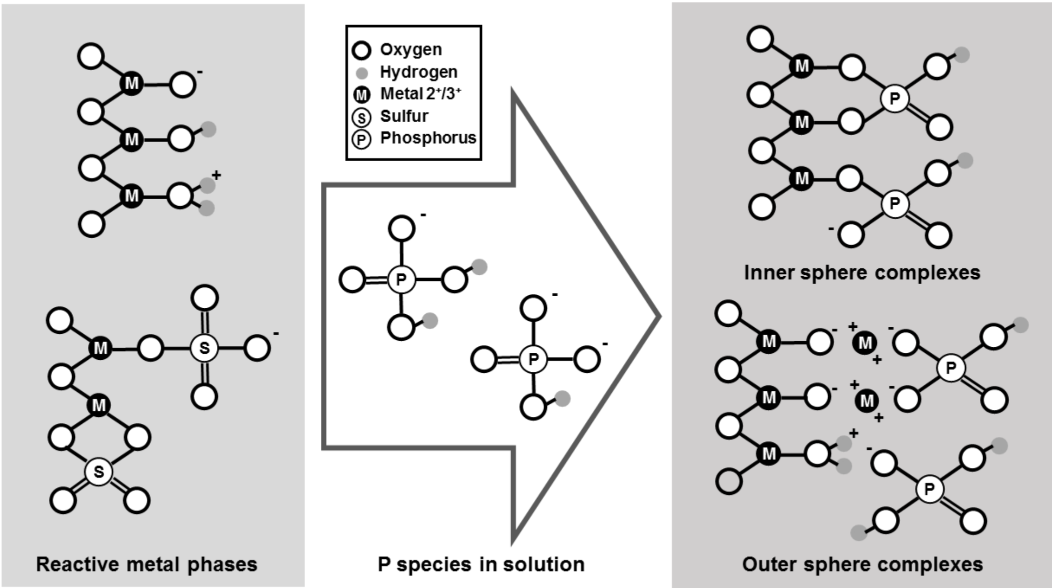

Figure 3.14 Phosphate-reactive metal phases on the biochar surfaces in these biochars. The degree of hydrogenation of the metal oxides decreases with increasing pH and is affected by the pyrolysis highest treatment temperature (HTT). Experimental observations indicate that in addition to hydroxyl ligand exchange, biochar phosphate capture also occurs at sites vacated by sulfate. These reactive sites can form inner sphere and outer sphere compounds with phosphate, with some examples shown.

In the 800 mg l^{-1} P experiments and not the 20 mg l^{-1} P experiments, however, K is negatively (but not significantly) associated with P release (Pearson's product-moment correlation = -0.636, p value = 0.175). This may be an electrostatic effect, where excess K from the higher concentration treatment (added with the phosphate solution as K_2HPO_4) interacts with the biochar surface making it more positively charged, reducing the repulsion effect that slows down P capture over time (Barrow, 2015). As ash is washed from the biochar during the experiment, more of the negative carbon functional groups of the biochar are exposed, increasing the possibility for K to interact in this way. For the higher concentration treatments at least, any effect of K on P capture and release is most likely an artefact of the experimental setup and may not be observed when the materials are used in a wastewater treatment plant.

3.4.3.4 Mixed Fe and Al minerals are involved in P capture

Biochar Fe concentration was significantly positively correlated with P capture and negatively correlated with P release. As well as P captured during the adsorption experiments, XPS analysis indicated that native P is associated with Fe in the biochars.

Phosphorus and Fe can react during pyrolysis, especially when ochre is present in the feedstock as during pyrolysis as it can act as an acid catalyst (Joseph et al., 2013). Clay, when heated, can liberate a range of chemical species including HF, HC1, HBr, H_2S and HP (Heller-Kallai et al., 1988). Interior biochar surfaces characterised by XPS showed the presence of Fe_3O_4 in both POCAD450 and EPOCAD450 as well as the surface of the latter, whilst Fe_2O_3 was only identified on the surface of POCAD450. It is possible that P exposure acts to prevent oxidation of the biochar surfaces, and that P sorption occurs without oxidising Fe(II), therefore possibly only occurring at Fe(III) sites, but additional XPS analysis would be required to fully explore these hypotheses.

For pelletised biochar from sludge–ochre mixes correlation analysis using LA-ICP-MS data showed strongly significant positive correlation between the concentration of P and Al after P exposure (EPOCAD450) or with Al, Si, K, Ca and Cu (EPOCAD550). PCA of LA-ICP-MS data for the P-exposed EPOCAD450 biochar showed that P concentration variation was related to that of Fe, Mn, Cu and Mg in the first and second PCs. Compared to POCAD450, the relationship between the variance of Fe and Mn with P was stronger whilst the relationship of P with the variance of S decreased, suggesting replacement of sulfate by phosphate as a potential sorption mechanism, which is supported by the SEM-EDX data. This was not the case for EPOCAD550, in which P concentration variation was not related to that of Fe, S and Mn in the first and second PCs, yet the relationship between the variance of Fe and S in POCAD550 was maintained after P exposure, suggesting a different mechanism of P capture compared to POCAD450. The bulk P capture for POCAD450 and POCAD550 were nearly identical (0.95 ± 0.18 mg P g^{-1} and 0.95 ± 0.23 mg P g^{-1}, respectively), so although it appears that different mechanisms predominate in biochars prepared at contrasting HTTs, the net effect on P capture is similar. The heterogeneity of the biochars and therefore P capture mechanisms most likely increases, as evidenced by the increased number of PCs in the EPOCAD compared to POCAD biochars, as well as the smaller relative contribution of PC1 in the former cases. These analyses provide information on the main sources of variation between sample locations on the biochar surface but also highlight the high amount of heterogeneity on the microscale.

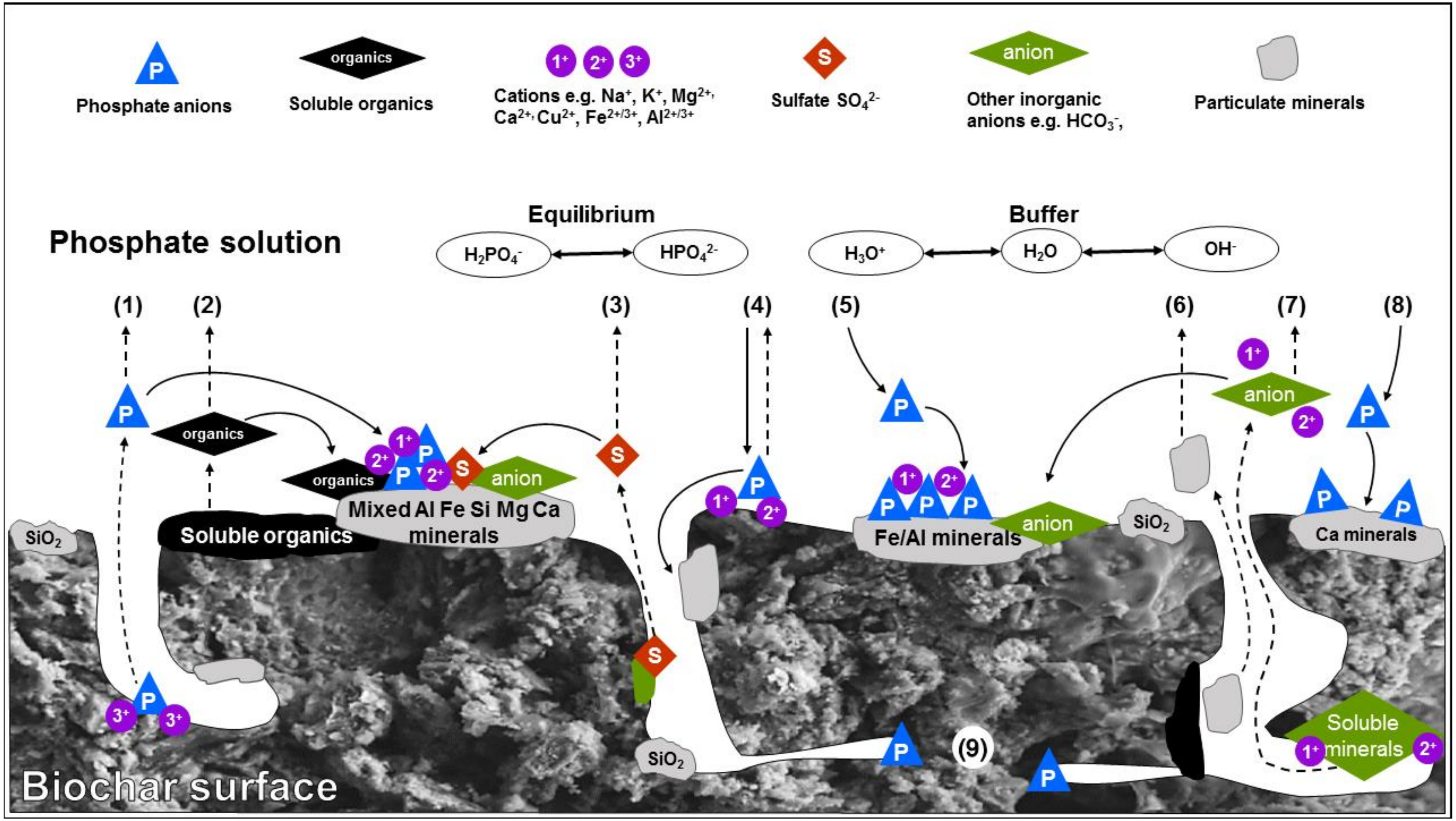

P
Phosphate anions
organics
Soluble organics
1+ 2+ 3+
Cations e.g. Na+, K+, Mg2+, Ca2+, Cu2+, Fe2+/3+, Al2+/3+
S
Sulfate SO4 2-
anion
Other inorganic anions e.g. HCO3-,
Particulate minerals
Phosphate solution
Equilibrium
H2PO4-
HPO4 2-
Buffer
H3O+
H2O
OH-
(1)
(2)
(3)
(4)
(5)
(6)
(7)
(8)
(9)
Soluble organics
Mixed Al Fe Si Mg Ca minerals
Fe/Al minerals
Ca minerals
Soluble minerals
SiO2
Biochar surface

Figure 3.15 Graphical representation of reactions which occur when biochar is placed in a pH 7 buffered phosphate solution. (1) Dissolution of phosphate from soluble ash/mineral phases. Phosphate may be released into solution or re-associate with biochar surfaces via mineral or organomineral interactions with other mixed species, such as Al, Fe, Si, Mg, Ca, K and Na in these materials. (2) Dissolution of soluble organic species from surfaces. These species may stay in solution or re-associate with species on the surfaces in organomineral clusters. (3) Dissolution of sulfate minerals (as observed in the biochars produced at 450°C). Sulfate may stay in solution or re-associate with surfaces in mineral or organomineral clusters. (4) Electrostatic association of phosphate to biochar surfaces via cation mediated interactions with surface organic functional groups. Phosphate may either be re-released into solution due to the relative weakness of the interactions or react chemically with mineral phases resulting in stronger retention. (5) Chemisorption of phosphate to iron and/or aluminium oxide phases on the biochar surfaces. (6) Release of insoluble ash and mineral phases into the aqueous phase due to weak binding or lack of binding to biochar surfaces. (7) Solubilisation of other minerals from within the biochar structure. (8) Precipitation of phosphates from solution with calcium mineral phases. (9) Native phosphate phases will be found within the biochar pore structure and will not be immediately accessible for dissolution, as per scenario (1). These phases will be released more gradually, over time.

Although Ca was only identified as strongly significantly correlated to P capture in the LA-ICP-MS analysis of EPOCAD550, as it is present at a relatively high abundance in the biochars it is likely that precipitation of P by Ca occurs in each of them to some extent. The buffered pH 7 of the system may not favour this reaction, which could explain why Ca concentration did not correlate with P capture consistently. High P capture from mallee tree biochar produced at 720°C HTT has been reported in the literature (Zhang et al., 2016). The authors suggest that the mechanism of P capture is via precipitation of P as $CaHPO_4$ by substituting for HCO_3^{2+} and OH^- on $CaHCO_3^+$ or $Ca(OH)_2$ mineral surfaces of the biochar. This seems quite likely, as the biochar had a pH of 10.2, which strongly favours Ca phosphate precipitation, and contained 1.3% Ca by weight but no Fe or Al. Importantly, whilst washing of the biochar with deionised water significantly increased P capture but did not greatly affect Ca concentration, washing with acid significantly decreased P capture, with an associated decrease of Ca content in the biochar to 0.1%. The precipitation of hydroxyapatite was observed in similar experiments obtained using cement-bound ochre to capture P from a non-buffered P solution (Littler et al., 2013).

3.4.4 Practical significance

Considered together, our results suggest that the mechanisms of P retention by biochar made from sewage sludge, although homogeneous and reproducible at the macroscale, will be highly heterogeneous at the micro and nanoscale and dependent on: (1) feedstock composition, in particular Fe and Al concentration (but also Ca and Mg); (2) pyrolysis conditions, where these affect the solubility of the mineral elements formed during the process; (3) the reactivity of the chemical elements released from the soluble mineral elements into solution during the P sorption/capture process; (4) the pH of the system, as this directly affects (3); and (5) the concentration of phosphate in solution as this will shift the equilibrium of the reaction, which has a similar activation energy in the forwards and backwards directions (Barrow, 2015).

This study has shown that pelletisation of sewage sludge leads to retention of elements within the biochar structure and/or contamination from the pelletising process compared to non-pelletised sewage sludge. This is a positive feature for retention of nutrients, but could lead to retention of potentially toxic elements (PTEs) inhibiting the environmental suitability of biochar.

Our results also highlight the importance of minerals within the biochar structure for their observed functionality in soil. When added to soil to improve soil quality in some way, biochar mineral composition should be considered in combination with the nutrient status of the biochar and the soil, as well as pH, in order to predict the effect on nutrient mobility in the system. The PZC of the different minerals is an important aspect, as this will dictate whether the mineral surfaces will be positively or negatively charged at the native pH of the biochar, controlling the interactions between these phases in biochar with nutrients or PTEs. The pH of the environment into which biochar is added will also have an effect on this, so it is important to consider when tailoring a biochar material to a specific purpose.

3.5 Conclusions

Sustainably produced biochar prepared from pelletised digested sewage sludge has an affinity for P in solution higher than activated carbon and thus potential for P capture and recycling. The inclusion of goethite-containing ochre as a minor ingredient prior to sludge prior to pelletising and pyrolysis results in biochar that captures more P than pelletised biochar from sludge only. Based on correlation analysis and surface examination, Fe and Al present in complex mineral phases containing also Si, Mg and Ca explained the P capture properties. Pyrolysis yields a greater proportion of less soluble Fe/S minerals at 550°C than at 450°C, which may result in lower P capture over the long term.

Chapter 4

Bioavailability of nutrients and potentially toxic elements from marginal biomass-derived biochar assessed in barley (*Hordeum vulgare*) growth experiments

J.G. Shepherd, W. Buss, S.P. Sohi and K.V. Heal

Published in *Science of the Total Environment* Volume 584-585 pages 448-457

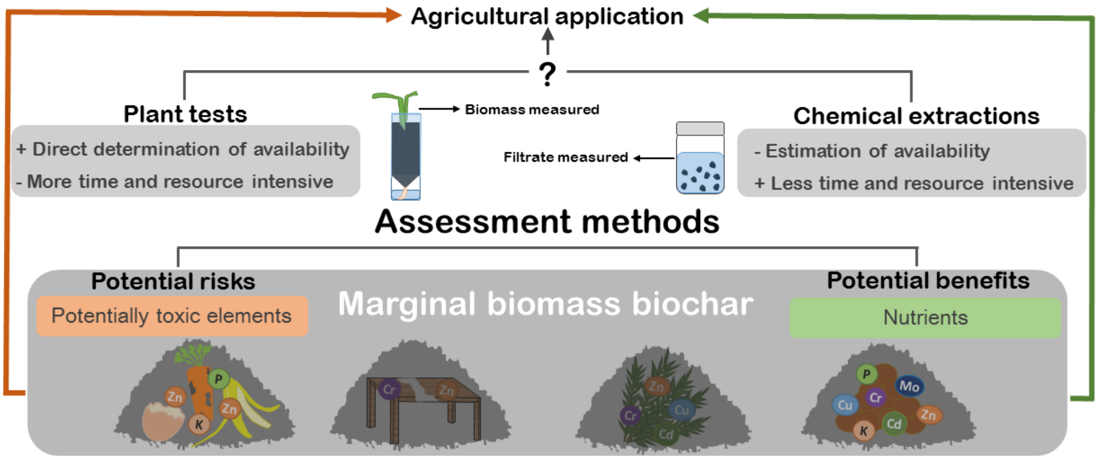

The candidate, as lead author, performed the experiments and laboratory analysis. Data analysis and writing of the paper was carried out by the candidate. Co-authors provided support and guidance on the scope and design of the project, the analyses performed and editing of the manuscript. Pyrolysis was performed by Dr Wolfram Buss, who also assisted with the experiments and ICP-OES analysis. Plant digestions were performed by Andy Gray and John Mormon. Dr Lorna Eades performed the ICP-MS analyses.

4.1 Introduction

The production of biochar from pyrolysis has potential to couple organic waste management to various improvements in agricultural systems (Shackley et al., 2011). If biochar is to become widely adopted in the long term, environmental acceptability must be demonstrated in order to address the concerns of industry and environmental regulators. Realising this potential must be underpinned by robust understanding of biochar properties, including the identification and mitigation of any risks posed to the environment. Assessment of risk initially relied heavily on analysis techniques that were developed for soils and compost. Biochar is physically and chemically distinct from these materials, however, so new protocols have been developed. Examples include a modified dry ashing method to assess total elemental concentrations (Enders and Lehmann, 2012) and extended hot toluene extraction to quantify polyaromatic hydrocarbons (PAHs) (Hale et al., 2012; Hilber et al., 2012). Measuring the bioavailability of potentially beneficial elements (nutrients) and potentially toxic elements (PTEs) in biochar also needs new protocols as methods currently used have been optimised for matrices that have very different properties to biochar.

Biochar produced from high-nutrient feedstocks, such as sewage sludge and food waste digestate, and modified feedstocks as in biochar mineral complexes (BMCs), have been suggested as replacements for traditional fertilisers (Hossain et al., 2010; Joseph et al., 2010; T. Wang et al., 2012; Wang et al., 2014). Although persistence of the carbon fraction or matrix may be desirable for carbon sequestration, nutrients, such as P and potassium (K), which unlike nitrogen (N) are predominantly preserved during pyrolysis, must be leachable or reactive towards plant exudates to be plant-accessible. If nutrient reactivity is central to an agricultural application of biochar, PTE reactivity needs to be minimised.

PTEs that may be conserved during biomass pyrolysis include chromium (Cr), nickel (Ni), zinc (Zn) and copper (Cu). Such elements must remain inert in biochar, to prevent phytotoxicity or soil pollution. Estimates for the bioavailability of PTEs in biochar require a high level of confidence. PTEs are often found to be less extractable in biochar than their parent feedstock, but their measured mobility in soil is also affected by soil-specific properties (Beesley et al., 2010; Buss et al., 2016b; Farrell et al., 2013; Khanmohammadi et al., 2015; Lu et al., 2013; Luo et al., 2014). Hence, reliable methods are required for assessing PTE bioavailability in a soils context, but where results are interpreted drawing on site-specific data such as soil composition, pH and land-use.

A variety of extraction methods have been used to estimate PTE and nutrient bioavailability of biochar and biochar–soil mixes. 'Mobile' PTEs in biochar have been measured using 0.1 M $CaCl_2$ (Méndez et al., 2012), whilst 0.01 M $CaCl_2$, ultra-pure water, 1 M NH_4NO_3, 0.5 M acetic acid and 0.05 M ethylenediaminetetraacetic acid (EDTA) were compared as estimators of plant availability of biochar PTEs by Farrell et al. (2013). Diethylenetriaminepentaacetic acid (DTPA) extraction at a relatively high pH of 7.3 has also been used, prepared using 0.01 M $CaCl_2$ and a buffering agent (triethanolamine) (e.g. Fellet et al., 2011; Lu et al., 2013; Luo et al., 2014).

Many studies have reported positive correlations between 0.01 M $CaCl_2$ (pH 7.0) and 1 M NH_4NO_3 (pH 4.6) extractable PTE concentrations in soil with uptake of PTEs by plants (e.g. Meers et al., 2007; Menzies et al., 2007; Zhang et al., 2010), including a study on biochar (Farrell et al., 2013). The German Federal Soil Protection and Contaminated Sites Ordinance (1999) stipulates the use of 1 M NH_4NO_3 soil extractions to compare against legislated threshold values for available As, Cd, Cr, Cu, Ni, Pb and Zn to assess the risk of toxicity in plants and to maintain crop quality. Correlations have also been investigated between plant uptake of nutrients and PTEs and soil bioavailability assessed using the Mehlich 3 extraction (pH 2.5) which was developed to extract P, K, Na, Ca, Mg, Mn, Zn and Cu from soils using a mixture of acid, buffer and complexing components, including NH_4NO_3 (Mehlich, 1984a). Various studies exist within the literature which assess the bioavailability of PTEs and nutrients in plant growth experiments and chemical extractions (Grzebisz et al., 1983; Monterosso et al., 1999; van Raij, 1998).

The solubility of both nutrients and PTEs in soils, a factor contributing to bioavailability, varies with the pH of the soil solution. The addition of biochar (like many other inputs) often changes soil pH, and consequently, feedstock properties, pyrolysis conditions and dose will affect the impact of biochar addition on soil pH and on bioavailability. Unless biochar is added in a high dose, however, the pH change in the soil system will not be as great as in the solutions used to assess bioavailability by extraction. Temporal control of extractant pH (at a designated pH, such as 7, or the pH of the soil to which the biochar will be added) by incorporation of a buffering agent should allow more accurate comparisons and prediction of nutrient and PTE extractability.

In addition to pH control, selection of appropriate methods for analysis should take into consideration the previous validation of methods and the number of studies and/or guidelines with which experimental results can be compared. Bioavailability assessed in plant growth experiments may be regarded as more representative than chemical extractions where soil and plants are not present, but is more resource intensive.

The purpose of the present study is to draw on established knowledge of pH, bioavailability and extraction in fertilisers and phytotoxicity contexts, to identify an appropriate protocol for bioavailability assessments in biochar. As pH is suggested as a main factor in biochar metal interactions, we compared five extraction solutions which covered a range of pH, with and without buffering, to explore fully the effect of biochar pH on nutrient and PTE bioavailability. In addition, a P-specific extraction method was tested (2% formic acid). We compared plant leaf concentrations of nutrients and PTEs to biochar extraction values to determine whether the low extractability of PTEs from biochar reported in the literature was also reflected in low bioavailability and whether high P biochars could act as P fertilisers in early plant growth stages.

4.2 Materials and methods

4.2.1 Biochar production and characterisation

The 17 biochars used in this study produced from nine different feedstocks were selected for their high content of different PTEs and nutrients. They were prepared at the UK Biochar Research Centre using the Stage II pyrolysis unit described in detail in (Buss et al., 2016a). Full characterisation data for 15 of the biochars can be found in Buss et al. (2016a, 2016b) and Chapter 3. Two of the biochars have not been described previously. These were prepared at 550°C and 700°C from rice husk grown on land in the vicinity of the Panipat thermal power station (Haryana, India). An overview of the biochars is provided in Table 4.1 General characteristics of the biochars used in this study. HTT = highest treatment temperature, PTEs = potentially toxic elements. [A] pH measured in a 1:10 ratio (m:v) in deionised water after 1.5 h shaking on an orbital platform shaker.

.

Four of the biochars (EPAD450, EPAD550, EPOCAD450 and EPOCAD550) are modified biochars which had been exposed to a P solution, to encompass captured as well as native nutrients within the study. The P-exposed biochars were created by addition of the biochars (PAD450, PAD550, POCAD450 and POCAD550) to a 20 mg l^{-1} P solution buffered at pH 7 using 0.01 M 3-(N-morpholino)ethanesulfonic acid (MOPS), parameters defined to simulate enrichment that might be achieved in a wastewater treatment plant (Chapter 2). Briefly, 30 g of each biochar with particles of diameter 0.25–15 mm were exposed to the P solution in a 1:20 solid to liquid ratio (m/v) and shaken for 24 h. After this time the solution was decanted and replaced with fresh P solution and this process was repeated for 6 days.

4.2.2 Plant growth experiments

Based on the methods of Farrell et al. (2013), spring barley (*Hordeum vulgare*) was grown in triplicate in 5% (dry mass basis) biochar/sand mixtures over 3 weeks, with five sand-only controls. No plant-free control was used as the experiment was designed to prevent leachate, therefore no analysis of leachates was to be performed The experiment was split between two batches with different biochars and dedicated controls for each batch (Control 1, Control 2 – sand only). The experimental set-up consisted of 50 ml disposable syringe tubes containing the sand/biochar mixtures, resting in 20 ml biotite containers. Five barley seeds were placed under the surface of the biochar/sand mixture in each tube (sand only in

Table 4.1 General characteristics of the biochars used in this study. HTT = highest treatment temperature, PTEs = potentially toxic elements. [A] pH measured in a 1:10 ratio (m:v) in deionised water after 1.5 h shaking on an orbital platform shaker.

Biochar	Feedstock	HTT (°C)	Post pyrolysis treatment	pH in water[A] (Mean ± 1 stdev n = 2)	Nutrients of interest (based on total concentration)	PTEs of interest (based on total concentration)	Characterised in
PAD450	Pelletised anaerobically digested sewage sludge (Edinburgh, UK)	450	None	7.49 ± 0.02	P, K	Cd, Cu, Mo, Ni, Zn	Chapter 3
PAD550	Pelletised anaerobically digested sewage sludge (Edinburgh, UK)	550	None	8.25 ± 0.08	P, K	Cd, Cu, Mo, Ni, Zn	Chapter 3
POCAD450	Pelletised anaerobically digested sewage sludge (Edinburgh, UK) and ochre (Fife, UK) in a 9:1 mass ratio	450	None	7.39 ± 0.05	P, K	Cu, Mo, Ni, Zn	Chapter 3
POCAD550	Pelletised anaerobically digested sewage sludge (Edinburgh, UK) and ochre (Fife, UK) in a 9:1 mass ratio	550	None	7.85 ± 0.03	P, K	Cu, Mo, Ni, Zn	Chapter 3
EPAD450	As for PAD450	450	Exposed to 20 mg l^{-1} P solution for 24 h x 6	-	P, K	Cd, Cu, Mo, Ni, Zn	Chapter 3
EPAD550	As for PAD550	550	Exposed to 20 mg l^{-1} P solution for 24 h x 6	-	P, K	Cd, Cu, Mo, Ni, Zn	Chapter 3
EPOCAD450	As for POCAD450	450	Exposed to 20 mg l^{-1} P solution for 24 h x 6	-	P, K	Cu, Mo, Ni, Zn	Chapter 3
EPOCAD550	As for POCAD550	550	Exposed to 20 mg l^{-1} P solution for 24 h x 6	-	P, K	Cu, Mo, Ni, Zn	Chapter 3
ADX350	Whole plant of *Arundo donax* without roots (Italy)	350	None	8.79 ± 0.44	None	Cd	Buss et al. (2016a,b)
DW550	Demolition wood (heterogeneous, glued, laminated, painted, coated or otherwise treated), (Germany)	550	None	7.65 ± 0.08	None	Cr, Cu, Pb, Zn	Buss et al. (2016a,b)
DW750	Demolition wood (heterogeneous, glued, laminated, painted, coated or otherwise treated) (Germany)	750	None	9.85 ± 0.27	None	Cr, Cu, Ni, Pb, Zn	Buss et al. (2016a,b)
FWD550	Solid residues from anaerobic digestion of food waste (UK)	550	None	8.88 ± 0.24	P, K	Cu, Zn	Buss et al. (2016a,b)
RHI550	Rice husk from plants grown on PTE contaminated land (Panipat, Haryana, India)	550	None	10.20 ± 0.15	K	Ni	n/a
RHI700	Rice husk from plants grown on PTE contaminated land (Panipat, Haryana, India)	700	None	10.40 ±0.25	K	Ni	n/a
WHI550	Water hyacinth (*Eichhornia crassipes*), whole plant, from contaminated water (New Delhi, India)	550	None	9.85 ± 0.11	P, K	Cd, Cr, Cu, Mo, Ni, Pb, Zn	Buss et al. (2016a,b)
WLB550	Willow logs with bark (*Salix* spp., species unknown) from PTE contaminated land (Belgium)	550	None	9.52 ± 0.16	None	Cd, Ni, Pb, Zn	Buss et al. (2016a,b)
WSI550	Wheat straw (*Triticum aestivum*) from PTE contaminated land (India)	550	None	10.12 ± 0.01	K	Mo, Ni	Buss et al. (2016a,b)

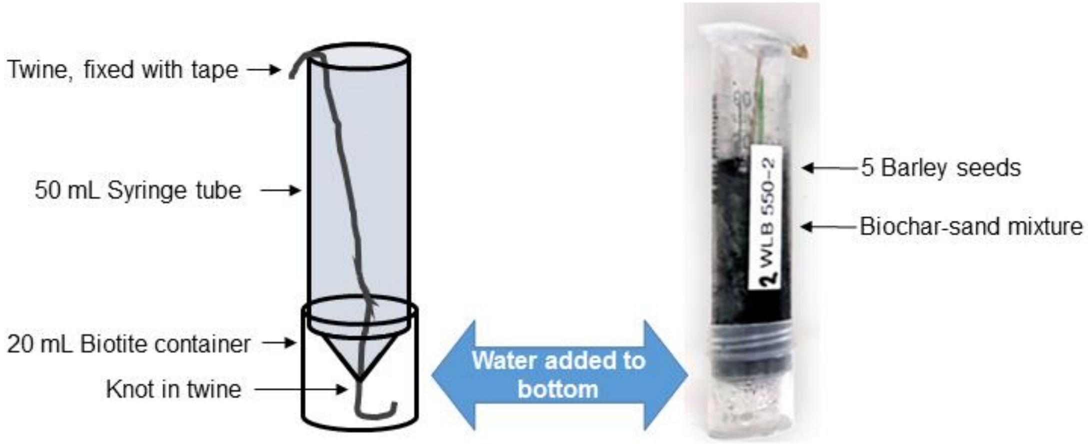

Figure 4.1 Plant growth experiment set-up

controls) and were grown in the laboratory at 20°C under constant fluorescent light for 21 days. Plants received deionised water wicked from 10 ml aliquots in the biotite containers via cotton twine inserted into the base of the syringe tube (see Figure 4.1 for a schematic diagram of the experimental set-up). This watering method was used to reduce leaching of biochar constituents out of the biochar/sand mixture, and was undertaken three times on Day 1 of the experiment as the water was taken up rapidly by the dry mixtures. Subsequently, the deionised water was replenished in the biotite containers every 2 days. At 21 days after seed planting the above ground biomass (comprising leaves only) was harvested from the tubes and rinsed in deionised water, and then oven-dried for 3 days at 80°C to determine dry biomass yield. Figure 4.2 depicts a subset of samples and controls after 21 days, immediately prior to harvest.

To assess nutrient and PTE uptake, at least 40 mg of dried biomass was digested. Where less than this amount of biomass was available, replicates were combined for DW550, EPAD450, FWD550 and WHI550. The dried biomass samples and blanks were digested with 18 M H_2SO_4 and 30% w/v H_2O_2 in a heating block at 330°C for 6 h, and analysed for As, Al, B, Ca, Cd, Co, Cr, Cu, Fe, Hg, K, Mg, Mn, Mo, Na, Ni, P, Pb and Zn using a 7500ce ICP-MS (Agilent Technologies, Santa Clara, USA). Where elemental concentrations were sufficiently high (e.g. P and Ca), ICP-OES was performed using an Optima 5300DV instrument (Perkin Elmer, Waltham, USA). Standards were prepared and run during each analysis session for calibration and to check the accuracy of measurements over time. The results for digestion blanks were subtracted from the experimental results. The limit of detection for each instrument was determined as described in Buss et al. (2016a) by analysing 10 blanks at the end of the run, but calculated for each sample due to the variable amounts of dry biomass produced in each replicate.

Figure 4.2 A subset of barley plants immediately prior to harvest on day 21 of the growth experiment

4.2.3 Buffering method development

4.2.3.1 Investigation of pH effect on extractable phosphorus

In order to determine the effect of pH and pH buffering on the extraction of elements from biochar, two UKBRC standard biochars were selected for extraction with both buffered and unbuffered 1 M NH_4NO_3 (pH 4.6) and 0.01 M $CaCl_2$ (pH 7.0) solutions. The two biochars (SWP550, produced from soft wood pellet feedstock, and RH550, produced from rice husk feedstock, both at a pyrolysis highest treatment temperature (HTT) of 550°C) were selected based on differences in their physical and chemical characteristics which would have an effect on the pH of the extraction solution. The characteristics of SWP550 and RH550 were determined as follows. Biochar pH was measured in duplicate using the method described in Rajkovich et al. (2012). Thermogravimetric analysis (TGA) was performed in triplicate using a Mettler Toledo TGA/DSC1 instrument to analyse ash content according to the method described in Buss and Mašek (2014). The biochars were digested in triplicate using a modified dry-ashing method described in Buss et al. (2016a) and phosphorus (P) determined by ICP-OES analysis of the sample digests as described in the same experiment. The results of these analyses can be found in Table 4.2.

Table 4.2 Contrasting characteristics of SWP550 and RH550 biochars relevant to the buffer testing experiment

	SWP550	**RH550**
pH	7.91 ± 0.30	9.71 ± 0.26
Ash (wt. %)	1.25 ± 0.42	47.8 ± 2.18
Total P (mg kg^{-1})	140	1680

Based on previous buffer testing carried out in Chapter 2 and the background provided in Yu et al. (1997) and Kandegedara and Rorabacher (1999), the non-complexing ‘Better Buffers’ MOPS (3-(N-morpholino)ethanesulfonic acid) and PIPPS (1,4-Piperazinedipropanesulfonic acid) were selected to buffer the $CaCl_2$ and NH_4NO_3 extraction solutions, respectively. Initial buffer concentrations were selected based on the buffer testing in Chapter 2. Four extraction solutions were prepared, unbuffered 0.01 M $CaCl_2$, unbuffered 1 M NH_4NO_3, 10 mM MOPS in 0.01 M $CaCl_2$, and 10 mM PIPPS in 1 M NH_4NO_3. The pH of the solutions was adjusted using HCl or NaOH to bring the buffered and unbuffered solutions to the same initial pH (4.6 for NH_4NO_3, and 7.0 for $CaCl_2$).

For each replicate (four for each treatment) 10 mL of the appropriate extraction solution was added to 1 g of crushed biochar and shaken on an orbital platform shaker at 150 rpm for 2 hours. The samples were centrifuged for 30 mins at 3500 rpm, then filtered through 0.45 µm syringe filters (Millipore, Watford, UK). A subsample of each extraction was taken and analysed for pH. The extractions were analysed for P by ICP-OES using a Perkin Elmer Optima 5300DV instruments (Waltham, USA). Axial mode was used and P standards prepared and run for calibration and to check the accuracy of the measurements. The results are summarised in Figure 4.3.

4.2.3.2 Optimisation of DEPP concentration for NH_4NO_3 extractions

Analysis of the results obtained in Section 1.1 revealed that PIPPS was not an ideal buffer for NH_4NO_3 extractions at a 10 mM concentration. The pKa1 of PIPPS is 3.73, which is 0.87 units more than the desired pH of the buffered system. DEPP (N,N'-diethylpiperazine) is another Better Buffer and has a pKa1 of 4.67, which is much closer to the desired pH of 4.6.

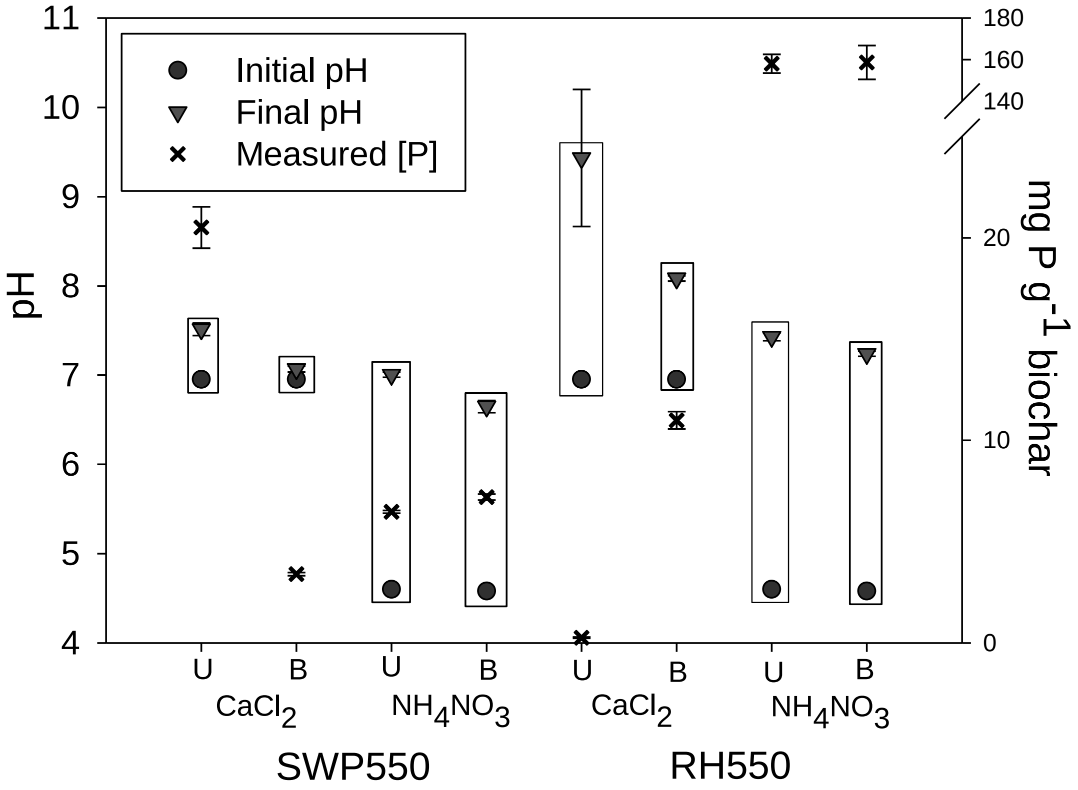

Figure 4.3 Changes in pH (y axis left) for buffered and unbuffered 0.01 M $CaCl_2$ and 1 M NH_4NO_3 extractions for SWP550 and RH550 compared to extractable P concentrations (y axis right). Each value is the mean of 4 replicates and error bars represent ± 1 standard deviation.

PIPPS was originally selected over DEPP due to its commercial availability from multiple sources, however it was clear that PIPPS would not be an appropriate buffer for the experimental system.

To determine the required concentration of DEPP for effective buffering of 1 M NH_4NO_3 extractions, solutions of the extractant containing 0, 10, 20, 50 and 100 mM of DEPP were prepared using NaOH or HCl as required to bring the pH of each solution to 4.6. As before, 20 mL of the appropriate solution was added to each treatment, in replicates of four, containing 1 g of crushed SWP550 biochar. The samples were shaken on an orbital platform shaker at 150 rpm for 2 hours and then centrifuged for 30 mins at 3500 rpm. They were syringe filtered as previously, however the extraction solution was only tested for pH, not also for extractable P The results of this experiment are given in Figure 4.4.

4.2.4 PTE and nutrient extractions

Based on a survey of the literature, two commonly used salt extractants (1 M NH_4NO_3 and 0.01 M $CaCl_2$) and one mixed component extractant (Mehlich 3) were selected. These provide relevant literature comparisons and were used to extract the 13 biochars not exposed to a P solution, i.e. all except EPAD450, EPAD550, EPOCAD450 and EPOCAD550. Buffered as well as un-buffered solutions were prepared for NH_4NO_3 (pH 4.6) and 0.01 M $CaCl_2$ (pH 7), as described in Section 4.2.3. Addition of a buffer to Mehlich 3 was not required, as it already contains a buffering agent.

The extraction solutions represent a range of pH as follows: Mehlich 3 (constantly at pH 2.5 when biochar is added), buffered 1 M NH_4NO_3 (constantly at pH 4.6), unbuffered 1 M NH_4NO_3 (starting at pH 4.6, increasing over the time of the extraction), buffered $CaCl_2$ (constantly at pH 7) and unbuffered $CaCl_2$ (starting at pH 7, increasing over the time of the extraction).Since Mehlich 3 contains a mixture of components which interact with elements via different mechanisms, factors other than pH are likely to affect the extractability of an element using this method. For the buffered and unbuffered 1 M NH_4NO_3 and 0.01 M $CaCl_2$

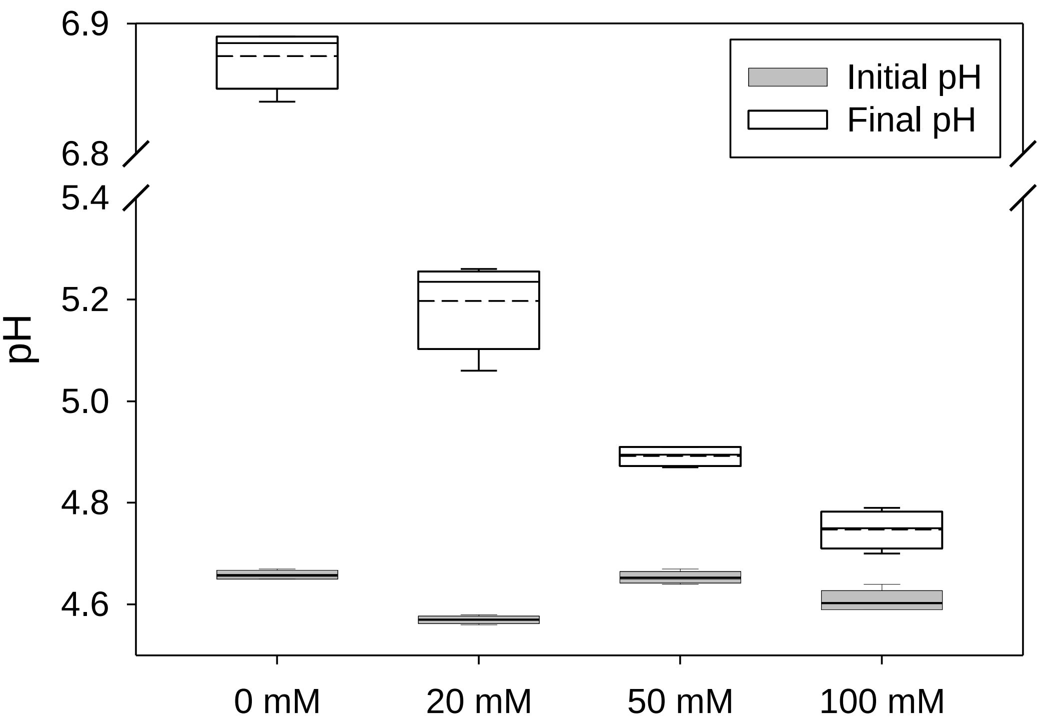

Figure 4.4 Optimisation of DEPP concentration for buffering 1 M NH_4NO_3 extractions of SWP550 biochar. DEPP buffer concentration is given on the x axis. The boxes represent the median pH (dotted line), the first quartile (lower edge of box), the third quartile (upper edge of box), as well as the minimum and maximum values (bars).

extractions, 1.5 g of biochar was weighed into a 50 mL centrifuge tube and 15 mL of the relevant extractant added. The choice of this biochar:extractant ratio is explained in Buss et al. (2016b). The extractions were performed in triplicate. The tubes were laid on their side and shaken on an orbital platform shaker at 150 rpm for 2 h, then centrifuged at 3500 rpm for 30 min and the supernatant filtered using 0.45 μm syringe filters (Millipore, Watford, UK). For Mehlich 3 extractions, the same mass of biochar and volume of extractant was used, but the mixtures were only shaken for 5 min, as per the standard Mehlich 3 procedure (Mehlich, 1984a). Due to the short extraction time, rather than centrifugation, the samples were double-filtered, first using Whatman No. 1 paper filters and then using 0.45 μm syringe filters (Millipore, Watford, UK). Blanks were prepared in triplicate for each extraction and their results subtracted from those of the experimental samples. All filtrates were stored briefly at 4°C before analysis for Al, B, Ca, Cd, Co, Cr, Cu, Fe, Hg, K, Mg, Mn, Mo, Na, Ni, P, Pb and Zn by ICP-OES using an Optima 5300DV instrument (Perkin Elmer, Waltham, USA). Most elements were analysed in axial mode, except for K and Na in the salt extracts and Al, Ca, Fe, K, Mg and Na in the Mehlich 3 extracts, which were analysed in radial mode as higher concentrations of these elements were expected. Due to the different ICP-OES analysis modes and extraction ratios used, the limits of detection for individual elements differ between the different methods. More details about the analyses and the calculation of the limit of detection can be found in Buss et al. (2016a) and their values can be found in Table 4.3 Table 4.4.

Since plant P uptake has previously been shown to correlate significantly with P extracted using 2% formic acid (2% FA) (T. Wang et al., 2012), all 17 biochars were also extracted using this method. In triplicate, 200 mg of each biochar was weighed into a 50 mL centrifuge tube and 20 mL of 2% FA was added. Reagent blanks were also prepared. The samples were shaken for 2 h, centrifuged for 30 min and syringe-filtered as described above. The extracts were analysed for soluble reactive P (SRP) by automated colorimetry (Auto Analyser III, Bran & Luebbe, Norderstedt, Germany).

4.2.5 Statistical analysis

Statistical analyses were performed using R Studio (R Core Team, 2015) with significance determined as $p < 0.05$. Data were tested for normality using the Shapiro-Wilk test. Where both sets of data being compared were normally distributed, Pearson's product-moment correlation coefficient was calculated, otherwise Spearman's rho was calculated to identify significant correlations. Plant element concentrations in above ground biomass were correlated against extraction concentrations for the same element. To investigate whether the extraction methods were behaving in a similar or different way, each was correlated against the other methods for each individual element.

To determine significant effects of biochar type in the plant uptake experiment, one-way ANOVA and Tukey HSD tests were performed on above ground biomass, plant P concentration and total above ground P mass for data in all treatments where at least 3 replicate results were obtained.

Table 4.3 Limit of detection for ICP-MS/OES analysis of digestions of plant leaves (in mg kg^{-1}) to 3 significant figures

µg/kg	**As**	**Al**	**B**	**Ca**	**Cd**	**Co**	**Cr**	**Cu**	**Fe**	**K**	**Mg**	**Mn**	**Mo**	**Na**	**Ni**	**P**	**Pb**	**Zn**
EPAD450	0.240	26.8	17.4	30.9	0.0100	0.0100	0.541	0.110	9.18	70.9	20.2	46.7	0.140	53.5	0.949	6.46	0.0501	0.240
EPAD550	0.150	16.7	10.9	19.3	0.00625	0.00625	0.338	0.0688	5.73	44.3	12.6	29.1	0.088	33.4	0.592	4.03	0.0313	0.150
EPOCAD450	0.203	22.6	14.7	26.1	0.00847	0.00847	0.457	0.0932	7.76	60.0	17.0	39.5	0.119	45.2	0.802	5.46	0.0423	0.203
EPOCAD550	0.139	15.5	10.1	17.9	0.00580	0.00580	0.313	0.0638	5.31	41.1	11.7	27.0	0.081	31.0	0.549	3.74	0.0290	0.139
PAD450	0.197	21.9	14.3	25.3	0.00819	0.00819	0.442	0.0901	4.03	58.0	16.5	38.2	0.115	43.7	0.776	5.28	0.0410	0.197
PAD550	0.160	17.8	11.6	20.6	0.00668	0.00668	0.361	0.0735	6.12	47.3	13.4	31.1	0.0935	35.7	0.633	4.30	0.0334	0.160
POCAD450	0.200	22.3	14.5	25.7	0.00834	0.00834	0.450	0.0917	4.10	59.0	16.8	38.8	0.117	44.5	0.790	5.37	0.0417	0.200
POCAD550	0.195	21.7	14.2	25.1	0.00813	0.00813	0.439	0.0895	7.45	57.6	16.4	37.9	0.114	43.4	0.770	5.24	0.0407	0.195
ADX350	0.239	7.08	17.3	30.7	0.00995	0.00995	0.537	0.109	9.11	70.4	20.0	46.3	0.139	53.1	0.942	6.41	0.0497	0.239
DW550	0.195	22.1	14.4	61.2	0.0104	0.00499	0.447	0.0938	7.59	62.6	45.1	38.6	0.114	147	0.0235	1.72	0.0445	1.029
DW750	0.157	17.8	11.6	85.5	0.00832	0.00401	0.359	0.0753	6.09	87.6	63.1	31.0	0.0911	118	0.0189	2.40	0.0357	0.826
FWD550	0.210	23.8	15.5	68.7	0.0111	0.00537	0.481	0.101	8.16	70.3	50.7	41.5	0.122	158	0.0253	1.93	0.0479	1.11
RHI550	0.210	23.4	15.2	27.0	0.0087	0.00875	0.472	0.0962	8.01	61.9	17.6	40.7	0.122	46.7	0.828	5.63	0.0437	0.210
RHI700	0.215	6.38	15.6	27.6	0.00896	0.00896	0.484	0.0986	8.21	63.4	18.0	41.7	0.125	47.9	0.849	5.77	0.0448	0.215
WHI550	0.308	34.3	22.3	39.6	0.0128	0.0128	0.693	0.141	11.8	90.9	25.8	59.8	0.180	68.6	1.22	8.27	0.0642	0.308
WLB550	0.140	15.8	10.3	103	0.00741	0.00357	0.319	0.0670	5.42	106	76.2	27.6	0.0812	105	0.0168	2.90	0.0318	0.736
WSI550	0.405	45.9	29.9	92.0	0.0215	0.0104	0.926	0.194	15.7	94.3	67.90	80.1	0.235	305	0.0487	2.58	0.0448	2.13
Control 1	0.251	27.9	18.2	32.2	0.0104	0.0104	0.564	0.115	9.57	74.0	21.0	48.7	0.146	55.8	0.990	6.73	0.0522	0.251
Control 2	0.204	22.7	14.8	26.2	0.00849	0.00849	0.458	0.0934	7.78	60.1	17.1	39.6	0.119	45.3	0.804	5.47	0.0424	0.204

Table 4.4 Limit of detection for ICP-MS/OES analysis of biochar extractions using buffered and unbuffered 0.01 M $CaCl_2$, buffered and unbuffered 1 M NH_4NO_3 and Mehlich 3 (in mg kg^{-1}) to 3 significant figures.

	Al	As	B	Ca	Cd	Co	Cr	Cu	Fe	Hg	K	Mg	Mn	Mo	Na	Ni	P	Pb	Zn
Mehlich 3	0.712	0.721	0.356	3.09	0.0352	0.0773	0.489	0.0608	0.492	0.232	7.08	2.01	0.0368	0.211	5.34	0.0947	0.644	0.739	0.473
Other methods	0.105	0.102	0.0165	0.0715	0.161	0.00753	0.0294	0.0186	0.00928	0.0178	0.830	0.0228	0.00220	0.0607	0.0840	0.0109	0.103	0.0370	0.139

4.3.1 Plant growth experiment

4.3.1.1 Above ground biomass yield

Results for above ground biomass (referred to henceforth as plant leaves) are given for all biochar treatments and controls in Table 4.5. Many of the biochar treatments resulted in plant leaf yields > 50% higher than the sand-only control. Plant leaf yield from the EPOCAD550 treatment was 83% higher than the relevant control, whilst the yield for WLB550 was 120% higher. Significantly more biomass grew with WLB550 than Control 2 ($p < 0.05$). No other significant differences in plant leaf yield between biochars were identified. Plant leaf yield for WSI550, WHI550 and RHI700 biochars were below the relevant control, but not significantly (-24.0, -44.8 and -60.5%, respectively). The increase in plant growth is discussed in Section 3.1.4.

Table 4.5 Dry weight yield of above ground biomass reported in descending order of values. Results are given to 3 significant figures as means ± 1 standard deviation, unless only one replicate was obtained. [A]: Combined yield of 3 replicates, not measured separately. The grey shading indicates Control 2 and the biochars to which it relates, whilst Control 1 relates to the remainder of the biochar treatments.

Biochar	Plant yield mg ± stdev (n reps)	% difference to relevant control
EPOCAD550	86.2 ± 15.0 (3)	83.1
WLB550	84.4 ± 4.1 (3)	120.4
EPAD550	80.0 ± 30.0 (3)	69.8
DW750	75.2 ± 25.1 (3)	96.3
PAD550	74.8 ± 7.1 (3)	58.9
POCAD550	61.5 ± 9.3 (3)	30.5
PAD450	61.0 ± 4.0 (3)	29.6
DW550	60.4 ± 14.8 (2)	57.7
POCAD450	60.0 ± 1.9 (3)	27.3
EPOCAD450	59.0 ± 12.6 (3)	25.3
RHI550	57.2 ± 20.1 (3)	21.4
FWD550	56.1 ± 5.5 (2)	46.5
ADX350	50.3 ± 6.6 (3)	6.7
EPAD450	49.9 ± 9.2 (2)	5.9
Control 1	47.1 ± 11.4 (5)	N/A
Control 2	38.3 ± 17.1 (5)	N/A
WSI550	29.1 (3)[A]	-24.0
WHI550	26.0 ± 13.8 (3)	-44.8
RHI700	18.6 ± 20.3 (3)	-60.5

4.3.1.2 Uptake of potentially toxic elements into leaves

The concentration of elements in the dried leaves of barley grown in the 5% biochar/sand mixtures (Tables 4.7 and 4.8) was determined by wet digestion. Although somewhat lower elemental recovery is achieved than using microwave digestion, recovery efficiencies greater than 95% can be achieved for most elements (Tüzen, 2003).The determined concentrations were compared with “Upper critical limits” (UCL) for the PTEs As, B, Cd, Co, Cr, Cu, Hg, Mn, Mo, Ni, Pb and Zn calculated for barley plants (Davis et al., 1978; MacNicol and Beckett, 1985, see Table 4.6). The UCL is the lowest element concentration in plant tissues before toxic effects are observed. Leaf tissue concentrations of B exceeded the UCL in PAD550, POCAD550, Control 1 and WHI550 treatments, but this does not appear to have affected the yield for PAD550 or POCAD550. Control 1 had a higher mean yield than Control 2, which suggests that it also was not negatively affected by high B or Cu content, as Control 1 also exceeded the UCL for Cu. Compared to other elements, the determination of B concentration by most standard methods is more variable, and so it is possible the absolute concentration values obtained do not reflect the actual values in the plants (Banuelos et al., 1992; Nyomora et al., 1997). DW550 exceeded the UCL for Mn, but again this did not appear to have an effect on yield. No other treatments resulted in leaf tissue PTE concentrations above the published UCL values. Overall, UCLs were exceeded in plants exposed to different biochars, however, this did not cause a direct effect on plant growth in this study.

According to the leaf tissue concentrations, Mn and Fe deficiency (defined as < 12 and < 30-50 mg kg^{-1} in shoots, respectively (Ohki et al., 1979; Römheld and Marschner, 1991) was observed in the WLB550 treatment, whilst Mn deficiency also occurred in the FWD550 and WSI550 treatments. The WLB550, FWD550, WSI550 and DW700 treatments all exhibited Cu deficiency (< 1-5 mg kg^{-1}) (Marschner, 1995). Given the increase in growth of barley compared to the control in both WLB550 and FWD550 treatments, it is unlikely that micronutrient deficiencies have negatively affected plant growth.

4.3.1.3 Uptake of phosphorus from biochar into leaves

Since a relatively large range of plant leaf yields occurred in this experiment, P concentration (in mg P kg^{-1}) and total P content (in mg P) in the plant leaves were compared to assess whether the P measured was mostly seed derived, or whether the biochar had contributed P to the plant tissues. Comparison of these two descriptors (Figure 4.5) shows that high leaf P concentration does not always map onto high total leaf P due to low yields in some treatments, e.g. WSI550, ADX350. This means that the leaf P concentrations give a false indication of plant P uptake when assessing the fertiliser value of biochars in this experiment.

Total leaf P mass in the EPOCAD550 treatment was significantly higher than that of the relevant control ($p < 0.05$) and was the only treatment which was significantly different to the control. The mean total leaf P mass was higher than the highest recorded value of the controls for PAD450, PAD550, POCAD450, POCAD550, EPAD550, EPOCAD450, EPOCAD550, WLB550 and DW750 (marginally), suggesting that biochar supplied P to the plants in these treatments. Notably absent from this list is EPAD450, which indicates that the P-exposure process resulted in less available P than for EPAD550. The plants also took up less P from EPOCAD450 compared to its 550°C-counterpart, which has implications for their potential application in wastewater treatment and agriculture (Chapter 2). Interestingly, whilst FWD550 contains very high total concentrations of P (Buss et al., 2016a) and significantly increased the length of cress (*Lepidium sativum*) shoot length compared to controls in germination tests (Buss et al., 2016b), in this experiment it did not result in higher P uptake into barley leaves compared to the control. This may be due to the way that P is bound in the biochar as, although a high concentration of P was present in FWD550, only 0.10% was 1 M NH_4NO_3 extractable (Buss et al., 2016b).

Table 4.6 Upper critical limits of elements before toxic effects occur in barley (dry weight basis) from Davis et al. (1978) and MacNicol and Beckett (1985).

	Upper Critical Limit (mg g^{-1})
As	20
B	80
Cd	15
Co	6
Cr	10
Cu	20
Hg	3
Mn	120
Mo	135
Ni	26
Pb	35
Zn	290

4.3.1.4 Overall plant response to biochar-amended sand

Comparing the plant response to biochar treatments to the controls as well as the plant leaf element composition, we can conclude that, in support of the findings of Buss et al. (2016b), at 5% application rates in sand some of the biochars restrict the growth of barley, most likely due to high extractable K concentrations (RHI700, WHI550 and WSI550 in Buss et al. (2016b)). Elevated concentrations of PTEs in the plant leaves in some biochar treatments did not appear to be associated with lower yield, but it is not possible to say whether the edible portion of the mature plant would have met safety regulations. The biochar treatments which resulted in the highest yield increase compared to the controls were those which had moderate to low extractable K concentrations (DW550, DW750 and WLB550, from Buss et al. (2016b)), and had been exposed to P solution prior to use (EPAD550, EPOCAD550) or contained a high concentration of native P. measured in the controls, above which P in the plant may have been contributed by biochar.

Overall, it is likely that the growth promoting and inhibiting effects observed in barley plants in this study can be explained by the competition between two factors, the negative effect caused by high K vs the positive effect of available P in the various biochars.

4.3.2 Biochar element concentrations

4.3.2.1 Biochar element total concentrations

Nine of the biochars investigated in this study contain one or more PTEs at concentrations exceeding the International Biochar Initiative (IBI) and European Biochar Certificate Basic (EBCB) and Premium (EBCP) threshold values for total PTE concentrations in biochar (See Table 4.9 for threshold values; total elemental concentrations in Buss et al., 2016b, and Chapter 3 in this thesis). The potential exceedance of guideline values by the P-exposed biochars (EPAD450, EPAD550, EPOCAD450 and EPOCAD550) was not assessed, as their concentrations are expected to be similar to their non-P exposed precursors (PAD450, PAD550, POCAD450 and POCAD550). The biochars containing elements present in concentrations above minimum threshold values for one or more of the guidelines are: DW750 (Cr), FWD550 (Zn) WSI550 (Mo), WLB550 (Cd, Zn), POCAD450 and POCAD550 (Cu, Mo and Zn), PAD450 and PAD550 (Cd, Cu, Mo and Zn) and WHI (Cr, Cu, Ni and Zn).

Dry ashing techniques generally result in lower recovery of elements than wet digestion or

Table 4.7 Element concentrations measured in barley leaves (mg kg^{-1}). Values given to 3 significant figures and are means ± 1 standard deviation. n = 3 for all biochar treatments except EPAD450, for which n = 2. [A]: only one replicate returned a valid value from ICP-MS analysis, so no standard deviation could be calculated. Control 1 (Table 3b) is the relevant control for these data.

	PAD450	**PAD550**	**POCAD450**	**POCAD550**	**EPAD450**	**EPAD550**	**EPOCAD450**	**EPOCAD550**
As	4.16 ± 2.42	3.52 ± 3.04	2.24 ± 2.89	1.11 ± 0.73	0.805 ± 0.063	2.48 ± 0.56	2.11 ± 1.13	1.19 ± 0.47
Al	61.4 ± 7.0	47.7 ± 3.6	42.8 ± 10.3	44.8 ± 17.8	53.6 ± 17.8	40.3 ± 6.4	52.5 ± 21.3	49.9 ± 6.0
B	57.6 ± 25.6	150 ± 106	32.7 ± 12.3	477 ± 366	43.0 ± 1.3	52.8 ± 10.1	61.2 ± 16.9	43.9 ± 2.7
Ca	5110 ± 631	5720 ± 279	6510 ± 460	5710 ± 605	4180 ± 335	5470 ± 1030	5380 ± 416	6170 ± 1080
Cd	0.152 ± 0.130	0.133 ± 0.093	0.449 ± 0.619	0.0320 ± 0.0132	0.0440 ± 0.0022	0.114 ± 0.122	0.0598 ± 0.0456	0.199 ± 0.262
Co	0.324 ± 0.111	0.288 ± 0.092	0.559 ± 0.319	0.284 ± 0.078	0.372 ± 0.073	0.344 ± 0.223	0.291 ± 0.113	0.250 ± 0.061
Cr	1.17 ± 0.67	1.43 ± 0.96	1.01 ± 0.27	1.18 ± 0.23	0.751 ± 0.385	2.37 ± 1.92	1.38 ± 0.68	1.44 ± 0.57
Cu	9.72 ± 0.84	17.0 ± 5.7	8.19 ± 0.76	18.9 ± 8.9	11.6 ± 1.8	11.4 ± 1.8	11.5 ± 2.0	10.2 ± 0.64
Fe	119 ± 11	90.5 ± 6.7	104 ± 15	106 ± 21	118 ± 4	122 ± 29.2	125 ± 44	398 ± 372
Hg	0.0125 ± 0.0217	0.0663 ± 0.016	0.0383 ± 0.0596	0.0327 ± 0.0054	0.0376 ± 0.0056	0.0381 ± 0.0138	0.0673 ± 0.0372	0.0436 ± 0.0145
K	44600 ± 3090	46300 ± 3540	48900 ± 3990	46500 ± 5520	52900 ± 1370	41800 ± 6089	54100 ± 4330	35100 ± 2220
Mg	2390 ± 120	2200 ± 82	2780 ± 309	2510 ± 290	2210 ± 1	2650 ± 131	2400 ± 12	2920 ± 202
Mn	72.9 ± 11.2	86.0 ± 8.7	93.5 ± 2.5	93.5 ± 9.2	80.8 ± 21.5	90.6 ± 1.0	100 ± 19	101 ± 22
Mo	12.1 ± 3.8	12.3 ± 0.6	10.9 ± 4.7	15.3 ± 2.5	23.2 ± 3.6	27.0 ± 5.9	20.3 ± 1.5	27.3 ± 1.7
Na	9470 ± 1490	8530 ± 1140	5460 ± 494	7400 ± 2150	10000 ± 1460	8670[A]	7550 ± 2010	8420 ± 408
Ni	2.22 ± 8.00	3.05 ± 3.00	2.38 ± 0.30	2.50 ± 0.40	3.71 ± 3.69	2.11 ± 1.14	1.06 ± 0.32	0.891 ± 0.133
P	9880 ± 317	8430 ± 369	9760 ± 186	9490 ± 429	11100 ± 695	10800 ± 1350	10500 ± 584	10200 ± 236
Pb	0.167 ± 0.055	0.961 ± 0.766	0.233 ± 0.037	0.698 ± 0.226	0.249 ± 0.088	0.327 ± 0.120	0.291 ± 0.250	0.193 ± 0.060
Zn	49.4 ± 5.4	43.7 ± 3.3	41.9 ± 4.5	45.9 ± 9.5	43.2 ± 5.0	47.2 ± 4.4	43.6 ± 9.9	46.5 ± 0.45

Table 4.8 Element concentrations measured in barley leaves ($mg\ kg^{-1}$). Values given to 3 significant figures and are means ± 1 standard deviation. n = 5 for Control 1 and 2, n = 3 for all other biochar treatments except DW550 and FWD550, for which n = 2 and RHI700 and WSI550, for which n = 1. [B]: Only one replicate available for analysis, so no standard deviation could be calculated. < LOD: Value obtained was below the limit of detection. ND: No data was obtained for this element. Columns are shaded according to which control is relevant for each treatment i.e. white columns refer to Control 1 and grey columns refer to Control 2.

	Control 1	**Control 2**	**ADX350**	**DW550**	**DW750**	**FWD550**	**RHI550**	**RHI700[B]**	**WHI550**	**WLB550**	**WSI550[B]**
As	2.03 ± 2.39	3.66 ± 4.31	1.48 ± 0.51	0.255 ± 0.309	< LOD	< LOD	4.69 ± 5.22	4.27	1.71 ± 1.34	0.291 ± 0.166	< LOD
Al	119 ± 16	103 ± 7	24.8 ± 3.0	31.9 ± 7.7	23.9 ± 4.3	37.4 ± 4.5	26.8 ± 12.9	25.1	57.4 ± 24.4	32.7 ± 9.1	130
B	430 ± 221	29.4 ± 6.4	56.2 ± 10.8	ND	ND	ND	31.6 ± 14.1	23.5	297 ± 341	ND	ND
Ca	1882 ± 24	1750 ± 289	1670 ± 340	10500 ± 1	7140 ± 1	6050 ± 0	1910 ± 273	1290	1020 ± 145	6450 ± 0	8010
Cd	0.0268 ± 0.0109	0.131 ± 0.147	0.395 ± 0.567	0.500 ± 0.015	0.659 ± 0.334	0.963 ± 0.139	0.0353 ± 0.0174	0.0508	0.207 ± 0.249	0.76 ± 0.05	2.26
Co	0.416 ± 0.298	0.370 ± 0.065	0.226 ± 0.105	< LOD	< LOD	< LOD	0.357 ± 0.096	0.581	0.289 ± 0.029	0.0037 ± 0.0046	BDL
Cr	1.02 ± 0.19	1.11 ± 0.41	0.757 ± 0.041	0.531 ± 0.024	< LOD	0.713 ± 0.222	0.871 ± 0.243	0.857	1.80 ± 0.72	3.15 ± 5.04	0.940
Cu	23.2 ± 4.8	9.10 ± 1.62	8.32 ± 2.03	2.39 ± 0.44	1.77 ± 0.47	1.98 ± 0.04	10.2 ± 2.2	7.50	17.9 ± 11.8	1.63 ± 0.23	1.71
Fe	60.5 ± 6.8	58.9 ± 3.8	64.8 ± 7.60	ND	ND	ND	86.7 ± 25.3	57.0	78.8 ± 10.4	14.6 ± 25.2	ND
Hg	0.049 ± 0.044	0.0248 ± 0.0211	0.170 ± 0.180	ND	ND	ND	0.0359 ± 0.0183	ND	0.0097 ± 0.0137	ND	ND
K	18500 ± 2640	20600 ± 3850	79700 ± 8730	29200 ± 5	55000 ± 7	65500 ± 5	63900 ± 1820	68200	86100 ± 2680	53300 ± 2	59300
Mg	2550 ± 180	2460 ± 266	1820 ± 402	2700 ± 0	2470 ± 1	2090 ± 0	2160 ± 158	1680	1270 ± 192	2040 ± 0	< LOD
Mn	ND	ND	ND	129 ± 0	113 ±16	< LOD	57.0 ± 6.3	ND	ND	< LOD	< LOD
Mo	1.56 ± 1.21	1.04 ± 1.19	ND	0.502 ± 0.015	0.659 ± 0.334	0.963 ± 0.139	1.45 ± 1.65	ND	6.34 ± 0.26	0.757 ± 0.053	2.26
Na	1710 ± 137	1800 ± 163	769 ± 93	4290 ± 0	2960 ± 2	11400 ± 1	1070 ± 147	1280	13600 ± 847	269 ± 0	14500
Ni	4.48 ± 4.54	3.06 ± 0.38	1.82 ± 0.44	ND	ND	ND	4.77 ± 2.05	3.43	5.61 ± 0.33	ND	ND
P	8930 ± 174	9390 ± 885	10500 ± 899	7580 ± 0	7150 ± 2	8380 ± 0	8470 ± 786	8730	10000 ± 5	8540 ± 0	11800
Pb	1.21 ± 0.37	1.00 ± 0.18	0.136 ± 0.050	0.185 ± 0.211	0.0431 ± 0.0402	<LOD	0.160 ± 0.148	0.454	0.620 ± 0.487	0.172 ± 0.096	< LOD
Zn	41.9 ± 3.7	45.1 ± 5.6	44.2 ± 6.3	17.0 ± 0.42	19.5 ± 0.6	20.3 ± 0.3	46.0 ± 12.4	43.2	60.5 ± 5.6	26.8 ± 7.5	49.8

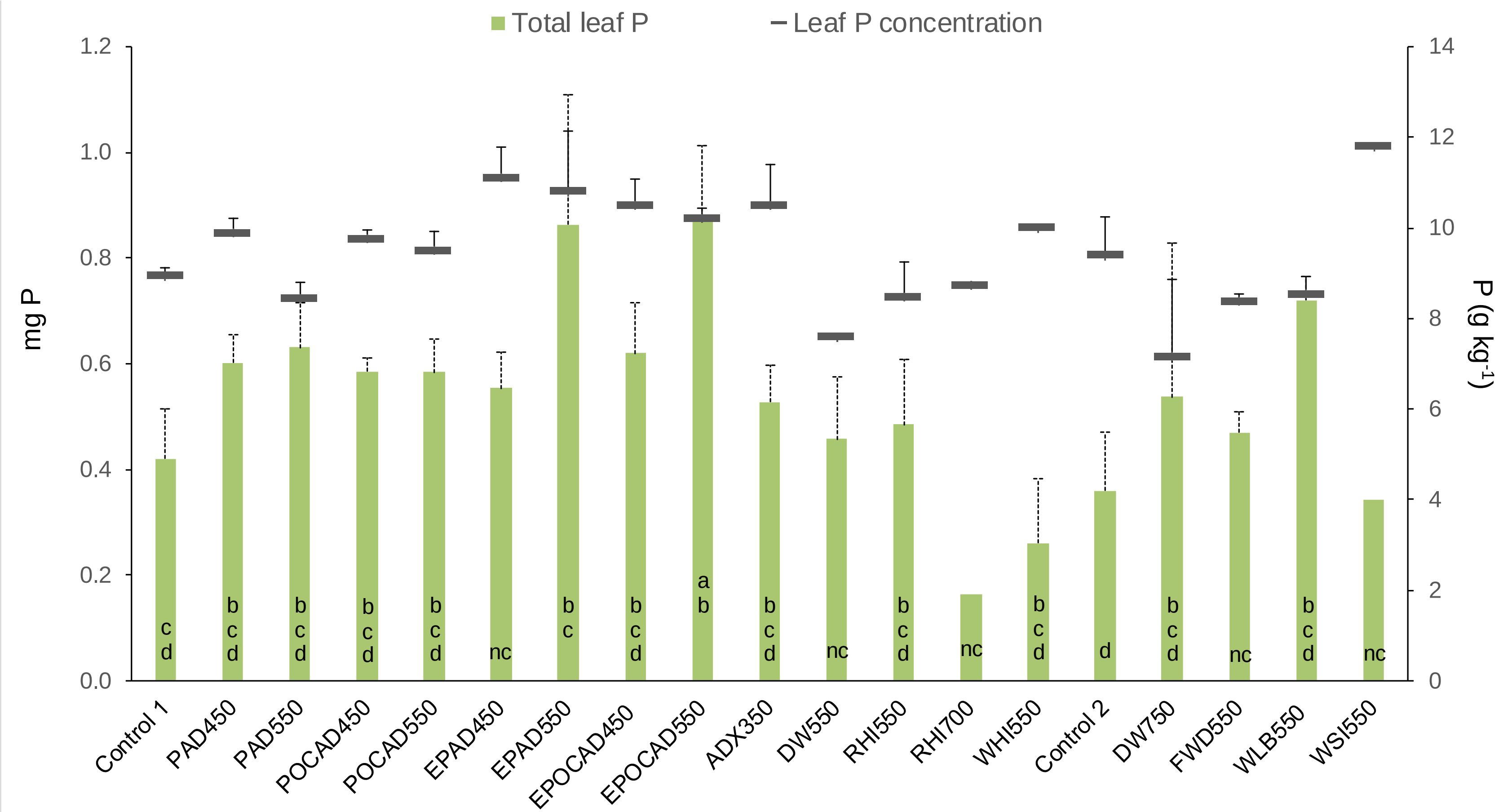

Figure 4.5 Concentration and total P mass in above ground biomass (leaves) on dry weight basis. Values are means ± 1 standard deviation, except where only one replicate was obtained (RHI700 and WSI550). Control 2 relates to WLB550, DW550, DW750, FWD550 and WSI550, whilst Control 1 relates to the rest of the treatments. Different letters symbolise significant differences between the treatments. nc = not included in statistical analysis as n < 3. The blue dashed line represents the highest leaf P mass.

microwave methods due to volatilisation (Ali et al., 1988; Banuelos et al., 1992; Enders and Lehmann, 2012; Huang and Schulte, 1985). In the case of biochar, however, wet digestion does not always result in complete dissolution due to the recalcitrant nature of the material (Enders and Lehmann, 2012). The Modified Dry Ashing technique is therefore a compromise, where some elements may be volatilised but others are dissolved that would not have been otherwise. With the exception of Ca and B, Enders and Lehmann (2012) found no significant difference in P, K, Ca, Mg, Zn, and Cu concentrations determined for an ApCk reference material by the Modified Dry Ashing method compared to microwave-assisted digestion. Given these results, and that the IBI threshold values are based on this method, without access to high-throughput microwave digestion facilities, this appears to be a suitable method for analysing and comparing a wide variety of different biochars.

4.3.2.2 Potentially toxic element and nutrient extractions

The amount of element that was extractable from the biochars varied between methods, partly due to differences in pH between methods. Based on the number of biochars for which each element could be extracted for each extraction method, the elements Al, B and Co could be extracted from many of the biochars investigated above the limit of detection (LOD) using Mehlich 3 and the higher pH extractions (Table 4.10). Calcium, Cu, Ni and Zn were could be extracted above the LOD from more of the biochars using lower pH extractions than high pH and, with the exception of Zn, were Mehlich 3 extractable. Cadmium and Pb were only extractable for 2 of the biochars above the LOD using Mehlich 3, whilst K, Mg, Mn, Mo, Na and P could be extracted above the LOD (although with differing extraction efficiencies) using any method, except Mehlich 3 for Mo. Of the remaining elements, Cr could be extracted using the buffered and unbuffered 1 M NH_4NO_3 solutions, Fe by Mehlich 3, unbuffered 1 M NH_4NO_3 and buffered 0.01 M $CaCl_2$ solutions, and Hg by unbuffered 1 M NH_4NO_3 and buffered 0.01 M $CaCl_2$ solutions. This suggests moderately acidic to neutral pH extractions are most effective for these three elements, and that Mehlich 3 targets a specific mechanism of Fe binding in biochar that the other methods do not.

Of the 13 biochars extracted following the established soil analysis method specified in the German soil ordinance (1 M NH_4NO_3), concentrations of PTEs extracted from five were higher than the recommended threshold. Arsenic was detected above threshold values from PAD450 and WHI550, Cd from POCAD550 as well as WLB550, which also exceeded threshold values for Zn. These results differ slightly to those of Buss et al. 2016b), but this is due to the low threshold values in question (0.1 mg kg^{-1}) and the relatively high Cd detection limit for the experiment. Rather than ICP-OES, ICP-MS appears to be a more suitable method for these analyses in future.

Considering that pure biochar was analysed in this study and the threshold values are referring to soil, as suggested in Buss et al. (2016b), if the biochars are applied to soil at a rate of 1% (< 20 t ha^{-1}) and the soil/biochar mixtures extracted, soil amendment with these biochars will not result in soil PTE concentrations exceeding threshold values.

4.3.3 Comparison of extraction methods

4.3.3.1 Mehlich 3, $CaCl_2$ and NH_4NO_3 extractions for potential assessment of elemental bioavailability in biochars

Multiple significant correlations between an element extracted from biochar with plant leaf concentrations (across methods) were revealed for 'generally extractable' elements, i.e. where elements were extracted from many biochars above the LOD for all (or most) extraction solutions, e.g. K, Mn, Mo and Na (Table 4.10). All significant correlations were positive apart from for unbuffered 1 M NH_4NO_3 where plant leaf concentrations of Ca and Zn decreased with higher concentrations extracted from the biochars. Whilst Mehlich 3 generally extracted elements at the highest concentrations and from the highest number of biochars, plant leaf concentrations were significantly correlated with these extractions only for Fe, K, Na and P, suggesting that the bioavailability of elements in biochar, apart from Fe, is not related to a chelation mechanism of extraction.

Despite the biochars in this study being selected for their known high concentrations of total PTEs, the quantities removed by extractions were sometimes below the experimental limit of detection. Although this limited examination of different extraction methods for assessing PTE bioavailability in biochars, it supports the findings of other studies where biochars with high concentrations of PTEs have proportionally low extractability (Buss et al., 2016b; Farrell et al., 2013; Khanmohammadi et al., 2015), indicating that soil amendment might be acceptable with a range of biochar types.

In general, both the buffered and unbuffered 0.01 M $CaCl_2$ extractions correlated well with plant uptake in this study. The extracted biochar and plant concentrations were significantly positively correlated for 6 elements (all micro- and macronutrients) (Table 4.10), although the extracted concentrations (data not shown) were one to three orders of magnitude lower than the measured plant leaf concentrations. Plant element concentrations probably correlate well with the $CaCl_2$ extractions because the extraction pH is closest to the pH of the biochars, and in an unbuffered system the biochar is the main control of pH.

Table 4.9 Quality guidelines for biochar assessment

		As	**Cd**	**Co**	**Cr**	**Cu**
IBI biochar guidelines (2012)	mg kg $^{-1}$	12 - 100	1.4 - 39	40 - 150	64 - 1200	63 - 1500
EBC basic grade biochar (2012)	mg kg $^{-1}$		1.5		100	100
EBC premium grade biochar (2012)	mg kg $^{-1}$		1		80	100
German soils ordinance [A]	mg kg $^{-1}$	0.4	0.1			1
		Hg	**Mo**	**Ni**	**Pb**	**Zn**
IBI biochar guidelines	mg kg $^{-1}$	1 - 17	5 - 20	47 - 600	70 - 500	200 - 7000
EBC basic grade biochar	mg kg $^{-1}$	1		50	150	400
EBC premium grade biochar	mg kg $^{-1}$	1		30	120	400
German soils ordinance	mg kg $^{-1}$			1.5	0.1	2

[A] German Federal Environmental Agency (1999) German Federal Soils Protection and Contaminated Sites Ordinance

128

Table 4.10 Correlation coefficients between element concentrations measured in plant biomass from the growth experiment and those determined in biochars extracted using different methods. ICP-OES was used to determine element correlations for all extractions except for the 2% formic acid extraction where P concentrations were determined by colorimetry. Values reported are Spearman's ρ, unless marked with ^{P}, where Pearson's correlation is stated. N.S. = correlation non-significant, * = $p < 0.05$, ** = $p < 0.01$, *** = $p < 0.001$. N/A = method is not applicable for that element. N.C. = not calculated as standard deviation = 0. The number in brackets indicates the number of data pairs in the dataset for which both plant and biochar extraction data were available with values above the experimental limit of detection.

	Mehlich 3		**Buffered 1 M NH_4NO_3**		**Unbuffered 1 M NH_4NO_3**		**Buffered 0.01 M $CaCl_2$**		**Unbuffered 0.01 M $CaCl_2$**		**2% formic acid**
pH	**2.5**		**4.6**		**4.6 +**		**7.0**		**7.0 +**		**2.1**
Al	N.S.	(12)	N.S.	(4)	N.S.	(7)	N.S.	(6)	N.S.	(8)	N/A
B	N.S.	(6)	**0.805***	(5)	N.S.	(8)	**0.738***	(8)	**0.738***	(8)	N/A
Ca	N.S.	(13)	N.S.	(13)	**-0.597**^{P*}	(13)	N.S.	(10)	N.S.	(7)	N/A
Cd	N.S.	(11)	N.S.	(1)	N.S.	(2)	N.C.	(0)	N.C.	(0)	N/A
Co	N.S.	(11)	N.S.	(1)	N.S.	(3)	N.S.	(2)	N.S.	(2)	N/A
Cr	N.S.	(3)	N.S.	(10)	N.S.	(6)	N.S.	(2)	N.S.	(1)	N/A
Cu	N.S.	(13)	N.S.	(13)	N.S.	(8)	N.S.	(2)	N.S.	(3)	N/A
Fe	**0.900****	(9)	N.S.	(4)	N.S.	(8)	N.S.	(4)	N.S.	(2)	N/A
Hg	N.C.	(0)	N.C.	(0)	N.S.	(3)	N.S.	(2)	N.C.	(0)	N/A
K	**0.835*****	(13)	**0.867****	(9)	N.S.	(13)	**0.810***	(8)	**0.929****	(8)	N/A
Mg	N.S.	(13)	N.S.	(13)	N.S.	(13)	N.S.	(13)	N.S.	(13)	N/A
Mn	N.S.	(10)	N.S.	(10)	$\mathbf{0.927***}$	(10)	**0.781**^{P**}	(10)	**0.806****	(10)	N/A
Mo	N.S.	(3)	**0.752****	(8)	N.S.	(6)	**0.758****	(7)	**0.801****	(6)	N/A
Na	**0.892**^{P***}	(10)	N.S.	(8)	N.S.	(6)	**0.935**^{P**}	(5)	**0.943**^{P***}	(8)	N/A
Ni	N.S.	(8)	**0.846****	(3)	N.S.	(7)	N.S.	(4)	N.S.	(3)	N/A
P	**0.588***	(13)	N.S.	(13)	N.S.	(13)	**0.692***	(13)	**0.583***	(12)	**0.507*** (17)
Pb	N.S.	(10)	N.S.	(2)	N.C.	(0)	N.S.	(2)	N.S.	(1)	N/A
Zn	N.S.	(13)	N.S.	(7)	**-0.566***	(9)	N.S.	(2)	N.C.	(0)	N/A

Despite the large difference in the plant and extract concentration values for individual elements, it is still possible to state the relative availability of nutrients and therefore compare element bioavailability between biochars.

Correlations of the total mass of the element in the leaves with the extraction methods were calculated, but this analysis did not highlight any stronger relationships than for leaf element concentrations (data not shown), except for P (discussed in 4.3.3.2).

Comparison of the results of our study to those of Farrell et al. (2013) reveals that there are no method correlations in common. This could be due to the different plant species used (wheat vs. barley) or the different number of biochars used (4 vs. 7 – 17).

4.3.3.2 Suitability of extraction methods to determine biochar P bioavailability

Significant correlations between P concentrations in plant tissue and biochar extractions were found for Mehlich 3, buffered and unbuffered 0.01 M $CaCl_2$ and 2% FA, however Spearman's rho was not high (< 0.7) (Table 4.10). The strongest correlation was with buffered 0.01 M $CaCl_2$, ($\rho = 0.692$, $p < 0.05$).

Considering the results of Wang et al. (2012) and their recommendation of the 2% FA method for the estimation of P bioavailability in high ash biochars, a curve was fitted to the plot of plant P concentration against 2% FA-extractable P (Figure 4.6a, $R^2 = 0.34$). There appears to be an upper concentration limit in the plant leaves of around 11 mg P g^{-1} which could be the optimal P concentration range for barley seedling growth, with most of the values between 8 and 10 mg P g^{-1}. There are three outliers in Figure 4.6a, one of which is due to low yield (WSI550), whilst the others appear to be related to over-estimation of P uptake by the 2% FA extraction. As previously discussed, 1 M NH_4NO_3 extractable P from FWD550 is low relative to uptake, whilst the opposite is true for 2% FA. This suggests that the latter method overestimates the P fraction from biochar by extracting a P fraction that is not plant available.

The comparison of total leaf P mass and 2% FA extractable P provides a better representation of the ability of the 2% FA extraction method for assessing P bioavailability from the biochars Figure 4.6b). This can be explained by the fact that when the optimal P concentration in the leaves is reached, the plant does not need to take up more P and thus increase the P concentration further. However, with growth of the plant, more P is taken up by the plant to maintain optimal tissue concentration. Correlation with total leaf P mass should identify the better indicator for bioavailability. This is further emphasised by the lack of relationship between leaf P concentration and plant yield (Figure 4.6c) and the strong linear relationship between total leaf P mass and yield Figure 4.6d, $R^2 = 0.8477$). Figure 4.6d also shows the sewage sludge-derived biochars perform consistently well as sources of plant P, providing evidence to support use of biochar from sewage sludge feedstocks as a fertiliser.

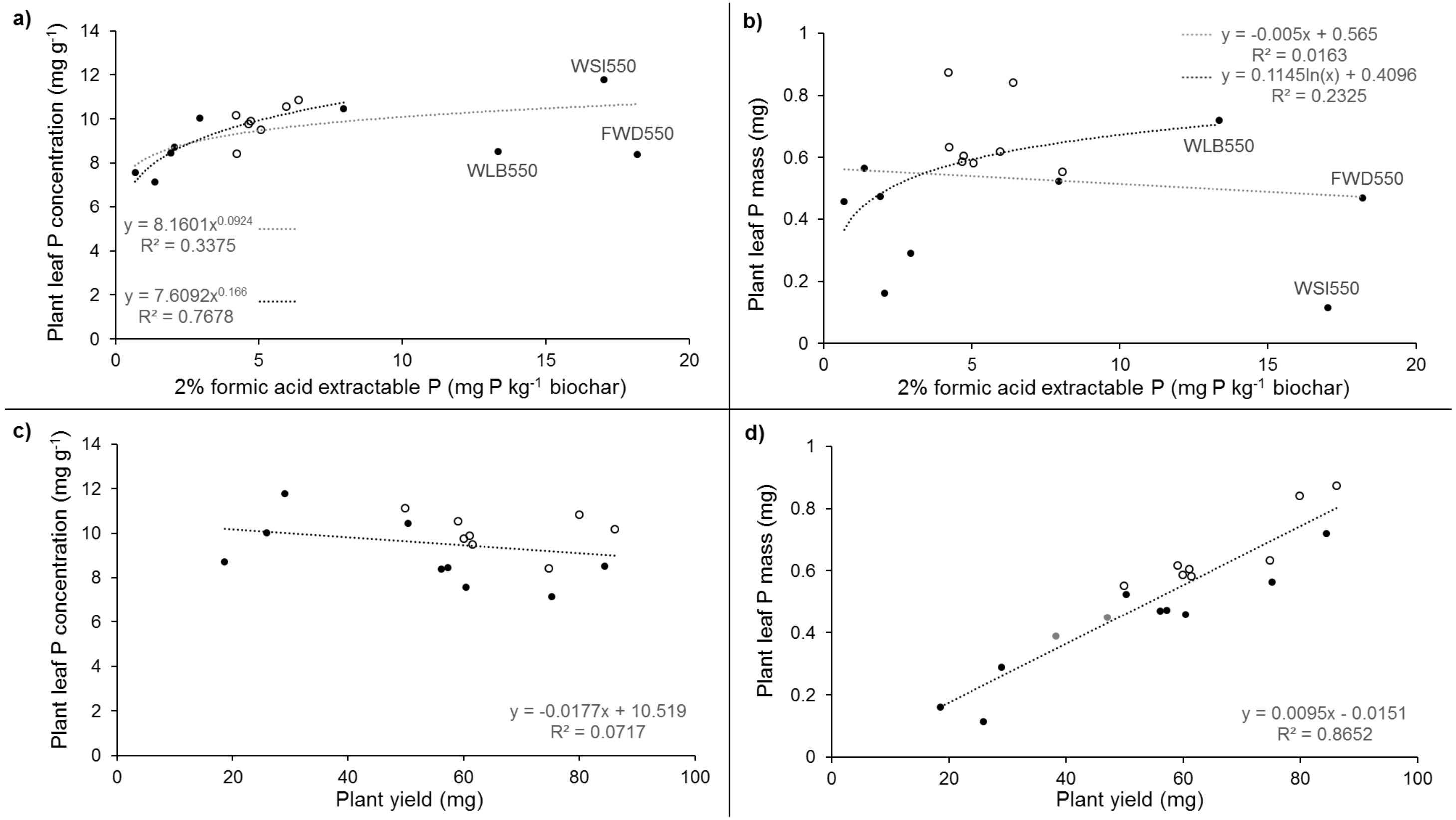

Figure 4.6 Relationships between plant leaf P mass and concentration and 2% formic acid extractable P from biochar and plant yield. White circles are the sewage sludge-derived biochars, black circles are the remaining biochars produced from various feedstocks, and grey circles in d) are controls. a) Plant P concentration and 2% formic acid extractable P from biochar. The grey fitted line includes all data points except the WSI550 and FWD550 outliers. The black fitted line also excludes the WLB550 outlier. b) Plant leaf P mass and 2% formic acid extractable P from biochar. The grey fitted line includes all data points. The black fitted line excludes WSI550 and FWD550. c) Plant P concentration and plant yield. d) Plant leaf P mass and plant yield.

It is important to consider the different spectrophotometry methods used for the 2% FA analysis method compared to the other extractions. The 2% FA method employs the molydnenum-reactive phosphate method, using colorimetry to determine the concentration of soluble reactive phosphate (SRP) in the extraction solution. The other extractants are analysed using ICP-OES, which measures the total amount on P in the extraction solution, not just SRP. This second scenario better represents the plant-root P acquisition system, as root exudates can convert non-SRP compounds into bioavailable phosphate, but it is also likely that some of the measured P is actually not bioavailable. Each of these methods has been designed to estimate bioavailability, which is a highly debated area of research. Taking this into consideration, it is likely that there are potentially bioavailable P compounds present in the 2% FA extraction solution which are overlooked in the colorimetry analysis, and non-bioavailable P compounds present in the other analyses, contributing to the relatively low R^2 values obtained for P (Table 4.10). Compared to the other extractants, with the exception of Mehlich 3, 2% FA extracted a much higher concentration of P. It would be useful in future work to analyse the 2% FA extracts using ICP-OES to determine whether this correlates better with plant leaf P uptake.

4.3.3.3 Comparison of extraction methods with each other: effect of pH and solution composition

Different extractant solutions have different native pH, indirectly and/or intentionally affecting the solubility of PTEs and nutrients, in addition to targeting different binding mechanisms according to the constituents of the solution. It has previously been reported that acidic extractants provide a more representative assessment of element bioavailability in acidic soils, with alkaline extractants better suited to alkaline soils (Fixen et al., 1990), but this conclusion has also been questioned (Jordan-Meille et al., 2012). Thus, pH is not the only factor influencing the suitability of methods for estimating bioavailability: solution composition is also important.

Of the 13 elements for which extraction methods were significantly correlated with each other, for nine a significant correlation was found between 0.01 M $CaCl_2$ buffered and unbuffered extracted concentrations (**Error! Reference source not found.**). Conversely, s ignificant correlations occurred between 1 M NH_4NO_3 buffered and unbuffered extracted concentrations for only 2 of the 13 elements. This is most likely related to the pH of the solutions compared to that of the biochars being extracted. The pH of the biochars were in the range 7.39 – 10.12, with most < 9 (Buss et al., 2016a and Chapter 3 in this thesis) whilst the pHs of 1 M NH_4NO_3 and 0.01 M $CaCl_2$ are 4.6 and 7.0, respectively. The potential pH change is therefore greater for the unbuffered 1 M NH_4NO_3 extractions than for 0.01 M $CaCl_2$, for which only minor pH changes were observed upon addition of the lower pH biochars (< pH 0.5, data not shown).

Table 4.11 Significant correlations for individual elements in biochars for the extraction methods investigated (except 2% formic acid, which was only used to extract P). Correlation coefficients shown are Spearman's ρ, except indicated ^{P}, where Pearson's r is stated. Significance levels are indicated as * = $p < 0.05$, ** = $p < 0.01$, *** = $p < 0.001$.

	Mehlich 3	**Buffered 1 M NH_4NO_3**	**Unbuffered 1 M NH_4NO_3**	**Buffered 0.01 M $CaCl_2$**
Buffered 1 M NH_4NO_3	B 0.679* Ca 0.703** Fe -0.747** K 0.917** Mg 0.890*** Na 0.705* Ni 0.571*			
Unbuffered 1 M NH_4NO_3	Al 0.780** Mg 0.632* P 0.720**	Cu 0.593* Na 1***		
Buffered 0.01 M $CaCl_2$	B 0.569* Ca 0.569* Fe -0.695** K 0.881** Mg 0.879*** Na 0.983^{P***}	B 0.663* Ca 0.619* K 1*** Mg 0.923*** Mn 0.841*** Mo 0.959*** Na 0.991*** Ni 0.739** P 0.769** Zn 0.662*	K -0.952** Mn 0.571* Na 0.904^{P*}	
Unbuffered 0.01 M $CaCl_2$	Ca 0.572* K 0.762* Mg 0.846*** Na 0.984^{P***} Ni 0.645*	K 0.833* Mg 0.901*** Mn 0.665* Mo 0.921*** Ni 0.608*	K -0.833* Mn 0.604*	B 0.855*** Ca 0.904*** Cu 0.851*** K 0.833* Mg 0.967*** Mn 0.676* Mo 0.961*** Na 0.999^{P***} Ni 0.757**

The extractants with the highest number of significant correlations for element concentrations were buffered 1 M NH_4NO_3 and buffered 0.01 M $CaCl_2$, with 10 elements (Table 4.10). Given the different pHs of these extractants (4.6 vs. 7), pH cannot be the main factor controlling element extractions from these biochars. The most probable explanation is that since both these extractants are buffered, the extraction pH remains constant at these values, which both happen to lie just outside the pH range at which the adsorption behaviour of many elements change (pH 5-7 for Zn, Co, Ni and Mn) (Basta et al., 2004). Supporting this further is the observation that no significant correlations between these methods was found for Pb, which has a different pH range for changing adsorption behaviour (pH 3-6), which includes the pH of the buffered 1 M NH_4NO_3 extractions (4.6). Therefore, whilst buffered 1 M NH_4NO_3 and buffered 0.01 M $CaCl_2$ extract different amounts of each element, the relationship between element concentrations from the two extractions remains constant for many elements. Predictably, the number of significant correlations was higher for Mehlich 3 and buffered 1 M NH_4NO_3 extractions (7) than for unbuffered NH_4NO_3 (3). None of the latter were in common with the former.

Elements for which significant correlations occurred in concentrations extracted from biochar by alternate methods were: Al (1), B (4), Ca (5), Cu (2), Fe (2), K (8), Mg (7), Mn (5), Mo (3), Na (7), Ni (5), P (2) and Zn (1). Insufficient data were obtained to determine whether there were correlations between the different extraction methods for Cd, Co, Cr, Hg, and Pb since extracted concentrations were generally below the detection limit, despite deliberate inclusion of high PTE-containing feedstocks. High concentrations of K, Na and Ca were extractable in most of the biochars, resulting in a higher number of data points to use for correlation analysis. Conversely, whilst Al and Fe were also present in high concentrations in many of the biochars, there were few significant correlations between extraction methods for these elements. Magnesium was not found in high concentrations in all of the biochars, but a high number of significant correlations were observed between extractable concentrations from different methods. However, extractable biochar concentrations from any of the methods were not significantly correlated with Mg leaf concentrations, so even though the extraction methods utilise similar extraction mechanisms, these do not represent the mechanisms the plant uses to access Mg from the biochars.

These observations emphasise the importance of pH for element extractability, as well as the general difficulty in determining the mechanisms controlling element extractability and thus plant accessibility of nutrients and PTEs in different biochars.

4.3.4 Broader context of the assessment of biochar bioavailability assessment

The results of this study contribute towards the development of standardised methods to assess bioavailability of nutrients and PTEs from biochar. Based on correlations of element concentrations in plant biomass with concentrations in biochar extracts, 0.01 M $CaCl_2$ (buffered or unbuffered) was the best estimator of element bioavailability for a range of elements. Spearman's ρ (or Pearson's r) correlation coefficient values were equal or slightly higher for all significantly correlated elements in the unbuffered solution compared to buffered 0.01 M $CaCl_2$, with the exception of P (Table 4.10). This suggests that methods using an extractant with pH closest to the pH of the biochar may provide the most accurate representations of element bioavailability in soils amended with biochar. It is important to note, however, that no method correlated well for plant uptake of key toxic metals.

Selection of (an) appropriate method/s to assess bioavailability of nutrients and PTEs from biochar involves consideration of a number of factors, including whether values exist in the literature and legislation with which results can be compared. Without the availability of biochar standard reference materials for which the elemental composition is precisely known, it is difficult to rely on element total concentrations to determine the potential for toxic effects. In addition, identification of significant positive correlations between plant tissue concentration/contents and extracted PTE concentrations does not necessarily mean that the extraction method gives an accurate absolute value for bioavailability, only that there is a relationship between the two sets of data. Calculations using conversion factors may need to be conducted on the extraction results to provide an estimate of bioavailability, or a ranking devised to demonstrate what constitutes a high or a low bioavailability value when plant tissue concentration/contents and extracted concentrations of an element are significantly positively correlated. Based on this observation, and in agreement with the recommendations of Farrell et al. (2013), we suggest that direct measurement of plant nutrient and PTE uptake from biochar is the most reliable method to determine bioavailability i.e. plant based tests. Whilst it is more time consuming than extraction methods, it is difficult to foresee the identification of a single extraction method which will a) extract enough of each element of interest for analysis and b) also correlate with plant uptake.

A combination of nutrient and PTE leaching from biochar/soil mixtures and plant uptake studies would provide the necessary information to determine whether the biochar in question could perform well as a fertiliser and/or have the potential to cause phytotoxicity. A soil-specific leaching experiment as described in Bastos et al. (2014) might provide an appropriate measure of leachability. Reflecting on our finding (in agreement with Buss et al. (2016b) that high K content in the 5% biochar application rate impacted negatively on plant yield, for the assessment of the suitability of biochars to be used as P fertiliser growth experiments using application rates in line with those of fertiliser (extractable or total P mass basis) should be performed. To provide compelling evidence as to whether the biochar can function as a P fertiliser 4-5 different crop species and different soils would need to be used. Assessment of these experiments may be as simple as yield comparison, as demonstrated by the highly significant positive relationship between plant P mass and yield reported from our experiments. Furthermore, for the assessment of PTEs and general biochar toxicity, both 5% and 1% application rates could be assessed for the same range of crops in a specific soil to separate PTE and salt effects.

4.4 Conclusions

Concentrations of B, K, Mn, Mo, Na and P in both buffered and unbuffered 0.01 M $CaCl_2$ extractions were significantly correlated with plant uptake in barley seedlings grown in a 5% biochar/sand medium. None of the extraction methods assessed for 17 biochars correlated well with plant uptake of any of the PTEs of most concern, such as As, Co, Cr, Cu, Ni, Pb or Zn. This can be explained mostly by the extractability of these elements at concentrations below the method limit of detection. These results indicate that plant experiments used in this study are better suited for risk assessment of PTEs than extraction methods, but the method needs to be further validated with long term pot experiments. Yield inhibition compared to controls was primarily due to high K concentrations in the 5% biochar applications. The bioavailability of P was highest in post-pyrolysis P-exposed biochars made from sewage sludge feedstocks at a HTT of 550°C, indicating that these production conditions could be suitable for producing biochars with optimised characteristics for use in the wastewater and agriculture industries.

Chapter 5

Plant availability of phosphorus from sewage sludge derived biochar used to capture aqueous phosphorus in barley rhizobox experiment

J.G. Shepherd, S.P. Sohi and K.V. Heal

Intended for development into a manuscript for submission to Science of the Total Environment

The candidate, as lead author, performed the experiments and laboratory analysis. Data analysis and writing of the chapter was carried out by the candidate. Co-authors provided support and guidance on the scope and design of the research, data analysis and editing of the chapter. The biochars were produced for Chapter 2, with pyrolysis performed by Dr Wolfram Buss. Lettice Hicks helped with plant watering. Plant and soil digestions were performed by Andy Gray and John Morman. ICP-OES was run by the candidate with the assistance of Dr Wolfram Buss and Dr Lorna Eades, who also performed the ICP-MS analyses.

5.1 Introduction

There are currently many drivers for the improvement of phosphorus (P) recovery and re-use from wastewater systems. The flux of P into oceans caused by human activity increased from pre-industrial levels of 15 Mt y^{-1} to 70 Mt y^{-1} the year 2000 (Smil, 2000). The natural P cycle occurs over a very slow timescale ($10^7 – 10^8$ years), but human activity accelerates the flow such that it can take just one year for P to be transported from rock reserves through the agriculture, food and sanitation systems to oceans, where cycling returns to natural rates once again (Cordell et al., 2009; Smil, 2000). Interception of P at wastewater treatment plants (WWTPs) is one strategy for preventing loss into the water system and is already a widespread practice to prevent environmental damage caused by eutrophication, (Haygarth and Condron, 2004; Pierzynski et al., 2000). The focus of P capture at WWTPS is slowly shifting from pollution prevention to resource recovery, reflecting a greater recognition of limited P rock reserves and system inefficiencies by environmental regulators and industry (Cordell et al., 2009; Desmidt et al., 2015). The EU recently placed phosphate rock on its list of Critical Raw Materials substances and is currently developing new fertiliser regulations which will include provisions for fertilisers made from recycled P sources, such as sewage sludge and other WWTP outputs (EU DG ENTR, 2014).

Sewage sludge is P-rich, but also contains high concentrations of potentially toxic elements and pathogens (Agrafioti et al., 2013). Application of sludge to land is practised in many EU countries, such as the UK, Denmark, France and Spain, but strict environmental regulations limiting the application of PTEs and mobile nutrients to soils is driving alternatives such as landfilling and sludge incineration (Desmidt et al., 2015; SEPA, 2015; Stutter, 2015). In the EU, 31% of sludge is sent to landfill, either as treated sludge or as ash (Scholz et al., 2014).

Pyrolysis has arisen as an appropriate alternative technology to incineration. The process can generate energy more efficiently than incineration (Kleemann, 2015) and kills pathogens due to the high temperatures involved. In addition to its long-term carbon storage value when applied to soils, the biochar produced can be used directly as P fertiliser, and the PTEs within the char may not leach into the soil system (Hossain et al., 2010; Khan et al., 2013a, 2013b; Waqas et al., 2014). The equivalent of 40% of total UK P imports were treated by WWTPs in 2009, so there is great potential for recycled P fertilisers to replace rock-based fertilisers in this case (Cooper and Carliell-Marquet, 2013). Application of sewage sludge biochars to soil must still meet environmental regulations, so investigations of the mobility of PTEs in the soil-plant system are necessary.

In previous work, we demonstrated the potential for anaerobically digested sewage sludge biochars to be used as substrates for the capture P from wastewater effluent (Chapter 2). In further studies, the native biochars and P-exposed biochars were shown to provide P to barley without causing phytotoxicity in rapid growth experiments (Chapter 4). The application rates used in the study were extremely high, as the focus of the experiment was to identify the worst-case scenario for PTE contact with the plants. The experiment did not reveal the extent of P bioavailability as there was an excess present in the system. The aims of the current study were to test sewage sludge biochars as P fertilisers to grow barley at application rates based on extractable P, to compare the bioavailability of native biochar P to that of captured P, and to determine whether biochar application at these rates causes soil PTE contamination or phytotoxicity.

5.2 Materials and methods

5.2.1 Biochar production

The production of the biochars PAD450, PAD550, POCAD450 and POCAD550 from pelletised feedstocks was described in Chapter 3. The PAD feedstock consisted of anaerobically digested sewage sludge, ochre and lignin binder in an 89.1:9.9:1.0 ratio. In this experiment, to assess the effect of exposure of these biochar to aqueous P (as would occur if used to capture P from wastewater), they were exposed to a 20 mg l^{-1} P solution buffered at pH 7 using 0.01 M 3-(N-morpholino)ethanesulfonic acid (MOPS) to produce the biochars EPAD450, EPAD550, EPOCAD450 and EPOCAD550. Briefly, 30 g of each biochar with particle diameters 0.25–15 mm were exposed to the P solution in a 1:20 solid to liquid ratio (m/v) and shaken for 24 h. After this time, the solution was decanted from the biochar and replaced with fresh P solution. This process was repeated for 6 days.

5.2.2 Biochar characteristics

The general characteristics of the biochars were investigated in Chapters 2 and 3 and are outlined in Table 1.

5.2.3 Barley rhizobox experiment

5.2.3.1 Soil characteristics

A sandy loam soil from the Rothamsted Research experimental farm at Woburn, Bedfordshire (UK), was used as it has been shown to be P-limited, with total P measured at 0.065% in previous studies (Garbouchev, 1966; Wang et al., 1993). The soil (Stackyard series, Catt et al., 1980) had been maintained as bare fallow for at least 40 years. Full historical data is not available for this soil, as it was not sampled from within the experimental plots, but rather adjacent to them on land which had not been used in the experiments to date. Soil pH was determined in deionised water (ratio 1:2.5, m:v) after shaking for 1.5 h. Soil moisture content was 8.7% (mean of 4 replicates) which was 16.7% of the soil water holding capacity (Prendergast-Miller et al. 2013).

Table 5.1 General characteristics of the biochars used in this experiment

Biochar	**Feedstock**	**HTT (°C)**	**pH (Mean ± 1 stdev, n = 2)**	**PTEs of interest (based on total concentration)**	**Nutrients of interest (based on total concentration)**	**2% formic acid extractable P ($g\ P\ kg^{-1}$) (Mean ± 1 stdev, n = 2)**
PAD450	Pelletised anaerobically digested sewage sludge (Edinburgh, UK) and lignin binder in a 99:1 ratio	450	7.49 ± 0.02	Cd, Cu, Mo, Ni, Zn	P, K	4.73 ± 0.11
PAD550	Pelletised anaerobically digested sewage sludge (Edinburgh, UK) and lignin binder in a 99:1 ratio	550	8.25 ± 0.08	Cd, Cu, Mo, Ni, Zn	P, K	4.24 ± 0.13
POCAD450	Pelletised anaerobically digested sewage sludge (Edinburgh, UK), ochre (Fife, UK) and lignin binder in a 89.1:8.9:1 ratio	450	7.39 ± 0.05	Cu, Mo, Ni, Zn	P, K	4.67 ± 0.29
POCAD550	Pelletised anaerobically digested sewage sludge (Edinburgh, UK), ochre (Fife, UK) and lignin binder in a 89.1:8.9:1 ratio	550	7.85 ± 0.03	Cu, Mo, Ni, Zn	P, K	5.08 ± 0.07
EPAD450	As for PAD450	450	*Not measured*	Cd, Cu, Mo, Ni, Zn	P, K	8.06 ± 0.23
EPAD550	As for PAD550	550	*Not measured*	Cd, Cu, Mo, Ni, Zn	P, K	6.41 ± 0.26
EPOCAD450	As for POCAD450	450	*Not measured*	Cu, Mo, Ni, Zn	P, K	5.97 ± 1.10
EPOCAD550	As for POCAD550	550	*Not measured*	Cu, Mo, Ni, Zn	P, K	4.21 ± 0.08

5.2.3.2 Rhizobox set up

The rhizobox experimental set up was the same as that described in Prendergast-Miller et al. (2013). Four replicates were prepared for all biochar treatments and controls. Soil was spread out in trays and air-dried for 5 days. The air-dried soil was then sieved to 2 mm and weighed equally into two separate bags for each treatment replicate based on the volume of the rhizoboxes (20 x 40 x 0.6 cm internal dimensions) and soil bulk density of 1.58 g cm^{-3}. The rhizoboxes were half-filled with soil from one of the bags poured through a flexible clear plastic funnel for all biochar treatments. The boxes were then shaken by hand until the soil settled at the correct density, assessed using a line drawn across the box to mark halfway. The rhizoboxes for two control treatments – NPK fertilised and NK fertilised – were completely filled with soil only using this method. Fertiliser application rates were based on the requirements of spring barley (*Hordeum vulgare)* in Index 0 soil (DEFRA, 2010). The contribution of biochar P and K was calculated based on bioavailable P (assessed by 2% formic acid extraction, see Table 1) and total K (assessed by modified dry ashing, see Chapter 3. The 2% formic acid extraction was selected to estimate P bioavailability has been previously correlated with plant uptake of P from high ash content biochars (Wang et al., 2012) Biochar application rate (Table 5.2) was calculated based on bioavailable P, with any deficiency in K at this application rate made up by the addition of KCl. The appropriate amount of biochar was mixed into the remaining soil for each biochar treatment replicate and then the mixture added to fill the rhizoboxes. KCl was also used to meet the K requirements of the P-fertilised and non-P fertilised controls. NH_4NO_3 was used to meet N fertilisation requirements in all treatments. $Ca(H_2PO4)_2$ was used to meet the P requirements of the P-fertilised control treatment. All fertilisers were added in aqueous solution (made up with deionised water) to the top of each rhizobox, as per their designated treatment. Four barley seeds were pushed just under the surface of the soil in each rhizobox, evenly spaced and away from the edges. The clear Perspex boxes were wrapped in foil to minimise light to the root zone and placed in a plant growth room (21°C, 16 h light (100 µmol m^{-2} s^{-1}), 65% humidity (day) 50% humidity (night)). The rhizoboxes were watered every second day by applying 10 ml deionised water to the top of each rhizobox. Watering based on change in mass compared to day 1 was originally planned, however the fragile nature of the plants, confined space in the growth chamber and sharp edges of the rhizoboxes meant it was difficult to measure rhizobox weight without disturbing the experiment. Therefore, the volume of water added was chosen based on initial changes in rhizobox weight with water

Table 5.2 Biochar application rates per rhizobox added to 670 g of soil , calculated based on the proportion of total biochar P which was extractable using 2% formic acid.

	Biochar added (g)
PAD450	1.22
PAD550	1.36
POCAD450	1.23
POCAD550	1.13
EPAD450	0.71
EPAD550	0.78
EPOCAD450	1.04
EPOCAD550	1.11

evaporation in the early days of the experiment. One week after shoot emergence, the seedlings were reduced to one plant in each rhizobox. The plants were left to grow for 12 weeks before harvest. Although grain had not yet set, the building in which the growth chamber was situated was to be demolished and thus it was decided to end the experiment, rather than transport the rhizoboxes to another building.

5.2.3.3 Experiment sampling

At harvest, the barley plants were photographed and the length of all leaves measured. The above ground biomass was removed from the top of the rhizobox and oven-dried for 3 days at 60°C, before being weighed to determine above ground biomass dry weight yield.

The rhizoboxes were opened and roots removed. The soil in each box was separated into three sections, the top 15 cm, middle 10 cm and bottom 15 cm, transferred to plastic zip-lock bags and hand-mixed to homogenise. They were then stored at -8°C until preparation for analysis. Only the top and bottom samples were analysed, as the middle soil fraction was collected to eliminate any effect of mixing between the original two applied layers.

5.2.3.4 Soil pH

Soil samples from the top and bottom sections of each rhizobox were weighed into small glass bottles, to which deionised water was added (1:2.5 m:v ratio). These were shaken on an orbital platform shaker at 150 rpm for 1.5 h before measurement of pH using a Mettler Toledo FE 30 pH probe calibrated with standards of pH 4 and 7.

5.2.3.5 Soil bioavailability analysis

Soil samples from the top and bottom sections of each rhizobox were sieved to 1 mm and oven-dried at 80°C before being weighed into a centrifuge tube (1.5 g). Mehlich 3 reagent (15 mL) was added and the mixtures shaken on an orbital platform shaker at 150 rpm for 5 min, as per the standard Mehlich 3 procedure (Mehlich, 1984b). This extractant was selected based on its common usage in the literature and the high amounts of nutrients and PTEs it was shown to extract in Chapter 4. The samples were double-filtered, first using Whatman No. 1 paper filters and then using 0.45 μm syringe filters (Millipore, Watford, UK). Blanks were prepared for each extraction (in triplicate) and values subtracted from the experimental samples. All filtrates were stored at 4°C before analysis for Al, B, Ca, Cd, Co, Cr, Cu, Fe, Hg, K, Mg, Mn, Mo, Na, Ni, P, Pb and Zn by ICP-OES, using a Perkin Elmer Optima 5300DV instrument (Waltham, USA). Most elements were analysed in axial mode, except for Al, Ca, Fe, K, Mg and Na, which were analysed in radial mode as higher concentrations of these elements were expected.

5.2.3.6 Soil elemental analysis

Soil samples from the top and bottom samples from each rhizobox were sieved to 1 mm, oven-dried at 80°C and milled before weighing, ashing at 430°C for 6 h followed by HCl/HNO_3 digestion. Duplicate digestions of randomly selected samples were conducted to test the precision of the method, which showed good replicability (< 10% variation). These were for POCAD450, EPOCAD450, Control NPK and Control NK, and the final results showed good method precision. ICP-OES was used to determine concentrations of Al, B, Ca, Cd, Co, Cr, Cu, Fe, Hg, K, Mg, Mn, Mo, Na, Ni, P, Pb and Zn using a Perkin Elmer Optima 5300DV instrument (Waltham, USA). Most elements were analysed in axial mode, except for Al, Ca, Fe, K, Mg and Na, which were analysed in radial mode as higher concentrations of these elements were expected. More details about the analysis method and the calculation of the limit of detection can be found in Buss et al. (2016a).

5.2.3.7 Leaf elemental analysis

The dried leaves were ball milled and approximately 100 mg of dried biomass was digested from each of the 4 replicates for each treatment. The dried biomass samples and 4 blanks were digested with 18 M H_2SO_4 and 30% w/v H_2O_2 in a heating block at 330°C for 6 h, and analysed for As, Al, B, Ca, Cd, Co, Cr, Cu, Fe, Hg, K, Mg, Mn, Mo, Na, Ni, P, Pb and Zn using an Agilent 7500ce ICP-MS (Agilent Technologies, Santa Clara, USA). Where elemental concentrations were sufficiently high (e.g. P and Ca), ICP-OES was performed using a Perkin Elmer Optima 5300DV instrument (Waltham, USA). Standards were prepared and run during each analysis session for calibration and to check the accuracy of measurements over time. Values obtained for the digestion blanks were subtracted from each reading. The limit of detection for each element for each instrument was determined as described in Buss et al. (2016b), except that it was calculated for each sample due to the small and variable amounts of dry biomass produced in the experiment.

5.2.4 Data analysis

Rhizobox total P budget was calculated using the total P concentrations of the unamended soil to determine the total mass of P in each rhizobox. The concentration of P in each biochar (and in the NPK fertilised control), along with the individual treatment application rates, were used to calculate the total mass of P added to each rhizobox. The sum of these two values equalled the total applied P per rhizobox (averaged for each replicate). The amount of total P in the rhizoboxes at the end of the experiment was calculated as the total applied P minus the mass of P measured in the barley leaves, giving the calculated final soil P mass. The soils were examined for total P at the end of the experiment, so a comparison between calculated final soil P mass and measured total soil P mass could be made. Any differences between the two values would reflect P taken up by the plant roots, as these were not analysed.

All statistical analyses were performed using SigmaPlot (SigmaPlot, v13.0). Dry above ground weight yield, total leaf length at harvest, leaf element concentrations, leaf P mass, soil element totals and soil Mehlich extracts were compared. The data were tested for normality using the Shapiro-Wilk test. Where data were normally distributed, one-way Analysis of Variance (ANOVA) and Tukey's Honest Significance Difference (HSD) test were used to identify differences between treatments. Where data were not normally distributed and could not be easily transformed to normality (most data), Kruskal-Wallis H test was used, followed by Dunn's method to identify differences between treatments. Statistical significance was considered to be at a level of at least $p < 0.05$.

5.3.5 Plant yields

There were no significant differences between treatments for plant yield or total leaf length (Figure 5.1), indicating the biochars were as effective as standard P fertiliser treatment. It was expected that growth would be lower in the NK fertilised control as it should have been P-limited, however this was not the case. It is possible that plant growth for all treatments was limited by the height of the growth chamber (1 m, 60 cm above the top of the rhizoboxes) and the lack of space in the rhizobox for 3-dimensional root growth to support the stems.

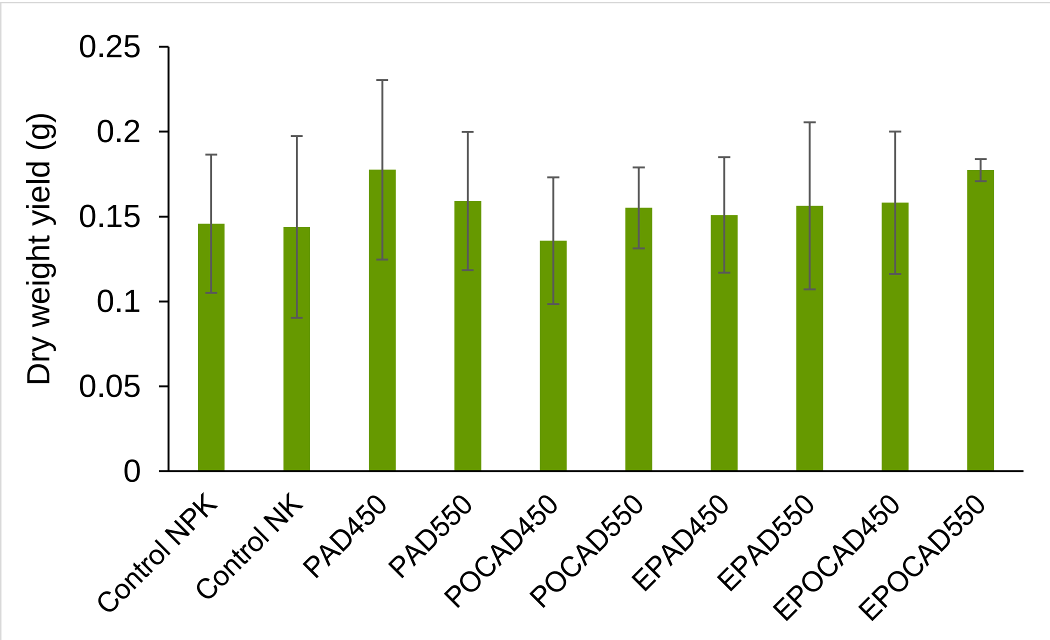

Figure 5.1 Dry weight yield of barley above ground biomass after 12 weeks growth. Means of 4 replicates are shown, ± 1 standard deviation.

5.3.6 Leaf composition

5.3.6.8 Phosphorus

No statistically significant differences in P concentration or P mass in the harvested barley leaves was identified between biochar and controls (Figure 5.2, Table 5.3). The variation between replicates was higher for the two controls than the biochar treatments, suggesting plant access to P was more ubiquitous in the biochar treatments.

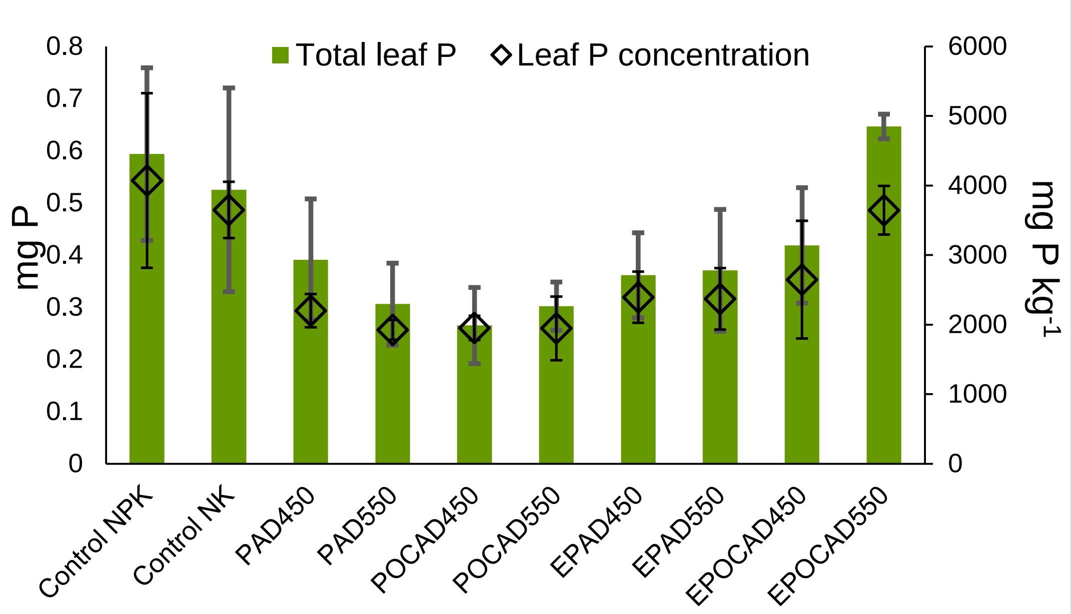

Figure 5.2 Comparison of barley leaf P concentration and leaf P mass for treatments and controls. Means of 4 replicates are shown ± 1 standard deviation

5.3.6.9 Other elements

There were statistically significant differences in the concentrations of Ca, Mg and Na in the plant leaves between treatments. Leaves harvested from the Control NPK fertiliser treatments contained a higher concentration of Ca on average than the Control NK fertiliser ($p < 0.001$), PAD550 ($p < 0.001$), EPOCAD450 ($p < 0.002$), EPAD550 ($p < 0.004$), and PAD450 ($p < 0.011$) treatments. They also contained a higher concentration of Mn than PAD550 ($p < 0.008$) and EPOCAD550 ($p < 0.35$). As there were no significant differences in yields and none of the treatments caused accumulation of PTEs in the barley leaves above the Upper Critical Limits for barley (based on Davis et al. (1978) and MacNicol and Beckett (1985), outlined in Chapter 4), these differences in leaf chemical composition did not have a measurable effect on plant growth (Table 5.4).

Table 5.3 Mean nutrient concentrations (n = 4) of the digested barley leaves determined by ICP-MS/OES, expressed in mg kg^{-1} ± 1 standard deviation.

	Control NPK	Control NK	PAD450	PAD550	POCAD450	POCAD550	EPAD450	EPAD550	EPOCAD450	EPOCAD550
Ca	22018 ± 1582	13959 ± 301	16554 ± 1425	15375 ± 1197	18186 ± 1773	17532 ± 1822	17539 ± 1558	16023 ± 1786	15528 ± 3050	17772 ± 1659
K	54969 ± 3947	49396 ± 2582	45867 ± 5236	46820 ± 3689	53375 ± 6492	56511 ± 6718	56447 ± 4823	54677 ± 4785	54133 ± 9409	54276 ± 3767
Mg	3401 ± 132	3013 ± 265	3111 ± 263	3206 ± 286	3591 ± 277	3519 ± 230	3456 ± 458	3248 ± 149	3079 ± 646	3460 ± 271
Mn	111 ± 23	86.1 ± 6.5	79.2 ± 16.9	61.0 ± 14.0	84.8 ± 21.5	82.7 ± 17.9	87.3 ± 10.1	75.7 ± 20.5	71.9 ± 17.6	68.5 ± 14.8
P	4073 ± 1254	3649 ± 406	2202 ± 240	1925 ± 143	1952 ± 175	1946 ± 459	2394 ± 367	2371 ± 442	2646 ± 847	3645 ± 351

Table 5.4 Mean PTE and other element concentrations (n = 4) of the digested barley leaves determined by ICP-MS/OES, expressed in mg kg^{-1} ± 1 standard deviation.

	Control NPK	Control NK	PAD450	PAD550	POCAD450	POCAD550	EPAD450	EPAD550	EPOCAD450	EPOCAD550
As	2.49 ± 2.15	0.911 ± 1.00	1.07 ± 0.21	0.84 ± 0.20	0.55 ± 0.23	0.94 ± 0.29	0.890 ± 0.282	0.65 ± 0.17	0.610 ± 0.13	1.12 ± 0.96
Al	64.1 ± 14.2	73.0 ± 34.2	90.0 ± 82.6	107 ± 35	68.3 ± 36.1	90.0 ± 77.5	58.9 ± 14.7	56.0 ± 23.6	73.4 ± 41.3	43.8 ± 8.5
B	24.8 ± 3.2	20.4 ± 3.9	22.0 ± 6.9	21.9 ± 6.8	22.4 ± 7.0	20.2 ± 5.7	16.3 ± 4.4	19.5 ± 2.9	16.5 ± 1.47	15.4 ± 2.4
Cd	0.459 ± 0.068	0.368 ± 0.078	0.415 ± 0.211	0.354 ± 0.089	0.371 ± 0.093	0.367 ± 0.081	0.371 ± 0.077	0.312 ± 0.024	0.409 ± 0.035	0.334 ± 0.050
Co	0.283 ± 0.151	0.360 ± 0.124	0.545 ± 0.210	0.25 ± 0.06	0.250 ± 0.111	0.334 ± 0.151	0.449 ± 0.342	0.352 ± 0.167	0.277 ± 0.181	0.243 ± 0.061
Cr	83.3 ± 70.9	121 ± 88	226 ± 133	64.8 ± 43.3	67.8 ± 45.3	108 ± 51	174 ± 172	130 ± 95	92.4 ± 97.0	89.1 ± 34.6
Cu	12.3 ± 1.5	12.9 ± 1.0	14.8 ± 1.4	13.2 ± 1.8	14.1 ± 1.71	14.3 ± 1.5	13.4 ± 1.6	13.4 ± 1.4	13.6 ± 0.89	12.7 ± 0.69
Fe	528 ± 283	1000 ± 220	1420 ± 711	576 ± 261	516 ± 271	784 ± 394	1170 ± 1060	845 ± 495	656 ± 510	576 ± 196
Hg	0.0820 ± 0.0621	0.00 ± 0.00	0.00 ± 0.00	0.00 ± 0.00	0.00 ± 0.00	0.00 ± 0.00	0.00 ± 0.00	0.00 ± 0.00	0.00 ± 0.00	0.00 ± 0.00
Mo	7.13 ± 3.83	2.99 ± 1.56	8.00 ± 3.77	2.94 ± 1.49	2.80 ± 1.26	3.72 ± 1.45	3.74 ± 2.32	3.44 ± 0.79	2.33 ± 1.45	2.63 ± 0.54
Na	2410 ± 376	2320 ± 345	8090 ± 19	8890 ± 557	7370 ± 873	5430 ± 523	5480 ± 1270	4760 ± 886	3900 ± 1740	3180 ± 503
Ni	185 ± 123	248 ± 62	83.4 ± 37.7	104 ± 80	156 ± 142	249 ± 86	197 ± 141	292 ± 160	179 ± 136	234 ± 94
Pb	1.25 ± 0.20	1.45 ± 0.62	1.80 ± 0.31	1.17 ± 0.16	4.84 ± 5.93	1.29 ± 0.44	1.46 ± 0.57	1.33 ± 0.33	1.51 ± 0.63	1.80 ± 0.92
Zn	131 ± 34	136 ± 37	114 ± 7	110 ± 22	118 ± 10	122 ± 4	132 ± 17	104 ± 5	106 ± 38	104 ± 21

5.3.7 Soils

5.3.7.10 Total element concentrations

A sample of untreated soil was set aside to be analysed in order to compare soil characteristics before and after the experiment, however it was inadvertently thrown away by a third party before the analysis could take place. For this reason, there was not a true set of 'before' characteristics with which to compare. For the purposes of this thesis, the characteristics of the bottom fraction of the non-P fertilised soil have been used, although these are unlikely to be exactly the same as the completely untreated soil. This does not, however, affect the comparisons of top and bottom soil fractions, or the end points of the different treatments.

5.3.7.10.1 Total phosphorus

No significant differences were identified between P concentrations in the bottom soil fraction of any of the treatments. There were significant differences ($p < 0.05$) in P concentration between the Control NPK top soil samples and top soil samples in the PAD550 ($p < 0.002$), PAD450 ($p < 0.003$), POCAD550 ($p < 0.004$) and POCAD450 ($p < 0.007$) treatments. As the biochar application rates were based on extractable P, rather than total P, it is not unexpected that the biochar treatments contain more P than the two controls, especially in the top soil sections, as the biochar contained additional P relative to the fraction which was assessed as bioavailable.

5.3.7.10.2 Other nutrients

Compared to the top soil fraction of Control NPK, the same fraction of POCAD550 treated soils contained significantly more Ca ($p < 0.006$), whilst EPOCAD450 ($p < 0.034$), EPOCAD550 ($p < 0.004$), EPAD450 (0.016) and PAD450 treated soils contained significantly more Mg.

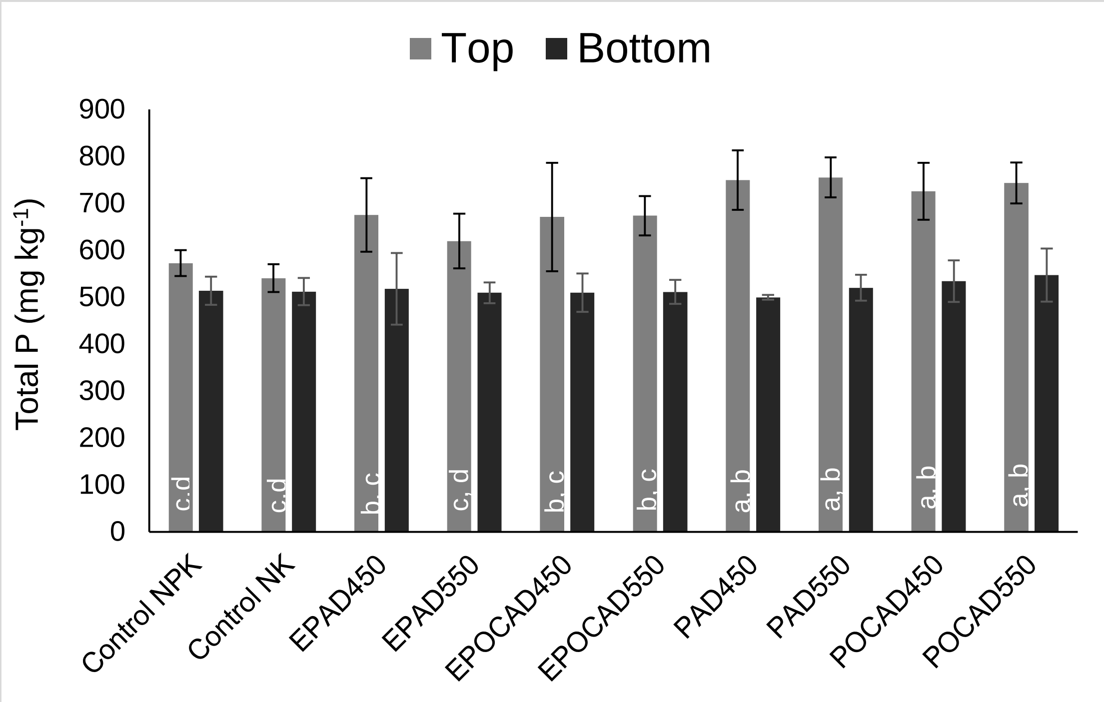

Figure 5.3 Total P in soils sampled from the top and bottom 15 cm of the rhizoboxes. Values are the mean of 4 replicates and error bars represent ± 1 standard deviation. Letters are used to designate significant differences between treatments

5.3.7.10.3 Potentially toxic and other elements

The top soil fraction of the PAD450 treatments contained significantly more As ($p < 0.001$), B ($p < 0.003$) and Fe ($p < 0.003$) than the NPK Control treatments. EPAD450 treatments contained significantly more B ($p < 0.05$) and Fe ($p < 0.023$) than the NPK Control, and PAD550 contained significantly more As (0.003) compared to the same control. No other significant differences between top soil fraction in the biochar treatments and the NPK Control were found. The increase in As concentration compared to the NPK Control was between 6.5-7.8 mg kg^{-1} and 16-21 mg kg^{-1} for B. This increase cannot be completely attributed to biochar application as even the top soil in the NK fertilised Control contained more As (~2.8 mg kg^{-1}) and B (~4.7 mg kg^{-1}) compared to the bottom soil fraction of the same treatments.

5.3.7.11 Mehlich extractable P

Significant differences in P concentration in Mehlich 3 extractions were found between treatments for top and bottom soil fractions ($p < 0.05$) (Figure 5.4). In the bottom soil fractions Mehlich 3-extractable P concentrations were significantly higher in the NPK Control, PAD450, PAD550, POCAD450 and POCAD550 compared to the other treatments. The top soil fraction extracts from the PAD450, PAD550, POCAD450 and NPK Control treatments contained higher concentrations of P than the Control NK treatment. These data confirm that the P present in the Control NK treatment was less extractable than in the other treatments.

Mehlich 3 extractable P in the non-P amended soil (Control NK, bottom fraction) was 36.0 ± 1.42 mg P kg^{-1}. Using the conversion method of Wolf and Baker (1985) suggested by Jordan-Meille et al. (2012), this equates to an Olsen-P value of between 13.5-14.4, which is classified as an Index 1 soil in the DEFRA Fertiliser Manual RB209 (2010). Thus, based on this assessment, the Woburn soil used was relatively P limited. As outlined in Table 5.5, the soil P index increased in all treatments except Control NK, which had no P addition.

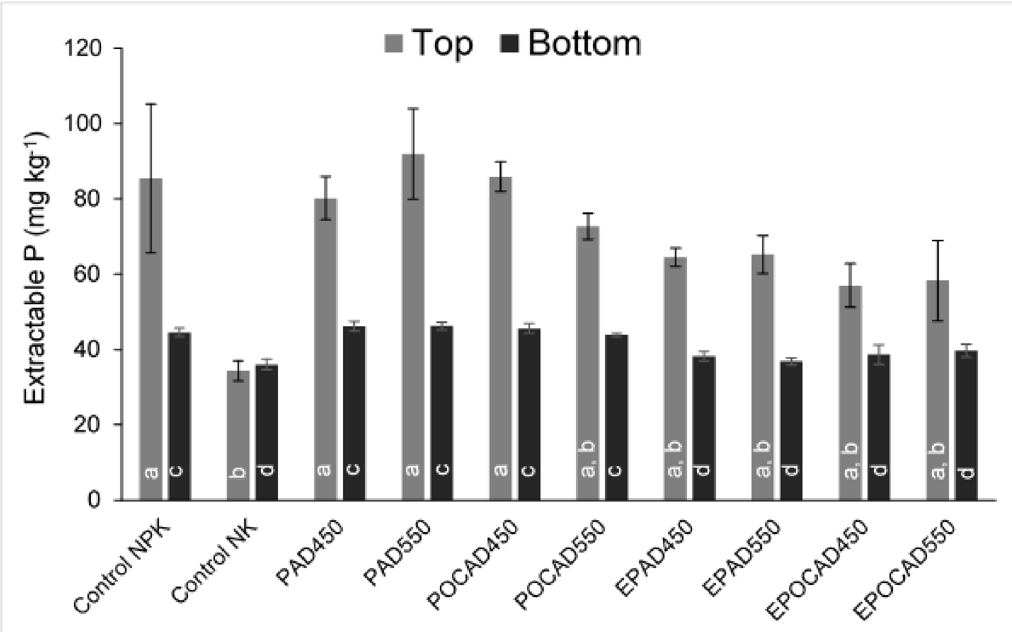

Figure 5.4 P concentrations in Mehlich 3 extractions of top and bottom soil samples , displayed as means of 4 replicates ± 1 standard deviation. Letters are used to designate significant differences between treatments.

Total P concentration in top soil samples was highest in the non P-exposed biochar treatments, as these contained lower proportions of 2% formic acid extractable-P and were thus applied at higher rates on a total P basis (data not shown). The data in Table 5.5 provide possible evidence for transport of biochar and fertiliser P to the bottom of the rhizobox, as the proportion of Mehlich 3-extractable P is significantly higher in the bottom soil fraction for the NPK control and PAD450, PAD550, POCAD450 and POCAD550 compared to the NK control. It is likely that some of the increase in extractable P proportion compared to the NK control is related to the presence of residual organic matter (roots) in the soil samples, which grew better in the presence of P fertiliser than without it.

Given the lower extractable P status of the Control NK treatment, it is apparent that the baseline level of P in the soil was sufficient for barley growth, even though it was not as extractable as the other treatments. The P-exposed biochars appear to have a lower proportion of Mehlich 3-extractable P compared to the non P-exposed biochars, which supports the hypothesis that the P present in the P-exposed biochars is more bioavailable than the native biochar P and has thus been taken up by the plant. Full evidence for this would have required a sub-sample of the fertilised soils at the beginning of the experiment to compare before and after values.

Table 5.5 Soil P bioavailability at harvest. Soil P index after plant harvest is for the top soil fraction, based on DEFRA soil classifications (DEFRA, 2010) and calculated using the Mehlich 3/Olsen P conversion equation proposed by Wolf and Baker (1985) : Olsen P = (Mehlich 3 P + 6.91)/3.08. For each treatment the mean Mehlich 3 extractable P value + one standard deviation and – one standard deviation have been used to calculate the range of Soil P Index values given. The proportion of Total P which was Mehlich 3 extractable is also given. Were one value for Soil P Index is given, both the minimum and maximum values fell in that classification.

Treatment	Soil P Index at harvest	Mehlich 3 extractable P (% Total P)	
		Top soil fraction	Bottom soil fraction
Control NPK	2 – 3	14.9	8.7
Control NK	1	6.4	7.0
PAD450	3	10.7	9.2
PAD550	3	12.2	8.9
POCAD450	3	11.8	8.5
POCAD550	2 – 3	9.8	8.0
EPAD450	2	9.6	7.4
EPAD550	2	10.5	7.2
EPOCAD450	2	8.5	7.6
EPOCAD550	2	8.7	7.8

5.3.8 Rhizobox phosphorus budgets

5.3.8.12 *Total phosphorus*

A total P budget was calculated for each rhizobox to compare the underlying concentration of P in the soil at the start and end of the experiment with the P added with the fertiliser and biochar treatments and present in the above ground plant biomass at the end of the experiment. The amount of P extracted by the plants in the experiments was a very small proportion of the total P that was present in the system (Figure 1.5).

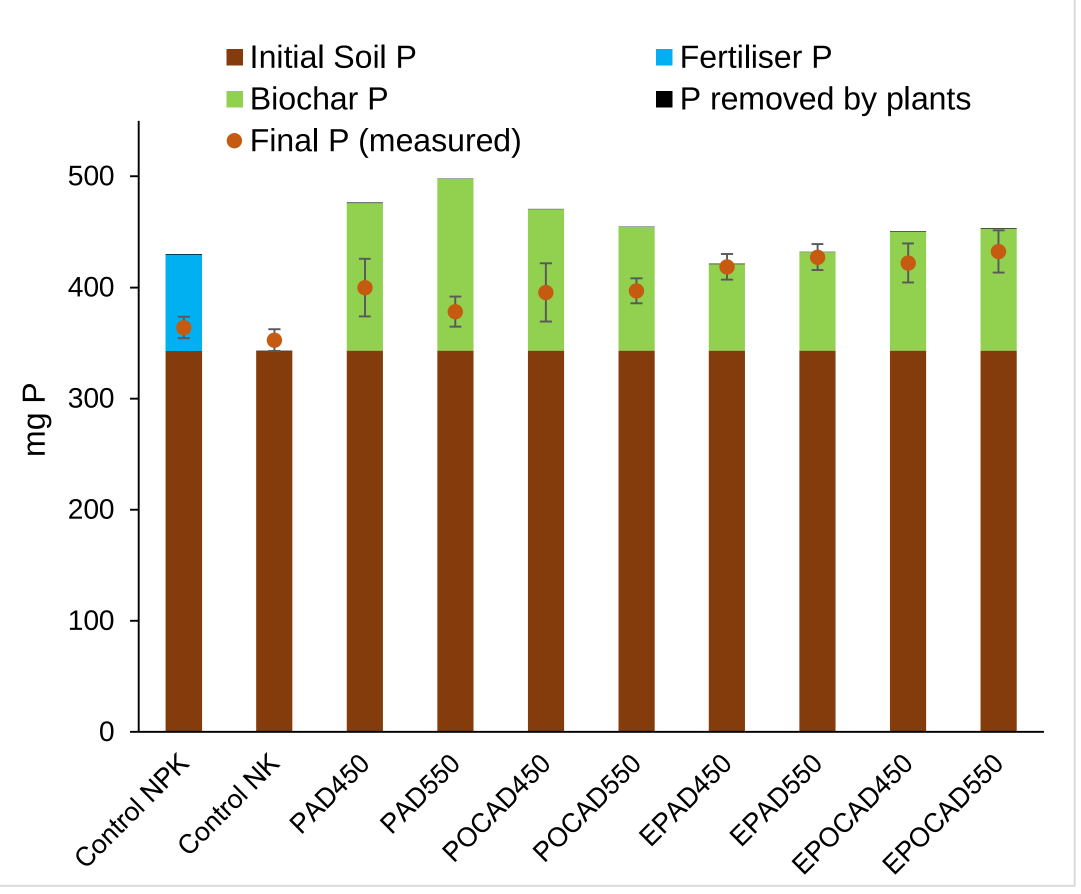

Figure 5.5 Total P budget showing initial mean P mass in the soil (670 g soil), fertiliser and biochar P additions to each treatment, as well as the amount of P taken from the soil system into the barley above ground biomass. The mean measured final P mass in the soils at harvest (n = 4) is also displayed as orange circles, ± 1 standard deviation.

The total P budget, based on initial soil and biochar/fertiliser added P, did not match total P measured in the soils after harvest. This was most pronounced in the Control NPK and non P-exposed biochars, where soil total P at the end of the experiment was less than the sum of the initial soil total P and the added P. It is also that some of the difference could be explained by the variation in the recovery efficiencies (95-100%) of the wet digestion technique used to analyse the leaf samples and the modified dry ashing technique used for the biochars and soil (Enders and Lehmann, 2012; Tüzen, 2003). It is also possible that some of the ‘missing’ P was located in the plant roots, which were not analysed for practical reasons. On the other hand, the calculated total P budget and final soil P mass are more similar for the Control NK and P-exposed biochars. This may indicate better P use efficiency in these treatments or that P was more available in these treatments, so less root mass development was required by the plants to access P.

5.3.9 General discussion

The original concept of biochar, in a research context, was to sequester carbon in soils as a means of climate change mitigation, whilst improving soil characteristics at the same time (Lehmann and Joseph, 2009). Thus, the application rates of biochar in most published experiments tend not to be based on nutrient concentrations, in contrast to this study, but rather in the order of tens to hundreds of tonnes per hectare (Jeffery et al., 2011). Many studies compare either the effect of biochar on plant yield to untreated, unfertilised controls (Liu et al., 2014; Song et al., 2014) or the additional yield effects when biochar is combined with fertiliser treatments compared to fertiliser alone (Glaser et al., 2015; Lehmann et al., 2003). The P-exposed biochars used in the present study are in a way similar to these biochar and fertiliser treatments, although at lower P fertiliser concentrations.

The application of biochars to the Woburn soil at an application rate based on 2% FA extractable P concentration compared to soluble P fertiliser at the equivalent application rate resulted in no significant differences in barley above ground biomass yield, leaf P concentration or leaf P mass. Biochar application rates were based on 2% FA extraction values, as this has been suggested as the best method for assessing bioavailability of P in high-ash biochars (Wang et al., 2012). The rhizobox experiment described in this chapter was initiated before the experiments described in Chapter 4 had been completed. The outcome of these experiments may have influenced the decision to use the selected method of bioavailability prediction, however no bioavailability method assessed in Chapter 4 was found to be a good predictor of plant uptake of P.

The concentration of P in the biochars used in this research are high at around 10% dry weight (as described in Chapter 3), considering the mass percentage of P in PO_4^{3-} is 33%, and at the native pH of the biochars (around 7) it is possible that a large proportion of this is bioavailable. In addition, biochar application is expected to be infrequent, with the biochar itself expected to last tens to hundreds of years in the soil (Lehmann and Joseph, 2009) so it is possible that far more P than can be extracted in laboratory tests could be accessed from each biochar particle by plants over time. Different testing methodologies need to be developed in order to be able to accurately determine the bioavailability of P from biochar fertilisers.

Sewage sludge-derived biochar produced at a HTT of 450°C increased plant height and fresh matter yield of Chinese cabbage in a pot experiment using low nutrient status or PTE polluted soil collected from nearby a zinc lead mine (Liu et al., 2014). The biochar application rate of 1:3 biochar to soil ratio was much higher than that used in the present study (7:3350 - 7:6700), similar to another study (1:6 – 1:2) which compared both sewage sludge-derived biochar HTT and application rates on plant height and yield in garlic (Song et al., 2014). The optimised application rate for yield increase using biochar produced at a HTT of 550°C was shown to be 1:5, whilst at this application rate biochar produced at 450°C was found to be more effective at increasing yield than biochar produced at 550°C. When assessing the optimal application rate of the biochar produced at 450°C, a 1:4 application rate was found to produce the highest yield (Song et al., 2014). Given the higher application rate required for the lower temperature biochar, a cost-benefit analysis would be required to determine the most efficient treatment for increasing yield.

Gwenzi et al., (2016) used much lower sewage sludge-derived biochar application rates of 7.5 and 15 t ha^{-1} in a maize pot experiment using tropical clay soil. Unlike the previously discussed studies, this experiment included a fertiliser treatment to compare the efficiency of biochar as a stand-alone fertiliser. The fertiliser used was “Compound D”, applied at 300 kg ha^{-1}, equivalent to 18.3 kg P ha^{-1}, whilst the biochar application rates were equivalent to 8.3 – 16.5 kg Total P ha^{-1}. Unsurprisingly, given the higher concentration of available P in the fertiliser treatments, total dry biomass yield was higher in the fertiliser treatments, but biochar application did increase maize yield compared to the untreated control. Interestingly, the biochar treatments promoted shoot growth relative to root growth compared to the fertiliser treatments. The root mass was not measured in the present study as it was generally low in volume and broke easily when handled, but future experiments should consider the root to shoot ratio when assessing the performance of these biochar fertilisers.

Addition of the biochars at the rates used in the present study did not cause PTE contamination of the soil or cause phytotoxicity, agreeing with the statement of (Buss et al., 2016b), which explains that when biochars (produced from marginal biomass, in particular) are applied at rates based on their nutrient content, PTE concentrations added to the soil should not cause environmental harm. These results support those in the literature which highlight the potential for biochar fertilisers to be produced from sewage sludge (Hossain et al., 2010; Khan et al., 2013a, 2013b).

Even at higher biochar application rates, PTEs from the biochar have not caused toxicity to plants. In low nutrient status, non-PTE contaminated soil, sewage sludge-derived biochar did not significantly increase the concentration of Cu, Pb, Zn, Cd or Cr in Chinese cabbage, and even significantly reduced the concentration of Pb, Cr and Cd in the cabbage grown in PTE contaminated soil when compared to a biochar-free control (Liu et al., 2014). Compared to soil-only treatments, Song et al. (2014) did not observe an increase in PTE accumulation in garlic plants, either. Application of sewage sludge-derived biochar to tropical clay soil at rates of 7.5 and 15 t ha^{-1} also did not cause accumulation of PTEs in maize shoots (Gwenzi et al., 2016). There is clearly a growing body of evidence within the literature that biochar does not cause phytotoxicity when applied at economically feasible rates and tends to reduce, rather than increase, concentrations of PTEs in plant tissue where contaminated soil is used.

Although the P delivered to the plants via the biochars was plant available, there were (non-significant) differences in total leaf P (and leaf P concentration, Figure 5.2). Barley leaves grown in the PAD450 and the P-exposed biochar treatments, especially EPOCAD550, contained more P than the other three biochar treatments, indicating that the plants were able to access P from these more easily.

Unlike in the rapid plant growth experiment described in Chapter 4, there was not a significant linear correlation between plant leaf P mass and above ground biomass yield, which indicates non-optimal growing conditions. There was also no relationship between leaf P concentration and above ground biomass yield, so some of the treatments may have been P limited due to differences in P bioavailability, or the P use efficiency in the plant varied between treatments. Without grain to analyse for comparison with quality criteria and without analysis of the roots, it is not possible to say whether lower P concentration in the plant leaves would have a positive or negative effect on the final crop characteristics such as grain yield and protein content.

Application of biochar to the P-constrained Woburn soil resulted in an overall increase in soil P bioavailability as measured by Mehlich 3 extraction compared to the non-P fertilised treatment. This is in agreement with previous literature findings, where the respective effects of biochar liming to increase soil-P availability compared to fertilisation by biochar-P on plant growth have been assessed (Shen et al., 2016). Previous studies have found application of biochar increases crop yield, but applying fertiliser with biochar increases yields even further (e.g. Hossain et al. (2010)). Additional experiments are required to calculate a full P budget for the biochars used in this study and account for the contribution of mobilised soil-derived P to plant growth.

Comparison of the total P budget and the final Mehlich 3 extractable values (Figures 5.4 and 5.5) reveals the high amount but relative low availability of P in the soil system in the experiment. This explains why, even though no P was added to the soil, barley plants grown in the NK Control treatments were no different to the NPK control in terms of yield and leaf P mass. The barley plants are able to access P from the soil. The additional leaf P mass is explained as P originating from the barley seed.

The hypothesis of soil pH differing in the top and bottom soil fractions of the biochar treatments due to a liming effect of biochar was disproven, as there were no significant differences in pH between the top and bottom soil fractions (data not shown). There was, however, an effect of biochar on P availability in the top soil fractions, so there may be localised changes in pH which could not be detected using bulk pH analysis, or there have been non-soil pH related reactions occurring which had an effect on P availability.

5.4 Conclusion

This study has shown that sewage sludge derived biochars can be used to fertilise barley growth in a P constrained soil, without causing PTE contamination or phytotoxicity. The P delivered to the soil-plant system from the P-exposed biochars appears to be more bioavailable than native biochar P. Based on P concentration measured in barley leaves, EPOCAD550 performed particularly well as a P fertiliser compared to the other biochar treatments. There is evidence for an increase in soil P bioavailability after biochar application, even at relatively low application rates, but this cannot be attributed to a bulk soil pH effect, as no significant increase in soil pH was observed. Further experiments are needed to calculate properly the proportion of biochar P which is bioavailable, which will ensure efficient use and reduce total P applied to soils. Investigations of pH changes around biochar particles in the soil would also assist in understanding the overall effect of application of sewage sludge derived biochars on P bioavailability in P constrained soils.

Chapter 6

General discussion

This discussion chapter brings together the research findings from Chapters 2-5 to address the aims presented in Chapter 1. The research has been necessarily interdisciplinary, as it aimed to address a problem in a complex system that spans industrial, agricultural and environmental spheres.

The overall purpose of this research was to design and test tailored biochars to be used as P recycling materials as a way of using wastewater effluent P to meet agricultural crop P requirements.

6.1 Material production

6.1.1 Feedstock selection and processing

The initial stages of material development required selection of appropriate feedstocks for biochar production. This required a decision regarding the chosen approach, as two broad pathways exist for incorporating ochre to create potentially phosphate-reactive biochar. The first is similar to that of activated carbon, involving the selection of a main carrier feedstock which would produce biochar with high porosity and surface area, such as wood (Chia et al., 2015). Methods for impregnating either the feedstock or biochar with ochre particles (or dissolved components of ochre) would then be investigated. This approach was not chosen as it was not clear that impregnation would be possible and if it was would require solvents and additional production steps. It was also not clear that a reliably consistent source of waste wood or feedstock with similar physical properties would be available on a large scale.

The chosen methodology involved selection of feedstock based on demonstrated P capture properties. A comparison of anaerobically digested and non-digested sugar beet tailings (Yao et al., 2011) drew attention to anaerobically digested feedstocks. A second study utilising biochar from another anaerobically digested feedstock also highlighted P capture properties (Streubel et al., 2012). Recognising the need for a non-cement binding medium for the powdered Minto MWTP ochre, it was decided to use anaerobically digested sewage sludge, an abundant feedstock, prior to pyrolysis and test the properties of these composite biochars compared to anaerobically digested sewage sludge biochar alone. As the biochars produced in this first stage of material development demonstrated P capture properties (covered in Chapter 2) this approach was considered successful and was adopted for the whole research project.

The upscaling of the production process required the use of a screw-fed kiln, for which the uncompacted dried sewage sludge and sewage sludge-mixtures used in the small-scale batch pyrolysis process were not suitable. Pelletisation of the feedstocks was chosen as the use of pellets in the particular pyrolysis unit had been well demonstrated, although no data has been published on such biochars to date. This decision is now further supported in literature discussion of feedstock size and form, and pyrolysis feeding equipment (Mašek et al., 2016). Whilst the pelletisation of the feedstock was successful in aiding the pyrolysis feeding process, the increase in PTE concentrations in the resulting biochars compared to the non-pelletised feedstocks (Chapter 3) highlights the need for this process to be reconsidered. It is possible that the relative retention of PTEs in the pelletised biochars is related in part to the dense packing of the pellets, which may restrict gas flow and thus volatilisation of PTEs into the gas stream. It can be concluded that the pelletisation process employed (at the Biorenewables Development Centre, York, UK) likely caused Cr, Cu and Zn contamination of the pellets, which may be related to the frequent 'burning out' of the pelletising apparatus as the feedstock caused clogging.

If this technology were to be adopted in an industrial-scale setting, the combination, drying/forming and pyrolysis process would need to be optimised appropriately. As this was not one of the aims of this research project, it was not pursued further.

6.1.2 Comparison to biochar quality guidelines

Generally, the non-pelletised biochars contained lower concentrations of PTEs than the pelletised biochars (as discussed in section 6.1.1). When these data are compared to quality guidelines published by the International Biochar Initiative and the European Biochar Foundation (basic and premium product levels), both of the non-pelletised mixed ochre-sewage sludge biochars (OCAD450 and OCAD550) meet the quality criteria (Chapter 2) (EBC, 2012; IBI, 2012). The anaerobically digested sewage sludge counterparts did exceed both IBI and EBC guidelines, as did all of the pelletised biochars (Chapter 3). The elements concerned are Cd, Cu, Mo and Zn, and the relevant guideline and biochar values are outlined in Table 6.1. These regulations seem to be the most appropriate to consider environmental regulation of sewage sludge-derived biochar application to soil in Scotland. Of the IBI guideline value exceedances, many are of the lower but not the higher of guideline range. Considering this, AD450 and AD550 both meet the IBI criteria, and the pelletised biochars only exceed IBI guideline values for Mo.

Considering the biochar application rates used in Chapter 5, based on the 2% formic acid extractable content of the different biochars, it is unlikely that application of the biochars to meet the P fertilisation requirements of crops will cause PTE pollution or phytotoxicity. When the application rates are used to calculate the amount of PTEs applied to soil at the relevant rates (Table 6.2) for the pelletised biochars, only PAD450 and PAD550 exceed the limits set out in the regulations for sewage sludge application in the UK (Public Health, England and Wales Public Health, Scotland 1989 No. 1263 Schedule 1, Regulation 3:

Testing of Sludge). These regulations seem to be the most appropriate to consider environmental regulation of sewage sludge-derived biochar application to soil in Scotland.

Table 6.1 Element concentrations for biochars where values exceed biochar quality guidelines for maximum PTE concentration. IBI - International Biochar Initiative, EBC - European Biochar Certificate. Values are the means of 3 replicates ± 1 standard deviation.

Material/Guideline	**Element**	**Value mg kg^{-1}**
IBI guidelines	Cd	1.4-39
	Cu	63-1500
	Mo	5-20
	Zn	200-7000
EBC basic guidelines	Cd	1.5
	Cu	100
	Mo	N/A
	Zn	400
EBC premium guidelines	Cd	1
	Cu	100
	Mo	N/A
	Zn	400
AD feedstock	Zn	461 ± 17
AD450	Cd	3.34 ± 0.40
	Mo	7.62 ± 1.44
	Zn	518 ± 42
AD550	Mo	5.56 ± 0.15
	Zn	900 ± 13
PAD450	Cd	1.77 ±0.00
	Cu	110 ± 2
	Mo	21.9 ± 0.5
	Zn	787 ± 10
PAD550	Cd	1.15 ± 0.01
	Cu	112 ± 8
	Mo	23.8 ± 0.8
	Zn	825 ± 16
POCAD450	Cu	103 ± 2
	Mo	26.7 ± 0.6
	Zn	746 ± 7
POCAD550	Mo	24.3 ± 0.3
	Zn	706 ± 12

The threshold exceedance is only for Cr, which, unlike the other elements, is regulated by concentration in the material, rather than by mass applied per unit area per year (Table 6.2). New fertiliser guidelines for the EU are currently being developed, which will include recycled P sources such as struvite, incineration ash and biochars. It is unclear whether the UK would adopt these in light of the imminent withdrawal from the EU, however it is likely that Cr will be regulated based on Cr(VI) concentrations, rather than total. If it can be shown that more biochar P is bioavailable than estimated by 2% formic acid, the required application rates would be even lower, again reducing the application rate of PTEs to levels at which they may be useful as micronutrients.

Table 6.2 Biochar application rates used in the growth experiment in Chapter 5 compared to the current relevant regulations in Scotland (Public Health, England and Wales Public Health, Scotland 1989 No. 1263 Schedule 1, Regulation 3: Testing of Sludge).

		Maximum permissible application of PTEs to soils					
		kg ha^{-1} y^{-1}					**mg kg^{-1}**
		Cd	**Cu**	**Ni**	**Pb**	**Zn**	**Cr**
		0.15	7.5	3	15	15	25
Biochar application rate t ha^{-1}		**% of total permitted concentration applied y^{-1}**					
PAD450	3.62	12.0	14.7	9.8	2.1	52.4	135.2
PAD550	4.03	8.0	15.0	8.8	2.0	55.0	120.5
POCAD450	3.66	1.1	13.8	7.7	1.7	49.7	99.8
POCAD550	3.36	2.1	13.2	6.3	1.9	47.1	84.3

6.1.3 Research outcomes

The research presented in this thesis provides a strong basis for further development of P recycling materials from anaerobically digested sewage sludge and ochre-based biochars. Additional development is required, to tailor the shape and density of the biochars to optimise P capture in WWTPs and allow for application to land using standard agricultural fertiliser technologies. The form of the fertiliser is important, as it must allow for the material to be spread onto fields effectively using the farm technologies which are already in place, otherwise farmers will not be interested in using it.

6.2 P capture from wastewater

6.2.1 The reactivity of the biochars towards phosphate

Discussion of technologies for P removal from wastewater in the literature use a variety of terms to describe the processes involved. Batch 'adsorption' experiments are used to determine the 'P sorption capacity' of materials. The term 'sorption' is widely accepted to describe the combination of processes that occur between aqueous phosphate and substrates, however it is sometimes considered inaccurate as it does not explicitly include other P removal processes such as precipitation. For that reason, the term 'P capture' and 'P capture capacity' has been adopted in this work, so it is clear that adsorption is not the only process described.

6.2.1.1 The effect of feedstock and processing on biochar P capture properties

6.2.1.1.1 Feedstock type

The OCAD biochars captured a significantly higher amount of P than the AD biochars in the repeated exposure experiment using a 20 mg l^{-1} P solution (Chapter 2). This was consistent over the whole 5 days of P exposure. In the 800 mg l^{-1} P experiment, the distinction between feedstock types was not observed, and there were no significant differences between the biochar treatments.

6.2.1.1.2 Feedstock processing

Because of the different experimental goals of Chapters 2 and 3, slight variations in P-enrichment procedures were employed. Initial capture experiments, which utilised the non-pelletised biochars (Chapter 2), were necessarily small-scale, using small masses (1 g) of small particle size (0.5-1 mm) biochar in replicates of 4 to enable statistical analysis of the results, and provide a well-controlled basis for designing larger-scale experiments. The P-enrichment of the pelletised biochars in Chapter 3 was performed to study differences in the surface properties of P-exposed and non-P exposed biochars, as well as preparing sufficient quantities of P-exposed biochar for the plant growth experiments performed in Chapters 4 and 5. Both experiments involved repeated application of 20 mg l^{-1} P solution, decanted and replenished after 24 h. A much larger mass of biochar (30 g) in larger and more varying particle sizes (0.25-15 mm) was used for the pelletised biochar experiment, over 6 rather than 5 days, and P capture was determined in duplicates, making the results more variable than those for the non-pelletised biochars. The consequence of this is that the cumulative P capture values between the pelletised and non-pelletised biochars cannot be compared directly. The P capture values obtained for the non-pelletised biochars (~0.99-1.3 mg P g^{-1}) were higher than for the pelletised biochars (~0.57-0.95 mg P g^{-1}). As discussed in Chapter 3, the differences are most likely due to the larger particle size used in the latter experiment, and so in real terms the differences are likely to be minimal.

6.2.1.2 The effect of pyrolysis highest treatment temperature

After repeated exposure to environmentally relevant concentrations of P for 5 days (Chapter 2), no significant difference in P capture between OCAD450 (1.24 ± 0.02 mg P g^{-1}) and OCAD550 (1.26 ± 0.01 mg P g^{-1}) was observed. On the other hand, a small but significant difference was observed in P capture between AD450 (1.06 ± 0.00 mg P g^{-1}) and AD550 (0.99 ± 0.01 mg P g^{-1}). Although not statistically significant, the inverse relationship was observed in the pelletised biochars (Chapter 3), with PAD450 capturing less P (0.57 ± 0.26 mg P g^{-1}) than PAD550 (0.70 ± 0.40 mg P g^{-1}). There was no difference between POCAD450 and POCAD550 (both 0.95 mg P g^{-1}).

Consideration of the results of the 800 mg l^{-1} P experiment using the non-pelletised biochars (Chapter 2) shows the same order of P capture values as the comparable 20 mg l^{-1} P experiment (OCAD550 > OCAD450, AD450 > AD550), but no significant differences were observed between the biochar treatments.

6.2.1.3 Batch adsorption experiments

The output of the Langmuir and Freundlich isotherm fits of the batch adsorption experiments in Chapter 2 do not agree with the observed reactivity of the biochars in the repeat exposure experiments. According to the Langmuir parameters calculated, the order of P sorption capacity should be AD550 (8.25 mg g^{-1}) > OCAD550 (7.33 mg g^{-1}) > OCAD450 (6.70 mg g^{-1}) ≈ AD450 (6.68 mg g^{-1}). The most interesting discrepancy is the highest ranking of AD550, where in all other experiments it was ranked last. The reciprocal of the Freundlich parameter *n* represents the affinity of the substrate for P. Interpreting the values obtained for the biochars suggests that the 450°C HTT biochars would have higher affinity for P than the 550°C HTT biochars. Comparing this to the total amount of P which could be extracted from the P-exposed (20 mg l^{-} P) non-pelletised biochars in pH 7 buffered deionised water, the calculated order does not reflect the affinity observed, measured by the % of captured P remaining after 5 x 24 h leaching events. If the different feedstocks are considered separately, the order is correct for the AD biochars, but not the OCAD biochars. The same is true for the Langmuir *K* parameter, which is also a measure of the substrate affinity for the solute. Taken together, this supports the conclusions of Chapter 2, which indicate that the batch adsorption method does not provide reliable results for estimating P capture capacity and performance of biochar materials as they do not model the range of mechanisms involved.

6.2.2 Chemical mechanisms of P capture

Statistical analysis of the capture and release results from Chapter 2 showed a significant ($p < 0.05$) positive correlation between P capture and material Fe concentration after 5 days P exposure at 20 mg l P^{-1}. There was a significant negative correlation between P capture and material Al concentration on day 1 of the experiment, but this was not significant by day 5. The statistical analyses were performed using data from each of the non-pelletised biochars, as well as ochre and activated carbon, which were included to represent two extremes – the properties of ochre without a biochar binder, and the properties of a low-mineral element containing biochar. This may explain why P capture was significantly correlated with Fe in these analyses, but not in the statistical analysis of the LA-ICP-MS data obtained from the pelletised mixed anaerobically digested sewage sludge and ochre biochars. In the latter analyses, Al, Si, and Ca were the strongest positively significantly correlated elements with P capture. Further evidence for an Al-mediated mechanism is given by the XRD results, where the only P mineral identified was $AlPO_4$, in EPOCAD450. Additionally, no Fe minerals detected, which may be because they are highly amorphous in the biochars.

The pelletised anaerobically digested sewage sludge and ochre biochars became the focus of the mechanistic investigation in Chapter 3 due to interesting differences identified between POCAD450 and POCAD550 in initial analyses. XPS analysis identified a unique peak at 708.82 eV for POCAD550 which was not present in POCAD450, indicating the presence of reduced Fe compounds such as FeS_2, FeO and/or FeS. The presence of oxidisible Fe in POCAD550 could explain the superior P capture properties of the equivalent non-pelletised biochar (OCAD550) observed in Chapter 2. Alternatively, it is possible that the observation that Fe is only strongly significantly correlated with S and Mn in POCAD550 and EPOCAD550 in the LA-ICP-MS analyses indicates that a large fraction of Fe is present in POCAD550 in unreactive mineral phases, which results in other P capture processes being more energetically and/or sterically favourable. More investigations of Fe speciation would be necessary to identify the exact processes occurring.

It is clear from the results of the many analyses performed that the processes involved in P capture using anaerobically digested sewage sludge and ochre biochar materials are complex. Given the micro-scale heterogeneity of the biochars, determining the exact nature of each component of the process using current analytical techniques would be exceptionally difficult, without contributing much to the overall aims of the work. An understanding of the main elements involved has now been obtained, and can be used in conjunction with the results of the plant experiments in Chapters 4 and 5 to optimise the materials for their intended use.

6.2.3 Research outcomes

The research presented demonstrates the P capture characteristics of the mixed anaerobically digested sewage sludge and ochre biochars, as well as the unmixed biochars. The mixed feedstocks result in biochar materials that capture more P than the anaerobically digested sewage sludge biochars over the timescales assessed in this research, which confirms the hypotheses developed during the material development stage. The chemical P capture mechanisms are driven by Fe and Al, as well as Si and Ca. For the POCAD biochars, the higher HTT of 550°C changes the characteristics of Fe such that during P-exposure it remains closely associate with S and Mn, unlike the 450°C analogue. This may partially explain the higher P capture of OCAD550 in Chapter 2.

6.3 Recycling of captured P to plants

6.3.1 Screening of nutrient and potentially toxic element bioavailability in biochar

Identification of an effective and cost-efficient method for estimating the bioavailability of nutrients and PTEs in biochar would help speed up the process of determining the potential risks and benefits of new biochars. To date, no such method/s have been identified with wide applicability. A study comparing the plant uptake of PTEs from biochar into wheat with concentrations extracted from biochar using common soil extractants concluded that the variability of binding mechanisms in the native biochar structure precludes identification of a single method (Farrell et al., 2013). Based on this work, a similar experiment was devised to assess a different (but overlapping) group of soil extractants against nutrient and PTE uptake into spring barley grown in 50 ml syringe tubes the laboratory (Chapter 4). The extraction solutions were selected to cover a range of pH values, as this was hypothesised to have an effect on the solubility of elements in biochar. To ensure sufficient data for a robust correlation analysis, in addition to the biochars produced in this research, an additional set of biochars containing high concentrations of PTEs were included in the experiment.

Significant positive correlations were found between barley leaf concentrations of P, K, B, Mn, Mo and Na and both buffered and unbuffered 0.01 M $CaCl_2$ extractions of the biochars. These two extractant solutions had the highest pH of the methods selected (both started at pH 7, with the unbuffered solution increasing with pH over the course of the extraction), which were closer to the native biochar pH in water than the other solutions. This finding supports the hypothesis that the bioavailability of elements from biochar is related to the pH of the biochar.

No significant correlations were identified between barley leaf concentrations for PTEs of relatively more concern (As, Co, Cr, Cu, Ni, Pb, Zn) and extraction methods. This supports the findings of Farrell et al. (2013) and the conclusion that plant growth tests are necessary to provide accurate bioavailability information for biochar.

Plant P concentration was significantly correlated with each of the Mehlich 3 (Spearman's ρ = 0.588), buffered 0.01 M $CaCl_2$ (ρ = 0.692) unbuffered 0.01 M $CaCl_2$ (ρ = 0.583) and 2% formic acid extraction methods for P extraction, but these were among the weakest (positive) correlations of the experiment (ρ ranged from 0.507 to 0.943). Without a clear relationship between the two variables, it is still difficult to predict the amount of bioavailable P in the biochars using these methods, although biochars can be ranked against each other using the values obtained.

Comparison of the non P-exposed pelletised biochars with their P-exposed counterparts in terms of the total percentage of P in each biochar and the proportion of that which is 2% formic acid extractable is shown in **Error! Reference source not found.**. The difference in e xtractable P between the PAD biochars and their EPAD counterpart is much greater than that of the POCAD biochars. This means the amount of biochar applied in the plant growth experiments in Chapter 5 was lower for the EPAD biochar treatments, and may have implications for the results of the rhizobox study in Chapter 5.

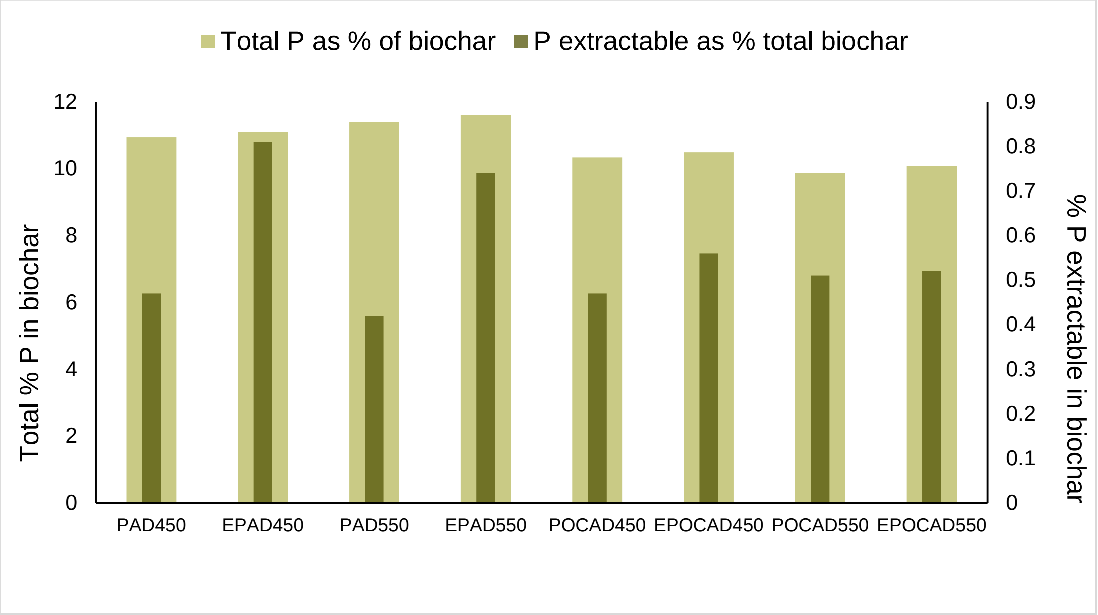

Figure 6.1 Comparison of the total P % in the pelletised biochars compared to total % of P in biochar which is 2% formic acid extractable.

6.3.2 Plant access to native and captured phosphorus from biochar

Plant uptake of various elements differed between biochar treatments in the rapid barley growth experiments (Chapter 4). All yields of barley were higher than the control for the biochar treatments. No significant differences between the dry weight above ground biomass yield of the PAD, POCAD, EPAD or EPOCAD biochars and the control was found, although yield was 83% higher than the control for EPOCAD550, 70% for EPAD550 and 59% for PAD550. The above ground P mass taken up by the barley plants was higher than the control for all biochar treatments, but the only significant yield increase was for EPOCAD550.

Biochar application rates for the rhizobox experiment in Chapter 5 were calculated based on the 2% formic acid extractable concentration of P in the biochars (**Error! Reference source n ot found.**), so each application rate was different on a biochar mass basis. The 2% formic acid method for assessment of P bioavailability has been suggested as an appropriate method for high ash (i.e. manure and sewage sludge) biochars (Wang et al., 2012) and was significantly positively correlated with plant uptake of P in Chapter 4 (see Section 6.3.1 for discussion of the validity of the method).

After 3 months growing time, there were no significant differences in barley yield or total leaf length between the biochar treatments and controls (neither the NPK nor NK control). It is not possible, then, due to the unexpectedly high yield of the NK control to say that the 2% formic acid extractable fraction of biochar P is as plant available as soluble P (from $Ca(H_2PO_4)_2$) based on these data. The same is true for both the leaf P concentration and leaf P mass, as no significant differences were observed between treatments, although the mass of P in leaves from the EPOCAD550 treatment was slightly higher (8.9%) than the NPK control, and 23% higher than the NK control. It can be concluded, however, that the application of biochar did not negatively affect barley growth, and that EPOCAD550 demonstrated positive characteristics for P fertilisation in both Chapter 4 and 5 experiments.

Analysis of the soils for total and Mehlich 3 extractable P did demonstrate significant differences between treatments. The biochar treatments contained more total P than both controls in the top fraction of the soils. For the same soil fraction, the NPK control, PAD450, PAD550 and POCAD450 treatments contained significantly higher concentrations of Mehlich 3 extractable P, showing that these treatments contained more extractable P than the appropriate control, even after 3 months of barley growth.

6.3.3 Research outcomes

A scoring system was devised to rank the biochars based on their performance in the plant tests in Chapters 4 and 5 (Table 6.3). The score is based on the ranking of the biochar for maximising plant yield and leaf P mass, and weighted by dividing the ranking by the percentage difference of each value from the experiment control (which has been divided by 100). Based on this scoring system, EPOCAD550 ranks far above the other biochars, although most of the biochars performed better than controls (but not significantly so), as shown by the fact that most of the conversion factors are above one. For all HTT biochar pairs except PAD, the 550°C biochar ranks better than the 450°C analogue. This may have a P interaction basis, related to the differences observed in the comparison of POCAD450 and POCAD550 Fe oxidation and binding chemistry after P-exposure (Chapter 3). The ranking score difference between PAD450 and PAD550 is much smaller than the other HTT pairs (5 units, compared to < 10 units for all others), which suggests that the materials have more similar properties than the other pairs. An interesting observation is the reversal of rank order of the PAD biochars (450 > 550 – 550 > 450) after P-exposure. This is driven by the relatively low performance of EPAD450 in the rapid plant growth experiment (Chapter 4) and yield performance in the rhizobox experiment (Chapter 5), especially compared to PAD450 for the latter. On the other hand, PAD550 and EPAD550 consistently rank between 2nd and 6th in each experiment. PAD450 appears to perform fairly well in the longer-term rhizobox experiment compared to the shorter-term rapid growth experiment, whilst the same is not true for EPAD450. It is possible that the process of P-exposure exposes reactive sites that are deleterious to plant growth by locking up nutrients in the soil. It is also possible that the process transfers native biochar P from bioavailable forms to less-available forms, although, as shown in **Error! Reference source not found.**, the formic acid extractable P f raction of EPAD450 is very similar to that of EPAD550.

Table 6.3 Ranking of biochar performance in plant growth tests based on both leaf yield and leaf P mass in the rapid uptake and rhizobox experiments. Lower ranking scores reflect better performance. The conversion factors are based on the difference of each treatment to the experimental control (% difference / 100), so values over 1 represent better performance than the control. The score for each experiment (expressed to 1 decimal place) = ranking / conversion factor. The lowest total score represents the best performing biochar.

	Yield						Leaf P mass						
	Rapid uptake experiment			Rhizobox experiment			Rapid uptake experiment			Rhizobox experiment			
Biochar	Ranking	Conversion factor	Score	Ranking	Conversion factor	Score	Ranking	Conversion factor	Score	Ranking	Conversion factor	Score	Total score
PAD450	5	1.30	3.8	2	1.22	1.6	5	1.55	3.2	3	0.66	4.5	13.1 (3)
PAD550	3	1.59	1.9	3	1.09	2.8	3	1.62	1.9	6	0.52	11.5	18.1 (5)
POCAD450	6	1.27	4.7	8	0.93	8.6	6	1.50	4.0	8	0.45	17.8	35.1 (8)
POCAD550	4	1.31	3.1	6	1.06	5.7	7	1.49	4.7	7	0.51	13.7	27.2 (6)
EPAD450	8	1.06	7.5	7	1.04	6.7	8	1.42	5.6	5	0.61	8.2	28.0 (7)
EPAD550	2	1.70	1.2	5	1.07	4.7	2	2.16	0.9	4	0.62	6.5	13.3 (2)
EPOCAD450	7	1.25	5.6	4	1.08	3.7	4	1.59	2.5	2	0.71	2.8	14.6 (4)
EPOCAD550	1	1.83	0.5	1	1.22	0.8	1	2.24	0.4	1	1.09	0.9	2.6 (1)

Chapter 7

Conclusions and further work

7.1 Conclusions

Feedstocks that met the desired criteria for functionality and sustainability were selected (anaerobically digested sewage sludge and ochre) and combined to produce feedstocks for pyrolysis. Additional feedstock processing was required to produce a material suitable for pyrolysis in a screw-fed kiln. Each feedstock was pyrolysed at two different highest treatment temperatures to determine whether these affected the phosphorus (P) capture and/or fertilisation characteristics of the resulting biochars. Biochar properties were assessed against published guidelines for biochars as an initial evaluation of the potential risk posed by the application of the biochars to soil. The biochars were tested for P capture in standard batch sorption experiments with the additional of a pH buffer to mitigate the large effect of biochar on the pH of the test system. A new P capture assessment method was designed, spanning over 5 days, which showed the standard batch sorption experiment underestimated the P sorption capacity of the biochars. Spectroscopic and microscopic analysis, in combination with other chemical analyses, were used to identify mechanistic detail behind the differences in biochar P capture observed. A variety of extraction methods were used to assess the bioavailability of the native and captured-P (and potentially toxic elements) in the biochars. Finally, plant growth tests using both excess (5% biochar, equivalent to < 100 t ha^{-1}) and P-fertilisation appropriate (up to 0.2% biochar, equivalent to ≤ 4 t ha^{-1}) application rates were performed, showing that both native biochar and additional captured P were bioavailable, whilst potentially toxic elements were not.

7.1.1 Material design

The research presented has shown that a mixed anaerobically digested sewage sludge and ochre biochar material can be produced using simple mixing techniques and standard pyrolysis systems. Further optimisation of mixture ratios and feedstock processing should be pursued, but the work presented demonstrates that materials such as these can be produced using technologies employed in the large-scale production of biochar.

The biochars produced did not uniformly meet current quality guidelines for biochar materials, but if applied to soil at rates appropriate for their use as P fertiliser, they should not pose any risk to soil or plants. This needs to be confirmed in larger-scale pot and field trials with the crops and soils of interest.

7.1.2 P capture from wastewater

The design and demonstration of the repeat-exposure P capture experiments showed that each of the biochar materials could be used to capture P over an extended period. This method was shown to be more informative for the screening of biochar materials for P capture properties than standard batch adsorption experiments. At an environmentally relevant concentration of P after 5 days exposure, the OCAD biochars performed better than the AD biochars. The effect of pyrolysis highest treatment temperature was opposite for the two different feedstocks. OCAD550 captured more P than OCAD450 (but not significantly), whilst AD450 captured significantly more P than AD550, giving the overall order of P capture as: OCAD550 ≈ OCAD450 > AD450 > AD550.

In repeated exposure experiments using a 800 mg l^{-1} P concentration the pyrolysis temperature relationships with P capture remained the same, but the overall order of P capture changed, giving: OCAD550 > AD450 > OCAD450 > AD550. None of the differences in P capture were significantly different, however.

Examination of the mechanisms of P capture revealed that Fe, Al, Si and Ca were all involved in recovering P from the 20 mg l^{-1} P solution. POCAD550 displayed different Fe binding characteristics to POCAD450, which may be related to the relatively superior P and consistent fertilising capabilities demonstrated by POCAD550 in the plant experiments.

7.1.3 Recycling of captured P to plants

Plant growth studies remain the best available method for determining bioavailability of nutrients and PTEs in biochar. Of the soil extraction methods tested, none correlated with the PTEs of most concern for soil application. The strongest correlation between extractable P and plant uptake was for the buffered 0.01 M $CaCl_2$ extractions, indicating that the bioavailability of P from biochar is influenced by the biochar pH. The plant experiments in Chapter 4 and 5 demonstrate that biochar P can be accessed by barley, and that the 2% formic acid extractable fraction of biochar P is probably as bioavailable as soluble P fertiliser, although further experiments are required to be certain. EPOCAD550 was the best performing biochar in both the rapid plant uptake and rhizobox experiments, warranting further testing in additional plant experiments

7.1.4 Research outcomes

Overall, the ochre and anaerobically digested sewage sludge biochar pyrolysed at a highest treatment temperature of 550°C (OCAD550) emerged as the best biochar for the capture of P. The P-exposed pelletised form of this biochar, EPOCAD550, was identified as the best performing P fertiliser. Interesting differences between Fe surface chemistry of the transition of POCAD550 to EPOCAD550, compared to that of POCAD450 to EPOCAD450, were also observed, which may account for the positive results demonstrated in the other experiments.

7.2 Further work

The research presented in this thesis forms the basis of the development of future technology for P recycling. The work is currently at a technology readiness level of one, and as such, there is much that can be done to further demonstrate and optimise the biochar materials for capture and re-use of P.

7.2.1 Material development

Investigation of different ochres: For an up-scaled production process in the UK, ochre from more than one MTWP may be required to satisfy demand. It would be more sustainable for WWTPs to source ochre from local MWTPs, but the chemical properties of local ochres may not be appropriate for incorporation into these materials. Much like the need for appropriate selection of biochar, each WWTP may need to select a specific ochre to optimise their P capture system. Additional experiments similar to those carried out in Chapters 2 and 4 could be used to screen new biochar materials made from anaerobically digested sewage sludge with different ochre.

Sewage sludge variability: As with ochre, the effect of varying sewage sludge source (location, time of year) has not been investigated. WWTPs keep detailed record of sludge composition changes over time, which would assist with predicting the possible effects on biochar properties (e.g. fluctuations in Al, Fe, Si, Ca and Mg concentrations). Additional experiments similar to those carried out in Chapter 2 could be performed to determine how transferrable the technology is to other WWTPs.

Optimisation of processing conditions: As it stands, pelletising successfully processed the feedstocks into materials that can be pyrolysed by a screw-fed pyrolysis kiln, however this appears to have caused PTE contamination of the products. It is not clear what kind of technology would be used for large-scale pyrolysis of anaerobically digested sewage sludge in WWTPs, so pelletisation may not be required. Consultation with WWTPs, pyrolysis technology developers and fertiliser companies would provide insights into the requirements for each system and thus inform material development.

7.2.2 Analysis of P capture properties

Release of elements during P capture: One area of the assessment of P capture properties that was not covered in this research project was an analysis of the components that are released when P is captured by the biochars. An experiment analysing concentrations of Total P, relevant cations such as $Ca^{2+}$and Mg^{2+}, PTEs and exchangeable ions such as carbonate and sulphate in the P solution after sorption would highlight any potential risks to water quality and also give more information on possible P capture mechanisms (such as sulphate exchange, for instance).

Column experiments: The hydraulic properties of the biochars were not assessed in this research as it was outside the scope of the project. Flow-through column experiments are required to calculate the hydraulic conductivity of the biochars and to identify the ideal particle size for optimum P capture and water flow. Testing of the 2-phase resting column design outlined by Sibrell et al., (2009) could also be performed, to determine whether resting results in enhanced P capture, as is the case with ochre.

Effect of competing elements: Depending on which stage of WWT the biochars would be used to capture P, they will be exposed to different wastewater compositions. Column experiments such as those described above using simulated sewage sludge or real wastewater could be used to assess whether there is any competition for P capture sites from other species in the water. It would also highlight whether the biochars capture more than just P, for example and As or organic contaminants present.

7.2.3 Analysis of P fertilisation properties

Plant growth studies: The bioavailability of biochar P is still not quantified. A number of different approaches could be used to determine the amount of P that is plant accessible over one or multiple growing seasons. In a truly P limited system it would be possible to calculate the P mass balance from biochar to plant, although proper cleaning of the roots to remove biochar particles can be difficult. Repeated cropping of a P sensitive plant such as lettuce on biochar amended P-limited soil may be one way to do this. As discussed in Chapter 4, a variation of the rapid plant growth experiment to compare biochar application rates to different application rates of P fertiliser would be another way to determine equivalency. Following the methodology of Chapter 4, using a selection of soluble P fertiliser rates ranging from P deficient to excess could be used to construct a fertiliser calibration curve (based on plant yield and/ or above ground biomass P mass) for a certain soil and certain crop. The same soil and crop system would be amended with biochar at 0.1, 0.2, 0.5 and 1% application rates (or t ha^{-1} equivalent) and the yield and/or above ground biomass P mass compared to the fertiliser calibration curve to identify the equivalent soluble fertiliser application rate.

P exposure at higher concentrations: An alternative approach to the development of sustainable P fertilisers would involve the exposure of the sewage sludge-derived biochars to much higher concentrations of P, saturating the reactive sites and producing a much higher P product per unit weight. Such materials could be investigated for their P retention properties, compared to the bioavailability of the P they contain, to determine whether P use efficiency is improved relative to soluble P fertiliser in the fertiliser-soil-plant system.

7.3 Relevance of the work

As has been emphasised in Chapter 1, the global P cycle is a flow, rather than a cycle, on an anthropogenic timescale, but cycling must be restored if food supply can be secured for the growing human population. This research targets one area of the P system where great potential for P recycling exists without the need for large-scale societal changes. The technology developments suggested in this thesis and required for the development of the P recovery materials discussed do not just address P cycle problems, but also result in the diversion of waste from landfill and prevention of eutrophication in aquatic environments.

The research addresses the themes discussed in Shepherd et al. (2016), which presents the outcomes of the 2014 Young Scientists Workshop held between the 4th Sustainable Phosphorus Summit and 5th International Symposium on Phosphorus in Soils and Plants. The main outcome of the workshop was a diagram (Figure 7.1) demonstrates that an

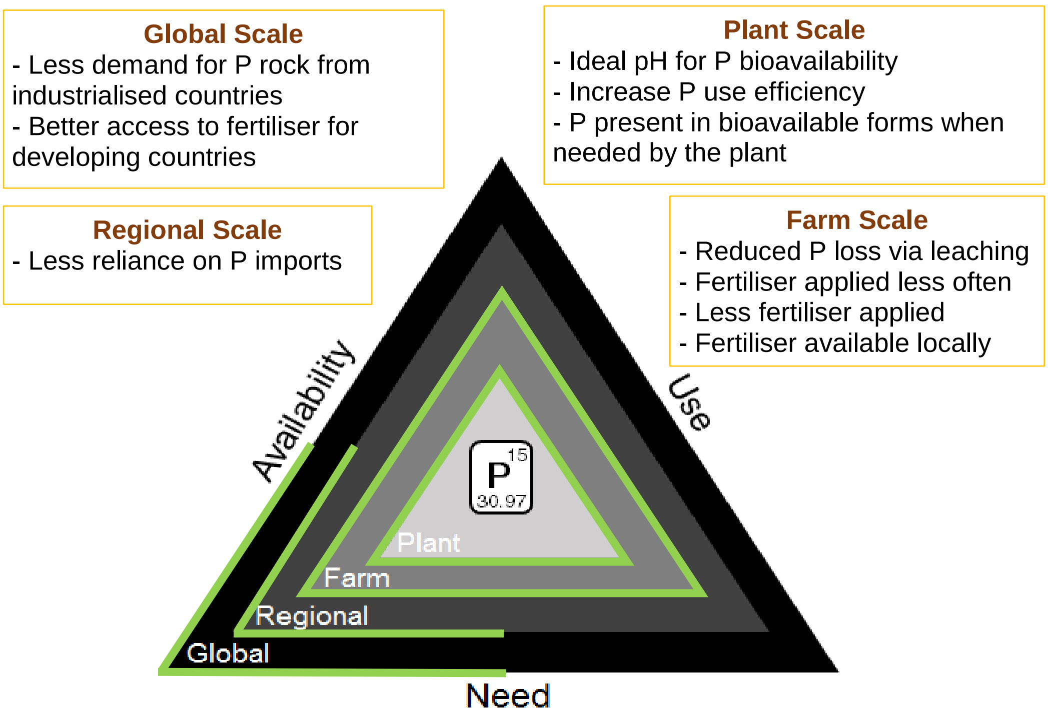

Figure 7.1 Conceptual model representing the three drivers (P availability, need and use) which must be in balance for equitable and safe P utilisation. Each driver has a different specific meaning at each geospatial scale (e.g. P availability can refer to physical access restrictions due to location and finance at a global scale, type of recyclable resource available based on local industries at a regional scale and bioavailability at the plant scale. The imbalances which are addressed by this research at each scale are highlighted in green and detailed in the boxes around the conceptual model.

effective P system requires balance between three drivers, P availability, P use and P need, at all relevant scales. The materials developed and WWT/agricultural system changes suggested in this thesis address the issue of P availability and P need imbalances at global and regional scales by increasing local/regional P recycling, which then reduces reliance on mined P resource imports. The materials developed also address P need, P use and P availability imbalances at the farm and plant scale, turning relatively mobile P in sewage sludge into less mobile but bioavailable P in biochar. If widely adopted, biochar technologies for transforming nutrient rich wastes into valuable materials may have a considerable impact on the re-stabilisation of the P cycle.

Chapter 8

References

Adler, P.R., Sibrell, P.L., 2003. Sequestration of phosphorus by acid mine drainage floc. J. Environ. Qual. 32, 1122–1129. doi:10.2134/jeq2003.1122

Agrafioti, E., Bouras, G., Kalderis, D., Diamadopoulos, E., 2013. Biochar production by sewage sludge pyrolysis. J. Anal. Appl. Pyrolysis 101, 72–78. doi:10.1016/j.jaap.2013.02.010

Agrawal, S.G., King, K.W., Fischer, E.N., Woner, D.N., 2011. PO4 3- removal by and permeability of industrial byproducts and minerals: Granulated blast furnace slag, cement kiln dust, coconut shell activated carbon, silica sand, and zeolite. Water. Air. Soil Pollut. 219, 91–101. doi:10.1007/s11270-010-0686-4

Ainsworth, C.C., Sumner, M.E., Hurst, V.E., 1985. Effect of Aluminum Substitution in Goethite on Phosphorus Adsorption: I. Adsorption and Isotopic Exchange. Soil Sci. Soc. Am. J. 49, 1142–1149. doi:10.2136/sssaj1985.03615995004900050015x

Ali, M.W., Zoltai, S.C., Radford, F.G., 1988. A comparison of dry and wet ashing methods for the elemental analysis of peat. Can. J. Soil Sci. 68, 443–447.

Amonette, J.E., Joseph, S., 2009. Characteristics of biochar: Microchemical properties, in: Lehmann, J., Joseph, S. (Eds.), Biochar for Environmental Management: Science and Technology. Earthscan, London, pp. 33–52.

Angst, T.E., Sohi, S.P., 2013. Establishing release dynamics for plant nutrients from biochar. GCB Bioenergy 5, 221–226. doi:10.1111/gcbb.12023

Antelo, J., Avena, M., Fiol, S., López, R., Arce, F., 2005. Effects of pH and ionic strength on the adsorption of phosphate and arsenate at the goethite-water interface. J. Colloid Interface Sci. 285, 476–486. doi:10.1016/j.jcis.2004.12.032

Arai, Y., Sparks, D.L., 2001. ATR–FTIR Spectroscopic Investigation on Phosphate Adsorption Mechanisms at the Ferrihydrite–Water Interface. J. Colloid Interface Sci. 241, 317–326. doi:10.1006/jcis.2001.7773

Arshadi, M., Zandi, H., Akbari, J., Shameli, A., 2015. Ferrocene functionalized nanoscale mixed-oxides as a potent phosphate adsorbent from the synthetic and real (Persian Gulf) waters. J. Colloid Interface Sci. 450, 424–433. doi:10.1016/j.jcis.2015.03.026

Ashley, K., Cordell, D., Mavinic, D., 2011. A brief history of phosphorus: From the philosopher's stone to nutrient recovery and reuse. Chemosphere 84, 737–746. doi:10.1016/j.chemosphere.2011.03.001

Bagreev, A., Bandosz, T.J., Locke, D.C., 2001. Pore structure and surface chemistry of adsorbents obtained by pyrolysis of sewage sludge-derived fertilizer. Carbon N. Y. 39, 1971–1979. doi:10.1016/S0008-6223(01)00026-4

Banuelos, G.S., Cardon, G., Pflaum, T., 1992. Comparison of dry ashing and wet acid digestion on the determination of boron in plant tissue. Commun. Soil Sci. Plant Anal. 23, 2383–2397. doi:10.1080/00103629209368745

Barrow, N.J., 2015. Soil phosphate chemistry and the P-sparing effect of previous phosphate applications. Plant Soil 397, 401–409. doi:10.1007/s11104-015-2514-5

Barrow, N.J., 1983. A mechanistic model for describing the sorption and desorption of phosphate by soil. Eur. J. Soil Sci. 66, 9–18. doi:10.1111/ejss.12198

Barrow, N.J., 1979. Three Effects of Temperature on the reactions between inorganic phosphate and soil. J. Soil Sci. 30, 271–279.

Basta, N.T., Ryan, J. a, Chaney, R.L., 2004. Trace element chemistry in residual-treated soil: key concepts and metal bioavailability. J. Environ. Qual. 34, 49–63. doi:10.2134/jeq2005.0049dup

Bastos, A.C., Prodana, M., Abrantes, N., Keizer, J.J., Soares, A.M.V.M., Loureiro, S., 2014. Potential risk of biochar-amended soil to aquatic systems: an evaluation based on aquatic bioassays. Ecotoxicology 23, 1784–1793. doi:10.1007/s10646-014-1344-1

BBF, 2014. British Biochar Foundation Biochar Quality Mandate.

Beesley, L., Inneh, O., Norton, G., 2014. Assessing the influence of compost and biochar amendments on the mobility and toxicity of metals and arsenic in a naturally contaminated mine soil. Environ. Pollut. 186, 195–202.

Beesley, L., Moreno-Jiménez, E., Clemente, R., Lepp, N., Dickinson, N., 2010. Mobility of arsenic, cadmium and zinc in a multi-element contaminated soil profile assessed by in-situ soil pore water sampling, column leaching and sequential extraction. Environ. Pollut. 158, 155–160. doi:10.1016/j.envpol.2009.07.021

Beesley, L., Moreno-Jiménez, E., Gomez-Eyles, J.L., Harris, E., Robinson, B., Sizmur, T., 2011. A review of biochars' potential role in the remediation, revegetation and restoration of contaminated soils. Environ. Pollut. 159, 3269–3282. doi:10.1016/j.envpol.2011.07.023

Bennett, E.M., Carpenter, S.R., Caraco, N.F., 2001a. Human Impact on Erodable Phosphorus and Eutrophication: A Global Perspective. Bioscience 51, 227. doi:10.1641/0006-3568(2001)051[0227:HIOEPA]2.0.CO;2

Bennett, E.M., Carpenter, S.R., Caraco, N.F., 2001b. Human impact on erodable phosphorus and eutrophication: a global perspective increasing accumulation of phosphorus in soil threatens rivers, lakes, and coastal oceans with eutrophication. Bioscience 51, 227. doi:10.1641/0006-3568(2001)051[0227:HIOEPA]2.0.CO;2

Bhatnagar, A., Sillanpää, M., 2011. A review of emerging adsorbents for nitrate removal from water. Chem. Eng. J. doi:10.1016/j.cej.2011.01.103

Biederman, L. a., Harpole, W.S., 2013. Biochar and its effects on plant productivity and nutrient cycling: A meta-analysis. GCB Bioenergy 5, 202–214. doi:10.1111/gcbb.12037

Brown, R.A., Kercher, A.K., Nguyen, T.H., Nagle, D.C., Ball, W.P., 2006. Production and characterization of synthetic wood chars for use as surrogates for natural sorbents. Org. Geochem. 37, 321–333. doi:10.1016/j.orggeochem.2005.10.008

Bryant, D., 2004. The Chemistry of Phosphorus, in: Valsami-Jones, E. (Ed.), Phosphorus in Environmental Technologies; Principles and Applications. IWA Publishing, London, pp. 1–19.

Buss, W., Graham, M.C., Shepherd, J.G., Mašek, O., 2016a. Suitability of marginal biomass-derived biochars for soil amendment. Sci. Total Environ. doi:10.1016/j.scitotenv.2015.11.148

Buss, W., Graham, M.C., Shepherd, J.G., Mašek, O., 2016b. Risks and benefits of marginal biomass-derived biochars for plant growth. Sci. Total Environ. 569–570, 496–506. doi:10.1016/j.scitotenv.2016.06.129

Buss, W., Kammann, C., Koyro, H.-W., 2012. Biochar Reduces Copper Toxicity in Willd. in a Sandy Soil. J. Environ. Qual. 41, 1157. doi:10.2134/jeq2011.0022

Buss, W., Mašek, O., 2014. Mobile organic compounds in biochar - A potential source ofcontamination - Phytotoxic effects on cress seed (Lepidiumsativum) germination. J. Environ. Manage. 137, 111–119. doi:10.1016/j.jenvman.2014.01.045

Campbell, A., Schwertmann, U., Campbell, P., 1997. Formation of cubic phases on heating ferrihydrite. Clay Miner. 32, 615–622. doi:10.1180/claymin.1997.032.4.11

Camps-Arbestain, M., Amonette, J.E., Singh, B., Wang, T., Schmidt, H.P., 2015. A biochar classification system and associated test methods, in: Lehmann, J., Joseph, S. (Eds.), Biochar for Environmental Management, Science, Technology and Implementation. London, pp. 165–193.

Cao, Y., Pawłowski, A., 2012. Sewage sludge-to-energy approaches based on anaerobic digestion and pyrolysis: Brief overview and energy efficiency assessment. Renew. Sustain. Energy Rev. 16, 1657–1665. doi:10.1016/j.rser.2011.12.014

Carpenter, S.R., Bennett, E.M., 2011. Reconsideration of the planetary boundary for phosphorus. Environ. Res. Lett 6, 14009–12. doi:10.1088/1748-9326/6/1/014009

Carr, S., 2012. An Investigation into Phosphorus Removal by Iron Ochre for the Potential Treatment of Aquatic Phosphorus Pollution. PhD Thesis. The University of Edinburgh.

Castaldi, P., Mele, E., Silvetti, M., Garau, G., Deiana, S., 2014. Water treatment residues as accumulators of oxoanions in soil. Sorption of arsenate and phosphate anions from an aqueous solution. J. Hazard. Mater. 264, 144–152. doi:10.1016/j.jhazmat.2013.10.037

Chen, B., Chen, Z., Lv, S., 2011. A novel magnetic biochar efficiently sorbs organic pollutants and phosphate. Bioresour. Technol. 102, 716–723. doi:10.1016/j.biortech.2010.08.067

Chernyakhovskii, V.A., 1985. Technology of unfired periclase-spinel parts with a phosphate binder. Refract. Ind. Ceram. 26, 41–44.

Chia, C.H., Downie, A., Monroe, P., 2015. Characteristics of Biochar: Physical and structural properties, in: Lehmann, J., Joseph, S. (Eds.), Biochar for Environmental Management: Science, Technology and Implementation. Routledge, London, pp. 89–110.

Chintala, R., Schumacher, T.E., McDonald, L.M., Clay, D.E., Malo, D.D., Papiernik, S.K., Clay, S.A., Julson, J.L., 2014. Phosphorus sorption and availability from biochars and soil/biochar mixtures. Clean - Soil, Air, Water 42, 626–634. doi:10.1002/clen.201300089

Clift, R., Shaw, H., 2012. An Industrial Ecology Approach to the Use of Phosphorus. Procedia Eng. 46, 39–44.

Cooper, J., Carliell-Marquet, C., 2013. A substance flow analysis of phosphorus in the UK food production and consumption system. Resour. Conserv. Recycl. 74, 82–100. doi:10.1016/j.resconrec.2013.03.001

Cooper, J., Lombardi, R., Boardman, D., Carliell-Marquet, C., 2011. The future distribution and production of global phosphate rock reserves. Resour. Conserv. Recycl. 57, 78–86. doi:10.1016/j.resconrec.2011.09.009

Cordell, D., Drangert, J.O., White, S., 2009. The story of phosphorus: Global food security and food for thought. Glob. Environ. Chang. 19, 292–305. doi:10.1016/j.gloenvcha.2008.10.009

Cordell, D., Neset, T.S.S., 2014. Phosphorus vulnerability: A qualitative framework for assessing the vulnerability of national and regional food systems to the multi-dimensional stressors of phosphorus scarcity. Glob. Environ. Chang. 24, 108–122. doi:10.1016/j.gloenvcha.2013.11.005

Cordell, D., Rosemarin, a., Schröder, J.J., Smit, a. L., 2011. Towards global phosphorus security: A systems framework for phosphorus recovery and reuse options. Chemosphere 84, 747–758. doi:10.1016/j.chemosphere.2011.02.032

Cordell, D., White, S., 2013. Sustainable phosphorus measures: strategies and technologies for achieving phosphorus security. Agronomy 3, 86–116. doi:10.3390/agronomy3010086

Cornel, P., Schaum, C., 2009. Phosphorus recovery from wastewater: Needs, technologies and costs. Water Sci. Technol. 59, 1069–1076. doi:10.2166/wst.2009.045

Cornell, R.M., Schwertmann, U., 1996. The iron oxides: Structure, properties, reactions, occurrence and uses, 1st ed. VCH, Weinheim.

Cucarella, V., Renman, G., 2009. Phosphorus sorption capacity of filter materials used for on-site wastewater treatment determined in batch experiments-a comparative study. J. Environ. Qual. 38, 381–392. doi:10.2134/jeq2008.0192

Cucarella, V., Zaleski, T., Mazurek, R., 2007. Phosphorus sorption capacity of different types of opoka. Ann. Warsaw Univ. Life Sci. L. Reclam. 18, 11–18.

Cucarella, V., Zaleski, T., Mazurek, R., Renman, G., 2008. Effect of reactive substrates used for the removal of phosphorus from wastewater on the fertility of acid soils. Bioresour. Technol. 99, 4308–4314. doi:10.1016/j.biortech.2007.08.037

Davis, R.D., Beckett, P.H.T., Wollan, E., 1978. Critical levels of twenty potentially toxic elements in young spring barley. Plant Soil 49, 395–408.

de la Rosa, J.M., Paneque, M., Miller, A.Z., Knicker, H., 2014. Relating physical and chemical properties of four different biochars and their application rate to biomass production of Lolium perenne on a Calcic Cambisol during a pot experiment of 79 days. Sci. Total Environ. 499, 175–184.

Deenik, J.L., McClellan, T., Uehara, G., Antal, M.J., Campbell, S., 2010. Charcoal volatile matter content influences plant growth and soil nitrogen transformations. Soil Sci. Soc. Am. J. 74, 1259–1270. doi:10.2136/sssaj2009.0115

Defra, 2011. Anaerobic digestion strategy and action plan 56.

DEFRA, 2010. Fertiliser Manual (RB209), 8th ed. Department for Environment, Food and Rural Affairs.

Desmidt, E., Ghyselbrecht, K., Zhang, Y., Pinoy, L., Van der Bruggen, B., Verstraete, W., Rabaey, K., Meesschaert, B., 2015. Global Phosphorus Scarcity and Full-Scale P-Recovery Techniques: A Review. Crit. Rev. Environ. Sci. Technol. 45, 336–384. doi:10.1080/10643389.2013.866531

Diaz, R.J., Rosenberg, R., 2008. Spreading dead zones and consequences for marine ecosystems. Science (80-.). 321, 926–929. doi:10.1126/science.1156401

Ding, Y., Liu, Y., Liu, S., Li, Z., Tan, X., Huang, X., Zeng, G., Zhou, Y., Zheng, B., Cai, X., 2016. Competitive removal of Cd(II) and Pb(II) by biochars produced from water hyacinths: performance and mechanism. RSC Adv. 6, 5223–5232.

Dobbie, K.E., Heal, K.V., Smith, K. a., 2005. Assessing the performance of phosphorus-saturated ochre as a fertilizer and its environmental acceptability. Soil Use Manag. 21, 231–239. doi:10.1079/SUM2005314

Dobbie, K.E., Heal, K. V., Aumônier, J., Smith, K. a., Johnston, a., Younger, P.L., 2009. Evaluation of iron ochre from mine drainage treatment for removal of phosphorus from wastewater. Chemosphere 75, 795–800. doi:10.1016/j.chemosphere.2008.12.049

Dodds, W.K., Bouska, W.W., Eitzmann, J.L., Pilger, T.J., Pitts, K.L., Riley, A.J., Schloesser, J.T., Thornbrugh, D.J., 2009. Eutrophication of U.S. freshwaters: analysis of potential economic damages. Environ. Sci. Technol. 43, 12–19. doi:10.1021/es801217q

Donatello, S., Cheeseman, C.R., 2013. Recycling and recovery routes for incinerated sewage sludge ash (ISSA): a review.Donatello, S. & Cheeseman, C.R., 2013. Recycling and recovery routes for incinerated sewage sludge ash (ISSA): a review. Waste management (New York, N.Y.), 33(11), pp.2328–40. Waste Manag. 33, 2328–40. doi:10.1016/j.wasman.2013.05.024

Doolette, A.L., Smernik, R.J., 2011. Soil organic P speciation using spectroscopic techniques, in: Bünemann, E., Oberson, A., Frossard, E. (Eds.), Soil Biology Volume 26. Phosphorus in Action. Biological Processes in Soil Phosphorus Cycling26. Phosphorus in Action. Springer-Verlag, Berlin and Heidelberg, pp. 3–36.

Downie, A., Crosky, A., Munroe, P., 2009. Physical Properties of Biochar, in: Lehmann, J., Joseph, S. (Eds.), Biochar for Environmental Management: Science and Technology. Earthscan, London, pp. 13–32.

Doyle, J.D., Parsons, S.A., 2002. Struvite formation, control and recovery. Water Res. 36, 3925–3940. doi:10.1016/S0043-1354(02)00126-4

Drizo, A., Forget, C., Chapuis, R.P., Comeau, Y., 2006. Phosphorus removal by electric arc furnace steel slag and serpentinite. Water Res. 40, 1547–1554. doi:10.1016/j.watres.2006.02.001

EBC, 2012. European Biochar Certificate - Guidelines for a Sustainable Production of Biochar, Version 6.1 1–22. doi:10.13140/RG.2.1.4658.7043

EC, 2013. Communication from the Commission to the European Parliament, the Council, the European Economic and Social Committee and the Committee of the Regions:

Consultative Communication on the Sustainable Use of Phosphorus.

Enders, A., Lehmann, J., 2012. Comparison of Wet-Digestion and Dry-Ashing Methods for Total Elemental Analysis of Biochar. Commun. Soil Sci. Plant Anal. 43, 1042–1052. doi:10.1080/00103624.2012.656167

EU DG ENTR, 2014. Report on Critical Raw Materials for the EU. Ares(2015)1819503.

European Commission, 2016. CALL FOR APPLICATIONS FOR MEMBERS AND OBSERVERS TO THE TECHNICAL WORKING GROUP FOR THE DEVELOPMENT OF POSSIBLE PROCESS AND PRODUCT CRITERIA FOR STRUVITE, BIOCHAR AND ASH-BASED PRODUCTS FOR USE IN FERTILISING PRODUCTS. Ares(2016)2078221. (STRUBIAS TWG).

Fang, L., Huang, L., Holm, P.E., Yang, X., Hansen, H.C.B., Wang, D., 2015. Facile upscaled synthesis of layered iron oxide nanosheets and their application in phosphate removal. J. Mater. Chem. A 3, 7505–7512. doi:10.1039/C4TA07083F

Farrell, M., Rangott, G., Krull, E., 2013. Difficulties in using soil-based methods to assess plant availability of potentially toxic elements in biochars and their feedstocks. J. Hazard. Mater. 250–251, 29–36. doi:10.1016/j.jhazmat.2013.01.073

Fellet, G., Marchiol, L., Delle Vedove, G., Peressotti, A., 2011. Application of biochar on mine tailings: Effects and perspectives for land reclamation. Chemosphere 83, 1262–1267. doi:10.1016/j.chemosphere.2011.03.053

Fenton, O., Healy, M.G., Rodgers, M., O Huallacháin, D., 2009. Site-specific P absorbency of ochre from acid mine-drainage near an abandoned Cu-S mine in the Avoca–Avonmore catchment, Ireland. Clay Miner. 44, 113–123. doi:10.1180/claymin.2009.044.1.113

Fenton, O., Kirwan, L., Huallacháin, D.Ó., Healy, M.G., 2012. The effectiveness and feasibility of using ochre as a soil amendment to sequester dissolved reactive phosphorus in runoff. Water. Air. Soil Pollut. 223, 1249–1261. doi:10.1007/s11270-011-0941-3

Fixen, P.E., Grove, J.H., Westerman, R.L., 1990. Testing soils for phosphorus, in: Westerman, R.L., Baird, J.V., Christensen, N.W., Fixen, P.E., WHitney, D.A. (Eds.), Soil Testing and Plant Analysis. Soil Science Society of America, Inc., Wisconsin, pp.

141–180.

Follmi, K., 1996. The phosphorus cycle, phosphogenesis and marine phosphate-rich deposits. Earth-Science Rev. 40, 55–124. doi:10.1016/0012-8252(95)00049-6

Franz, M., 2008. Phosphate fertilizer from sewage sludge ash (SSA). Waste Manag. 28, 1809–1818. doi:10.1016/j.wasman.2007.08.011

Frossard, E., Achat, D.L., Bernasconi, S.M., Bünemann, E.K., Fardeau, J.-C., Jansa, J., Morel, C., Rabeharisoa, L., Randriamanantsoa, L., Sinaj, S., Tamburini, F., Obertson, A., 2011. The use of tracers to investigate phosphate cycling in soil, in: Bünemann, E., Oberson, A., Frossard, E. (Eds.), Soil Biology Volume 26. Phosphorus in Action. Biological Processes in Soil Phosphorus Cycling. Springer-Verlag, Berlin and Heidelberg, pp. 59–91.

Frossard, E., Brossard, M., Hedley, M.J., Metherell, A., 1995. Reactions Controlling the Cycling of P in Soils. Phosphorus Glob. Environ. Transf. Cycles, Manag. 107–138.

Fytili, D., Zabaniotou, A., 2008. Utilization of sewage sludge in EU application of old and new methods-A review. Renew. Sustain. Energy Rev. doi:10.1016/j.rser.2006.05.014

Garbouchev, I.P., 1966. Changes occurring during a year in the soluble phosphorus and potassium in soil under crops in rotation experiments at Rothamsted , Woburn and Saxmundham. J. Agric. Sci. 66, 399–412.

German Federal Environmental Agency, 1999. German Federal Soil Protection and Contaminated Sites Ordinance (BBodSchV). Germany.

Glaser, B., Wiedner, K., Seelig, S., Schmidt, H.P., Gerber, H., 2015. Biochar organic fertilizers from natural resources as substitute for mineral fertilizers. Agron. Sustain. Dev. 35, 667–678. doi:10.1007/s13593-014-0251-4

Goldberg, S., Sposito, G., 1985. On the mechanism of specific phosphate adsorption by hydroxylated mineral surfaces: A review. Commun. Soil Sci. Plant Anal. 16, 801–821. doi:10.1080/00103628509367646

González Ponce, R., López-de-Sá, E.G., Plaza, C., 2009. Lettuce response to phosphorus fertilization with struvite recovered from municipal wastewater. HortScience 44, 426–430.

Greenop, R., Wentworth, J., 2014. Phosphate Resources. UK Parliamentary Office of Science and Technology. POSTnote 477.

Grzebisz, W., Kocialkowski, W.Z., Chudzinski, B., 1983. Copper geochemistry and availability in cultivated soils contaminated by a copper smelter. J. Geochemical Explor. 58, 301–307. doi:10.1016/s0375-6742(96)00065-9

Gull, M., Zhou, M., Fernández, F.M., Pasek, M.A., 2014. Prebiotic phosphate ester syntheses in a deep eutectic solvent. J. Mol. Evol. 78, 109–117. doi:10.1007/s00239-013-9605-9

Gwenzi, W., Muzava, M., Mapanda, F., Tauro, T.P., 2016. Comparative short-term effects of sewage sludge and its biochar on soil properties, maize growth and uptake of nutrients on a tropical clay soil in Zimbabwe. J. Integr. Agric. 15, 1395–1406. doi:10.1016/S2095-3119(15)61154-6

Hale, S.E., Alling, V., Martinsen, V., Mulder, J., Breedveld, G.D., Cornelissen, G., 2013. The sorption and desorption of phosphate-P, ammonium-N and nitrate-N in cacao shell and corn cob biochars. Chemosphere 91, 1612–1619. doi:10.1016/j.chemosphere.2012.12.057

Hale, S.E., Lehmann, J., Rutherford, D., Zimmerman, A.R., Bachmann, R.T., Shitumbanuma, V., O'Toole, A., Sundqvist, K.L., Arp, H.P.H., Cornelissen, G., 2012. Quantifying the total and bioavailable polycyclic aromatic hydrocarbons and dioxins in biochars. Environ. Sci. Technol. 46, 2830–2838. doi:10.1021/es203984k

Hancock, S., 2005. Output from the UK Coal Authority's Mine Water Treatment Sites, in: Loredo, J., Pendás, F. (Eds.), Mine Water 2005 – Mine Closure. pp. 392–402.

Haygarth, P.M., Condron, L.M., 2004. Background and Elevated Phosphorus Release From Terrestrial Environments, in: Valsami-Jones, E. (Ed.), Phosphorus in Environmental Technologies; Principles and Applications. IWA Publishing, London, pp. 79–92.

Heal, K., Younger, P.L., Smith, K., Glendinning, S., Quinn, P., Dobbie, K., 2003. Novel use of ochre from mine water treatment plants to reduce point and diffuse phosphorus pollution. L. Contam. Reclam. doi:10.2462/09670513.808

Heal, K. V., Dobbie, K.E., Bozika, E., McHaffie, H., Simpson, a. E., Smith, K. a., 2005. Enhancing phosphorus removal in constructed wetlands with ochre from mine drainage treatment. Water Sci. Technol. 51, 275–282.

Heller-Kallai, L., Miloslavski, I., Aizenshtat, Z., Halicz, L., 1988. Chemical and mass spectrometric analysis of volatiles derived from clays. Am. Mineral. 73, 376–382.

Hilber, I., Blum, F., Leifeld, J., Schmidt, H.P., Bucheli, T.D., 2012. Quantitative determination of PAHs in biochar: A prerequisite to ensure its quality and safe application. J. Agric. Food Chem. 60, 3042–3050. doi:10.1021/jf205278v

Holford, I.C.., 1982. The comparative significance and utility of the Freundlich and Langmuir parameters for characterizing sorption and plant availability of phosphate in soils. Aust. J. Soil Res. 20, 233–42.

Hollister, C.C., Bisogni, J.J., Lehmann, J., 2013. Ammonium, Nitrate, and Phosphate Sorption to and Solute Leaching from Biochars Prepared from Corn Stover (Zea mays L.) and Oak Wood (Quercus spp.). J. Environ. Qual. 42, 137–44. doi:10.2134/jeq2012.0033

Hossain, M.K., Strezov, V., Yin Chan, K., Nelson, P.F., 2010. Agronomic properties of wastewater sludge biochar and bioavailability of metals in production of cherry tomato (Lycopersicon esculentum). Chemosphere 78, 1167–1171. doi:10.1016/j.chemosphere.2010.01.009

Hossain, M.K., Strezov Vladimir, V., Chan, K.Y., Ziolkowski, A., Nelson, P.F., 2011. Influence of pyrolysis temperature on production and nutrient properties of wastewater sludge biochar. J. Environ. Manage. 92, 223–228. doi:10.1016/j.jenvman.2010.09.008

Huang, C.-Y.L., Schulte, E.E., 1985. Digestion of plant tissue for analysis by ICP emission spectroscopy. Commun. Soil Sci. Plant Anal. 16. doi:10.1080/00103628509367657

IBI, 2012. Standardized Product Definition and Product Testing Guidelines for Biochar That Is Used in Soil. International Biochar Initiative (IBI).

Ippolito, J.A., Spokas, K.A., Novak, J.M., Lentz, R.D., Cantrell, K.B., 2015. Biochar elemental composition and factors influencing nutrient retention, in: Lehmann, J., Joseph, S. (Eds.), Biochar for Environmental Management: Science, Technology and Implementation. Routledge, New York, pp. 139–164.

Jasinski, S.M., 2016. U.S. Geological Survey - Mineral Commodity Summaries 2015 - Phosphate Rock. Virginia.

Jasinski, S.M., 2012. U.S. Geological Survey - Mineral Commodity Summaries 2012 - Phosphate Rock.

Jasinski, S.M., 2010. Phosphate Rock, Mineral Commodity Summaries. US Geological Survey.

Jeffery, S., Bezemer, T.M., Cornelissen, G., Kuyper, T.W., Lehmann, J., Mommer, L., Sohi, S.P., van de Voorde, T.F.J., Wardle, D.A., van Groenigen, J.W., 2015. The way forward in biochar research: Targeting trade-offs between the potential wins. GCB Bioenergy 7, 1–13. doi:10.1111/gcbb.12132

Jeffery, S., Verheijen, F.G.A., van der Velde, M., Bastos, A.C., 2011. A quantitative review of the effects of biochar application to soils on crop productivity using meta-analysis. Agric. Ecosyst. Environ. doi:10.1016/j.agee.2011.08.015

Johansson Westholm, L., 2006. Substrates for phosphorus removal - Potential benefits for on-site wastewater treatment? Water Res. 40, 23–36. doi:10.1016/j.watres.2005.11.006

Johnston, D., Potter, H., Jones, C., Rolley, S., Watson, I., Pritchard, J., Agency, T.E., 2008. Abandoned mines and the water environment, Science Report. Environment Agency, Bristol. doi:978-1-84432-894-9

Jordan-Meille, L., Rubæk, G.H., Ehlert, P. a I., Genot, V., Hofman, G., Goulding, K., Recknagel, J., Provolo, G., Barraclough, P., 2012. An overview of fertilizer-P recommendations in Europe: Soil testing, calibration and fertilizer recommendations. Soil Use Manag. 28, 419–435. doi:10.1111/j.1475-2743.2012.00453.x

Joseph, S., Graber, E.R., Chia, C., Munroe, P., Donne, S., Thomas, T., Nielsen, S., Marjo, C., Rutlidge, H., Pan, G., Li, L., Taylor, P., Rawal, A., Hook, J., 2013. Shifting paradigms: development of high-efficiency biochar fertilizers based on nano-structures and soluble components. Carbon Manag. 4, 323–343. doi:10.4155/cmt.13.23

Joseph, S.D., Camps-Arbestain, M., Lin, Y., Munroe, P., Chia, C.H., Hook, J., Van Zwieten, L., Kimber, S., Cowie, A., Singh, B.P., Lehmann, J., Foidl, N., Smernik, R.J., Amonette, J.E., 2010. An investigation into the reactions of biochar in soil, in: Australian Journal of Soil Research. pp. 501–515. doi:10.1071/SR10009

Kandegedara, A., Rorabacher, D.B., 1999. Noncomplexing tertiary amines as “better” buffers covering the range of pH 3-11. Temperature dependence of their acid dissociation constants. Anal. Chem. 71, 3140–3144. doi:10.1021/ac9902594

Kanematsu, M., Young, T.M., Fukushi, K., Sverjensky, D. a., Green, P.G., Darby, J.L., 2011. Quantification of the effects of organic and carbonate buffers on arsenate and phosphate adsorption on a goethite-based granular porous adsorbent. Environ. Sci. Technol. 45, 561–568. doi:10.1021/es1026745

Khan, S., Chao, C., Waqas, M., Arp, H.P.H., Zhu, Y.G., 2013a. Sewage sludge biochar influence upon rice (Oryza sativa L) yield, metal bioaccumulation and greenhouse gas emissions from acidic paddy soil. Environ. Sci. Technol. 47, 8624–8632. doi:10.1021/es400554x

Khan, S., Wang, N., Reid, B.J., Freddo, A., Cai, C., 2013b. Reduced bioaccumulation of PAHs by Lactuca satuva L. grown in contaminated soil amended with sewage sludge and sewage sludge derived biochar. Environ. Pollut. 175, 64–68. doi:10.1016/j.envpol.2012.12.014

Khanmohammadi, Z., Afyuni, M., Mosaddeghi, M.R., 2015. Effect of pyrolysis temperature on chemical and physical properties of sewage sludge biochar. Waste Manag. Res. 33, 275–283. doi:10.1177/0734242X14565210

Kleemann, R., 2015. Sustainable phosphorus recovery from waste. University of Surrey.

Kloss, S., Zehetner, F., Dellantonio, A., Hamid, R., Ottner, F., Liedtke, V., Schwanninger, M., Gerzabek, M.H., Soja, G., 2012. Characterization of Slow Pyrolysis Biochars: Effects of Feedstocks and Pyrolysis Temperature on Biochar Properties. J. Environ. Qual. 41, 990. doi:10.2134/jeq2011.0070

Kumar, P., Sudha, S., Chand, S., Srivastava, V.C., 2010. Phosphate Removal from Aqueous Solution Using Coir-Pith Activated Carbon. Sep. Sci. Technol. 45, 1463–1470. doi:10.1080/01496395.2010.485604

Laird, D., Rogovska, N., 2015. Biochar Effects on Nutrient Leaching, in: Lehmann, J., Joseph, S. (Eds.), Biochar for Environmental Management, Science, Technology and Implementation. Routledge, Oxon, pp. 521–542.

Lehmann, J., Da Silva, J.P., Steiner, C., Nehls, T., Zech, W., Glaser, B., 2003. Nutrient availability and leaching in an archaeological Anthrosol and a Ferralsol of the Central Amazon basin: Fertilizer, manure and charcoal amendments. Plant Soil 249, 343–357.

doi:10.1023/A:1022833116184

Lehmann, J., Joseph, S., 2009. Biochar for environmental management: An introduction, in: Lehmann, J., Joseph, S. (Eds.), Biochar for Environmental Management, Science and Technology. Earthscan, London, pp. 1–12.

Li, J., Lv, G., Bai, W., Liu, Q., Zhang, Y., Song, J., 2016. Modification and use of biochar from wheat straw (Triticum aestivum L.) for nitrate and phosphate removal from water. Desalin. Water Treat. 57, 4681–4693. doi:10.1080/19443994.2014.994104

Littler, J., Geroni, J.N., Sapsford, D.J., Coulton, R., Griffiths, A.J., 2013. Mechanisms of phosphorus removal by cement-bound ochre pellets. Chemosphere 90, 1533–1538. doi:10.1016/j.chemosphere.2012.08.054

Liu, F., Zuo, J., Chi, T., Wang, P., Yang, B., 2015. Removing phosphorus from aqueous solutions by using ironmodified corn straw biochar. Front. Environ. Sci. Eng. doi:10.1007/s11783-015-0769-y

Liu, T., Liu, B., Zhang, W., 2014. Nutrients and heavy metals in biochar produced by sewage sludge pyrolysis: Its application in soil amendment. Polish J. Environ. Stud. 23, 271–275.

Lu, H., Zhang, W., Wang, S., Zhuang, L., Yang, Y., Qiu, R., 2013. Characterization of sewage sludge-derived biochars from different feedstocks and pyrolysis temperatures. J. Anal. Appl. Pyrolysis 102, 137–143. doi:10.1016/j.jaap.2013.03.004

Lua, A.C., Yang, T., Guo, J., 2004. Effects of pyrolysis conditions on the properties of activated carbons prepared from pistachio-nut shells. J. Anal. Appl. Pyrolysis 72, 279–287. doi:10.1016/j.jaap.2004.08.001

Luo, F., Song, J., Xia, W., Dong, M., Chen, M., Soudek, P., 2014. Characterization of contaminants and evaluation of the suitability for land application of maize and sludge biochars. Environ. Sci. Pollut. Res. 21, 8707–8717. doi:10.1007/s11356-014-2797-8

MacDonald, G.K., Bennett, E.M., Potter, P.A., Ramankutty, N., 2011. Agronomic phosphorus imbalances across the world’s croplands. Proc. Natl. Acad. Sci. U. S. A. 108, 3086–91. doi:10.1073/pnas.1010808108

Mackenzie, F.T., Ver, L.M., Lerman, A., 2002. Century-scale nitrogen and phosphorus controls of the carbon cycle. Chem. Geol. 190, 13–32. doi:10.1016/S0009-2541(02)00108-0

MacNicol, R.D., Beckett, P.H.T., 1985. Critical tissue concentrations of potentially toxic elements. Plant Soil 85, 107–129.

Magdziarz, A., Wilk, M., 2013. Thermal characteristics of the combustion process of biomass and sewage sludge. J. Therm. Anal. Calorim. 114, 519–529. doi:10.1007/s10973-012-2933-y

Mallet, M., Barthélémy, K., Ruby, C., Renard, A., Naille, S., 2013. Investigation of phosphate adsorption onto ferrihydrite by X-ray Photoelectron Spectroscopy. J. Colloid Interface Sci. 407, 95–101. doi:10.1016/j.jcis.2013.06.049

Mao, Y., Ninh Pham, A., Xin, Y., David Waite, T., 2012. Effects of pH, floc age and organic compounds on the removal of phosphate by pre-polymerized hydrous ferric oxides. Sep. Purif. Technol. 91, 38–45. doi:10.1016/j.seppur.2011.09.045

Marschner, H., 1995. Mineral nutrition of higher plants, Boston, MA, USA: Academic Press. Academic Press, Boston, MA, USA.

Mašek, O., Ronsse, F., Dickinson, D., 2016. Biochar production and feedstock, in: Shackley, S., Ruysschaert, G., Zwart, K., Glaser, B. (Eds.), Biochar in European Soils and Agriculture: Science and Practice. ROutledge, New York, pp. 17–40.

McGrath, J.W., Quinn, J.P., 2004. Biological Phosphorus Removal, in: Valsami-Jones, E. (Ed.), Phosphorus in Environmental Technologies; Principles and Applications. IWA Publishing, pp. 272–290.

Meers, E., Du Laing, G., Unamuno, V., Ruttens, A., Vangronsveld, J., Tack, F.M.G., Verloo, M.G., 2007. Comparison of cadmium extractability from soils by commonly used single extraction protocols. Geoderma 141, 247–259. doi:10.1016/j.geoderma.2007.06.002

Mehlich, A., 1984a. Mehlich 3 soil test extractant: A modification of Mehlich 2 extractant. Commun. Soil Sci. Plant Anal. doi:10.1080/00103628409367568

Mehlich, A., 1984b. Mehlich 3 soil test extractant: A modification of Mehlich 2 extractant. Commun. Soil Sci. Plant Anal. 15, 1409–1416. doi:10.1080/00103628409367568

Méndez, A., Gómez, A., Paz-Ferreiro, J., Gascó, G., 2012. Effects of sewage sludge biochar on plant metal availability after application to a Mediterranean soil. Chemosphere 89, 1354–1359. doi:10.1016/j.chemosphere.2012.05.092

Menzies, N.W., Donn, M.J., Kopittke, P.M., 2007. Evaluation of extractants for estimation of the phytoavailable trace metals in soils. Environ. Pollut. 145, 121–130. doi:10.1016/j.envpol.2006.03.021

Mills, N., Pearce, P., Farrow, J., Thorpe, R.B., Kirkby, N.F., 2014. Environmental & economic life cycle assessment of current & future sewage sludge to energy technologies. Waste Manag. 34, 185–95. doi:10.1016/j.wasman.2013.08.024

Monterosso, C., Alvarez, E., Fernández Marcos, M.L., 1999. Evaluation of Mehlich 3 reagent as a multielement extractant in mine soils. L. Degrad. Dev. 10, 35–47.

Moorhouse, A., Watson, I., 2015. Mine water derived iron as a national opportunity for phosphate removal. Coal Authority., in: Proceedings of the 9th European Wastewater Management Conference.

Morales, M.M., Comerford, N., Guerrini, I. a., Falcão, N.P.S., Reeves, J.B., 2013. Sorption and desorption of phosphate on biochar and biochar-soil mixtures. Soil Use Manag. 29, 306–314. doi:10.1111/sum.12047

Mukherjee, A., Lal, R., Zimmerman, A.R., 2014. Effects of biochar and other amendments on the physical properties and greenhouse gas emissions of an artificially degraded soil. Sci. Total Environ. 487, 26–36. doi:10.1016/j.scitotenv.2014.03.141

Mukherjee, A., Zimmerman, A.R., Harris, W., 2011. Surface chemistry variations among a series of laboratory-produced biochars. Geoderma 163, 247–255. doi:10.1016/j.geoderma.2011.04.021

Na, Y.-M., Park, S.S., 2004. Retardation of phosphate release from freshwater benthic sediments by application of ocher pellets with calcium nitrate. J. Environ. Sci. Health. A. Tox. Hazard. Subst. Environ. Eng. 39, 1617–1629. doi:10.1081/ESE-120037858

Namasivayam, C., Sangeetha, D., 2004. Equilibrium and kinetic studies of adsorption of phosphate onto ZnCl2 activated coir pith carbon. J. Colloid Interface Sci. 280, 359–65. doi:10.1016/j.jcis.2004.08.015

Nelissen, V., Ruysschaert, G., Müller-Stöver, D., Bodé, S., Cook, J., Ronsse, F., Shackley, S., Boeckx, P., Hauggaard-Nielsen, H., 2014. Short-Term Effect of Feedstock and Pyrolysis Temperature on Biochar Characteristics, Soil and Crop Response in Temperate Soils. Agronomy 4, 52–73. doi:10.3390/agronomy4010052

Nyomora, A.M.S., Sah, R.N., Brown, P.H., Miller, R.O., 1997. Boron determination in biological materials by inductively coupled plasma atomic emission and mass spectrometry : effects of sample dissolution methods. Fresenius J. Anal. Chem. 357, 1185–1191.

Ohki, K., Boswell, F.C., Parker, M.B., Shuman, L.M., Wilson, D.O., 1979. Critical manganese deficiency level of soybean related to leaf position. Agron. J. 71, 233–234.

Oleszczuk, P., Jośko, I., Kuśmierz, M., 2013. Biochar properties regarding to contaminants content and ecotoxicological assessment. J. Hazard. Mater. 260, 375–382. doi:10.1016/j.jhazmat.2013.05.044

Oliveira, M., Ribeiro, D., Nobrega, J.M.M., Machado, A.V. V, Brito, A.G.G., Nogueira, R., 2011. Removal of phosphorus from water using active barriers: Al2O3 immobilized on to polyolefins. Environ. Technol. 32, 989–995. doi:10.1080/09593330.2010.522597

Onay, O., Kockar, O.M., 2003. Slow, fast and flash pyrolysis of rapeseed. Renew. Energy 28, 2417–2433. doi:10.1016/S0960-1481(03)00137-X

Parfitt, R., 1989. Phosphate reactions with natural allophane, ferrihydrite and goethite. J. Soil Sci. 40, 359–369. doi:10.1111/j.1365-2389.1989.tb01280.x

Parfitt, R.., Russell, J.., 1977. Adsorption on hydrous oxides. IV. mechanisms of adsorption of various ions on goethite. J. Soil Sience 28, 297–305.

Parfitt, R.L., Atkinson, R.J., Smart, R.S.C., 1975. The Mechanism of Phosphate Fixation by Iron Oxides. Soil Sci. Soc. Am. 39, 838–841. doi:10.2136/sssaj1975.03615995003900050017x

Park, J.H., Ok, Y.S., Kim, S.H., Cho, J.S., Heo, J.S., Delaune, R.D., Seo, D.C., 2015. Evaluation of phosphorus adsorption capacity of sesame straw biochar on aqueous solution: influence of activation methods and pyrolysis temperatures. Environ. Geochem. Health 37, 969–983. doi:10.1007/s10653-015-9709-9

Parsons, S.A., Berry, T.A., 2009. Chemical phosphorus removal, in: Valsami-Jones, E. (Ed.), Phosphorus in Environmental Technologies. IWA Publishing, London, pp. 260–271.

Parsons, S.A., Smith, J.A., 2008. Phosphorus removal and recovery from municipal wastewaters. Elements 4, 109–112. doi:10.2113/GSELEMENTS.4.2.109

Parsons, S.A., Stevenson, T., 2004. Waste Water Treatment Principles, in: Valsami-Jones, E. (Ed.), Phosphorus in Environmental Technologies; Principles and Applications. IWA Publishing, London, pp. 249–259.

Pierzynski, G.M., Sims, J.T., Vance, G.F., 2000. Soil phosphorus and environmental quality, in: Soils and Environmental Quality. CRC Press, Boca Raton, pp. 155–207.

Plaza, C., Sanz, R., Clemente, C., Fernández, J.M., González, R., Polo, A., Colmenarejo, M.F., 2007. Greenhouse evaluation of struvite and sludges from municipal wastewater treatment works as phosphorus sources for plants. J. Agric. Food Chem. 55, 8206–8212. doi:10.1021/jf071563y

Pretty, J.N., Mason, C.F., Nedwell, D.B., Hine, R.E., Leaf, S., Dils, R., 2003. Environmental costs of freshwater eutrophication in England and Wales. Environ. Sci. Technol. 37, 201–208. doi:10.1021/es020793k

Prommer, J., Wanek, W., Hofhansl, F., Trojan, D., Offre, P., Urich, T., Schleper, C., Sassmann, S., Kitzler, B., Soja, G., Hood-Nowotny, R.C., 2014. Biochar decelerates soil organic nitrogen cycling but stimulates soil nitrification in a temperate arable field trial. PLoS One 9. doi:10.1371/journal.pone.0086388

Qiu, Y., Zheng, Z., Zhou, Z., Sheng, G.D., 2009. Effectiveness and mechanisms of dye adsorption on a straw-based biochar. Bioresour. Technol. 100, 5348–5351. doi:10.1016/j.biortech.2009.05.054

Quilliam, R.S., Marsden, K.A., Gertler, C., Rousk, J., DeLuca, T.H., Jones, D.L., 2012. Nutrient dynamics, microbial growth and weed emergence in biochar amended soil are influenced by time since application and reapplication rate. Agric. Ecosyst. Environ. 158, 192–199. doi:10.1016/j.agee.2012.06.011

Rajkovich, S., Enders, A., Hanley, K., Hyland, C., Zimmerman, A.R., Lehmann, J., 2012. Corn growth and nitrogen nutrition after additions of biochars with varying properties to a temperate soil. Biol. Fertil. Soils 48, 271–284. doi:10.1007/s00374-011-0624-7

Rawal, A., Joseph, S.D., Hook, J.M., Chia, C.H., Munroe, P.R., Donne, S.W., Lin, Y., Phelan, D., Richard, D., Mitchell, G., Pace, B., Horvat, J., Beau, J., Webber, W., 2016. Mineral-Biochar Composites: Molecular Structure and Porosity. Environ. Sci. Technol. 50, 7706–7714. doi:10.1021/acs.est.6b00685

Reddy, K.R., Kadlec, R.H., Flaig, E., Gale, P.M., 1999. Phosphorus retention in streams and wetlands: a review. Crit. Rev. Environ. Sci. Technol. 29, 83–146. doi:10.1080/10643389991259182

Reijnders, L., 2014. Resources , Conservation and Recycling Phosphorus resources , their depletion and conservation , a review. "Resources, Conserv. Recycl. 93, 32–49. doi:10.1016/j.resconrec.2014.09.006

Ren, J., Li, N., Li, L., An, J.-K., Zhao, L., Ren, N.-Q., 2015. Granulation and ferric oxides loading enable biochar derived from cotton stalk to remove phosphate from water. Bioresour. Technol. 178, 119–125. doi:10.1016/j.biortech.2014.09.071

Rockstrom, J., 2009. A safe operating space for humanity. Nature 461, 472–475. doi:10.1109/TIP.2011.2165549

Römheld, V., Marschner, H., 1991. Function of micronutrients in plants. In Micronutrients in agriculture, in: Mortvelt, J.J., Cox, F.R., Shuman, L.M., Welch, R.M. (Eds.), Micronutrients in Agriculture. Soil Science Society of America, Inc., Wisconsin, pp. 297–328.

Rondon, M.A., Lehmann, J., Ramirez, J., Hurtado, M., 2007. Biological nitrogen fixation by common beans (Phaseolus vulgaris L.) increases with bio-char additions. Biol. Fertil. Soils 43, 699–708. doi:10.1007/s00374-006-0152-z

RStudio Team, 2015. RStudio: Integrated Development for R.

Sakadevan, K., Bavor, H.J., South, N., 1998. Phosphate Adsorption Characteristics of Soils , Slags a N D Zeolite To Be Used As Substrates in Constructed Wetland Systems. Water Res. 32, 393–399. doi:10.1016/S0043-1354(97)00271-6

Sapsford, D., Santonastaso, M., Thorn, P., Kershaw, S., 2015. Conversion of coal mine drainage ochre to water treatment reagent: production, characterisation and application for P and Zn removal. J. Environ. Manage. 160, 7–15.

Schneider, F., Haderlein, S.B., 2016. Potential effects of biochar on the availability of phosphorus — mechanistic insights. Geoderma 277, 83–90. doi:10.1016/j.geoderma.2016.05.007

Scholz, R.W., Roy, A.H., Hellums, D.T., Ulrich, A.E., Brand, F.S., 2014. Sustainable phosphorus management: A global transdisciplinary roadmap, Sustainable Phosphorus Management: A Global Transdisciplinary Roadmap. doi:10.1007/978-94-007-7250-2

SEPA, 2015. Briefing for the Scottish Parliament's Public Petitions Committee: Oral Evidence Session on Use of Sewage Sludge on Land - 23 June 2015. Edinburgh.

Shackley, S., Hammond, J., Gaunt, J., Ibarrola, R., 2011. The feasibility and costs of biochar deployment in the UK. Carbon Manag. 2, 335–356. doi:10.4155/cmt.11.22

Sharpley, A.N., 2000. Phosphorus availability, in: Sumner, M.E. (Ed.), Handbook of Soil Science. CRC Press, pp. 18–38.

Shen, Q., Hedley, M., Camps Arbestain, M., Kirschbaum, M.U.F., 2016. Can biochar increase the bioavailability of phosphorus? J. soil Sci. plant Nutr. doi:dx.doi.org/10.4067/S0718-95162016005000022

Shenbagavalli, S and Mahimairaja, S., 2012. Characterization and Effect of Biochar on Nitrogen and. Intern. J. Adv. Biol. Res. 2, 249–255.

Shepherd, J.G., Joseph, S., Sohi, S.P., Heal, K.V., 2017. Biochar and enhanced phosphate capture: mapping mechanisms to functional properties. Chemosphere 179, 57–74.

Shepherd, J.G., Kleemann, R., Bahri-Esfahani, J., Hudek, L., Suriyagoda, L., Vandamme, E., van Dijk, K.C.K.C., 2016a. The future of phosphorus in our hands. Nutr. Cycl. Agroecosystems 104, 281–287. doi:10.1007/s10705-015-9742-1

Shepherd, J.G., Sohi, S.P., Heal, K.V., 2016b. Optimising the recovery and re-use of phosphorus from wastewater effluent for sustainable fertiliser development. Water Res. 94, 155–165. doi:10.1016/j.watres.2016.02.038

Sibrell, P.L., 2007. Method of removing phosphorus from wastewater. U.S. Patent No. 7,294,275.

Sibrell, P.L., Montgomery, G. a., Ritenour, K.L., Tucker, T.W., 2009. Removal of phosphorus from agricultural wastewaters using adsorption media prepared from acid mine drainage sludge. Water Res. 43, 2240–2250. doi:10.1016/j.watres.2009.02.010

Sibrell, P.L., Tucker, T.W., 2012. Fixed bed sorption of phosphorus from wastewater using iron oxide-based media derived from acid mine drainage. Water. Air. Soil Pollut. 223, 5105–5117. doi:10.1007/s11270-012-1262-x

Silber, A., Levkovitch, I., Graber, E.R., 2010. PH-dependent mineral release and surface properties of cornstraw biochar: Agronomic implications. Environ. Sci. Technol. 44, 9318–9323. doi:10.1021/es101283d

Smil, V., 2000. Phosphorus in the environment: Natural flows and human interferences. Annu. Rev. Energy Environ. 25, 53–88. doi:10.1146/annurev.energy.25.1.53

Smith, V.H., Schindler, D.W., 2009. Eutrophication science: where do we go from here? Trends Ecol. Evol. doi:10.1016/j.tree.2008.11.009

Song, X.D., Xue, X.Y., Chen, D.Z., He, P.J., Dai, X.H., 2014. Application of biochar from sewage sludge to plant cultivation: Influence of pyrolysis temperature and biochar-to-soil ratio on yield and heavy metal accumulation. Chemosphere 109, 213–220. doi:10.1016/j.chemosphere.2014.01.070

Spokas, K. a., Cantrell, K.B., Novak, J.M., Archer, D.W., Ippolito, J. a., Collins, H.P., Boateng, A. a., Lima, I.M., Lamb, M.C., McAloon, A.J., Lentz, R.D., Nichols, K. a., 2012. Biochar: a synthesis of its agronomic impact beyond carbon sequestration. J. Environ. Qual. 41, 973–989. doi:10.2134/jeq2011.0069

Steen, I., 1998. Phosphorus availability in the 21st century Management of a non-renewable resource. Phosphorus & Potassium 217, 25–31.

Steenari, B., Lindqvist, O., 1998. High Temperature Reactions of Straw Ash and the Anti-Sintering Additives Kaolin and Dolomite. Biomass and Bioenergy 14, 67–76.

Steffen, W., Richardson, K., Rockström, J., Cornell, S., Fetzer, I., Bennett, E., Biggs, R., Carpenter, S.R., de Wit, C. a., Folke, C., Mace, G., Persson, L.M., Veerabhadran, R., Reyers, B., Sörlin, S., 2015. Planetary Boundaries: Guiding human development on a changing planet. Science 347. doi:10.1126/science.1259855

Steffen, W., Stafford Smith, M., 2013. Planetary boundaries, equity and global sustainability:

Why wealthy countries could benefit from more equity. Curr. Opin. Environ. Sustain. doi:10.1016/j.cosust.2013.04.007

Streubel, J.D., Collins, H.P., Tarara, J.M., Cochran, R.L., 2012. Biochar produced from anaerobically digested fiber reduces phosphorus in dairy lagoons. J. Environ. Qual. 41, 1166–74. doi:10.2134/jeq2011.0131

Stutter, M.I., 2015. The composition, leaching, and sorption behavior of some alternative sources of phosphorus for soils. Ambio 44, 207–216. doi:10.1007/s13280-014-0615-7

Systat Software, 2016. SigmaPlot V 13.0.

Talboys, P.J., Heppell, J., Roose, T., Healey, J.R., Jones, D.L., Withers, P.J.A., 2016. Struvite: a slow-release fertiliser for sustainable phosphorus management? Plant Soil 401, 109–123. doi:10.1007/s11104-015-2747-3

Team, R.C., 2015. R: A language and environment for statistical computing.

Tiessen, H., Ballester, M.V., Salcedo, I., 2011. Phosphorus and global change, in: Bünemann, E., Oberson, A., Frossard, E. (Eds.), Soil Biology Volume 26. Phosphorus in Action. Biological Processes in Soil Phosphorus Cycling. Springer-Verlag, Berlin and Heidelberg, pp. 459–471.

Tilman, D., Cassman, K.G., Matson, P.A., Naylor, R., Polasky, S., 2002. Agricultural sustainability and intensive production practices. Nature 418, 671–7. doi:10.1038/nature01014

Torrent, J., Schwertmann, U., Barrón, V., 1992. Fast and slow phosphate sorption by goethite-rich natural materials. Clays Clay Miner. 40, 14–21. doi:10.1346/CCMN.1992.0400103

Tüzen, M., 2003. Determination of heavy metals in soil , mushroom and plant samples by atomic absorption spectrometry. Microchem. J. 74, 289–297. doi:10.1016/S0026-265X(03)00035-3

Uchimiya, M., Klasson, K.T., Wartelle, L.H., Lima, I.M., 2011. Influence of soil properties on heavy metal sequestration by biochar amendment: 1. Copper sorption isotherms and the release of cations. Chemosphere 82, 1431–1437. doi:10.1016/j.chemosphere.2010.11.050

Uzoma, K.C., Inoue, M., Andry, H., Zahoor, A., Nishihara, E., 2011. Influence of biochar application on sandy soil hydraulic properties and nutrient retention. J. Food, Agric. Environ. 9, 1137–1143.

Valsami-Jones, E., 2004. The Geochemistry and Mineralogy of Phosphorus, in: Valsami-Jones, E. (Ed.), Phosphorus in Environmental Technologies; Principles and Applications. IWA Publishing, London, pp. 20–50.

van Raij, B., 1998. Bioavailable tests: alternatives to standard soil extractions. Commun. Soil Sci. Plant Anal. 29, 1553–1570. doi:10.1080/00103629809370049

van Zwieten, L., Kimber, S., Morris, S., Chan, K.Y., Downie, A., Rust, J., Joseph, S., Cowie, A., 2010. Effects of biochar from slow pyrolysis of papermill waste on agronomic performance and soil fertility. Plant Soil 327, 235–246. doi:10.1007/s11104-009-0050-x

Verheijen, F.G. a, Graber, E.R., Ameloot, N., Bastos, A.C., Sohi, S., Knicker, H., 2014. Biochars in soils: New insights and emerging research needs. Eur. J. Soil Sci. 65, 22–27. doi:10.1111/ejss.12127

Villalba, G., Liu, Y., Schroder, H., Ayres, R.U., 2008. Global phosphorus flows in the industrial economy from a production perspective. J. Ind. Ecol. 12. doi:10.1111/j.1530-9290.2008.00050.x

Volceanov, E., Georgescu, M., Volceanov, A., Mihalache, F., 2003. Zirconium phosphate binder for periclase refractories. Silic. Ind. 3–4, 31–36.

Walker, T.W., Syers, J.K., 1976. The fate of phosphorus during pedogenesis. Geoderma 15, 1–19. doi:10.1016/0016-7061(76)90066-5

Wang, G.M., Stribley, D.P., Tinkler, P.B., Walker, C., 1993. Effects of pH on arbuscular mycorrhiza I. Field observations on the long-term liming experiments at Rothamsted and Woburn. New Phytol. 124, 465–472. doi:10.1111/j.1469-8137.1993.tb03837.x

Wang, T., Camps-Arbestain, M., Hedley, M., 2014. The fate of phosphorus of ash-rich biochars in a soil-plant system. Plant Soil 375, 61–74. doi:10.1007/s11104-013-1938-z

Wang, T., Camps-Arbestain, M., Hedley, M., Bishop, P., 2012. Predicting phosphorus bioavailability from high-ash biochars. Plant Soil 357, 173–187. doi:10.1007/s11104-

012-1131-9

Wang, Z., Nie, E., Li, J., Yang, M., Zhao, Y., Luo, X., Zheng, Z., 2012. Equilibrium and kinetics of adsorption of phosphate onto iron-doped activated carbon. Environ. Sci. Pollut. Res. 19, 2908–2917. doi:10.1007/s11356-012-0799-y

Waqas, M., Khan, S., Qing, H., Reid, B.J., Chao, C., 2014. The effects of sewage sludge and sewage sludge biochar on PAHs and potentially toxic element bioaccumulation in Cucumis sativa L. Chemosphere 105, 53–61. doi:10.1016/j.chemosphere.2013.11.064

Wei, X., Viadero, R.C., Bhojappa, S., 2008. Phosphorus removal by acid mine drainage sludge from secondary effluents of municipal wastewater treatment plants. Water Res. 42, 3275–3284. doi:10.1016/j.watres.2008.04.005

Wolf, A.M., Baker, D.E., 1985. Comparisons of soil test phosphorus by Olsen, Bray P1, Mehlich I and Mehlich III methods. Commun. Soil Sci. Plant Anal. 16, 467–484. doi:10.1080/00103628509367620

Xie, T., Reddy, K.R., Wang, C., Yargicoglu, E., Spokas, K., 2015. Characteristics and Applications of Biochar for Environmental Remediation: A Review. Crit. Rev. Environ. Sci. Technol. 45, 939–969. doi:10.1080/10643389.2014.924180

Yao, Y., Gao, B., Inyang, M., Zimmerman, A.R., Cao, X., Pullammanappallil, P., Yang, L., 2011. Biochar derived from anaerobically digested sugar beet tailings: Characterization and phosphate removal potential. Bioresour. Technol. 102, 6273–6278. doi:10.1016/j.biortech.2011.03.006

Yao, Y., Gao, B., Zhang, M., Inyang, M., Zimmerman, A.R., 2012. Effect of biochar amendment on sorption and leaching of nitrate, ammonium, and phosphate in a sandy soil. Chemosphere 89, 1467–1471. doi:10.1016/j.chemosphere.2012.06.002

Yu, Q., Kandegedara, A., Xu, Y., Rorabacher, D.B., 1997. Avoiding interferences from Good's buffers: A contiguous series of noncomplexing tertiary amine buffers covering the entire range of pH 3-11. Anal. Biochem. 253, 50–56. doi:10.1006/abio.1997.2349

Zhang, H., Chen, C., Gray, E.M., Boyd, S.E., Yang, H., Zhang, D., 2016. Roles of biochar in improving phosphorus availability in soils: A phosphate adsorbent and a source of available phosphorus. Geoderma 276, 1–6. doi:10.1016/j.geoderma.2016.04.020

Zhang, L., Zhang, J.S., 2013. Biochar from Sewage Sludge: Preparation, Characterization and Ammonia-Phosphorus Capture. Adv. Mater. Res. 830, 473–476. doi:10.4028/www.scientific.net/AMR.830.473

Zhang, M., Gao, B., Yao, Y., Inyang, M., 2013. Phosphate removal ability of biochar/MgAl-LDH ultra-fine composites prepared by liquid-phase deposition. Chemosphere 92, 1042–1047. doi:10.1016/j.chemosphere.2013.02.050

Zhang, M., Gao, B., Yao, Y., Xue, Y., Inyang, M., 2012. Synthesis of porous MgO-biochar nanocomposites for removal of phosphate and nitrate from aqueous solutions. Chem. Eng. J. 210, 26–32. doi:10.1016/j.cej.2012.08.052

Zhang, M.K., Liu, Z.Y., Wang, H., 2010. Use of single extraction methods to predict bioavailability of heavy metals in polluted soils to rice. Commun. Soil Sci. Plant Anal. 47, 820–831.

Chapter 9

Appendix

Appendix 1

The following documents can be found on the CD supplied with the PhD thesis:

- The published manuscripts associated with this thesis